COMPUTERIZED MODELING OF GEOTECHNICAL STRATIGRAPHIC DATA

by

ALEXANDER DONNAN SMITH

B.C.E. University of Delaware
Newark, Delaware
(1973)
M.S. Lehigh University
Bethlehem, Pennsylvania
(1974)

SUBMITTED TO THE DEPARTMENT OF CIVIL ENGINEERING
IN PARTIAL FULFILLMENT
OF THE REQUIREMENTS FOR THE
DEGREE OF

DOCTOR OF PHILOSOPHY

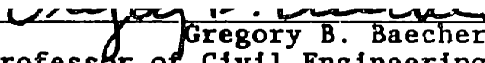at the

MASSACHUSETTS INSTITUTE OF TECHNOLOGY
June 1989

Signature of Author_____
Department of Civil Engineering
June 28, 1989

Certified by_____
Gregory B. Baecher
Professor of Civil Engineering
Thesis Supervisor

Accepted by_____
Ole S. Madsen
Chairman, Department Committee on Graduate Students

1

COMPUTERIZED MODELING OF GEOTECHNICAL STRATIGRAPHIC DATA

by

Alexander Donnan Smith

ABSTRACT

A computerized framework for incorporating available geotechnical information, subjective input, and probability-based profiling into the geometric modeling of soil stratigraphy for site characterization is developed. The developed techniques are demonstrated using typical geotechnical test data from selected case histories.

Existing surface modeling algorithms are reviewed with respect to their applicability to soil profiling. Selected analytical techniques including hand contouring are compared. Existing surface modeling techniques are shown to exhibit unacceptable results with respect to strata overlap and continuous models of discontinuous strata. Currently available probability-based mapping techniques are reviewed and assessed with respect to their applicability to soil profiling.

Clustering and regional merging techniques are applied, separately and in combination, as soil data preprocessing methods using visual description information to identify potential soil strata. Probabilistic profiles are developed treating the single surface models as random variables and assuming the geologic sequence is known. Probabilistic relaxation methods are applied to the probabilistic profiles to resolve the strata overlap and discontinuity issues.

The surface modeling and profiling methods are applied to two case history data sets. The case history applications demonstrate the relative performance of the developed soil data preprocessing, probabilistic profiling and probabilistic relaxation methods.

Thesis Supervisor: Dr. Gregory B. Baecher
Title: Professor of Civil Engineering

ACKNOWLEDGEMENTS

I would like to express appreciation   ofessor Gregory B. Baecher for his willingness to supervise this thesis during a transition period of his own, and for his encouragement throughout the research. I also want to acknowledge Professors Einstein, Veneziano and Whitman for their contributions as members of my thesis committee.

I want to thank Dr. Samson Liao for his friendship and encouragement, and Haley & Aldrich, Inc. for their financial support and commitment to professional development.

I want to acknowledge the graphics work performed by Mrs. Acey Welch to prepare the figures. Her assistance, advice and the professional end product is greatly appreciated.

Finally and yet foremost, I want to acknowledge the love and support of my wife, Cathy, and children, Elizabeth and Andrew. They have been a constant source of support throughout my MIT experience at the cost of lost time together. Their sacrifices and support have always been appreciated and will never be forgotten. I can only hope to repay them in the future.

TABLE OF CONTENTS

LIST OF TABLES

8

LIST OF FIGURES

CHAPTER 1

INTRODUCTION

1.1 Introduction

A common element to most design and construction projects is the acknowl-
edged need for an accurate definition and understanding of existing soil
and rock conditions and their impact on project design and construction.
In geotechnical engineering this process is referred to as site charac-
terization. Although site characterization is applied to every geotech-
nical design project, formal understanding of the process is limited.

A schematic of the general site characterization process is shown in Fig-
ure 1.1. The schematic presents the major activities in the site charac-
terization process. Although the activities are presented in a segmented
fashion, often several of the activities are performed concurrently with
little distinction between them.

The inherent complications in the process of site characterization (dis-
cussed below), coupled with the fact that no two sites are identical, and
that the process, as it is practiced, is largely subjective, have
restricted the development of objective site characterization procedures.

1.2 "Typical" Problems in Site Characterization

The process of site characterization has inherent complications, which
are present to varying extents on all sites. These complications
include:

1) sparse data,

2) 3D conditions which vary in space,

3) necessity of judgement in data interpretation, and

4) the empirical and heuristic (rule of thumb) nature of
   many analytical geotechnical models.

Geotechnical data is gathered in the field using various exploration techniques, most commonly test borings. Test borings are drilled for the purpose of gathering information for the evaluation of soil stratigraphy and soil properties. The geotechnical engineer relies on the information from the test borings as the main basis of the site characterization.

The horizontal spacing of test borings depends on the project. In practice, the horizontal spacing of the test borings is determined by the geotechnical engineer based on his experience with similar types of projects, the anticipated soil/rock conditions, and truthfully, at times, the budget available for explorations.

In addition to the spacing between test borings, the information obtained in the test borings is both objective and subjective. Objective information is obtained when Standard Penetration (SPT) tests (ASTM D-1586) are performed to quantify the resistance of the soil to a 1-1/2 foot penetration of a standard sampler, and to obtain a soil sample for visual classification and possible laboratory testing. The resistance is measured by the number of blows with a 140 pound hammer falling freely 30 inches, required to drive the sampler 1-1/2 feet into the soil. Even this relatively objective information can be biased by, among other things, deviations from the specified amount of energy applied to the sampler.

The vertical frequency of testing is variable and could, in fact, be continuous; however, in practice, it is common to perform Standard Penetration tests at five foot intervals (see Figure 1.2). Regular sampling intervals facilitate the field work, but it is unlikely that all soil strata changes will fall within the sampling interval of 1-1/2 feet in every 5 feet. Therefore, if there is a change in soil strata between samples, other information must be used by the driller to try to identify the elevation of the soil strata interface.

In addition to the objective SPT information, subjective information concerning the soil conditions is obtained by observing the performance of the drilling equipment, advance rate of casing, and other observations which indirectly reflect changes in the soil conditions with depth. Due to the nature of the information and the range of skill and experience in the drillers, this information is very subjective. It is this information which is used by the driller to estimate the strata change elevation, if the change does not fall within a SPT sampling interval. Often, in practice, the strata change is arbitrarily indicated by the driller. Therefore, as a consequence of the process of planning and performing the test borings, the resulting information is sparse with respect to spatial concepts and relatively subjective as well.

Soil and rock conditions need to be assessed in 3 dimensions as part of site characterization. As discussed above, the spacing between test borings and between samples is established in part in response to the anticipated spatial variation of the soil/rock stratigraphy. In general the test borings produce objective and subjective information, which the geotechnical engineer uses to infer the conditions between test borings with a considerable amount of personal judgement and experience.

The combined effect of sparse 3D data is that developing profiles as part of the site characterization process requires, by necessity, judgement in data interpretation. It is this need for judgement based on experience that makes this a challenging, and yet frustrating, area for the application of expert systems (Rehak, 1985). In fact, the application of expert systems to site characterization may be questioned by some due to the highly subjective nature of the process.

Although the site characterization process is subjective, there are several steps which are common to almost all projects (see Figure 1.3). The data obtained in the exploration and sampling, and measurement of properties phases of the site characterization process (see Figure 1.3) are used to develop design values needed for the implementation of geotechnical models for the analysis of the specific design issues. These

17

models are usually based upon empirical relationships and heuristics. Therefore, it is difficult at the completion of a project to assess whether differences in predicted vs. observed behavior can be attributed to the level of uncertainty in the general site characterization process, the geotechnical model itself, or a combination of the two. As a result, while ideally our understanding of the general site characterization process should improve by evaluating prediction versus performance, the rate of advancement in understanding is slowed by the inherent complexity of the process.

This research addresses the expanded steps of the site characterization process, and demonstrates that computerized techniques can be developed and applied to the process to not only improve the process, but at the same time improve our understanding of the process.

In Figure 1.3 there are several phases to the expanded site characterization process; however, all of these phases are concerned with assessing soil properties and soil stratigraphy which are discussed in the next two sections.

1.3 Soil Properties

1.3.1 Evaluation of Uncertainty

Samples obtained from the test borings are selectively tested in the laboratory to classify the soils and to evaluate their engineering properties. The number of tests performed varies considerably depending in part on the project and the soils encountered. However, in general, more classification type tests (Atterberg Limits, grain size analyses, etc.) are performed than tests of engineering properties (deformability, strength and permeability).

The difference in the testing frequency is due in part to the lower cost of the classification tests. Less expensive classification tests and empirical relationships between classification test results and estimated engineering properties are often used.

Engineering property tests are normally performed at a higher cost on "undisturbed" soil samples. Using classification test results to identify similar soils, the results of the engineering tests are used to develop design properties for soil strata or possibly sub-strata. Although the engineering tests typically indicate some uncertainty in their results, this uncertainty is often not extended into the analysis of the soil properties for the design soil strata.

1.3.2 Determination of Design Parameters

Assuming that classification tests have been performed to assist with the identification of design soil strata, design parameters are usually assigned to each soil stratum using the results of the engineering tests, if any, and a considerable amount of personal judgement by the geotechnical engineer. In the absence of engineering test results, empirical relationships between classification tests and engineering properties developed for "similar" soils are often used, along with even more personal judgement, to assign design parameters.

Decisions concerning whether or not soils are similar are made in a subjective manner by the geotechnical engineer using the available information (test boring logs, classification test results, and engineering test results), which may have been used also to develop design profiles. This process would be advanced considerably if by using the same available information the identification of "similar" soils could be handled in an objective fashion. However, regardless of the method, the geotechnical engineer must always be given the opportunity to input his personal judgement and experience.

1.4 Soil Stratigraphy

1.4.1 Test Borings

Soil stratigraphy is normally assessed using the results of the field and laboratory programs. Strata change information from the test boring log

is typically used with little questioning of the strata change information. The geotechnical engineer normally reviews the test boring information, particularly the visual descriptions of the recovered soil samples, and develops the soil stratigraphy in a very subjective manner.

To aid in the process of assessing the soil stratigraphy, the geotechnical engineer prepares soil profiles. These profiles are vertical sections through the site at selected locations with the adjacent test boring information projected into the plane of the profile. Based on judgement, the geotechnical engineer decides which test borings are close enough to a particular profile to be used in assessing soil stratigraphy in that profile. The geotechnical engineer also decides the number and orientation of the profiles that are developed to assess the soil stratigraphy for the project.

Once the test boring information is projected into the profile plane, soil stratigraphy is developed using techniques considered acceptable to the state of practice in geotechnical engineering. When the soil stratum being considered is continuous, straight lines are normally drawn from test boring to test boring connecting the observed stratum top and bottom elevations. If the stratum appears to be discontinuous, the geotechnical engineer uses personal judgement as to the interpretation that is shown and the manner, if any, in which the level of uncertainty is indicated.

1.4.2 Stratum Thickness

Another potential complication in assessing the soil stratigraphy is the fact that the test borings are usually drilled to varying depths. Thus, unless the test boring is drilled to the top of rock or below, the boring only partially penetrates the deepest soil stratum encountered. Therefore, the boring provides limited information concerning the total thickness of the deepest encountered stratum.

20

1.4.3 Discontinuities

Identification of discontinuous soil strata and representation of the strata in geotechnical models is one of the most difficult, and challeng-ing, phases of site characterization. The geologic sequence of the strata encountered in the test borings provides some information on the continuity of a particular stratum; however, due to the spacing between the test borings, the lateral extent of a discontinuous stratum is largely undetermined.

1.4.4 Evaluation of Uncertainty

During the development of the soil profiles, the level of uncertainty in the information is assessed subjectively by the geotechnical engineer. However, once the soil profiles are developed, too often the information is treated as deterministic data with no quantifiable attention given to the level of uncertainty.

1.5 Objectives of Stratigraphy Assessment

Ideally, the assessment of soil stratigraphy should include an objective consideration of all the available information. This should include the test boring log data, the visual description of the recovered soil sam-ples, and laboratory test results. The geotechnical engineer should have the opportunity during the process to input his personal judgement and experience. The stratigraphy should be developed by considering numerous soil profiles, not just those that are most convenient or that were selected prior to starting the test boring program.

Soil profiles should be developed objectively in an efficient manner so that more profiles can be considered as part of resolving the soil stra-tigraphy issues. The soil profiles should reflect the level of uncer-tainty in both the information and interpretation.

1.6 Geologic Modeling

1.6.1 Introduction

Geologic modeling, as the term is used here, is the process of gathering the available geology information concerning a specific site for the ultimate purpose of site characterization. One of the challenging tasks facing the engineer responsible for site characterization is to develop a preliminary concept of site conditions based on the available geology information, and then to modify this preliminary concept using the actual site information as that information is available.

The preliminary concept of the site conditions may be relatively sketchy on a site with little background information, or it may be fairly detailed if there is site characterization data available for the subject site or adjacent sites. It is the obligation of the geotechnical engineer to gather and assimilate available information as the first part of the site characterization process.

1.6.2 Objectives of Geologic Modeling

The objective of the preliminary geologic modeling is to develop an understanding of the anticipated geologic environment. The geologic environment may be very complex depending on the depositional environment. Other factors, such as changes in the site conditions by man (development, filling, etc.), may also contribute to the complexity.

The preliminary geologic model will be modified as the site specific information (test borings, laboratory data, etc.) becomes available, but it represents the geotechnical engineer's working hypothesis of the conditions.

It is very important to develop the preliminary geologic model prior to the planning of the field exploration program. When properly developed, the preliminary geologic model will heavily influence the scope of the

field exploration program. Anticipated geologic conditions influence the type, spacing, and depth of the field explorations, as well as, the equipment required and the anticipated costs.

Geologic modeling continues throughout the site characterization process. Any surface modeling and profiling of the subsurface conditions must be consistent with the overall geologic model concepts for the site. Therefore, throughout the site characterization process, the preliminary geologic model is revised as additional information is available. The revision process should include a review of the preliminary geologic model to make sure that the final geologic model is developed in an objective fashion.

1.7 Organization of Thesis

Although extremely complex as practiced, site characterization and in particular, the development of soil stratigraphy models, can be conceptualized. In simplest terms developing computerized models of soil stratigraphy consists of using the available information and general geology concepts to develop stratigraphic models based on a combination of mathematical reasoning and geology principles.

Computerized stratigraphic modeling can be conceptualized as indicated in Figure 1.4. This is a representation of a very complex process; however, the conceptual approach provides a basis for explaining the methodology of this research. Each of the modules shown in Figure 1.4 has been researched separately with the goal of ultimately combining the modules into an integrated computerized method for stratigraphic modeling of geotechnical data.

The chapters following this introduction provide a detailed statement of the research objectives (Chapter 2), summary of research by others in topics related to stratigraphic assessment (Chapter 3), a detailed presentation of the methods and results of this research regarding computerized modeling of geotechnical stratigraphic data (Chapters 4, 5 and 6), and summary and conclusions (Chapter 7). References to and critical

23

results from two applied case histories are presented throughout Chapters 4, 5 and 6. Details of the two applied case histories are presented in Appendices A and B.
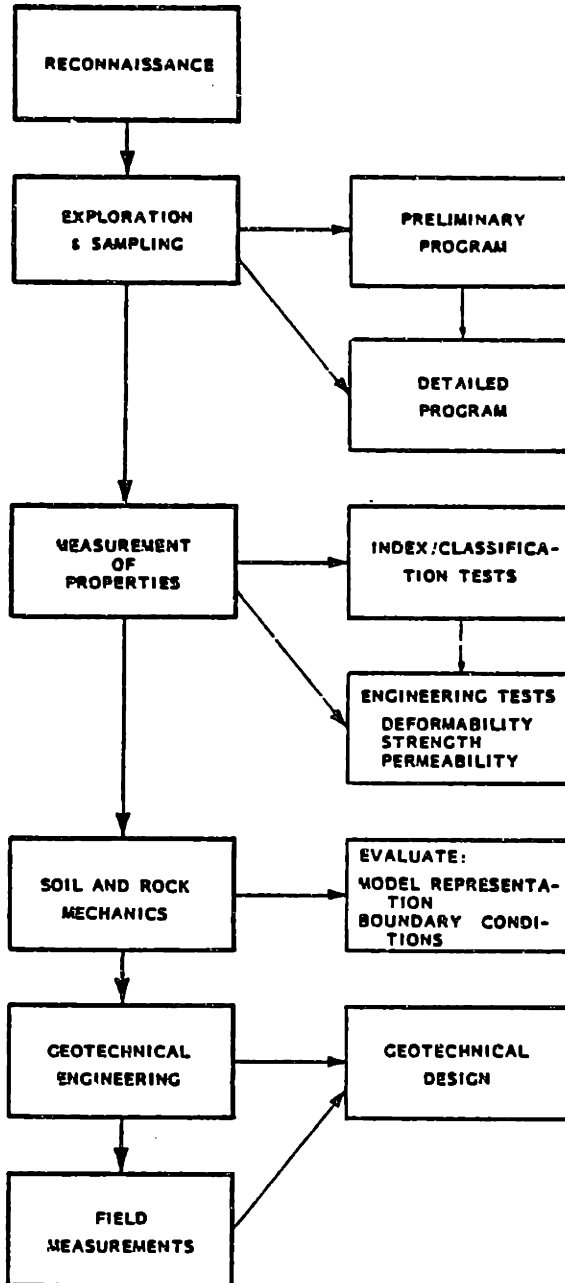
Figure 1.1 - General Site Characterization Process (after Einstein, personal communication).

Test boring

Typical boring spacing

30 to 50 ⁺ ft.

Ground surface

Stratum A

Strata Interface

Typical sample spacing 5 ft.

Depend heavily on strata change elevation for strata interfaces (change seldom in sample interval)

Stratum B

Stratum C

Sample interval typically 1 1/2 ft.
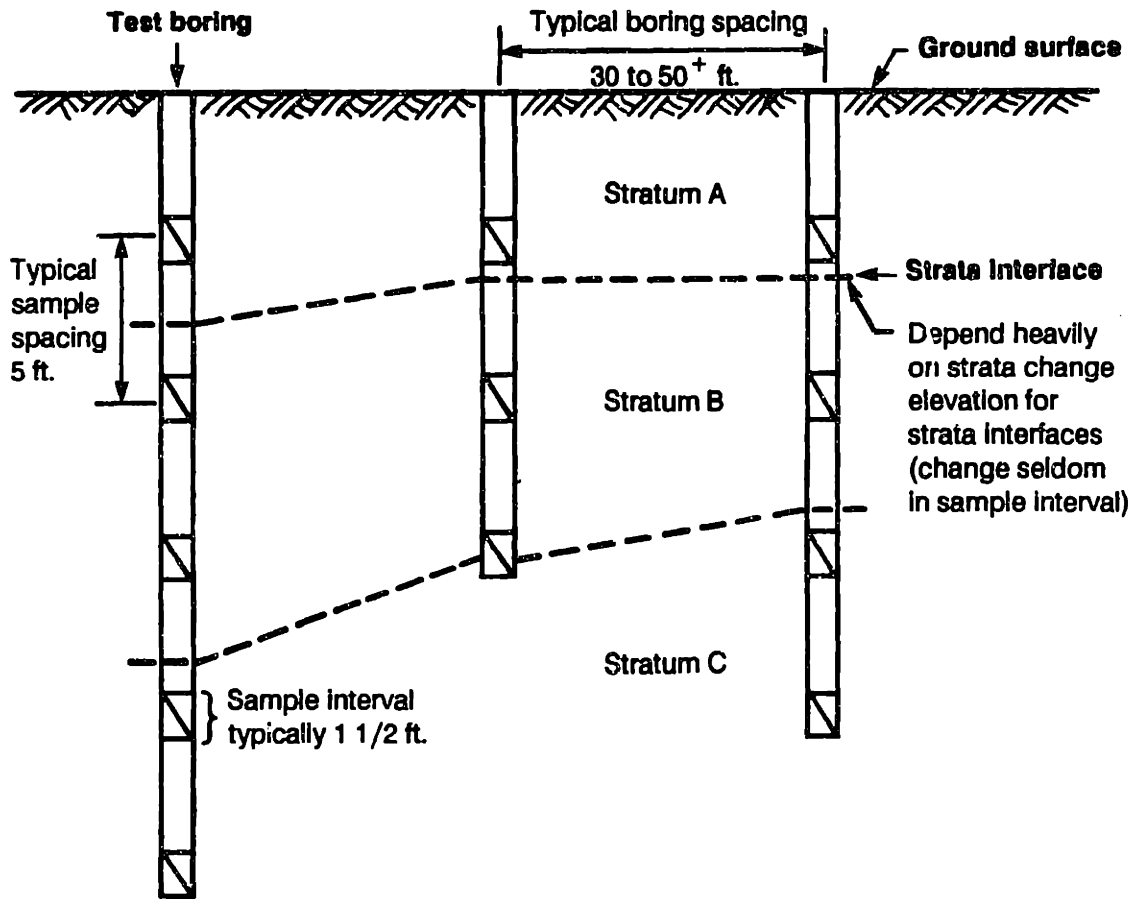
Figure 1.2 - Typical Test Boring and Sampling Spacings.
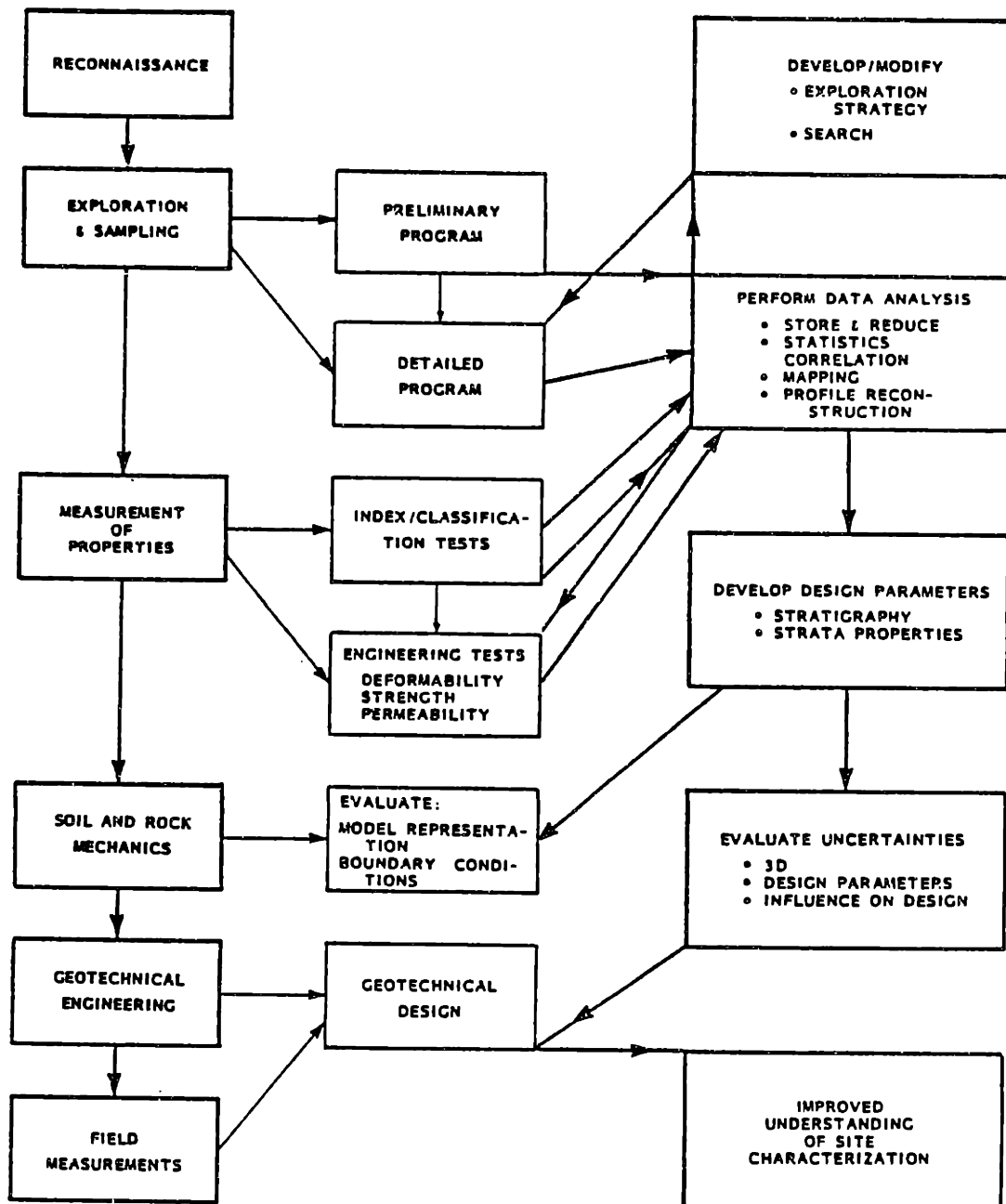
Figure 1.3 - Expanded Site Characterization Process.

GECLOGIC MODELING

PROBABILISTIC MAPPING/PROFILING

BORING DATA

SOIL DATA PREPROCESSING

GEOLOGY THEORY

GEOLOGY INFORMATION/GEOMORPHOLOGY

GEOLOGIC/GEOMETRIC CONSTRAINTS

SURFACE MODELING

PROFILING

ENHANCED PROFILES

(Stratigraphic profile
with indication of uncertainty)
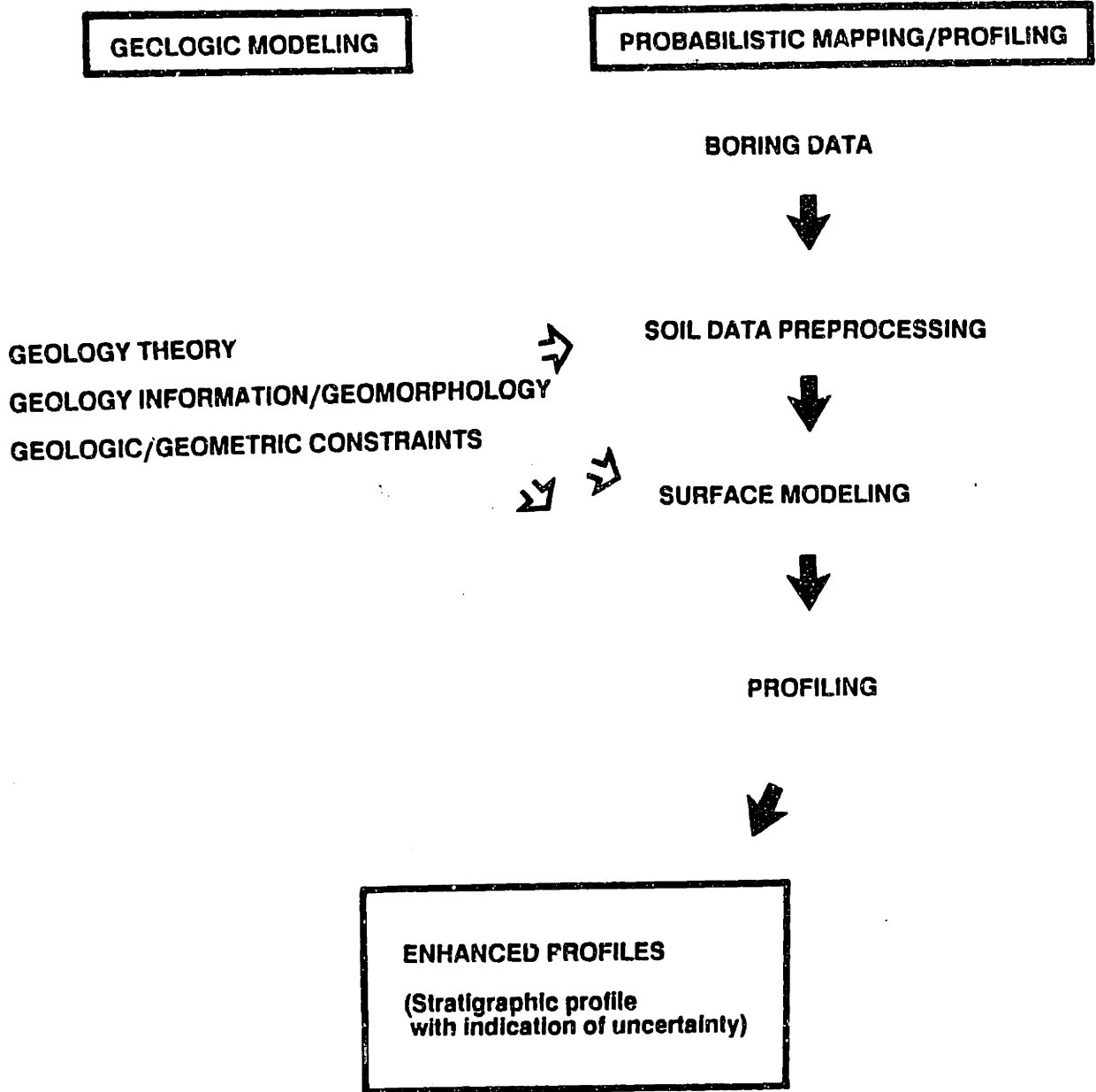
Figure 1.4 - Conceptual Representation of Stratigraphic Modeling.

CHAPTER 2

RESEARCH OBJECTIVES

2.1 Statement of Overall Objectives

The objectives of this thesis research are (1) to develop a computerized framework for incorporating available information, the engineer's subjective input, and probability-based profiling into the geometric modeling of soil stratigraphy, and (2) to demonstrate the application of the developed techniques using typical geotechnical test data from selected case histories.

The overall objectives can be further sub-divided into more specific objectives, which are discussed in the following section.

2.2 Statement of Specific Objectives

Surface Modeling:

Review existing surface modeling algorithms and assess their applicability to the development of geotechnical stratigraphic models - Numerous algorithms have been developed for modeling surfaces in disciplines other than geotechnical engineering. Some of these algorithms have been applied by geotechnical engineers to model soil strata interfaces. However, no thorough study of the algorithms applied to geotechnical stratigraphic modeling has been performed. This research includes an assessment of existing algorithms with respect to modeling soil strata surfaces and the applicability of various techniques to two applied case histories.

Profiling:

Assess the applicability of probability-based mapping techniques to the process of soil profiling - Review available probability-based mapping

techniques and apply appropriate techniques to the process of soil pro-
filing. Assess the applicability of the selected techniques to soil pro-
filing.

Develop computer techniques for probabilistic soil profiling - Soil pro-
files in practice today are generally accepted to have a level of uncer-
tainty; however, the level of uncertainty is not indicated or quantified.
Develop a computerized, efficient method for the assessment of soil
stratigraphy with a direct expression of the uncertainty level.

Develop methods for incorporating discontinuity into stratigraphic models
- Mathematical models of single surfaces typically imply continuity of
the surface over space. This is a serious deficiency when the models are
applied to soil stratigraphy, which is often discontinuous due to geo-
logic formation processes. This research summarizes methods for identi-
fying potentially discontinuous soil strata, and developed methods for
creating a discontinuous model in an objective fashion.

**Develop methods for incorporating available stratigraphic data as well as
subjective input from the engineer knowledge** - Computer techniques used
to develop probabilistic profiles should include direct consideration of
the available data. The considerations should be objective, and yet
allow for the input of the engineer's personal judgement and experience.

<u>Case Histories:</u>

Demonstrate the application of existing and developed techniques for sur-
face modeling and profiling using actual case history data - The existing
and developed techniques should be applied to create surface models and
profiles for case histories to demonstrate the relative advantages and
disadvantages of the existing and developed methods.

Demonstrate the influence of the interpretation of available data and the
engineer's subjective input on the results of the surface modeling and

30

profiling - The case history applications should be used to demonstrate the ability of the developed techniques to incorporate the influence of available information as well as the engineer's subjective input.

CHAPTER 3

LITERATURE REVIEW

3.1 Introduction

This chapter presents an overview of the existing literature concerning theoretical and applied research in areas which are addressed in Chapters 4, 5 and 6. The material in this chapter is presented at an introductory level for the benefit of the reader. Numerous references are provided so that the reader can consult the original publications for additional detail.

3.2 Surface Modeling

3.2.1 Introduction

The objective of surface modeling is to develop a mathematical representation of a "real" surface using the available data. The process of surface modeling is complicated by the typically sparse, irregular data that is obtained in the site characterization process.

There are a variety of methods that have been proposed for surface modeling. Many of these have been developed for the purpose of contouring surfaces. Dowd (1985) and Sabin (1985) have prepared detailed summaries of methods for the purpose of contouring for general and geostatistical problems. Several of the methods discussed by Dowd and Sabin are discussed in the following sections.

3.2.2 Triangulation (Piecewise Planar)

Automatic triangulation of irregularly spaced points has been summarized by others (Watson and Philip, 1984b). The size of the data set influences the complexity of triangulation since a data set containing N points has N(N-1)/2 possible edges and N(N-1)(N-2)/6 possible triangles (Watson and Philip, 1984b).

32

Watson and Philip identify three basic triangulation methods - Optimal, Greedy and Delaunay. The methods are briefly described in the remainder of this section.

Optimal triangulation is accomplished by minimizing the length of the resulting edges. The Optimal triangulation is not unique since there may be at least two different triangulations with the same minimal edge length.

Greedy triangulation is controlled by the requirement that no edge can be included if there exists a shorter edge which intersects the first. The Greedy triangulation is accomplished by searching for the longest edge which can not be intersected by a shorter edge and then repeating the search with the longest edge removed from the search. The Greedy triangulation algorithm is neither unique (two edges may be the same length) nor efficient (considerable ordering of lengths is required for large data sets).

Delaunay triangulation is achieved by triangulating the points such that no data point lies within the circumcircle of any other triangle. This requirement maximizes the smallest interior angle. The data points at the vertices of the Delaunay triangulations are in a sense nearest natural neighbors since they are closer to their circumcenter than to any of the other data points. Delaunay triangulation is unique unless four or more of the data points are cocircular.

Figure 3.1 shows the Optimal, Greedy and Delaunay triangulation of a small data set. The ramifications of the different triangulation methods are significant with respect to triangulation based surface models. Since the methods are piecewise planar, the inclination of the base triangle at any point is a function of the spatial orientation of the three vertices. Therefore, these three different triangulation methods can potentially result in significantly different contours using the same data set.

It should be noted that "linear interpolation", a common method of sur-
face modeling in geotechnical engineering, is in practice a
triangulation-based method. The actual triangulation is performed, in a
highly arbitrary fashion, by the individual who decides between which
data points to apply linear interpolation. In practice it is typical to
select by eye only those data points in the neighborhood of a central
point. This selection is a crude form of triangulating (i.e., determina-
tion of triangle side). Therefore, the surface model resulting from lin-
ear interpolation is not consistent and reproducible between users (see
Chapter 5 and Appendix A for an applied example).

Miles (1970) derived expressions for the expected values and variances of
critical properties of Delaunay triangles formed from random points cho-
sen from a Poisson process. The expected values of the properties are
as follows:

Equation 3.1:

$$E(A) = 1/(2\rho)$$

Equation 3.2:

$$E(S) = 32/(3\pi\sqrt{\rho})$$

Equation 3.3:

$$E(R) = 3/(4\sqrt{\rho})$$

Equation 3.4:

$$E(I) = 1/(4\sqrt{\rho})$$

Equation 3.5:

$$E(L) = 32/(9\pi\sqrt{\rho})$$

where

A = the triangle area,

S = the triangle perimeter,

R = the circumcircle radius,

I = the inradius,

L = the length of any arbitrary side,

ρ = the Poisson intensity of points.

Recent research in triangulation algorithms has concentrated on the Delaunay triangulation method and the development of numerous algorithms with varying efficiencies (Aurenhammer and Edelsbrunner, 1984; Fortune, 1987; Green and Sibson, 1978; Lee and Schachter, 1980; Preparata and Shamos, 1985; and Watson and Philip, 1984a).

3.2.3 Dirichlet Polygons

If the subject area is sub-divided into polygons with a single data point within each polygon such that all points within any polygon are closer to the enclosed data point than any other data point, the polygons which result are known as Dirichlet polygons. Dirichlet polygons have also been referred to as Voronoi polygons, Thiessen polygons, Wigner-Seitz polygons, cell-model, and S-mosaics (Upton and Fingleton, 1985).

Dirichlet polygons are constructed using the following steps (see Figure 3.2 for examples of Dirichlet polygons and Delaunay triangles):

1. Identify the nearest neighbors to the subject data point using the Delaunay triangulation method.
2. Connect the subject data point to its nearest neighbor.
3. Construct the perpendicular bisectors to the lines connecting the nearest neighbors.
4. The intersection of the perpendicular bisectors forms a polygon with the subject data point in the interior. This is the Dirichlet polygon for the subject data point.

Various properties of Dirichlet polygons have been determined by other researchers (Meijering, 1953; and Gilbert, 1962). These properties are summarized as follows:

Equation 3.6:

$$E(N) = 6$$

Equation 3.7:

$$E(A) = 1/\rho$$

Equation 3.8:

$$E(S) = 4/\sqrt{\rho}$$

Equation 3.9:

$$E(A^2) = 1.28/\rho^2$$

where

$A =$ *the polygon area,*

$S =$ *the polygon perimeter,*

$\rho =$ *the Poisson intensity of points.*

Dirichlet polygons are in some disciplines the desired end product. They have been used in research areas as diverse as the study of ancient cultures and commerce (Hodder and Orton, 1976), and plant ecology and territorial animals (Pielou, 1977).

Watson and Philip (1984a) present a thorough presentation of triangle-based interpolation including methods which are based upon Delaunay triangulation of the initially irregularly spaced data points. According to Lee and Schachter (1980), the Delaunay triangulation is an "excellent" choice for terrain fitting and display since the minimum angle is maximized and the resulting visual characteristics are good.

3.2.4 Trend Surface Analysis

Trend surface analysis as it is applied in geology is the process of using mathematical models to separate known data into a regional trend and a local variation. The process is somewhat arbitrary due to the subjective nature of the concepts of regional and local.

36

Trend surface analysis has been applied in geology since the mid-1960's
(Harbaugh and Merriam, 1968; Whitten, 1975). Reasons for the early
apparent popularity of trend surface analysis included its relatively
simple mathematical expressions and ease in computerization. However,
with the increase in computer computation resources other surface model-
ing methods discussed below have grown in popularity to surpass trend
surface analysis.

Mathematical expressions for surface modeling normally take the form $z = f(x,y)$ where z is the elevation of the surface being modeled, and x and y
are Cartesian coordinates. The function used to model the surface can
take any mathematical form. A unique solution can be obtained as long as
the number of parameters in the mathematical function is less than or
equal to the number of known data points.

When the number of known data points exceeds the number of parameters in
the modeling function, the method of least-squares is typically used to
determine the values for the function parameters which result in the
minimum sum of squared deviations between the known data points and the
surface model.

It should be noted that all of the data points are used in the calcula-
tion of the function parameters regardless of the spacing between data
points or the distance from an unknown value location.

The method of least-squares does not limit the form of the modeling func-
tion. Either linear or non-linear functions could be used. However,
linear models are more typically used due in part to their simpler form.
Polynomial expressions of degree 5 or less are the most common modeling
functions. Polynomial expressions are used as a matter of convenience
since they have the ability to fit reasonably complicated surfaces.

The degree of the polynomial expression used for trend surface analysis
determines the general shape of the surface that will be fit to the data.
Minimization of the least square error determines the coefficients of the

parameters in the polynomial expression. Figure 3.3 demonstrates the general shapes that result from changing the degree of the polynomial expression from one to three for up to three independent variables.

Another example of the surface shapes that result from changes in the degree of the polynomial expression is shown in Figure 3.4. Ripley (1981) analyzed the data from Davis (1973, Table 6.4) using trend surface analysis with first through fifth degree polynomials with the results as shown in Figure 3.4.

Linear models can be interpreted as (Watson, 1972):

Value at any point - Value of deterministic function + Random error

which can be also expressed as

Value at any point - Regional component + Local residual

When the random error terms are uncorrelated, have zero mean, and the same variance, it can be proved that the least-squares estimators of the function parameters are best linear unbiased estimates. If the error terms are also normally distributed, then the least-squares estimator is also the maximum-likelihood estimator (Tipper, 1979).

According to Tipper (1979), the least-squares estimators are optimal only when the error terms are truly random. If they are spatially autocorrelated (which is generally true unless the number of degrees of freedom used in the function is almost as great as the number of data points), then the assumptions of the least-squares method are violated, and the estimated parameters are neither unbiased nor of minimum variance. The error terms of any application of least-squares should be tested for spatial autocorrelation, using appropriate methods (Cliff and Ord, 1975). Tipper (1979) further states that failure to appreciate this point has caused most of the misuse of the least-squares method in surface fitting, including most of the earlier geological work using trend surfaces.

The process of trend surface analysis is highly dependent on the spatial distribution of the data set. One relatively early study of the effects of the spatial data distribution on trend surface analyses is the work by

Shaw (1977). However, although there is a spatial distribution effect, Shaw concluded that for the particular data set analyzed the measurable amount of distortion did not influence the interpretation of the structural data.

After further research by others in the more general field of regression analysis, Unwin and Wrigley (1987) present a discussion of the spatial problems with regression analysis. The spatial difficulties that they addressed included edge effects and the consequences of highly clustered data. Their analysis is based on the application of leverage methods to geologic data. Leverage is a means of assessing the relative influence of individual data points based on their spatial relationship to the "center of the data" (Hoaglin and Welsch, 1978; Belsley, Kuh, and Welsch, 1980).

Unwin and Wrigley (1987) conclude, in part, that:

"The analyses reported here should make it clear that the edge, frame shape, and data-point clustering effects noted by previous workers are an endemic feature of polynomial trend-surface models. The concept of the leverage of the data point provides an analytical framework for discussion of these effects. In particular, it demonstrates clearly that, unless a buffer region is created around the area of interest into which the worst edge effects can be concentrated, higher order surfaces are almost certain to give excessive influence to points lying at the extreme of the distribution of control."

Olea (1975) summarized the limitations of trend surface analysis as follows:

1. Trend surface analysis is based on the method of least squares and as such results in mathematical models without physical meaning.

2. Trend surface analysis is not statistically optimal.

3. Trend surface analysis does not provide a measure of the error of the estimate.

4. Trend surface analyses are unstable on the fringes of the data and
    can have severe edge effects.

5. The only controlled parameter in trend surface analysis is the order
    of the polynomial.

6. Although trend surface analysis uses all the data points, it does
    not use the information concerning the relationships of data points
    like the kriging methods discussed below.

3.2.5 Kriging

Kriging, which is discussed in this section, is a subset of a larger
field known as geostatistics or regionalized variable theory. The meth-
odology described here was developed by Matheron (1965 and 1971) for the
purpose of estimating spatial functions to develop mines. Since its
inception, geostatistics has grown to be a major field of research.
Although originally developed for the purpose of mineral exploration,
regionalized variable theory has been applied to diverse problems asso-
ciated with spatially distributed data.

In order to present the basics of kriging, it is necessary to discuss the
fundamental principles of regionalized variable theory. The following is
a synopsis of discussions found in a couple of sources (Dowd, 1984; Olea,
1982). The reader is referred to Rendu (1978) for a thorough, yet brief,
presentation of the subject of regionalized variable theory.

A surface model can be developed as realizations of a random variable
over x,y locations of interest. This can also be expressed as the value
z measured at location x (bold indicates vector) as a value of the random
variable $Z(x)$. There are, however, many random variables all belonging
to a random function which could result in the observed values.

Due to the spatial variation of the random variable $Z(x)$, conventional
statistical methods of either describing the mathematical model or devel-
oping a model based on relative frequency analysis are not possible. The

complexity of spatial functions nearly precludes developing a
mathematical model, and relative frequency analysis is not plausible
since there is only a single observation at each point.

In order to overcome the difficulties with conventional statistical meth-
ods, geostatistics imposes a restraint of stationarity in order to use
observations to estimate the first two moments of the random variable.
The "intrinsic hypothesis" is the assumption that all the observations
are from the same population. This assumption results in an increase in
the sample size to the number of observations.

Assuming that the distributions of all the random variables are identical
(the stationarity hypothesis) results in the following equations for the
first two moments of linear estimators:

Equation 3.10:

$$E[Z(x)] = m \quad (a \quad constant)$$

Equation 3.11:

$$Cov[Z(x_i)Z(x_j)] = E[Z(x_i)Z(x_j)] - m^2$$

$$Cov[Z(x_i)Z(x_j)] = C(h)$$

where

$$h = |x_i - x_j|$$

The covariance depends on the vector distance h which separates the two
locations, $Z(x_i)$ and $Z(x_j)$ and not on the actual locations x_i and x_j. The
variance of $Z(x)$ is $C(0)$.

If the random variable does not have a finite variance, the stationarity
hypothesis is replaced by the intrinsic hypothesis under which stationar-
ity is limited to the first order differences:

$$Z(x_i) - Z(x_j)$$

With the intrinsic hypothesis, the corresponding moments of the differ-
ences are:

41

Equation 3.12:

$$E[Z(x_i) - Z(x_j)] = 0$$

Equation 3.13:

$$Var[Z(x_i) - Z(x_j)] = 2\gamma(h)$$

and the variance of the differences exists and depends only on the vector distance h which separates $Z(x_i)$ and $Z(x_j)$ and not on the particular locations x_i and x_j. This variance is known as the variogram. The variance is related to the variogram by:

Equation 3.14:

$$C(h) = C(0) - \gamma(h)$$

where

$\gamma(h) =$ *the variogram*

With the variogram defined as above, the variogram is 1/2 the variance of the differences.

Geostatistics can be applied to special cases where the intrinsic hypothesis is not valid. Of interest here is the special case where removal of drift from the raw data results in residuals which satisfy the intrinsic hypothesis (see Figure 3.5).

Every regionalized variable which is second-order stationary satisfies the intrinsic hypothesis; however, the converse is not true. If the second order stationary conditions are satisfied , then

Equation 3.15:

$$\sigma^2 = \gamma(h) + cov(h)$$

where

$\sigma^2 =$ *the population variance*

$cov(h) =$ *the classical statistics autocovariance for a lag of h*

$\gamma(h) =$ *the semivariance*

The semivariance term is often studied with the use of semivariograms (Clark, 1979; Chung, 1984; Dowd, 1984; Huijbregts, 1975; Omre, 1987). The purpose of this process known as structural analysis is to interpret the available information regarding the regionalized variable, and to determine parameters for the estimation of the variable at unknown locations.

Kriging is a minimum variance, unbiased, linear method of estimating the value of a random variable at one location using values available at surrounding locations. More complex forms of kriging will permit the estimation of values over areas or volumes. However, these methods are more applicable to mining applications and will not be addressed here.

Kriging has desirable statistical properties. It minimizes the variance of the estimate at unknown locations which is a desirable property (minimum variance). It also is unbiased, meaning that the expected value of the unknown parameter is equal to the actual value of the parameter. In addition to these desirable statistical properties, kriging has additional advantages. It is an exact interpolator (i.e., it honors the data points), and it provides an estimate of the variance or uncertainty of the estimate at any location.

The estimated value of a random variable Z(x) at the location x_o is Equation 3.16:

$$Z'(x_o) = \sum_{i=1}^{n} \lambda_i Z(x_i)$$

λ_i = weights

where for x_i, i = 1, ... n are the locations of the observed values. The weights are determined by minimizing the estimation variance Equation 3.17:

$$Var\left[Z(x_o) - \sum_{i=1}^{n} \lambda_i Z(x_i) \right] = Var[Z(x_o) - \hat{Z}(x_o)]$$

43

with the unbiasedness constraint that

Equation 3.18:

$$E[\hat{Z}(x_o)] = E[Z(x_o)] = m$$

where m is the mean value of the observations.

The constrained minimization results in a set of simultaneous equations of the form

Equation 3.19:

$$\sum_{j=1}^{n} \lambda_j C_{ij} + \mu = C_0 i$$

for i - 1,...n

Equation 3.20:

$$\sum_{i=1}^{n} \lambda_i = 1$$

where

$$C_{ij} = C|x_i - x_j|$$

and

$$C_{0i} = C|x_o - x_i|$$

The kriging variance or minimum estimation variance is

Equation 3.21:

$$\sigma_K^2 = C(0) - \mu - \sum_{i=1}^{n} \lambda_i C_{0i}$$

Using the relationship between the covariance/variogram stated above, the simultaneous equations can be re-written as:

Equation 3.22:

$$\sum_{j=1}^{n} \lambda_j \gamma_{ij} - \mu = \gamma_{0i} \qquad for \quad i = 1,...n$$

44

Equation 3.23:

$$\sum_{i=1}^{n} \lambda_i = 1$$

Equation 3.24:

$$\sigma_K^2 = \sum_{i=1}^{n} \lambda_i \gamma_0 i - \mu$$

There are two alternatives to evaluate the simultaneous equations - evaluation of either the variograms or the covariances. In mining applications the common practice is the evaluation of the semivariogram (see Figure 3.6). This process is usually greatly facilitated by the relatively dense data which is often available. Irregularly spaced data can present problems in the interpretation of the semivariograms.

Various statistical methods including jackknifing and robust statistics have been used for the purpose of estimating the variogram (Chung, 1984; Dowd, 1985; Omre, 1984). The major difficulty with the variogram approach to kriging is that it requires considerable judgement in developing and evaluating the variogram model.

The variogram can be expressed in a general form as:

Equation 3.25:

$$Var[Z(x_i) - Z(x_j)] = Var\left[\sum_{i=1}^{2} \beta_i Z(x_i)\right] \quad with \quad \beta_1 = 1, \quad \beta_2 = -1$$

Equation 3.26:

$$Var[Z(x_i) - Z(x_j)] = \sum_{i=1}^{2} \sum_{j=1}^{2} \beta_i \beta_j C(|x_i - x_j|)$$

Constant drift is filtered out in the stationary case by the first order difference, $Z(x_i)$ - $Z(x_j)$. However, in a non-stationary case, higher order differences are required to remove the drift. This approach is the method of generalized covariances proposed by Matheron (1973, 1976) and Delfiner (1976).

45

An intrinsic random function of order K is defined as a random function whose k-th order increments are second order stationary. This is expressed mathematically as:

Equation 3.27:

$$E\left[\sum_{i=1}^{m}\beta_i Z(x_i)\right] = 0$$

Equation 3.28:

$$Var\left[\sum_{i=1}^{m}\beta_i Z(x_i)\right]$$

exists and does not depend on the location of x_i.

The higher order differences filter out polynomial drifts, just as the intrinsic random function of order zero removes the constant mean.

Matheron (1973) and Delfiner (1976) express the most common form of the generalized covariances as polynomials of the general form:

Equation 3.29:

$$C(h) = b_o + \sum_{j=0}^{K}(-1)^{(j+1)}b_j + 1|h|^{(2j+1)}$$

The coefficients of the common form of the generalized covariance function are controlled such that C(h) is conditionally positive definite. The conditions for the common values of K (0 to 2) are as follows:

$K = 0$

$$C(h) = b_o - b_1|h|$$

$$b_o \geq 0, \qquad b_1 \geq 0$$

$K = 1$

$$C(h) = b_o - b_1|h| + b_2|h|^3$$

$$b_0 \geq 0, \quad b_1 \geq 0, \quad b_2 \geq 0$$

46

$$C(h) = b_o - b_1|h| + b_2|h|^3 - b_3|h|^5$$

$$b_o \geq 0, \quad b_1 \geq 0, \quad b_3 \geq 0, \quad b_2 \geq -2\sqrt{(b_1 b_3)}$$

If the estimation variance is minimized adhering to the constraint of unbiasedness, the simultaneous equations result in:

Equation 3.30:

$$\hat{Z}(x_o) = \sum_{i=1}^{n} \lambda_i Z(x_i)$$

Equation 3.31:

$$\sum_{j=1}^{n} \lambda_j C_{ij} + \sum_{k=0}^{K} \mu_k f_k(x_i) = C_{io} \quad for \quad i = 1, 2, \ldots n$$

Equation 3.32:

$$\sum_{i=1}^{n} \lambda_i f_k(x_i) = f_k(x_o) \quad for \quad k = 0, 1, \ldots K$$

Equation 3.33:

$$\sigma_K^2 = C(0) - \sum_{i=1}^{n} \lambda_i C_{io} - \sum_{k=0}^{K} \mu_k f_k(x_o)$$

where C_{ij} signifies the generalized covariance $C(|xi-xj|)$. Using the generalized covariance, the simultaneous equations no longer require an estimation of the drift, but do require the generalized covariance.

Kafritsas and Bras (1981) developed the program AKRIP (A Kriging Program) which performs point kriging using the method of generalized covariance as originally described by Matheron (1970, 1979) and Delfiner (1976). In summary AKRIP has options for the performance of the following steps to krige a set of observations:

1. Up to 15 structural models (consisting of the order of the intrinsic function and the generalized covariance) can be compared by kriging

the data using each structural model. AKRIP then ranks the models based on the relative error at each known point to select the preferred structural model.

2. AKRIP determines the coefficients of the generalized covariance model by using the results from the structural model comparison. These results are used to generate differences of order k and than the unknown coefficients are calculated by minimizing the sum of the squares of the differences between the kriging errors and the corresponding estimation variances. Iteration can be continued until the user decides whether the solution has converged.

3. Once the order of the intrinsic function and the coefficients of the generalized covariance are determined, AKRIP has an option for assessing the parameters. This is done by estimating values at each data location, subdividing the data points into two groups and determining a jackknife estimator.

Various forms of kriging have been developed to address applications with differing assumptions regarding the distribution and stationarity of the data (see Figure 3.7). For a more detailed discussion of the various kriging methods as they may be applied to surface modeling, the reader is referred to Clark (1979), Rendu (1978), Olea (1975), and Dowd (1985).

Kriging studies have been performed using numerous data sets from a wide variety of disciplines. Of interest here are two studies, one on large data sets and one on very small data sets. Davis and Culhane (1984) researched the application of kriging for contouring large data sets. The specific problem they addressed was the analysis of extremely large offshore seismic data sets. They concluded in part that large kriging systems could be solved without numerical instability if local or moving neighborhood methods were properly applied.

Of more interest to geotechnical engineering, where the data sets are usually very small, is the research by Puente and Bras (1986). They concluded that universal (linear) kriging using the program AKRIP

resulted in better estimates using small data sets than disjunctive (non-linear) kriging or local mean estimators for both stationary and non-stationary fields. Based on their analysis of predicted estimation error, Puente and Bras conclude that predicted errors should not be used in an absolute sense, but as a relative measure of spatial estimation accuracy.

3.2.6 Other Methods

In addition to trend surface analysis and kriging, discussed above, there are a variety of other methods commonly used for surface modeling based on irregularly spaced data points. These methods include cubic splines, weighted or unweighted inverse distance, inverse distance with weighted gradients, and additional forms of polygonal interpolation. Detailed discussions of these methods are presented elsewhere (Henley, 1981; Ripley, 1981; Sabin, 1985; Watson and Philip, 1984a).

3.2.7 Comparison of Surface Modeling Methods

The relative advantages/disadvantages of a surface modeling method are highly dependent on the background of the user, access to computer code and resources, and ultimate objective of the application (contouring, point estimation, etc.). Although the comparative studies have been somewhat limited, there are a number of references that have used a particular data set from Davis (1973) (Ripley, 1981; Watson, 1982; Watson and Philip, 1984a). Surface contours generated by applying a variety of techniques to the same data set are shown in Figure 3.8.

The surface models shown in Figure 3.8 have been developed using a variety of analytical methods. Selection of the "best" model is primarily personal preference. However, in geotechnical engineering practice with sparse data, it is believed that the surface model must honor the few available data points. Using this criteria, the acceptable methods shown in Figure 3.8 are the manual, inverse distance, and kriging models.

There appear to be two factions in the area of surface modeling. Those who proposed kriging methods, and those that proposed one of the other methods. The comparative studies have typically been undertaken by a member of one of the factions in an effort to substantiate their claims of a "superior" method. It appears that the two factions differ in two other regards. Those that propose kriging appear to be much more mathematically inclined and are satisfied with extremely complex mathematical methods which require considerable computer code and resources to perform. The non-kriging faction appears to be satisfied with geometry based methods which are easily implemented on the computer and require limited computer resources to perform.

3.3 Profiling/Mapping

3.3.1 Introduction

There are several analytical methods developed for a variety of other applications, which have been used for the purpose of identifying soil stratigraphy. For discussion purposes, these methods have been separated into the categories of non-spatial and spatial methods. The distinction between the groups is arbitrary; however, the inclusion or exclusion of spatial considerations is significant.

3.3.2 Non-Spatial Methods

3.3.2.1 Introduction

Non-spatial, or object-oriented, methods, which are described in this section, treat the available data as a set of individual objects each with a vector of measured attributes. The key distinction in this discussion is that the object-oriented methods do not necessarily include any consideration of the spatial relationship between the objects. Depending on the method, this lack of consideration of spatial relationships may be artificially imposed.

3.3.2.2 Clustering Techniques

Clustering is the process of assigning objects to clusters based on the similarity between objects. The clustering process may be based on divisive or agglomerative methods using multidimensional data. The applications of agglomerative clustering techniques are considerably greater than for divisive methods, and therefore, the following discussion is limited to agglomerative methods.

Agglomerative methods can be simplified into four major steps. First, calculation of a distance (similarity) matrix between the objects. Second, identification of the minimal element in the distance matrix. Third, clustering the two most similar objects or clusters and calculation of a new distance matrix. Fourth, repetition of steps two through four as necessary until all objects have been clustered.

The two most critical stages for the application of agglomerative clustering techniques are steps one and three. In step one it is necessary to quantify the similarity between the objects being considered. In step three the similarity between objects and newly formed clusters must be updated as the clustering process continues. There are documented methods for performing these two critical stages (Sneath and Sokal, 1973). The selection of the technique for a specific application is largely dependent on the judgement of the researcher.

The results of the clustering process are usually presented in the form of a dendrogram (see Figure 3.9), which is a representation of the hierarchical clustering of objects into groups. The vertical axis of the dendrogram is either distance between the objects or its inverse similarity. In clustering vernacular distance refers to the inverse of similarity, and not the Euclidean distance that first comes to mind.

The dendrogram is often referred to as a "tree" with the initial objects being the "leaves" and the connectors between groups the "branches". The

"root" is the vertex at which all the objects have been joined into a single group. The maximal distance between the root and leaf, measured in the number of vertices, is called the "height" of the tree.

If the grouping is restricted such that there are only two branches from each vertex, then the tree is called a binary tree. In most applications binary trees are used because higher order trees can usually be substituted by binary trees, and binary trees lend themselves to computer implementation (Zupan, 1982).

In a binary tree with N original objects, there are 2N-1 vertices regardless of the branching or clustering method. The maximal height of the tree is N-1. The minimum height (fully balanced tree) is the smallest integer greater than the base 2 logarithm of N (Deo, 1974).

Considering agglomerative methods, there are seven common methods for the calculation of the similarity between clusters. These methods are: single linkage, complete linkage, group average, weighted group average, centroid, median and Ward's (Zupan, 1982). The methods are presented elsewhere (Sneath and Sokal, 1973; Zupan, 1982) along with discussions of the relative merits of the techniques.

Of interest, particularly in Chapter 4, is Ward's method which is known by various other names including minimum variance, sum of squares, error sum of squares, and optimal agglomeration (Grimm, 1987). In Ward's method the central point is calculated for any possible combination of two clusters and then the total sum of squared distances from this point to all objects in the hypothetical cluster is evaluated. The association of the two clusters with the smallest sum of squares is then taken as the next cluster. In Ward's method the distance between two clusters has no geometric meaning. According to Zupan (1982), Ward's method is commonly regarded as a very efficient clustering technique although it often results in the clustering of small groups.

The majority of the applications of clustering techniques to soils data to date have dealt with the ecological characteristics of the soil (Anderson, 1971; Muir et al., 1970; Rayner, 1966). While these studies have demonstrated the application of clustering to soils data in general, they address the problem of identifying surficial soil series for agricultural/ecology purposes.

Grimm (1987) presents a method for analyzing biostratigraphic sequences using cluster techniques that are stratigraphically constrained. The specific application in the work is analysis of pollen count data using Ward's method (incremental sum of squares) to define groups. Grimm references research by Birks and Gordon (1985) regarding unconstrained clustering of data from more than one stratigraphic section to identify regional zones.

As stated previously, calculation of the similarity matrix is one of the more critical, and complicated, steps of cluster analysis. One reason for this is the variety of the data types. With respect to geotechnical data, there are three types of characters: two-state, multistate (ordered and qualitative), and quantitative. Two-state characters may be the presence or absence of a particular soil component. Characters, such as soil density based on Standard Penetration test blow counts or color, are multistate ordered and qualitative characters, respectively. Quantitative characters are typically Standard Penetration test blow counts or laboratory test values.

Quantification of the similarity between objects (soil samples) to be clustered is complicated by the three types of characters typically present in geotechnical data. There are numerous methods (Sneath and Sokal, 1973) for calculating similarity coefficients between the objects; however, many of the methods are not applicable if the character types are mixed.

Sneath and Sokal (1973) in their landmark text on numerical taxonomy state that clustering analysis should use one of the extensively used association (similarity) coefficients so that the ensuing results can be understood and reviewed by others. They recommend using one of the basic similarity coefficients in consideration of "ease of interpretation."

One of the similarity coefficients presented for review and use by Sneath and Sokal (1973) is the General Similarity Coefficient of Gower (Gower, 1971). Gower's coefficient is one similarity coefficient which is applicable to all three character types. In principle the Gower similarity coefficient is calculated between two objects by comparing the various attributes and assigning a score for the level of agreement. Then a weighted average of the various scores is calculated by summing the product of the scores and weights for each attribute and dividing by the sum of the weights.

Mathematically, the Gower Similarity Coefficient is calculated between objects j and k by assigning a score, $0 \leq s_{ijk} \leq 1$, and a weight w_{ijk} for the attribute i. The coefficient is then defined as

Equation 3.34:

$$S_G = \frac{\sum_{i=1}^{n} w_{ijk} s_{ijk}}{\sum_{i=1}^{n} w_{ijk}}$$

Typically the weight w_{ijk} is set to 1 when the comparison is considered valid for the two objects and 0 when the comparison is inappropriate regardless of the character type. The score is dependent on the type of characters being compared. Usually s_{ijk} is set to 1 for a match between two-state characters and 0 if there is no match. The same process is typically used for multistate characters, and no consideration is given to the number of possible matches due to the multistates. With quantita-

tive characters it is normal practice to weight the score by dividing the
difference between the two observations being compared by the observed
range.

Gower's coefficient has been used in a variety of studies including two
studies on soils (Rayner, 1965 and 1966).

According to Sneath and Sokal (1973) there have been repeated attempts by
various researchers to define a probabilistic similarity index. One of
the other coefficients discussed by Sneath and Sokal is a probability
based coefficient proposed by Goodall (1966). In principle, Goodall's
probabilistic similarity index computes the cumulative probability that a
pair of objects will be as similar or more similar than can be empiri-
cally ascertained for each attribute on the basis of the observed distri-
bution of the attributes in the total set of objects. Sneath and Sokal
(1973) indicate serious reservations with the Goodall probabilistic
similarity index since it gives a greater weight to the rarer occur-
rences, a contradiction with the basic principles of phenetic (overall)
similarity to use unequal weights for the attributes.

3.3.3 Spatial Methods

3.3.3.1 Introduction

Spatial methods discussed in this section include methods which
inherently treat the objects (samples) with consideration of spatial
relationships with other objects. Most of these methods, including
regional merging which is discussed below, have been developed in the
study of pattern recognition and image processing/enhancement as applied
to the general problem of scene analysis (Duda and Hart, 1973; Pavlidis,
1977).

Scene analysis is the process of using the information available at the
pixel level to identify objects, boundaries or shapes in the scene. The

available information at the pixel level may be the result of remote observations, such as satellite observations. Therefore, the information is often incomplete or in the vernacular of scene analysis "fuzzy".

By its nature, scene analysis is limited to dealing with two dimensional pictures. In most applications scene analysis is also limited to a single observation at each location or pixel. This observation may be color, but in most research the more general problem observation of shade of grey (often referred to as brightness) is addressed.

Scene analysis is accomplished by a variety of techniques including splitting/merging regions based on some form of "average" shade of grey for the regions. Since the problem of soil stratigraphy is mainly one of joining regions to identify natural strata, the following section presents a discussion of the process of regional merging.

3.3.3.2 Nearest Neighbor (Switzer Model)

Switzer (1965, 1967) performed research on the problem of using discrete, irregularly spaced data to estimate the state of unsampled points. The research was limited to two color mapping in two dimensions.

Simply stated Switzer's model assumes that points close to observed data points (nearest neighbors) tend to be of the same class as the observation. Points further away from a known data point will be less likely to be of the same class as the observed point.

Switzer's model is for two class (i and j), isotropic, two dimensional maps. For an existing two color map the major class i and the minor class j are defined as follows:

Equation 3.35:

$$p_i = A_i / A$$

Equation 3.36:

$$p_j = A_j / A$$

56

Equation 3.37:

$$A_i + A_j = A$$

Equation 3.38:

$$p_i + p_j = 1$$

where A_i is the area belonging to class i, A_j is the area belonging to class j, and A is the total area of the map.

If a two color map is sampled at discrete locations, the probability of any point being of the same class (i) decreases asymptotically to the global frequency p_i as the distance from the known data point of class i increases. Switzer (1967) suggested that the decay function is of the form:

Equation 3.39:

$$p_{ii} = p_i + (1 - p_i)e^{(-\gamma r)}$$

Equation 3.40:

$$p_{ij} = p_j(1 - e^{(-\gamma r)})$$

$\gamma =$ *the decay parameter,*

where p_{ii} is the probability of both the known point and a point at distance r belonging to class i; and p_{ij} is the probability that the point at distance r is in class j while the known data point is in class i.

The relationships can be extended to:

Equation 3.41:

$$p_{jj} = p_j + (1 - p_j)e^{(-\gamma r)}$$

Equation 3.42:

$$p_{ij} = p_i(1 - e^{(-\gamma r)})$$

Equation 3.43:

$$p_{ii} + p_{ij} = 1$$

Equation 3.44:

$$p_{jj} + p_{ij} = 1$$

Figure 3.10 shows the relationships of the decay functions and demonstrates that p_{ii} and p_{ji}, as well as p_{jj} and p_{ij} are non-intersecting functions. Since $p_i > p_j$, p_{jj} and p_{ji} intersect at probability - 0.5 where r - r_c. Therefore, at distances greater than r_c from a known point belonging to class j, the probability of an unknown point belonging to the major class i is greater than the probability of belonging to the minor class j.

The rate of decay in the Switzer model is governed by the value of the decay parameter. The work by Nucci (1979) described in more detail below confirmed the visual properties of the effects of the decay parameter on isotropic maps. If the areas of a class are small, the decay parameter will be smaller since the extrapolation distance is less. Irregular or convoluted boundaries should also tend to reduce the value of the decay parameter, as well, for the same reason.

The Switzer model is based on isotropic conditions (i.e., the decay function is independent of direction). Schematic examples of an isotropic map and trending map were given by Nucci (1979) (see Figure 3.11). According to the Switzer model, the shapes of the two classes should be isotropic and therefore, the decay parameter will be isotropic. However, in a trending map the extrapolation distance will be greater in the direction of the trend and consequently the decay parameter will be anisotropic.

In the applied studies of the Switzer model performed by Nucci (1979) and Lee (1982) the maps chosen for study were selected to generally satisfy the isotropy assumption.

Baecher (1972) describes two methods (direct and indirect) for evaluating the decay parameter for known maps. The direct method requires knowledge of the entire "true" map; while the indirect method requires knowledge of a finite number of data points.

In the direct method selected sampling locations are chosen and a series of concentric circles is constructed centered on the sampling point (see Figure 3.12). A frequency diagram of the percentage of the circle perimeter belonging to class i and j is plotted versus the circle radius (see Figure 3.13). The value of the decay parameter can then be estimated using nonlinear regression techniques and the appropriate equation for P_{ii}, P_{ij}, P_{jj}, or p_{ji}. The value of the decay parameter should be independent of the value of r.

The accuracy of the direct method estimate of the decay parameter can be improved by increasing the number of circle centers used and by increasing the radii by smaller increments.

The indirect method of estimating the decay parameter, described by Baecher (1972) and Nucci (1979), is based on statistical estimation based on a finite number of observed points. The indirect method consists of calculating the distance between all the known data pairs and classifying the pairs into one of three groups (ii, jj, or either ij or ji). Plots similar to Figure 3.8 can then be constructed and the decay parameter can be estimated using non-linear regression analysis.

Nucci (1979) studied the application of the Switzer model to two color, isotropic geology maps to evaluate the ability of the model to predict known "true" maps using discrete sample points. The influence of the sampling pattern and density on the resulting error between the predicted map and the known "true" map was also evaluated.

Nucci's analysis included evaluating eight separate "true" maps using six different square grids and five random sampling patterns of varying sampling densities.. All of the analysis was the indirect method except for a single direct method evaluation of one map.

Nucci's conclusions are summarized as follows:

1. A better approximation of the true maps is achieved if the decay function is a first order function of r rather than r^2.

2. The single map comparison of the decay parameter estimated by direct and indirect methods was 11.76 ± 3.93 (90% confidence limits) and 10.68 ± 2.76, respectively.

3. If fewer than 50 data points are used to estimate a map, 20 to 30% of the area may be misclassified. The accuracy of the estimated map can be improved by increasing the number of data points used for the analysis; however, the marginal improvement decreases as the number of points increases.

4. The Switzer model provides a reasonable estimate of the error in an inferred map. Typically the model over estimated the error. The overestimation was attributed to data scatter, model variance, and uncertainty in the decay parameter.

Lee (1982) applied the Switzer model to the prediction of states at unobserved points along a line of known state and between two parallel lines of known states. Lee used several of the same maps as Nucci (1979). Lee concluded that the line-pair applications resulted in more accurate predicted maps than the methods used by Nucci, and that the actual error, which was typically less than 10%, was lower in small or convoluted regions.

Another application involving the Switzer mode was performed by Solow (1986) following the application of the kriging algorithm to indicator data by Switzer (1976). Solow used simple indicator kriging (classification into binary states) on isotropic binary maps with stationarity. According to Solow, the benefit of the indicator kriging is that it allows the estimated probability at an unmeasured location to be based on samples of $n > 2$, which presents problems with estimating the misclassification probability and with the combination of $n > 2$ samples when using models similar to the Switzer model. Solow's study was based on the analysis of parametric (known distribution) random fields.

3.3.3.3 Cross-Correlation and Cross-Association

Cross-correlation is a process of comparing a time series to itself while incrementing the shift distance between the two. The process is described by Davis (1973). Cross-correlation was a predecessor in terms of geology applications to cross-association.

Cross-association as applied to geology problems is the comparison of two series of states (mutually exclusive, and incapable of meaningful ranking), such as the lithographic states identified in two boreholes. The process consists of shifting the one sequence past the other and measuring the degree of agreement between the two series. The results of cross-association are typically calculated as the ratio of number of matches to number of comparisons for a range of match positions.

According to Davis (1986), the early statistical geology literature is full of applications of cross-correlation (eg, Matuszak (1972)). However, Davis states that since the process of cross-correlation assumes that the sampling is uniformly spaced with respect to time, applications using cross-correlation procedures are valid only under special conditions, such as with varved deposits.

Applications of cross-association techniques to geologic data include Sackin, Sneath, and Merriam (1965); Harbaugh and Merriam (1968); Merriam (1971); and Davis (1973, 1986).

3.3.3.4 Dynamic Programming

Considerable proprietary research has been performed in the area of stratigraphy assessment by mineral and oil exploration companies. Due to the highly competitive nature of resource evaluation, this work is essentially unreported in the open literature.

Before discussing several of the more recent publications in the area of stratigraphic correlation, it is important to point out some of the differences between stratigraphic studies in resource exploration and geotechnical engineering. In resource exploration, the potential cost

benefit is a real incentive for the application of sophisticated and expensive testing in boreholes that are often very deep and expensive to drill offshore. This testing is typically continuous downhole testing using a variety of geophysical techniques simultaneously. In comparison to the high cost of drilling the borehole, the cost of the downhole testing is relatively small.

By comparison, in geotechnical engineering applications, which are the subject of this research, the boreholes are typically relatively inexpensive when compared to the structure. Also, the testing in the boreholes is limited to non-continuous empirical type testing (i.e., Standard Penetration tests on five foot spacings) in many applications.

As a result of these differences, the methods developed for resource exploration, such as dynamic programming, are not readily or practically adaptable to geotechnical engineering.

Howell (1983) and Waterman and Raymond (1987) present research on the problem of stratigraphic correlation of borehole data using dynamic programming methods. The advantage of the dynamic programming methods over previous works using cross-association were that the methods could handle "gaps" in the correlated sections. Both papers deal with correlation of stratigraphy in sedimentary rock, typical of the conditions encountered in oil and gas exploration.

3.3.3.5 Stratigraphic Models

Jones et al. (1986) present a very thorough discussion of contouring geologic surfaces with the ultimate goal of developing stratigraphic models for use in oil exploration. Their recommended approach for the analysis of rock stratigraphy consists of geologic interpretation of the available data followed by the identification of conformable surfaces. These surfaces are then modeled using conventional contouring techniques such as those described in Section 3.2. Truncated or baselap surfaces are then modeled by adding or subtracting stratum thickness from the respective adjacent conformable surface.

Since the methods proposed by Jones et al. (1986) are based on globally conformable surfaces, the methods may be more properly applied to oil exploration, which is the specific problem that they have researched, than the assessment of soil stratigraphy in geotechnical engineering.

3.3.3.6 Regional Merging

Simply stated regional merging is the process of joining adjacent regions into a single combined region based on an arbitrarily determined criteria such that the uniformity of the newly formed region satisfies the objectives of the process. It is important to note that the regions must be adjacent (i.e., share a common boundary) in order to even be considered for merging.

The criteria for decisions concerning merging are referred to as uniformity predicates. Pavlidis (1977) defines the uniformity predicate as:

Let X denote the grid of sample points of a picture, i.e., the set of pairs

$$(i,j) \quad i = 1, 2, \ldots N , j = 1, 2, \ldots M$$

Let Y be a subset of X containing at least two points. Then a uniformity predicate $P(Y)$ is one which assigns the value true or false to Y, depending only on the properties of the brightness matrix $f(i,j)$ for the points of Y. Furthermore, P has the property that if Z is a non-empty subset of Y then $P(Y)$ = true implies always $P(Z)$ = true.

Erikson (1985) researched methods for determining soil profiles. Included in his work was a study of the application of regional merging techniques to the problem of identifying soil stratigraphy. Specifically, Erikson used a search process to identify reciprocating optimality between regions before merging decisions were made based on the difference between average properties of the regions and the possible merged region. The method was applied to two case histories to develop

63

soil profiles based on single attribute data vectors (shear strength and Standard Penetration test blow count data). The issue of multidimensional data or non-quantitative data was not addressed.

3.3.3.7 Probabilistic Relaxation

Digital image processing techniques have been the subject of intense research during the 1970's and 1980's. In many cases the objective of the techniques is to take a "fuzzy" or low quality image and improve the image using numerical techniques including segmentation, pattern recognition, and other techniques. One area of research has been image enhancement, where numerical techniques are used to improve the "quality" of an image through iterative processes.

Probabilistic relaxation (Rosenfeld and Kak, 1982) is an iterative process of calculating successive estimates of the probability of n objects belonging to m classes with the assignments being interdependent. The compatibility matrix c(i,j;h,k) is a measure of the compatibility of object i belonging to class j and object h belonging to class k.

The process of probabilistic relaxation is summarized as follows:

1. An initial estimate of the probability of each of the n objects belonging to each of the m classes is determined. Each of the prior probabilities must be less than or equal to 1.0 and greater than or equal to 0.0, and the sum of the prior probabilities for each object belonging to the m classes must total 1.0.

For objects (A's):

$$A_1, A_2, \ldots, A_n$$

For classes (C's):

$$C_1, C_2, \ldots, C_m$$

$$P_{ij}^{(0)}$$

is the initial probability that

64

$$P(A_i \in C_j)$$

where

$$1 \le i \le n \qquad 1 \le j \le m$$

for each i

$$0 \le P_{ij}^{(0)} \le 1$$

and

$$\sum_{j=1}^{m} P_{ij}^{(0)} = 1$$

2. The compatibility matrix c(i,j;h,k) is developed for the neighboring cells (maximum of eight for the two dimensional problem common to image enhancement) surrounding any cell. The value of c(i,j;h,k) is limited to the range -1 to +1. Incompatibility is indicated by a low value (-1) and compatibility by high values (+1). Neutrality is indicated by a value of 0.0 .

3. The increment q_{ij} is defined as follows:

Equation 3.45:

$$q_{ij} = 1/(n-1) \sum_{h=1, h \neq i}^{n} \left(\sum_{k=1}^{m} c(i,j;h,k) P_{hk} \right)$$

such that

$$-1 \le q_{ij} \le +1$$

4. By applying the increment to the current estimate of p_{ij}, revised probabilities are estimated:

Equation 3.46:

$$P_{ij}^{(r+1)} = P_{ij}^{(r)} \cdot (1 + q_{ij}^{(r)}) / \sum_{j=1}^{m} (P_{ij}^{(r)} \cdot (1 + q_{ij}^{(r)}))$$

where

$$q_{ij}^{(r)}$$

65

is defined in 2 above.

Note that prior probabilities of 0 and 1 will not be changed by any iterations.

Rosenfeld and Kak (1982) outlined several analytical methods to define the compatibility matrix $c(i,j;h,k)$. However, they also indicate that the coefficients of the compatibility matrix can be assigned arbitrarily or by measuring the individual and joint frequencies of the events A_i belonging in C_j in a single picture.

Rosenfeld and Kak (1982) address performance evaluation as follows:

"Ideally, we would like a probability adjustment scheme of (probabilistic relaxation) to exhibit the following type of behavior; During the first few iterations, appreciable changes in the estimates should occur, as 'noisy' initial estimates are brought in line with the concensus of evidence from their neighbors. Once this has happened, there should be little further change; the estimates should be relatively stable. We would also expect these 'final' estimates to be less ambiguous than the initial ones.

Quantitatively, we expect the sum of absolute probability differences

Equation 3.47:

$$\sum_{i,j} \left| p_{ij}^{(r)} - p_{ij}^{(r+1)} \right|$$

to become small after a few iterations. At the same time, the final probabilities should not be too far away, on the average, from the initial ones; we would not be satisfied with the process if it converged to an arbitrary set of final probabilities unrelated to the initial ones. Thus

66

Equation 3.48:

$$\sum_{i,j} \left| p_{ij}^{(r)} - p_{ij}^{(0)} \right|$$

should not become very large. In addition we expect the entropy of our probabilistic classification to decrease; in other words, we expect

Equation 3.49:

$$-\sum_{i,j} p_{ij}^{(r)} \cdot \ln p_{ij}^{(r)}$$

to be smaller than

Equation 3.50:

$$-\sum_{i,j} p_{ij}^{(0)} \cdot \ln p_{ij}^{(0)}$$

Rosenfeld and Kak also indicated that it is customary to use only the eight adjacent neighbors when evaluating the revised probabilities for a given cell. They also state that typically the maximum number of iterations is ten or less.

3.4 Summary

The literature review in this chapter presents a variety of analytical techniques which will be referenced in Chapters 4, 5 and 6 describing this research. Specific discussion of the previous research by others will be included where appropriate in those chapters.
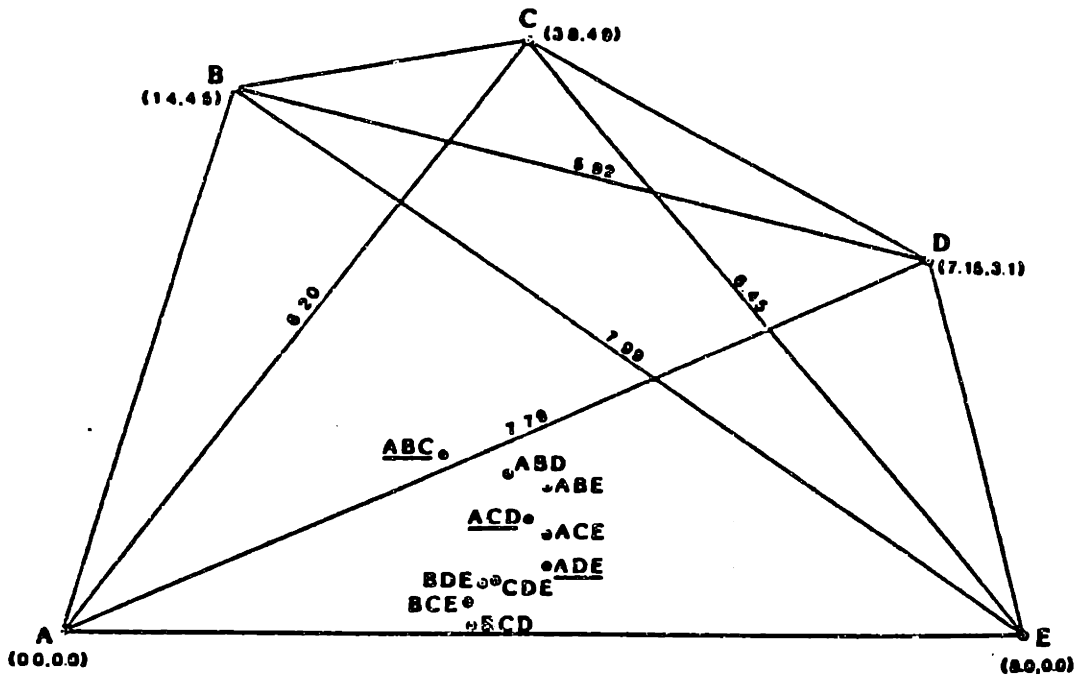
Figure 3.1 - Optimal, Delaunay, and Greedy Triangulation of a Small Data
Set (Watson and Philip, 1984b): Optimal triangulation
(ABC/ACE/CDE), Delaunay triangulation (ACD/ABC/ADE), and
Greedy triangulation (BCD/ABD/ADE). (Interior points indi-
cate center of circumcircles.)
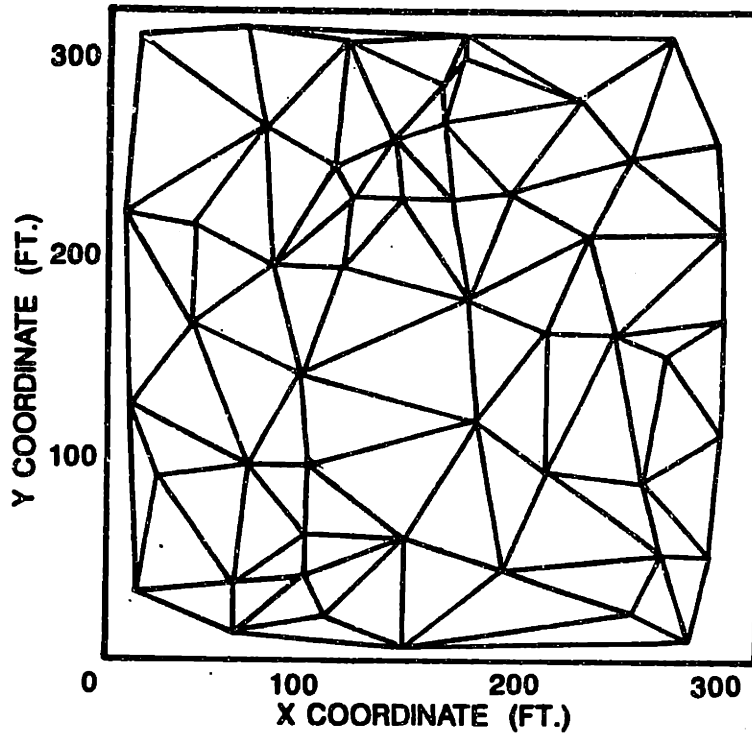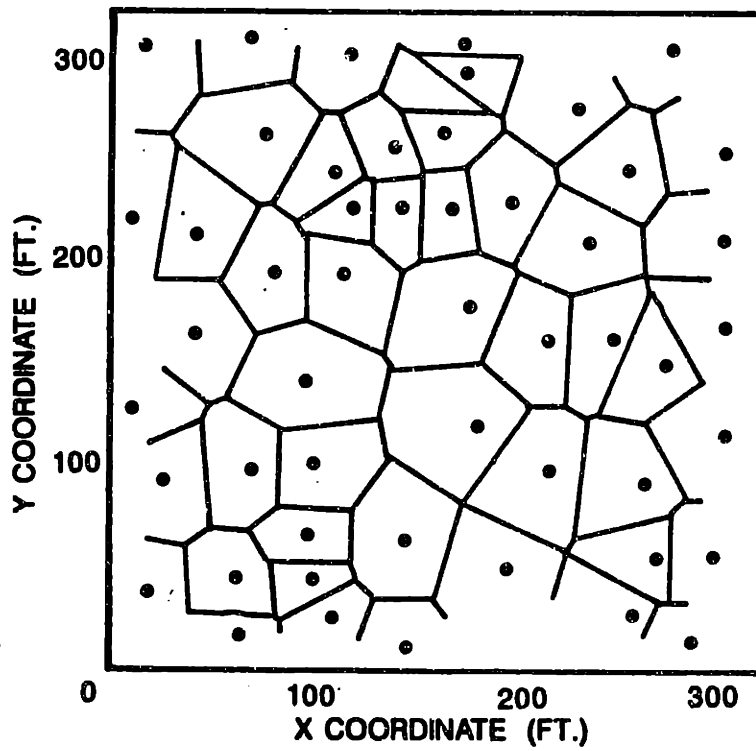
Figure 3.2 - Delaunay Triangulation (a) and Voronoi (Dirichlet) Polygons
(b) of Davis (1973, Table 6.4) Data Set (Watson and Philip,
1984b).

69
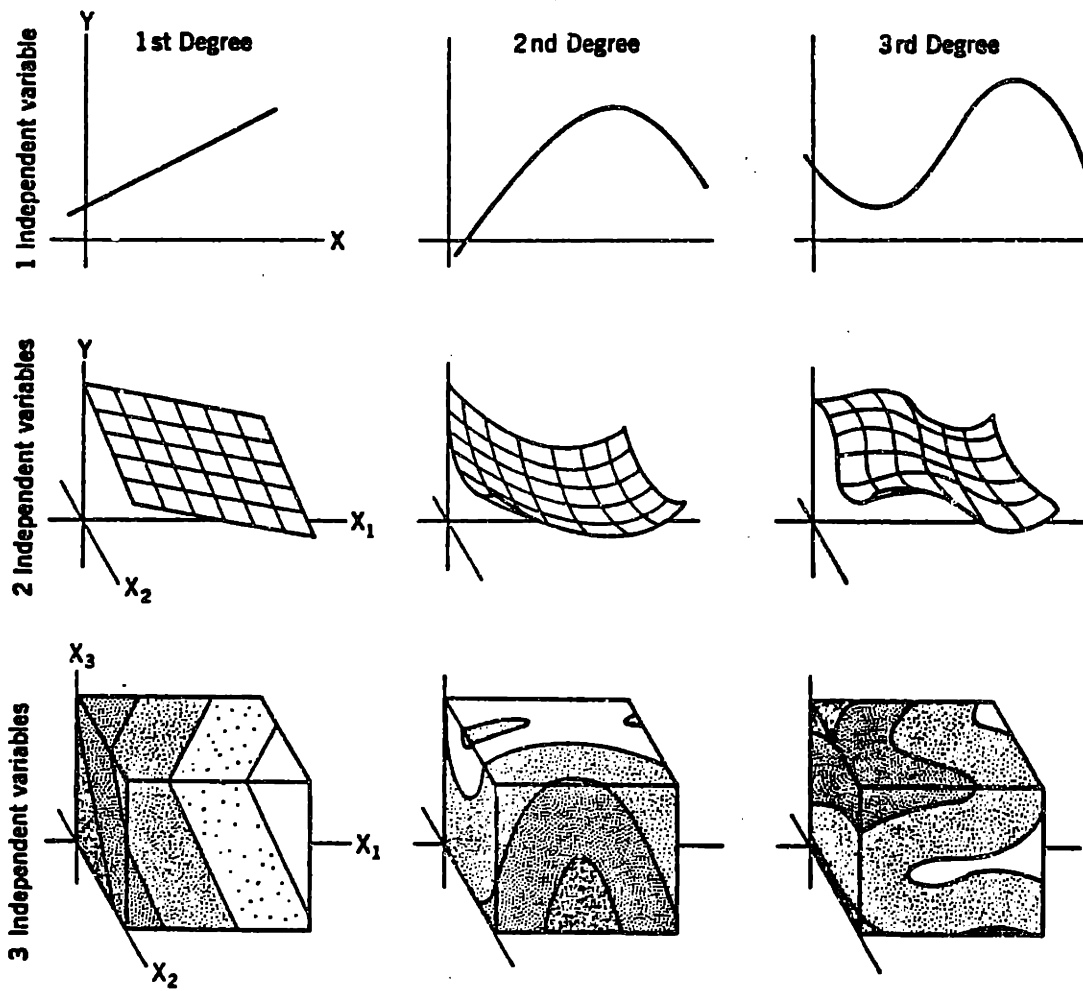
Figure 3.3 - General Shapes of Functions of One to Three Independent
Variables for First through Third Degree Polynomial Expres-
sions (Davis, 1986).
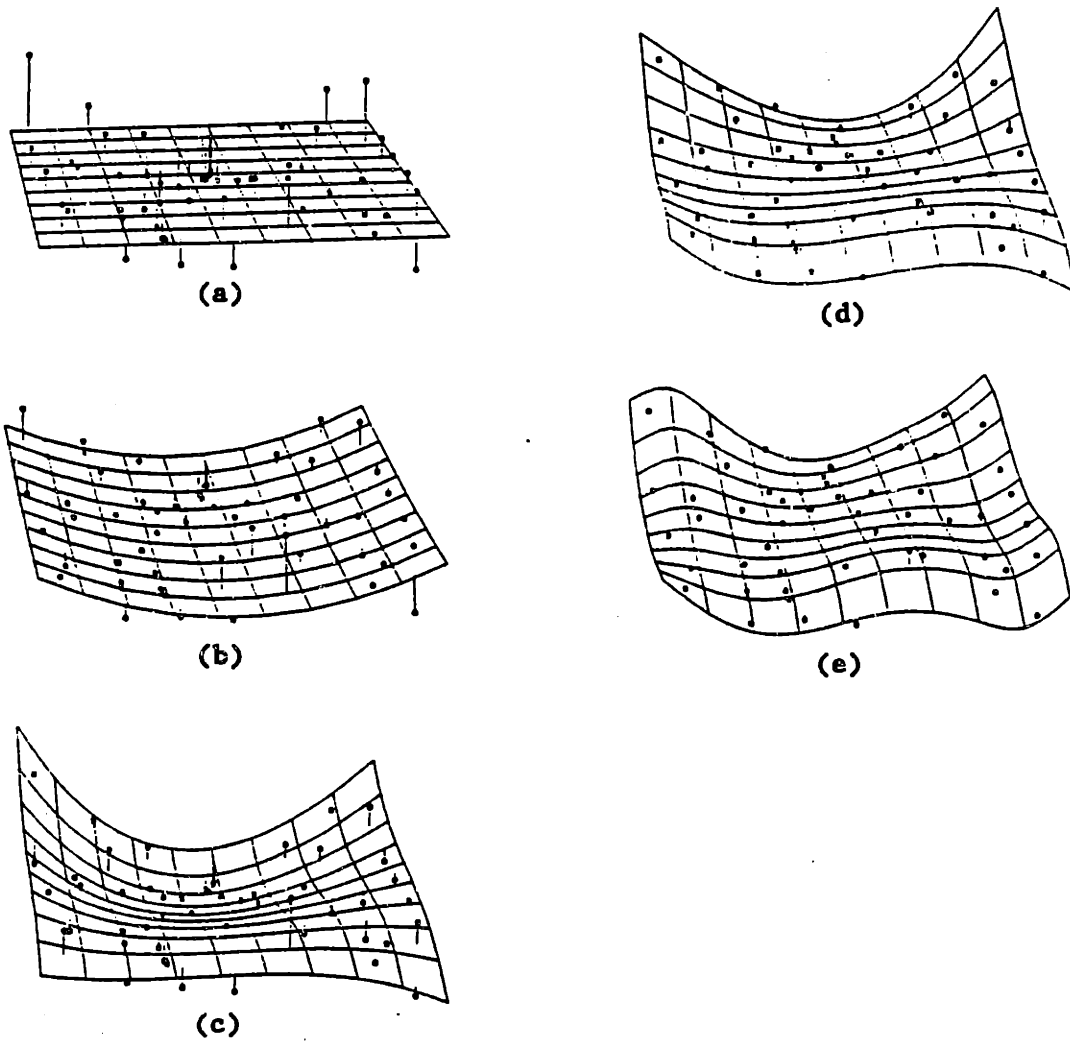
Figure 3.4 - Trend Surfaces of Polynomials of Degrees One (a) through
Five (e) for Data Set from Davis (1973, Table 6.4) (Ripley,
1981).
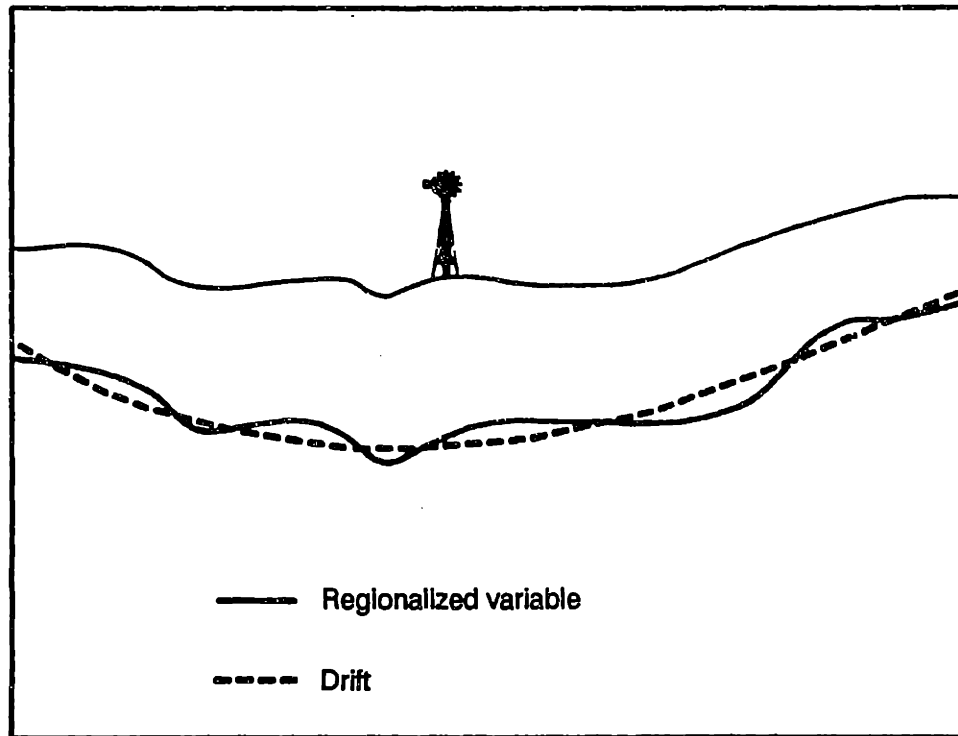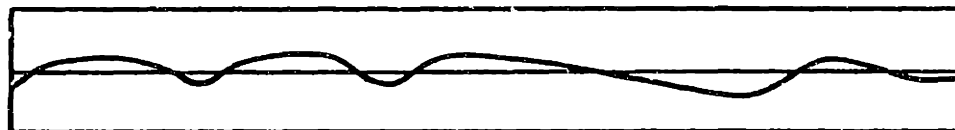
Figure 3.5 - Basic Elements in the Theory of Regionalized Variables: a)
Regionalized variable and the drift, b) Residual after
removal of the drift (Olea, 1984).

72

SPHERICAL MODEL

$$\gamma(h) = \sigma_0^2 \left(3\frac{h}{2a} - \frac{h^3}{2a^3} \right)$$

EXPONENTIAL MODEL

$$\gamma(h) = \sigma_0^2 \left(1 - e^{-\frac{h}{c}} \right)$$

LINEAR MODEL

$$\gamma(h) = ph^\lambda$$

p = slope of line
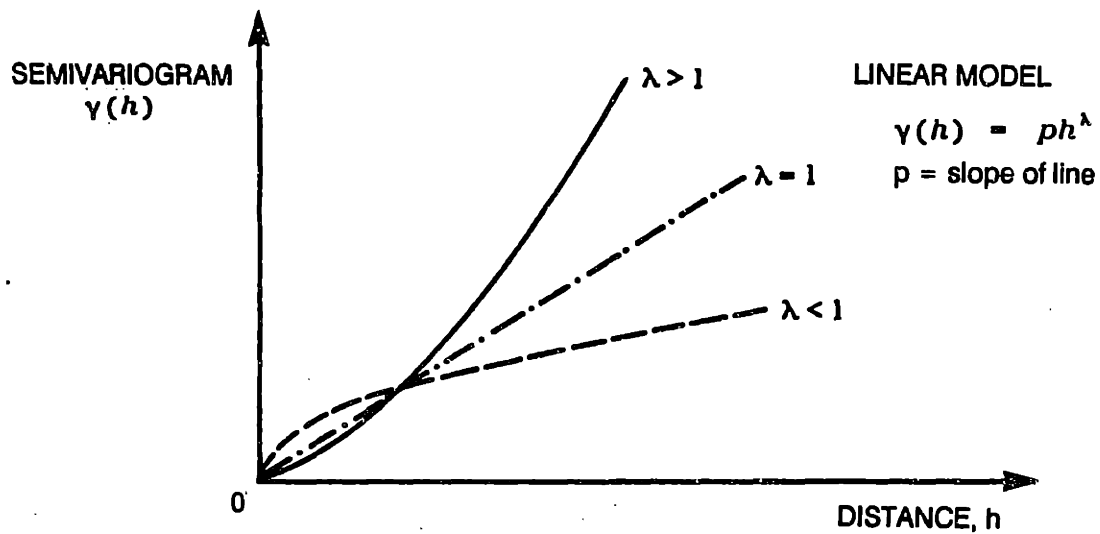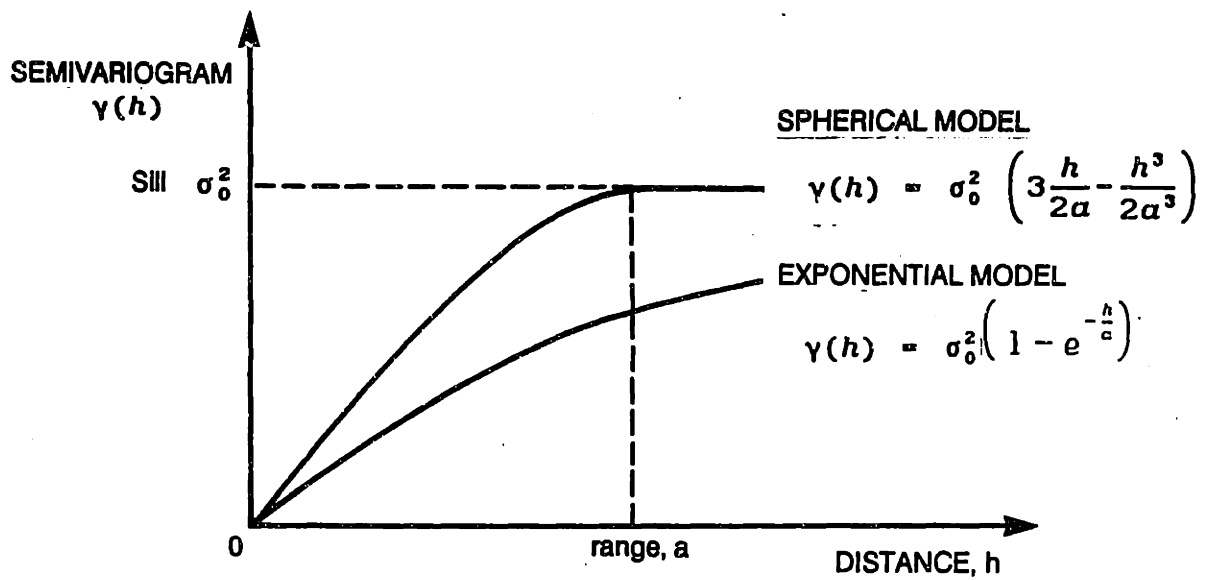
Figure 3.6 - Examples of Variogram Models (after Clark, 1979).

	Stationary	Simple drift	Local trends	Severe anisotropy
Complex	Disjunctive kriging		?	?
Simple known (e.g. lognormal)	Lognormal kriging	?	?	?
Normal	Simple kriging (point or block)	Universal kriging	Generalised covariances	?

DISTRIBUTION (vertical axis) — STATIONARITY (horizontal axis)

Figure 3.7 - Kriging Methods Available When Stationarity Assumptions or Distribution Assumptions Are Not Satisfied (Henley, 1981).
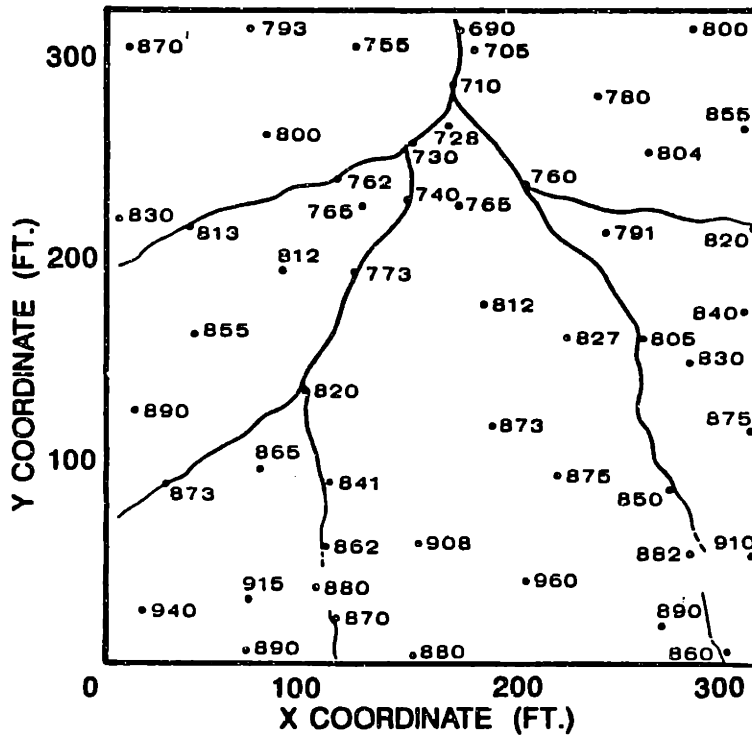
(a) Initial Data - Elevations in ft. (Davis, 1986).
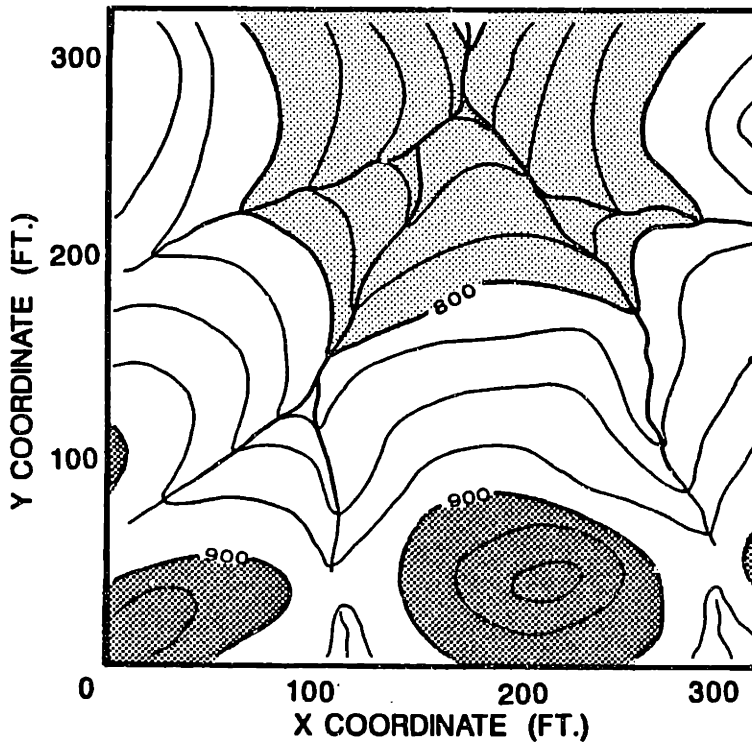
(b) Manual Contouring - Note inferred effect of streams on the form of the contour lines and smooth, equal spaced contours (after Davis, 1986).

Figure 3.8 - Surface Models of the Davis Data Set (1973, Table 6.4).
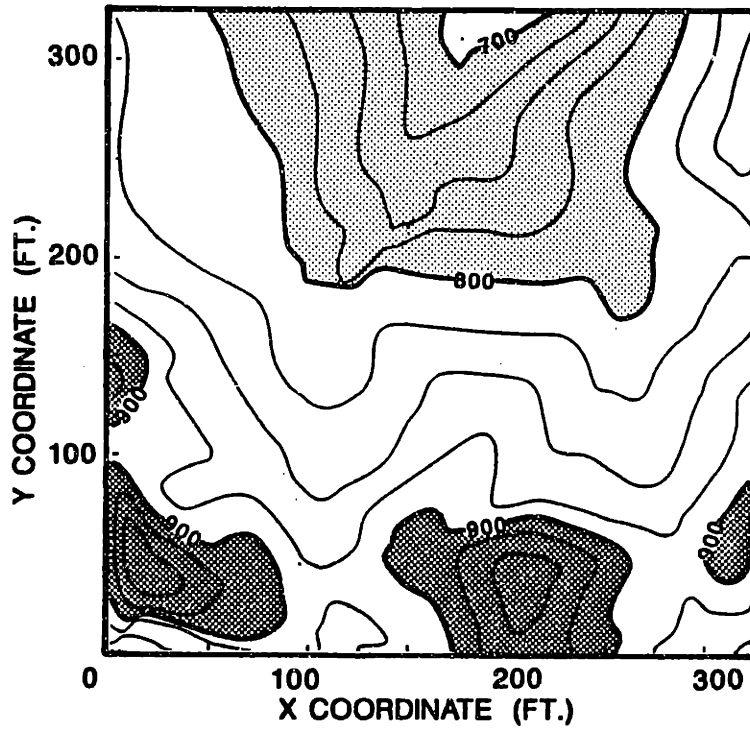
(c) Triangular Mesh Contour (McCullagh, 1981) - Note irregularly shaped contours (after Davis, 1986).
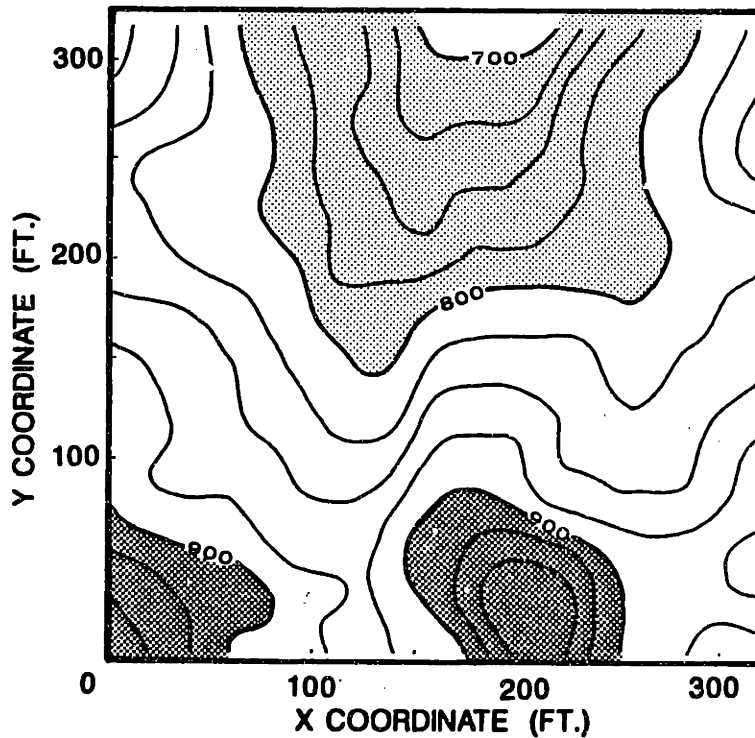
(d) Regular Grid Based on Inverse Distance Squared Contours - Used 16 nearest points in calculations. Note lack of similarity to (h). (after Davis, 1986).

Figure 3.8 Continued.

76
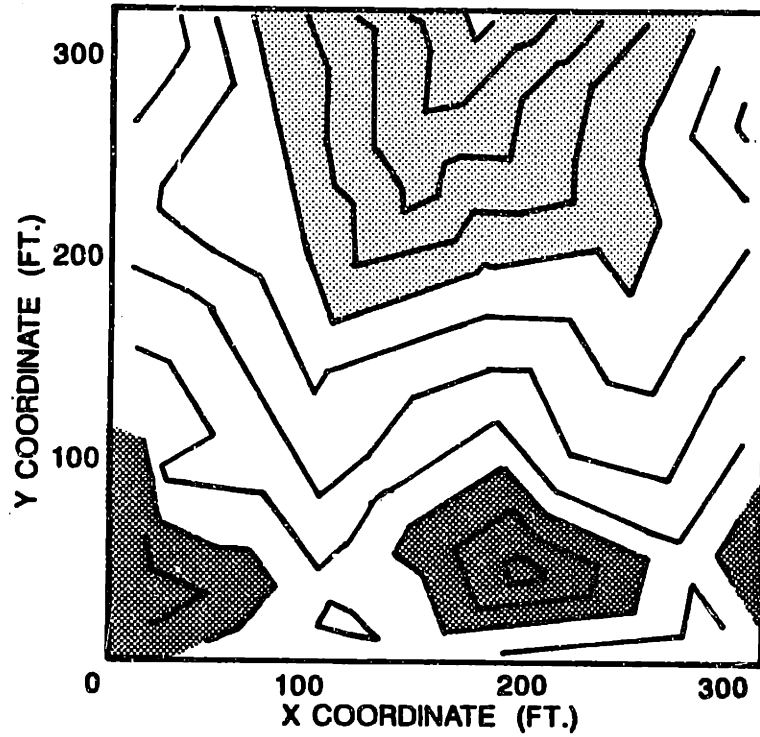
(e) Linear Interpolation Contours - Note angular lines (after Watson and Philip, 1984a).
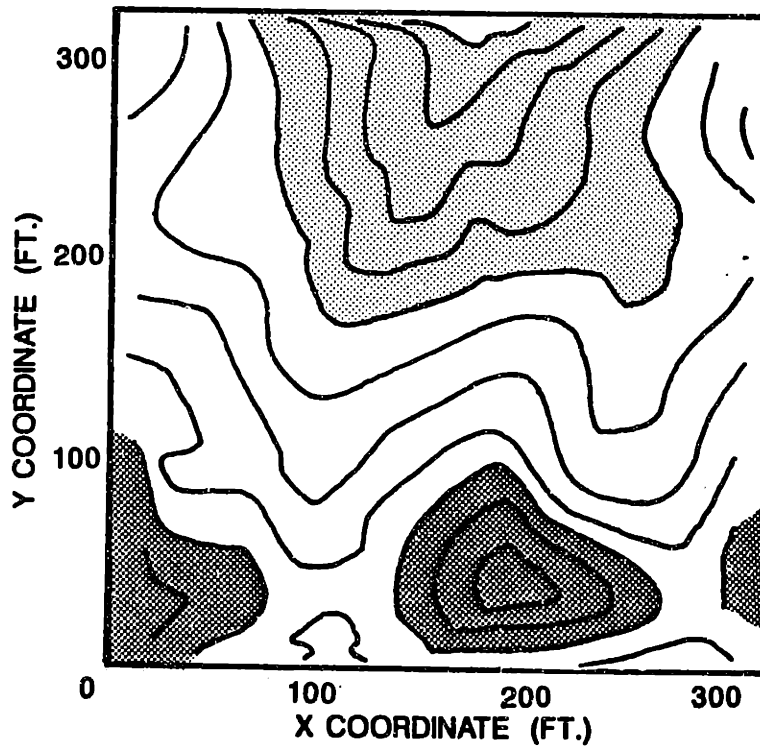
(f) Curvilinear Interpolation Contours - Note similarity to (e) with smoother contours (after Watson and Philip, 1984a).

Figure 3.8 Continued.
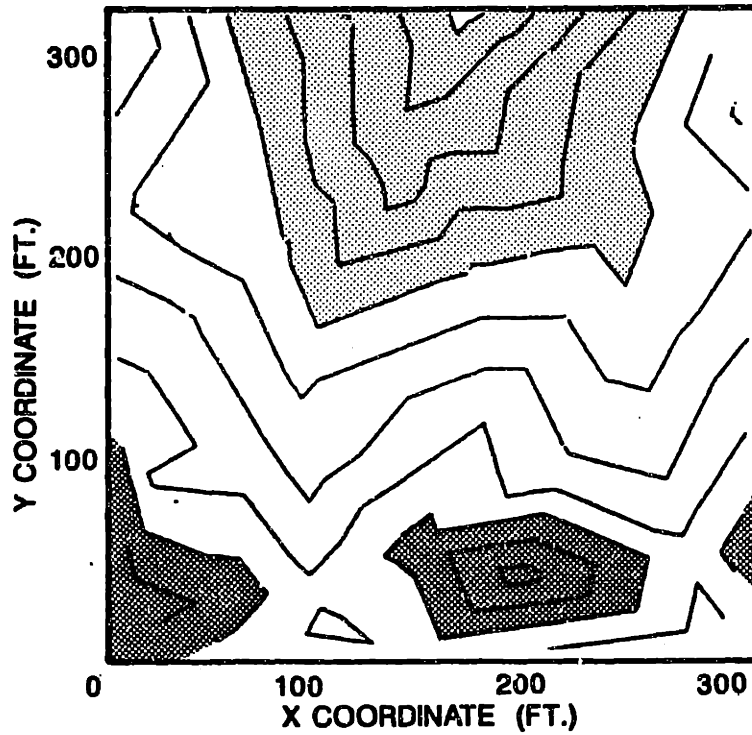
(g) Delaunay Triangulation Contours - Note angular contour lines and similarity to (e) (after Watson, 1982).
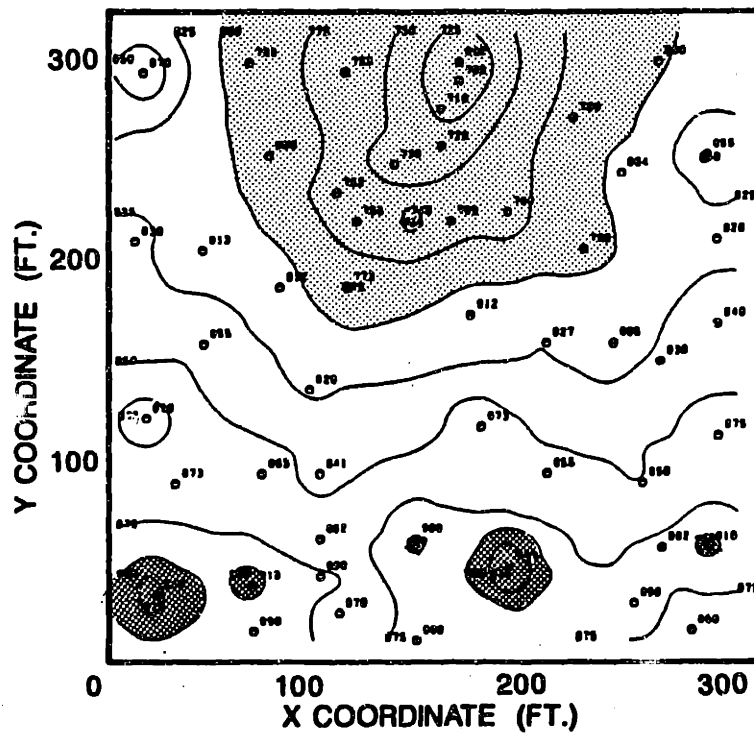
(h) Inverse Distance Squared Contours - Note lack of similarity to (d) (after Ripley, 1981).

Figure 3.8 Continued.

78
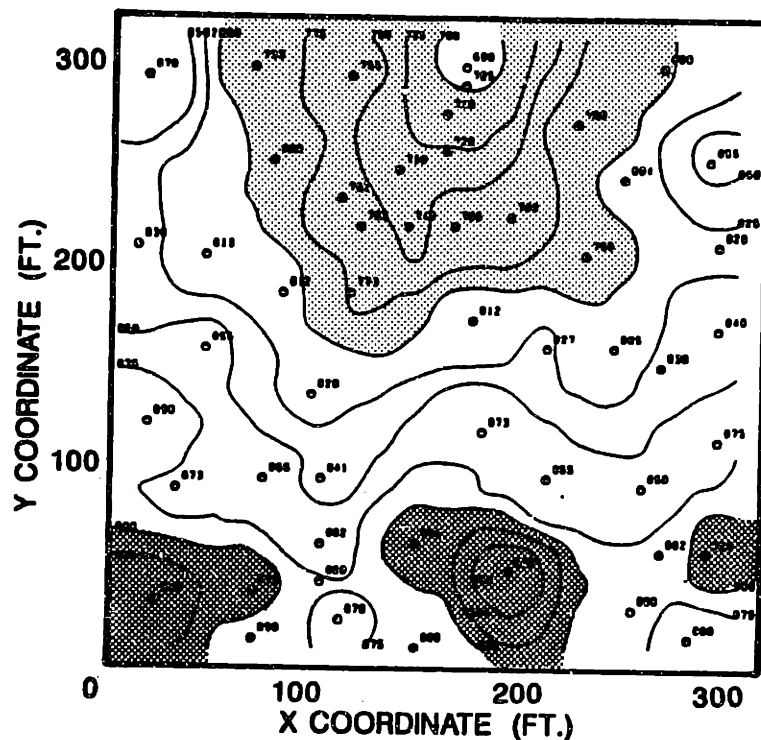
(i) Inverse Distance to the Fourth Power Contours - Note general similarity to (b) (after Ripley, 1981).
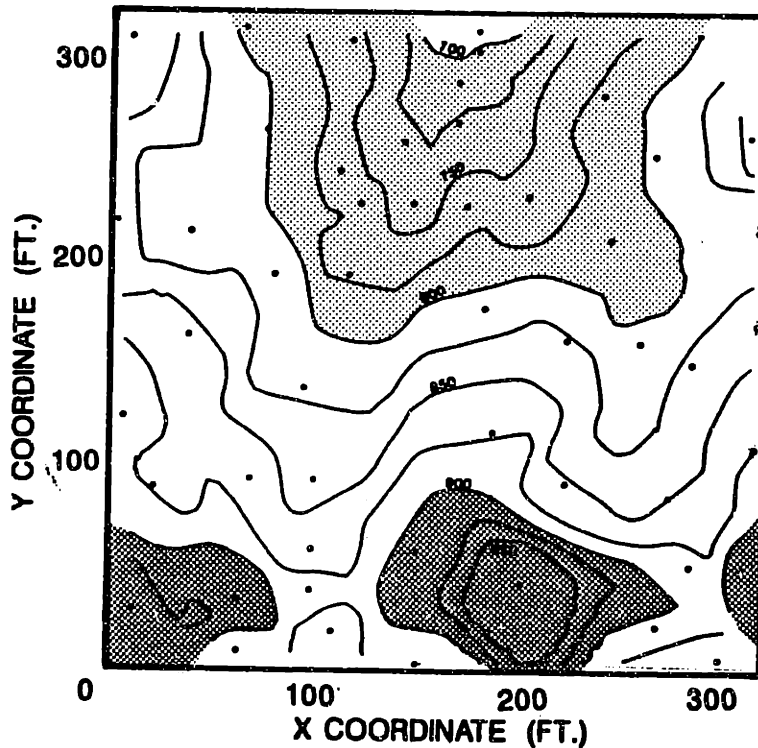
(j) Inverse Distance Weighted Gradient Contours - Interpolation based on the gradient of the Delaunay triangles (after Watson and Philip, 1985).

Figure 3.8 Continued.
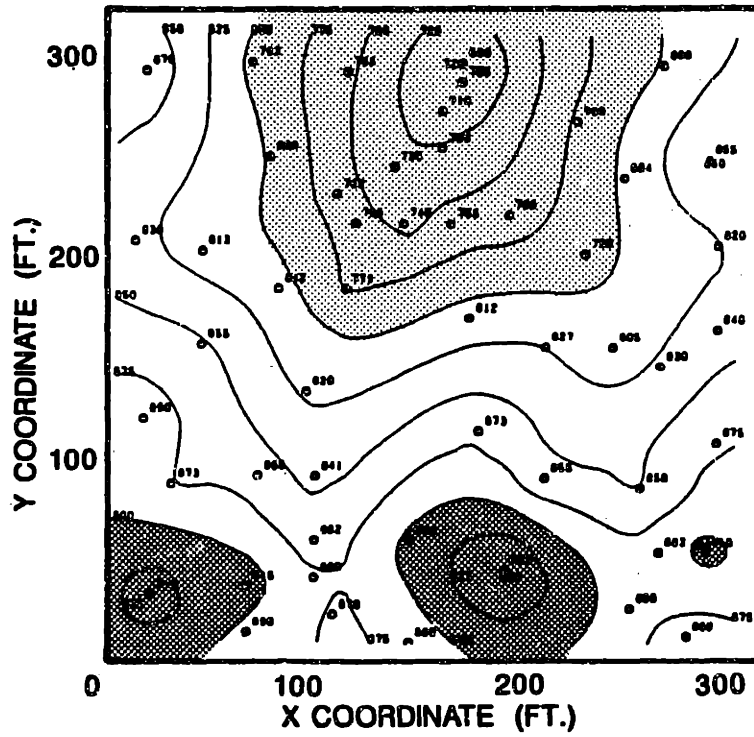
(k) Kriging Estimate Contours - Exponential model of covariance with r_o = 2 (after Ripley, 1981).
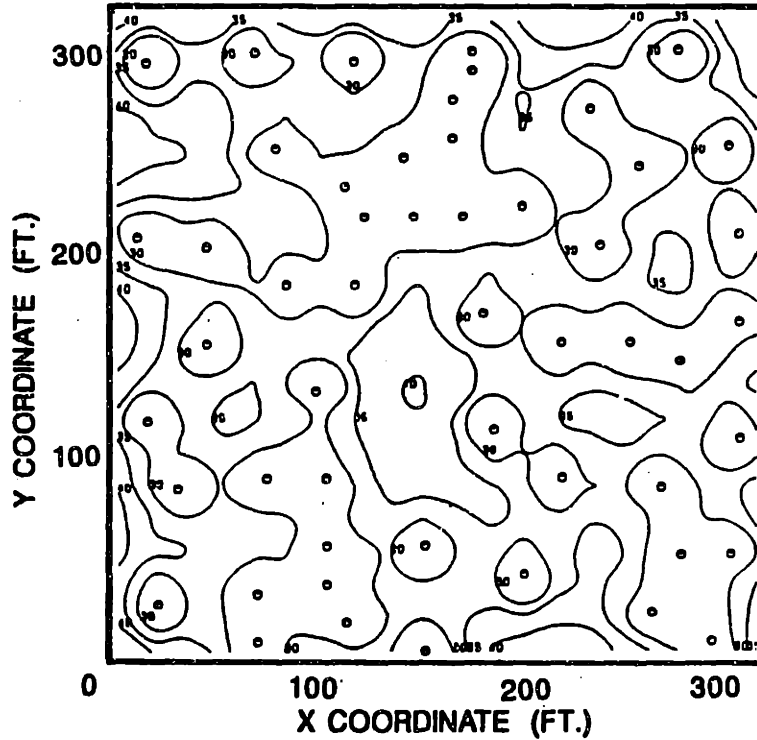
(l) Standard Deviation of Prediction Error in (k) (Ripley, 1981).

Figure 3.8 Continued.
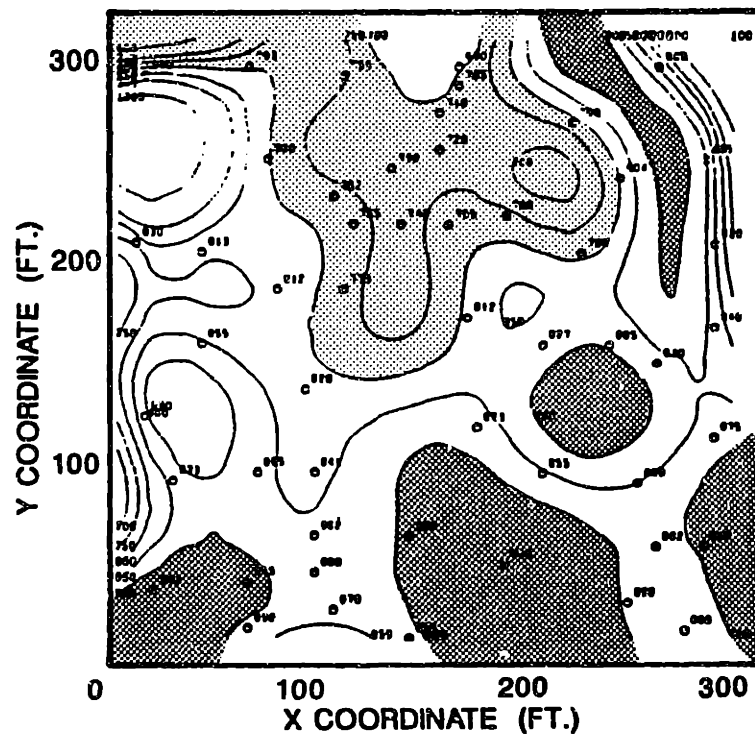
(m) Kriging Estimate Contours - Gaussian model of covariance with r_o = 2. Note greater relief than other models (after Ripley, 1981).
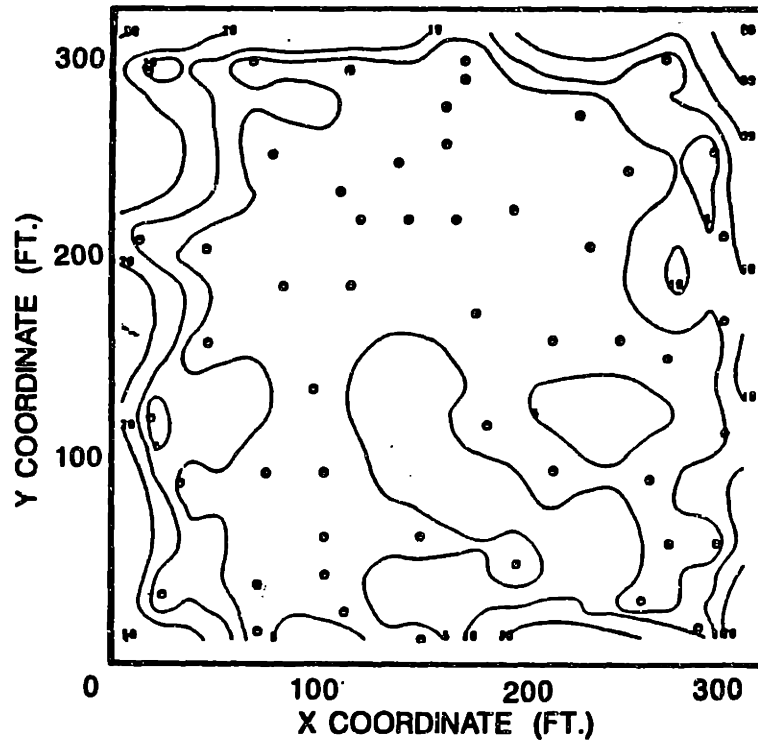
(n) Standard Deviation of Prediction Error in (m) - Note lower prediction error than model in (m) (Ripley, 1981).

Figure 3.8 Continued.
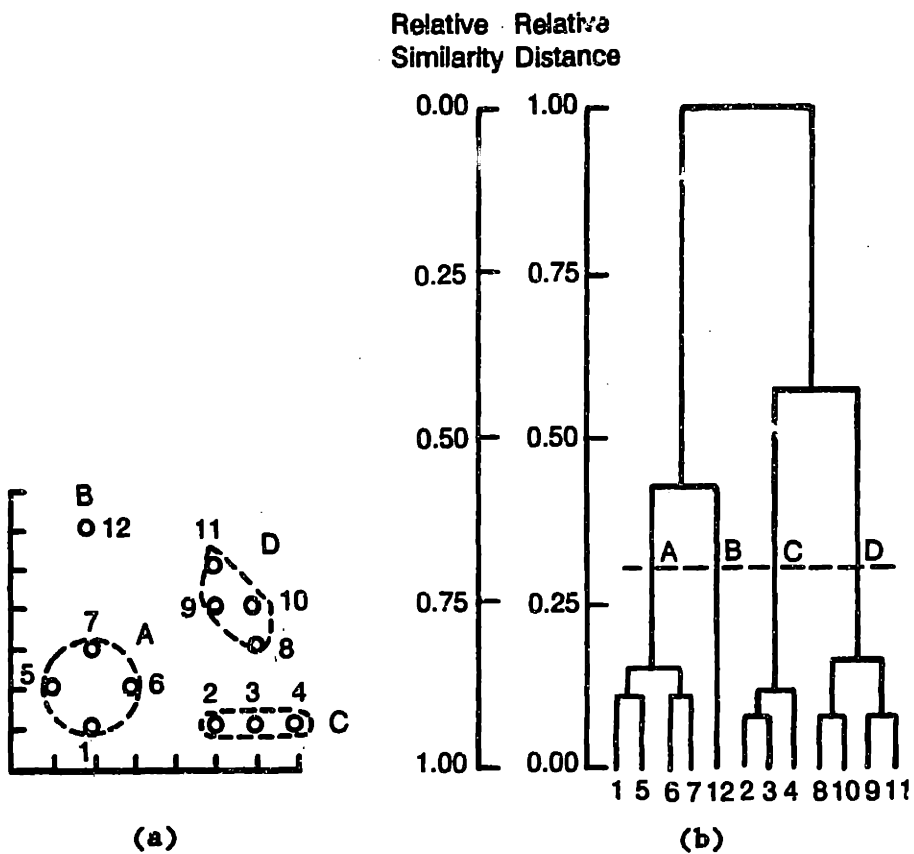
Figure 3.9 - Clustering Dendrogram: (a) 12 objects in two dimensional
space; (b) Dendrogram for clustering using Ward's method
(after Zupan, 1982).
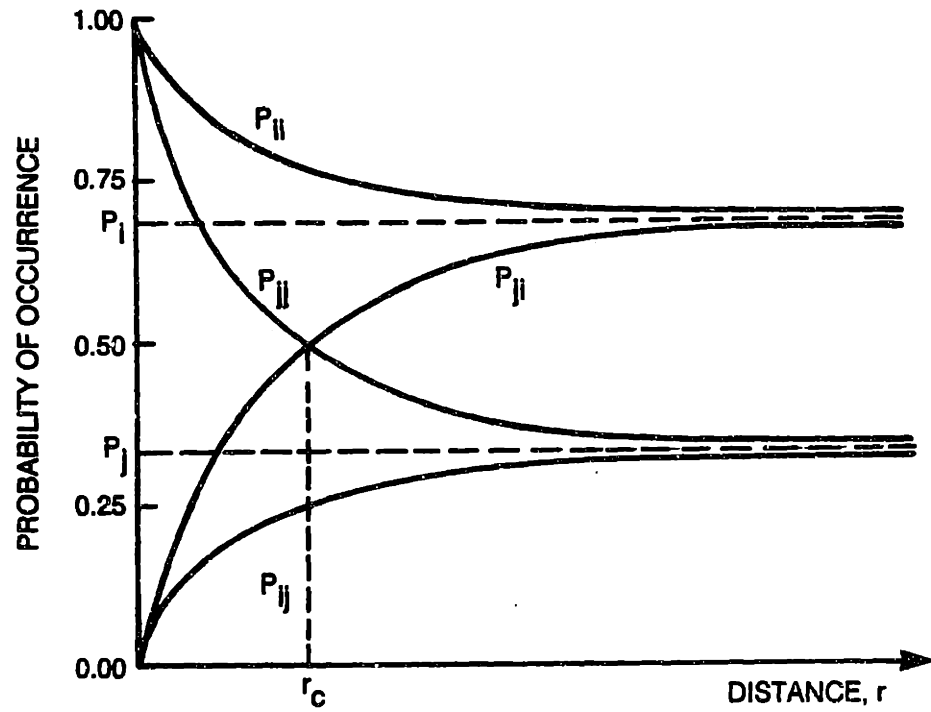
Figure 3.10 - Probability Decay Functions (Nucci, 1979).
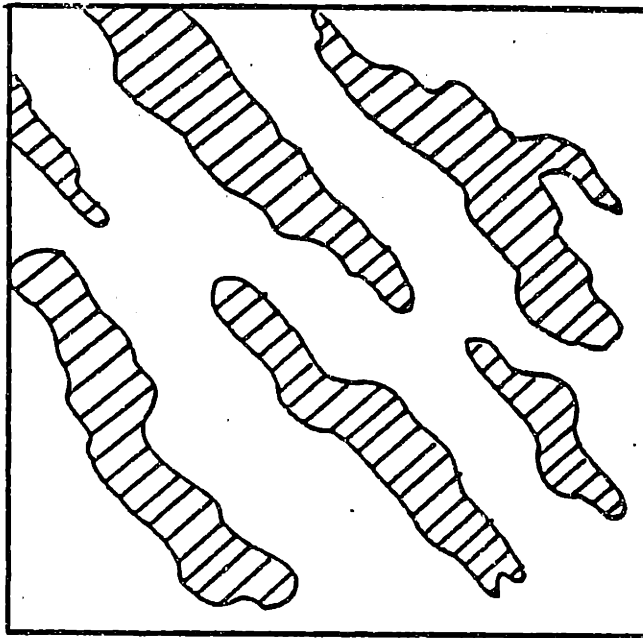
(a)
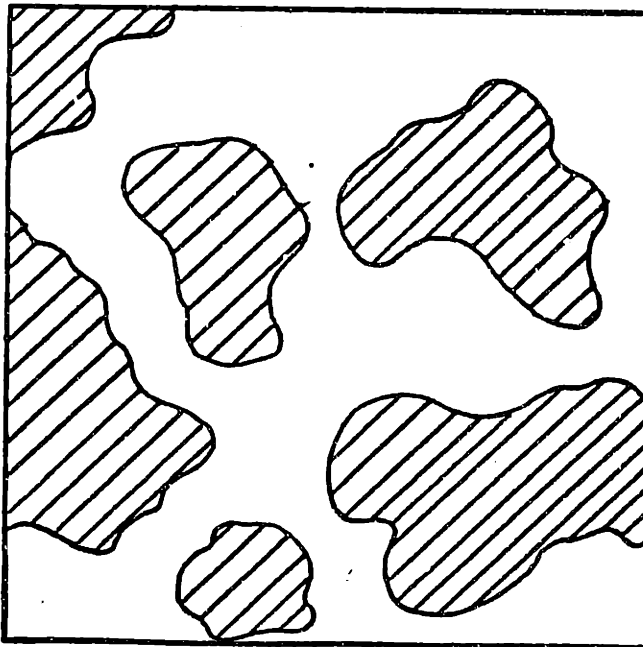
(b)

Figure 3.11 - Comparison of (a) Trending and (b) Isotropic Maps (Nucci, 1979).
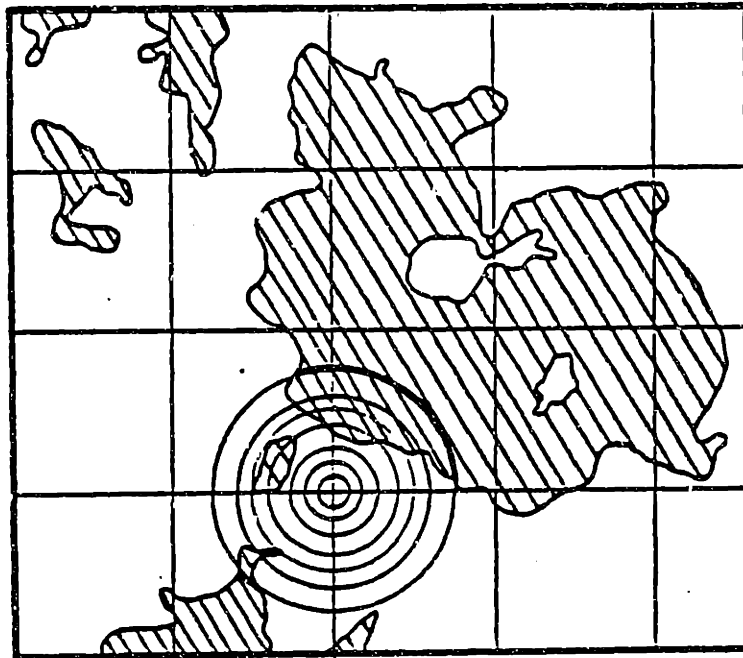
Figure 3.12 - Direct Method of Evaluation of Decay Parameter (Baecher, 1972).
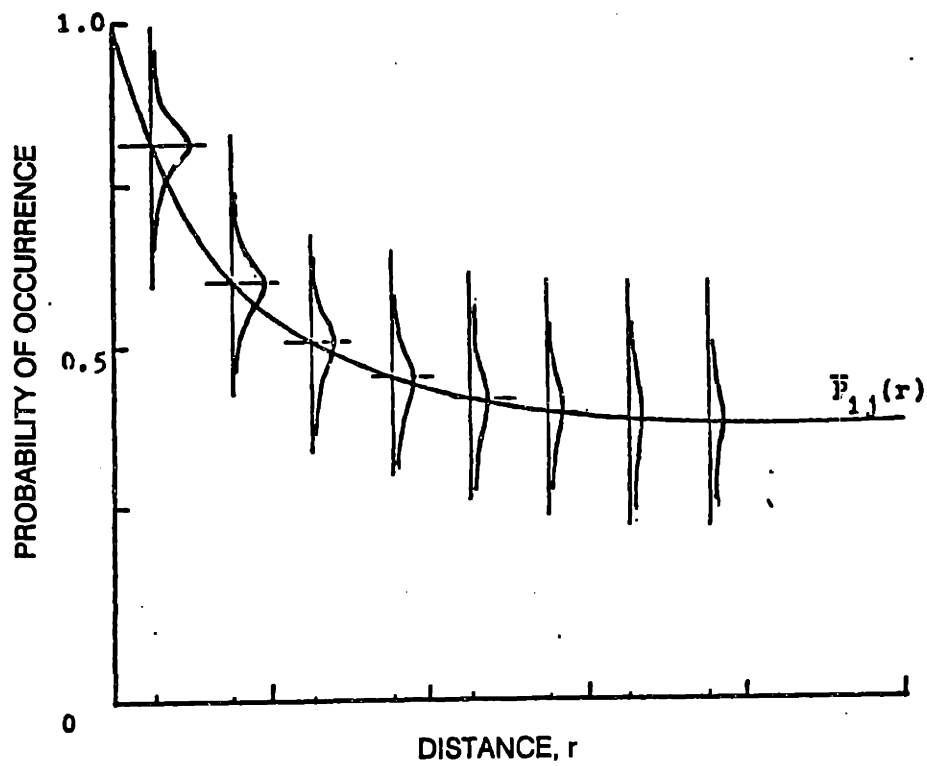
Figure 3.13 - Direct Method Probability Decay Function (Nucci, 1979).

CHAPTER 4

SOIL DATA PREPROCESSING

4.1 Introduction

This chapter deals with soil data preprocessing which for discussion purposes is defined as the process of assimilating the available soil data in order to make objective decisions concerning the grouping of the soil samples into similar groups or strata.

One of the major difficulties in the process of site characterization is identifying similar soils, meaning soils which in the judgement of the geotechnical engineer belong in the same soil stratum or sub-stratum. This process is hindered by factors which are discussed in Chapter 1. Not only is the available data usually sparse, but the type and amount of information varies from point to point. Also, the level of uncertainty in the available information, which is not quantified, is understood to vary considerably. The objective of soil data preprocessing is to develop objective analytical techniques that can be used by the geotechnical engineer to analyze the information available concerning soil strata.

The geotechnical engineer commonly has available for analysis the test boring log including observed strata changes and the Standard Penetration test blow counts for the samples, the visual description of the recovered soil samples, and possibly laboratory test data. Not all of the information is available for all the soil samples, so the geotechnical engineer must make judgements using variable amounts of data concerning the similarity of the different soil samples. More often than not the geotechnical engineer is biased by the soil strata identified by the driller and makes decisions concerning whether or not all of the samples belong to the same stratum identified by the driller.

4.2 Objectives

The objective of this research in soil data preprocessing is to develop
an objective process for the grouping of soil samples into similar groups
so that the groups could be used to assist with the development of soil
stratigraphy. The developed soil data preprocessing technique must be
capable of using variable type data with flexibility so that the geotech-
nical engineer can input his personal judgement and experience into the
process.

Two distinct approaches to soil data preprocessing, clustering and
regional merging, are presented in this chapter along with applications
using case history data. The research includes separate applications of
the methods, as well as, a combination of the methods.

4.3 Application of Clustering Techniques

Clustering techniques were presented briefly in Chapter 3 including a
discussion of their application by others to problems dealing with soils
in general. As noted in Chapter 3, the previous research with the clus-
tering of soils data has dealt with soil types from the perspective of
agriculture or flora/fauna/pollen contents (Anderson, 1971; Birks and
Gordon, 1985; Grimm, 1987; Muir et al., 1970; Rayner, 1966).

The research presented here uses clustering techniques for the first
time, known to the author, to identify soil strata from the perspective
of the geotechnical engineer, and compares the clustering solutions to
those developed independently by geotechnical engineers using hand meth-
ods. Before discussing the results of the research, a discussion of the
clustering methodology will be presented.

As discussed in Chapter 3, clustering is the process of assigning objects
to clusters based on the similarity between the objects. Agglomerative
methods, which start with all single objects and then iteratively join

the most similar objects or groups into larger groups, are the most common. Divisive methods start with all of the objects grouped and iteratively separates the groups into smaller parts until ultimately each group is a single object. Since the collection of soil samples is intuitively agglomerative and also since the agglomerative methods are used much more widely, agglomerative clustering methods were used for the soil data preprocessing research presented here.

The general algorithm of the agglomerative methods is:

1) Calculate a distance (similarity) matrix between the objects;

2) Identify the minimal element in the distance matrix;

3) Cluster the two most similar objects or groups and re-calculate the distance matrix considering the grouping; and

4) Repeat steps 2 through 4 until all the objects are clustered.

Step 1 is the calculation of the distance or similarity matrix. If the data available are of a single type (two-state, multistate (ordered and qualitative), or quantitative), determination of the distance matrix is greatly simplified. However, in geotechnical engineering the available data can be any or all of these types. Examples of geotechnical data of different types are as follows:

Two-state: presence/absence of a soil type

Multistate:

Ordered - soil density based on SPT blow counts

Qualitative - color

Quantitative: SPT blow counts, laboratory test results

As discussed in Chapter 3, the General Similarity Coefficient of Gower (Gower, 1971) is one similarity coefficient that can accommodate all of the data types. Therefore, it is an appropriate similarity coefficient for soil data preprocessing. In principle the Gower similarity coefficient is calculated between two objects by comparing the various attributes and assigning a score for the level of agreement. Then a weighted

average of the various scores is calculated by summing the product of the scores and weights for each attribute and dividing by the sum of the weights.

Use of the Gower General Similarity Coefficient requires determination of the attributes to be considered, and the corresponding weights and scores for matching. Usually a score of 1 is used for matches, and 0 if there is no match. If the data are quantitative, the score is usually expressed as a ratio of the data range such that the score is between 0 and 1. The selection process for the scores and weights is arbitrary, and when possible, can be adjusted to result in the most satisfactory clustering.

The similarity coefficient is used only to create the initial distance or similarity matrix which is the similarity between original objects. Once the initial matrix has been calculated, updating of the matrix requires consideration of similarity between objects and groups and, therefore, the original similarity coefficient can no longer be used.

As discussed in Chapter 3, Ward's method combines the groups with the smallest sum of squares. The method considers potential grouping of all possible combinations and calculates the squared distance of each point in the potential group from the group central point. The combined groups with the smallest sum of squares are then combined and the process is repeated.

4.4 Case History Examples Using Clustering Techniques

4.4.1 Calculation of the Similarity Matrix

The process of soil data preprocessing using clustering techniques was studied using the Gower General Similarity Coefficient. The clustering study is based entirely upon information available in the visual description of the soil samples recovered in the Standard Penetration tests.

89

In the initial research the clustering was limited to consideration of the soil consistency/density based on the SPT blow counts, the soil color, the minor constituent (35 to 50%), and the major constituent (>50%). For instance, if the visual description reads: Stiff, olive-gray silty clay, then the available information is:

Consistency/density:	Stiff
Color:	Olive-gray
Minor constituent:	Silt
Major constituent:	Clay

The information in the visual descriptions is from two sources. The consistency/density is based upon the SPT blow counts and the engineer's determination whether the soil is granular or cohesive. The consistency/density is determined by:

GRANULAR SOILS		COHESIVE SOILS	
SPT Blows/ft	DENSITY	SPT Blows/ft	CONSISTENCY
0-4	Very Loose	0-2	Very Soft
4-10	Loose	2-4	Soft
10-30	Medium Compact	4-8	Medium Stiff
30-50	Compact	8-15	Stiff
50+	Very Compact	15-30	Very Stiff

Consistent with the recommendations concerning use of the Gower coefficient, the score used was 1 for a match and 0 for no match. As discussed below, various weights were assigned to the attributes to see if the resulting clustering differed significantly.

Three profiles (Profiles B, M, and O) from the Cambridge Center case history (see Appendix B) were used to study the application of clustering techniques. Visual descriptions of the soil samples were availa   for use in the preparation of the similarity matrix. All of the visual descriptions were originally prepared by the staff of the same geotechnical engineering company using a company visual description procedure.

The hand drawn profiles for Profiles B, M and O are shown in Figures 4.1 through 4.3, respectively. The locations of the profiles are shown in Figure B.2. Note that some of the observed strata appear to be discontinuous. The uncertainty in the interpretation of stratigraphy has been implied by the use of dashed lines which tend to be wavy where the geotechnical engineer is unsure of the strata interface.

The three profiles were selected for analysis to provide a variety of subsurface conditions. Profile B (Figure 4.1) has consistent stratigraphy with the exception of Stratum IVA (see Appendix B for strata descriptions) which appears to be discontinuous. Profile M (Figure 4.2) has more discontinuous strata than Profile B. Profile O (Figure 4.3) is particularly complex with respect to Strata VA and VB, which are both discontinuous and irregular with respect to the vertical sequence.

Using Gower's similarity coefficient and the visual descriptions, an original similarity or distance matrix was calculated with variations in the weighting of the attributes (consistency/density, color, minor constituent, and major constituent). Seven different clustering methods were reviewed and used in the preliminary analysis using the algorithms presented by Zupan (1982). The preliminary analysis indicated that use of Ward's method for clustering resulted in a higher level of agreement with the hand drawn profiles than the six other clustering methods. Ward's method was selected to be used for the final clustering analysis for the following additional reasons:

1) its use by others (see Chapter 3) on other clustering studies,

2) the grouping is always monotonic (increasing dissimilarity) (Zupan, 1982),

3) the method is intuitively attractive because it minimizes the sum of squares in the grouping process, and

4) the method is computationally efficient (Zupan, 1982).

4.4.2 Analysis of Dendrograms

Figures 4.4 through 4.6 are examples of the dendrograms resulting from clustering the visual description data for Profiles B, M and O, respectively, using Gower's coefficient and Ward's method of clustering. Note that the height of the trees has been normalized by the greatest branch length so that the range of dissimilarity is between 0 to 1. Multiple objects that are joined on the x axis indicate that the relative dissimilarity, based on the scoring and weights, was zero.

The dendrograms for all three profiles visually appear to be nearly balanced considering the theoretical minimum maximum length of the chains indicated in Figures 4.4 through 4.6 (see Section 3.3.2.2). However, due to the number of objects joined along the x-axis, the chains are in fact considerably longer than they appear visually. Intuitively, the trees should be balanced only when there are the same number of soil samples in each of the "true" soil strata. It is unlikely that this will occur due to differences in the strata thicknesses and test boring lengths. A visual check of Figures 4.1 through 4.3 shows that Stratum IVB (Boston Blue Clay) is considerably thicker than the other soil strata and therefore, has more soil samples taken from it. Consequently, balanced trees would not be expected.

One of the major disadvantages of clustering is that the clustering normally continues until all the objects, no matter how dissimilar, are grouped into a single group. With respect to soil stratigraphy this presents the problem of determining the level at which to cut the dendrogram to identify potentially significant soil strata. By cutting the dendrograms with a single horizontal line or a series of horizontal line segments, it is possible to separate the groups into any number of clusters.

In order to compare the clusters with the hand drawn profiles, a single horizontal line was drawn at a level that resulted in the same number of groups as observed strata in the hand drawn profiles (see Figures 4.4 through 4.6).

By cutting the dendrogram with a horizontal line, it is possible to compare the clusters with the soil strata identified in the hand drawn profiles and determine the number of "mis-classified" samples assuming that the hand drawn profile is the "true" profile.

The level of the horizontal line lies between 0.14 and 0.18 on the normalized dissimilarity scale. In actual similarity distance the horizontal line falls in the range of 1.65 to 1.97 (Profile B), 1.68 to 1.71 (Profile M), and 1.96 to 2.32 (Profile O). These ranges appear to be fairly consistent with the exception of Profile O, which is anticipated to be the more difficult profile to develop.

Figure 4.7 presents the results of comparing the clustered groups to the hand drawn "true" profile using various interpretations of the data as discussed below. Accepting the hand drawn profile as the "true" profile and the method discussed above, the percent of the samples mis-classified ranges from 18 to 28 for the three profiles. As expected the percentage is higher in Profile O where the apparent soil stratigraphy is more complex.

4.4.3 Alternative Data Interpretations

The dendrograms shown in Figures 4.4 through 4.6 are totally objective in that the scoring process was strictly 1 for a match and 0 for no match, and each attribute is given equal weight. It is possible to modify the scoring process so that if key attributes of two or more objects match, then the objects are identified as complete matches and thus grouped at the x-axis (i.e., totally similar).

The use of key attributes is very attractive from the soil stratigraphy perspective because there is often a single attribute, such as color, or

a combination of attributes that is used to distinguish a specific stratum. For instance, in the Cambridge Center case history Stratum IVA is a very stiff to stiff, yellow silty clay which overlies Stratum IVB a stiff, grey silty clay. Stratum IVA is commonly distinguished from Stratum IVB by the yellow color, which is believed to be a result of oxidation of the Boston Blue Clay during periods of lower groundwater levels.

The clustering algorithm was adjusted by varying the weights assigned to the attributes and also in the method of determining the matches. It should be noted that these modifications are made at the sacrifice of objectivity. However, the sacrifice is considered minor if the result is an improvement in the mis-classification error.

The data interpretations used in the clustering analysis are summarized as follows:

<u>Data Interpretation B1</u>: Totally objective similarity matrix calculated using equal weights and scores for each of the four attributes (consistency/density, color, minor constituent, major constituent).

<u>Data Interpretation B2</u>: Similarity matrix calculated using three attributes (color, minor constituent, major constituent) and using selected key attributes or combinations of key attributes to identify samples from either Stratum I or II (fill and organic silt) and automatically setting the distance between the samples to 0 such that they are grouped into separate groups at the start of clustering.

<u>Data Interpretation B3</u>: Same as Data Interpretation B2 (initial grouping of samples from Stratum I and Stratum II) except that all four attributes are used.

<u>Data Interpretation B4</u>: Same as Data Interpretation B3 except that key attributes are used to initially group samples from Stratum IVA (stiff yellow clay), Stratum IVC (sandy clay) and Stratum VA (glacial outwash) in addition to those in Data Interpretation B3.

Figures 4.7 and 4.8 present the results of the adjustments to the match-
ing process. Depending on the level of adjustment to the matching, it is
possible to reduce the total mis-classification error to about 3 to 11%.
This reduction in the mis-classification error has been achieved while
still making the horizontal cut in the dendrogram at any arbitrary level
(in this case that level resulting in the same number of strata). If in
fact the cut is made with full knowledge of the profile, the mis-
classification error can be reduced to 0 to 4%.

Using the mis-classification error in the totally objective clustering
(Data Interpretation B1) as 100%, the mis-classification error with the
other matching options can be normalized (see Figure 4.8). The relative
mis-classification error can be lowered to about 20 to 55% by modifying
the matching options. Using modified matching options and full knowledge
of the profile to establish the dendrogram cut (Data Interpretation B4),
it is possible to lower the relative mis-classification error to 0 to
29%.

Figures 4.7 and 4.8 indicate that the best agreement is consistently with
Profile M which has two apparently discontinuous strata. The only stra-
tum that was mis-classified by all the matching options was Stratum IVC -
Sandy Clay which was grouped with Stratum VB - Glacial Till. This is not
totally unexpected based on the slight differences in the visual descrip-
tions of the strata (see Appendix B).

Profile B, which was anticipated to be the easier profile to model, had a
consistently higher mis-classification error than Profile M. The higher
mis-classification error in Profile B is due to several factors. The
distinction between the lower portions of the Stratum IVC - Sandy Clay
and the upper part of Stratum VB - Glacial Till was consistently mis-
classified. Although in this analysis discrepancies between Strata IVC
and VB were reported as mis-classification errors, it is interesting to
note that the original test boring logs, in fact, refer to the lower
portions of Stratum IVC as "till like". Because the clustering methods
continually group the most similar groups, the clustering of Profile B

95

grouped the Stratum IVA samples with Stratum IVB at a relatively low level (i.e., below the arbitrary horizontal line). Therefore, the apparent inability of the clustering to distinguish these two profile strata resulted in mis-classification error.

It is interesting to note that although the clustering of Profile B resulted in mis-classification error, it raised two questions with respect to the hand drawn profiles (see Figure 4.9). In Boring CC1040W the highest silty clay sample was included in Stratum IVB Silty Clay even though the visual description is "stiff, yellow gray, silty clay". The clustering models consistently correctly placed the sample in Stratum IVA - Stiff Yellow Clay.

The hand drawn profile refers to the middle stratum as Stratum IVB (Silty Clay) and IVC (Sandy Clay) indicating that although both soil types were observed, the mixing of the two types is such that the geotechnical engineer apparently did not want to make the distinction between the two strata on the profile. The clustering models consistently grouped the upper portion of the hand drawn profile Stratum IVB and IVC into Stratum IVB and the lower portion either into a stratum that could be interpreted to be Stratum IVC or Stratum VB as discussed above. In this case it appears that due to the totally objective nature of the clustering models, groupings that may either not be apparent to the engineer or that the engineer was unwilling or unable to differentiate are distinguished.

The clustering models of Profile O are particularly interesting because the models were able to group the discontinuous Strata VA and VB with a relatively low mis-classification error (about 11% in Figure 4.7). The total mis-classification error was due to an inability to differentiate between Strata VA and VB. Although it has been considered mis-classification error here, this inability could raise questions concerning the ability of an individual to consistently distinguish between these two strata objectively. Therefore, a portion of the total

mis-classification error may in fact be due to the differences between the actual "true" profile, which is unknown, and the assumed "true" profile (hand drawn profile).

4.4.4 Clustering to Estimate Soil Properties

To demonstrate how clustering techniques could be used to assist with the determination of design soil properties for soil strata, Profiles B, M and O were used for additional clustering analysis using the available shear strength and consolidation test data from the Cambridge Center case history.

The analysis was similar to that described above for the analysis of soil stratigraphy with one exception. The visual descriptions of all soil samples for which test data (compressive strength and consolidation properties) were available were included along with those of the soil samples for the test borings in three subject profiles. The clustering was performed using the same procedure (Ward's method of clustering with Data Interpretation B1), and then average soil properties were assigned to the groups based on the clustering results.

The results are shown in Figures 4.10 through 4.12. There was considerably more data available for the shear strength clustering. Consequently the clustering results for the shear strength are more conclusive.

The initial observation in Figures 4.10 through 4.12 is that there is more variation vertically between samples than horizontally. This is consistent with the intuitive impression of shear strength variation. The next observation is that the clustering has sub-divided the major strata into sub-strata based on shear strength. This is a significant improvement with respect to the selection of design soil parameters because it provides a rational method for sub-dividing major strata. In detailed engineering analysis, such as slope stability, it is advantageous to sub-divide the strata if there is a rational basis for doing so. Often in practice the sub-dividing is very limited or is done based primarily on elevation.

The clustering of the consolidation properties appears to less successful than the shear strength clustering due mainly to the lack of data. It is interesting to note that the consolidation values are not completely consistent with the shear strength values.

4.5 Discussion of Clustering Applications

It should be noted here that the clustering models are based on the individual objects and selected object attributes. The analysis described above did not include any attributes that indicate the spatial relationship of the objects. Limited analysis (not reported here) using sample elevations as another attribute did not result in any noticeable improvement in the mis-classification error. There is no reason why spatial attributes such as the coordinates of the test boring and/or sample elevation could not have been included in the analysis. In fact, they were purposefully excluded from the above analysis in order to see how successful the cluster analysis approach would be without any spatial attributes.

The clustering results described above have demonstrated that non-spatial clustering can very reasonably reproduce hand drawn soil profiles with a generally acceptable level of mis-classification. In the process the clustering results have presented additional insight into possible substrata. When applied to the shear strength and consolidation data, the clustering results provide an objective method for assigning design soil properties.

Use of the clustering methods requires cutting the resulting dendrogram to identify the strata. If the "real" profile is completely unknown, there is no rational basis for determining the level to cut the dendrogram. However, the dendrogram itself indicates the relative similarity level of the groupings so that cuts can be made at a level considered reasonable for the application. Also, in actual applications the initial cuts should be made at a level consistent with the initial geologic model hypothesis.

98

4.6 Application of Regional Merging Methods

Regional merging methods were discussed in Chapter 3. They represent another analytical method which can be applied to soil data preprocessing; however, regional merging has distinctly different characteristics than clustering. Before presenting regional merging applied to soil data preprocessing, a brief comparison of clustering and regional merging is merited.

Clustering and regional merging differ with respect to handling spatial concepts. Clustering typically addresses individual objects independent of spatial relationships, unless spatial attributes are purposefully included. It should be noted here that spatial attributes are not normally included in the conventional use of clustering techniques which are often applied to taxonomy. In contrast regional merging has definite spatial relationships since only adjacent regions are considered for merging.

Another important difference between the methods is that the level of grouping is typically controlled in regional merging, while clustering ultimately groups all the objects. Even though the eventual dendrogram can be cut to sub-divide the groups, the results will be different than with regional merging where a ˉefined merging criteria is used at each decision point.

One common characteristic of the methods when applied to soil data pre-processing is that an initial distance (similarity) matrix is needed for both methods. Therefore, as discussed below, it is possible to compare the two methods, if the same initial distance matrix is used.

4.7 Case History Examples Using Regional Merging Methods

A regional merging computer program, based on the split-merge methods presented by Pavlidis (1977), was developed. Split-merge methods are used to either divide or join regions to increase the similarity of the final regions. The code was developed to consider only merging since the

intuitive process is the combining of samples into soil strata. General merging techniques consider adjacency in any direction. However, the code was written so that the regional merging process was restricted to vertical neighboring cells (samples) so that it could be applied to the samples from a single boring. Therefore, adjacency was initially defined as neighboring les within a single test boring.

Using this vertical adjacency constraint and regional merging, the test borings in Profiles B, M and O were evaluated using the same distance matrix techniques as for the clustering methods. One significant variable in the regional merging application is the predicate, meaning criterion, used to assess whether the regions should or should not be merged. In the applications discussed here, the predicate was the difference in similarity between the adjacent samples of the region and the sample being considered for merging.

Various data interpretations were used with the regional merging analysis. These data interpretations are summarized as follows:

Data Interpretation C1: Totally objective similarity matrix calculated using equal weights for the four attributes with merging restricted to samples in single test borings.

Data Interpretation C2: Same as Data Interpretation C1 except that the consistency/density attribute was not used.

Data Interpretation C3: Similarity matrix calculated using all four attributes and using selected key attributes or combinations of attributes to automatically set distance between samples from Stratum I, II, IVA, IVC and VA to 0 before starting regional merging. Additional merging of samples with the initially defined regions was allowed to occur.

Data Interpretation C4: Same as Data Interpretation C3 except that merging of initially defined regions was restricted.

Figures 4.13 and 4.14 present a summary of the regional merging analysis of the three profiles. Figure 4.13 is a plot of the percent of the samples mis-classified for various interpretations of the data with different values for the predicate difference. As the predicate difference is increased (meaning that the acceptable difference between regions is higher and there will be more merging) the mis-classification error increases. It should be noted that due to the method of calculating mis-classification error, by comparison to the hand profiles, the method is biased in favor of smaller regions. In the extreme if the regional merging resulted in no merging, the mis-classification error, as defined here, would be zero. The major conclusion from Figure 4.13, when compared to Figure 4.7, is that the level of mis-classification error using regional merging is significantly lower than for the clustering methods.

Figure 4.14 shows the effect of increasing the predicate difference for the test borings in Profile B. As the predicate difference increases, the number of regions decreases such that at a level of 1± there is a single region in two of the three test borings. The horizontal lines on Figure 4.14 show the relative number of regions actually observed in the test borings.

Based on the results of the analysis presented in Figures 4.13 and 4.14, a predicate difference of 0.26 was selected for additional analysis of the three profiles. Since the initial distance matrix is based on four attributes with equal weights, the 0.26 value means that two samples would be merged if they match in two or more attributes. The value of 0.26 is therefore dependent on the number of attributes and is not site specific.

Using the 0.26 predicate difference, regional merging/clustering of the individual test borings from the profiles resulted in the profiles shown in Figures 4.15 through 4.17. It must be noted that the profiles in Figures 4.15 through 4.17 were developed from individual test borings

using regional merging to identify strata within each individual test boring, and then strata interfaces between borings were constructed by hand.

4.8 Discussion of Regional Merging Applications

Based on the results in Figure 4.13, regional merging of the individual test borings has a lower mis-classification error than the clustering of all the samples as separate objects. In the process of investigating regional merging, the flexibility of the method in assigning the predicate difference was a very convenient feature because the level of merging could be easily controlled unlike the cutting the dendrogram. Compared to cutting the dendrograms which is arbitrary, assigning the predicate difference was preferable since the difference can be based on a level of similarity.

4.9 Combination of Clustering and Regional Merging Methods

Since both clustering and regional merging are based on use of an initial distance matrix, it is possible with only minor modifications to the processes to combine the methods. In the application presented here the regional merging process was performed first followed by a constrained clustering which resulted in grouping of all the individual merged regions. With respect to the objective application, this means that the samples within all the individual test borings are considered for merging, and then all of the regions for all the borings are treated as objects and clustered.

The clustering was constrained in the sense that those objects that wanted to merge according to the regional merging analysis were initially forced to be grouped together as totally similar. This was accomplished by increasing the number of attributes by one with the additional attribute coded to the regions after regional merging. When calculating the initial distance matrix for the clustering process, the distance between samples with the same region attribute was set to 0 (meaning totally similar) so those regions would be clustered first.

102

Figures 4.18 through 4.20 present a summary of the soil data preprocessing methods discussed in this chapter. The summary is presented as a plot of the percent mis-classified versus the percent of the total area in an average region. This plot was selected to summarize the results because it demonstrates the potential trade-off of mis-classification error versus region size. The ultimate objective of soil data preprocessing is to determine groups or regions of a size in proportion to the relative penetrated thickness of each stratum with minimal mis-classification error.

In Figures 4.18 through 4.20 the results of the clustering methods plot as vertical lines because the size of the average region is established by the level of the horizontal cut in the dendrogram. Since the regional merging process resulted in smaller regions, the results plot to the left of the clustering methods. Although certainly part of the difference is due to the biased methods of calculating mis-classification error discussed above.

The combined regional merging/clustering models are shown in Figures 4.18 through 4.20 with two series of points. One set, referred to as the estimated cut, represents the results if the dendrogram is cut to create the same number of strata as the hand profile. These points therefore, plot on the same vertical line as the results of the clustering model due to the same underlying assumption. The other set of points, referred to as the optimal cut, for the regional merging/clustering model is for the cut of the dendrogram that results in the lowest mis-classification error.

The results presented in Figures 4.18 through 4.20 demonstrate that when comparing regional merging/clustering to regional merging alone there is some increase in the mis-classification error; however, the regional merging/clustering results in considerable larger average regions. If the geotechnical engineer can employ personal judgement with respect to the

level of cut in the dendrogram of the regional merging/clustering pro-
cess, the results in Figures 4.18 through 4.20 show that the mis-
classification error can be reduced at a slight decrease in the average
region size.

4.10 Summary

The research described in this chapter was performed to develop an objec-
tive process for the grouping of soil samples into similar groups to aid
in the analysis of soil stratigraphy. The results of the regional
merging/clustering (i.e., merge samples vertically within separate bor-
ings first then cluster borings horizontally) demonstrate that the devel-
oped methods can be successfully applied to actual case history profiles.
Also, it has been demonstrated that the same methods can be applied to
the determination of soil strata design properties.

Although in selected profiles the clustering and regional merging methods
identified sub-strata missing from the hand drawn profiles or apparent
inconsistencies in the hand drawn profiles, it is difficult to judge
whether the developed computerized methods are better than an experience
engineer. However, it has been demonstrated that the clustering and
regional merging methods can be easily computerized to consider multiple
soil samples/profiles in an efficient, objective manner.
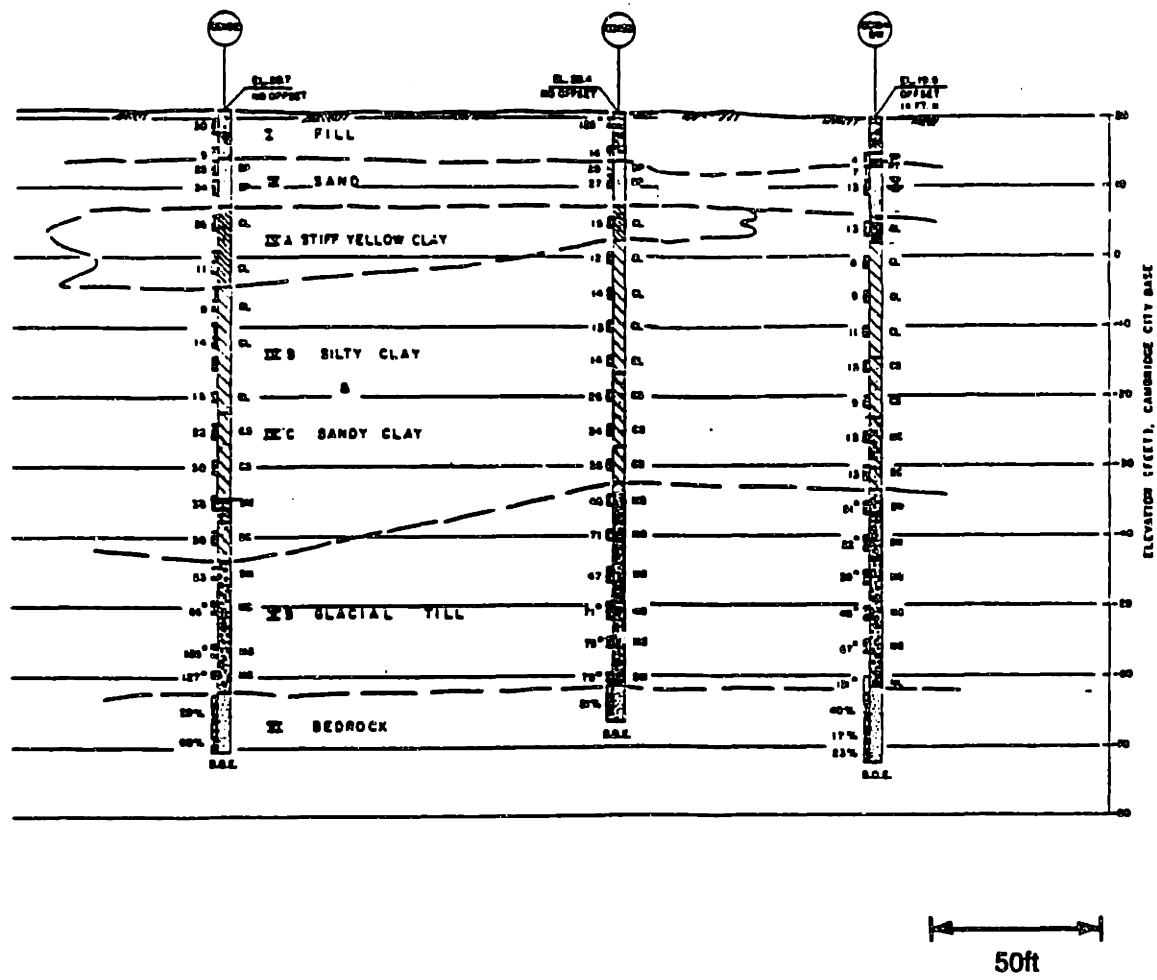
Figure 4.1 - Hand Drawn Profile B, Cambridge Center (see Appendix B for
    strata descriptions).
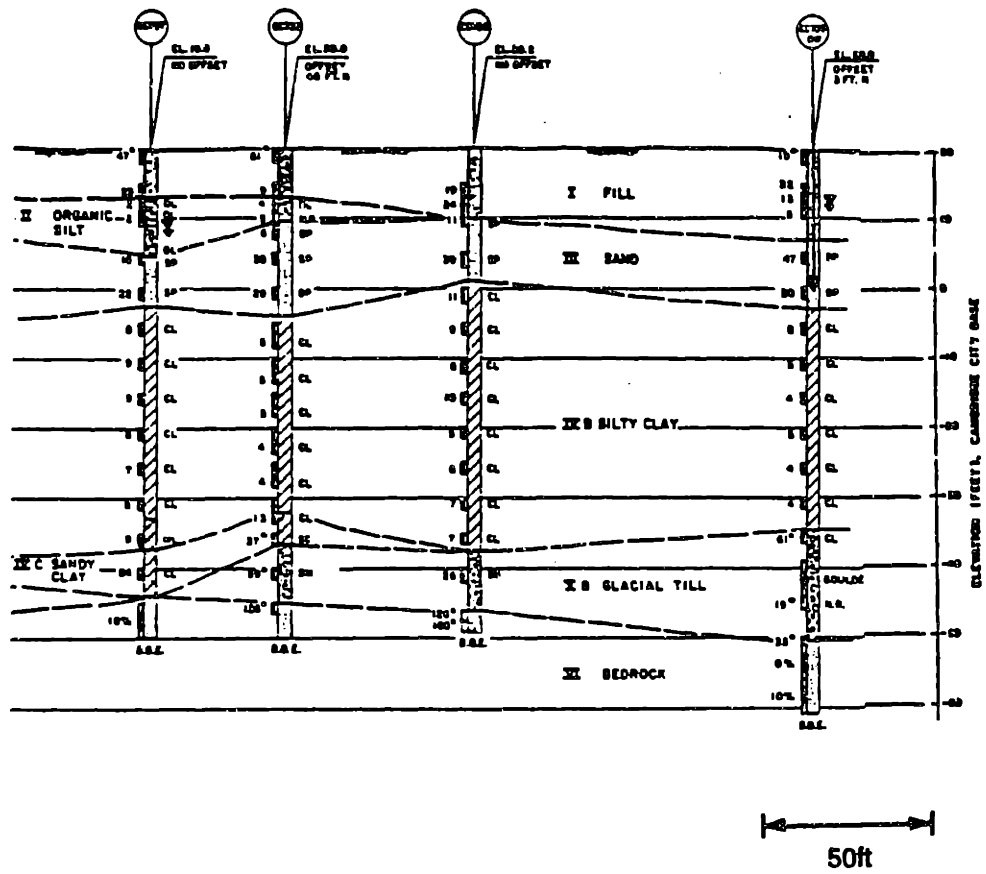
Figure 4.2 - Hand Drawn Profile M, Cambridge Center (see Appendix B for strata descriptions).
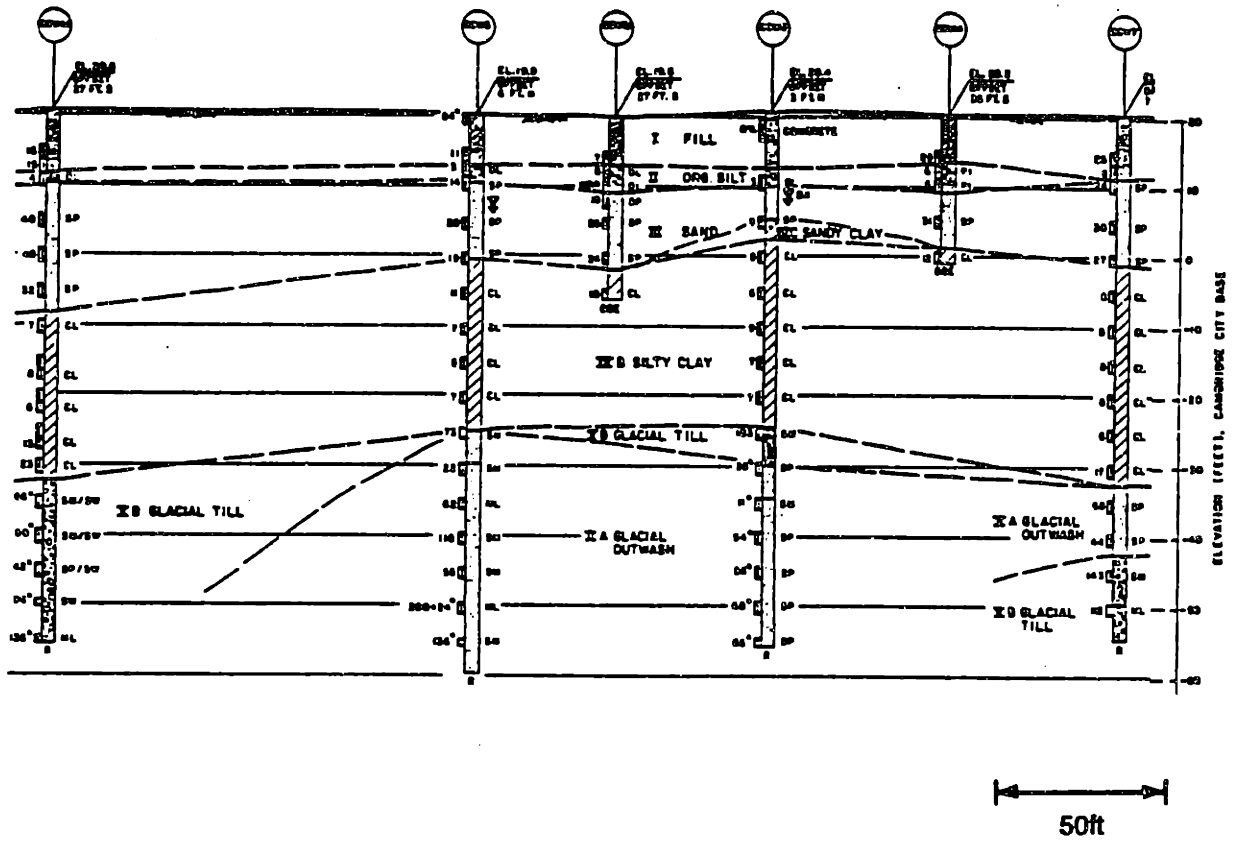
Figure 4.3 - Hand Drawn Profile 0, Cambridge Center (see Appendix B for strata descriptions).
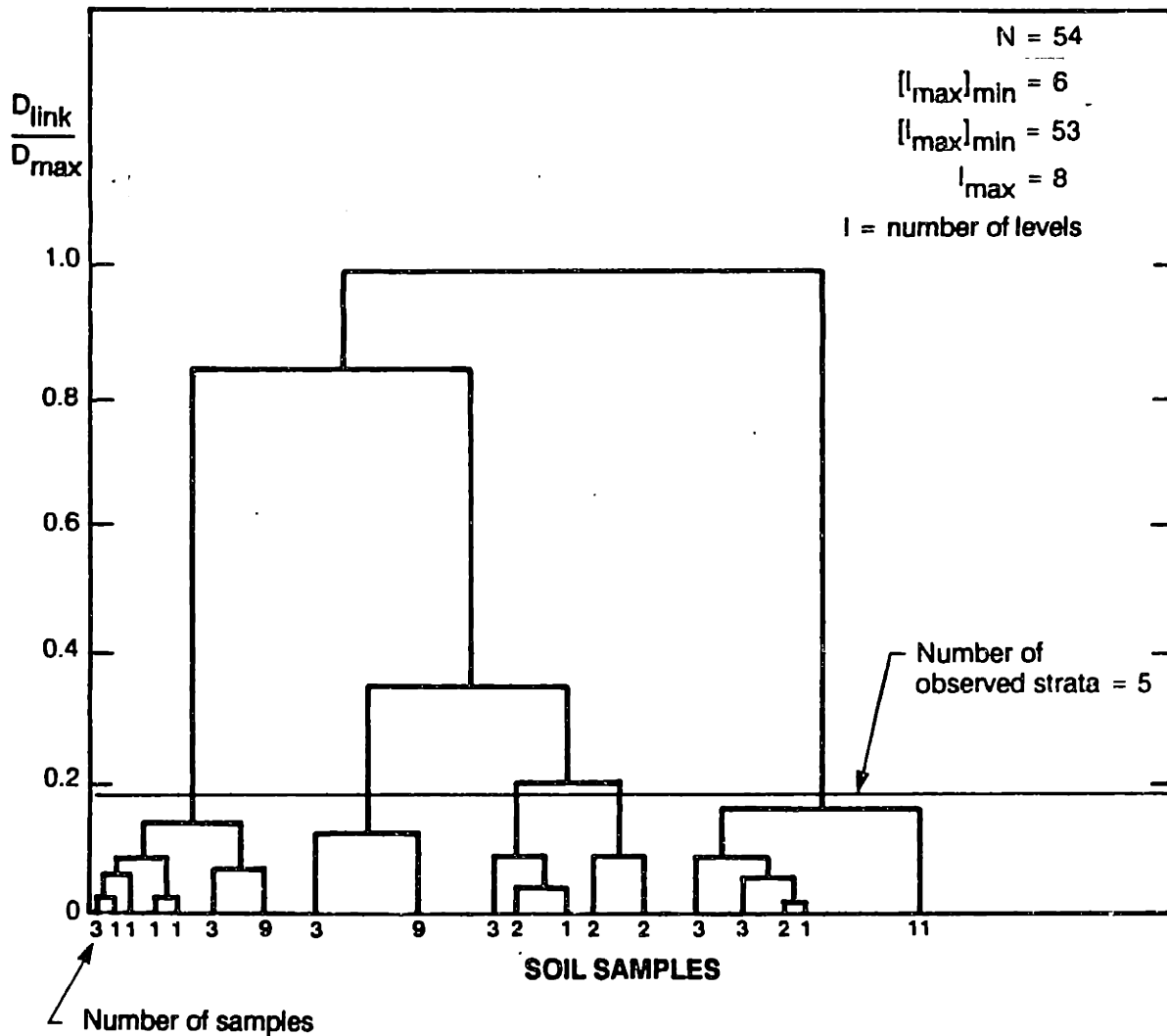
Figure 4.4 - Dendrogram for Profile B, Cambridge Center.
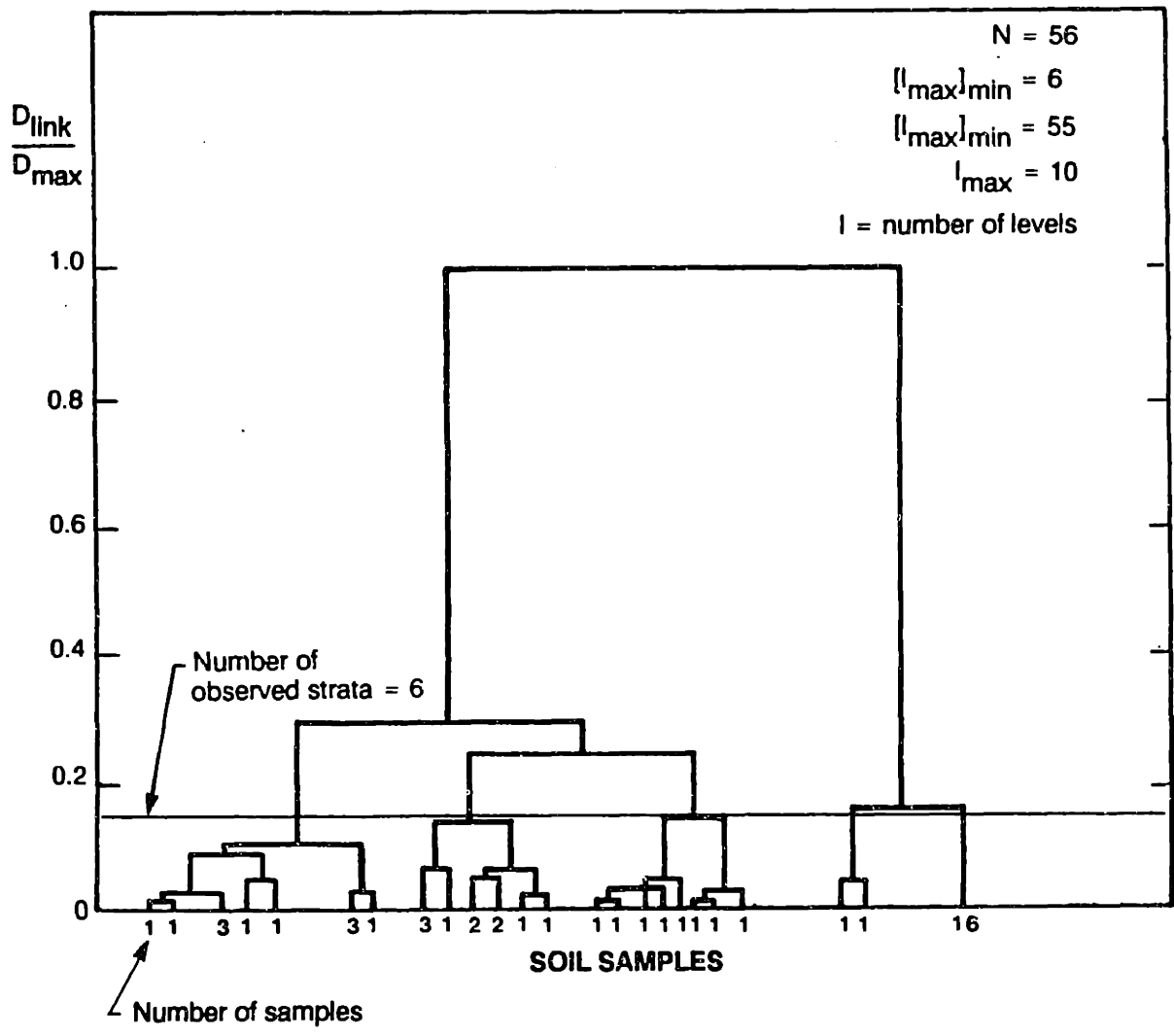
Figure 4.5 - Dendrogram for Profile M, Cambridge Center.
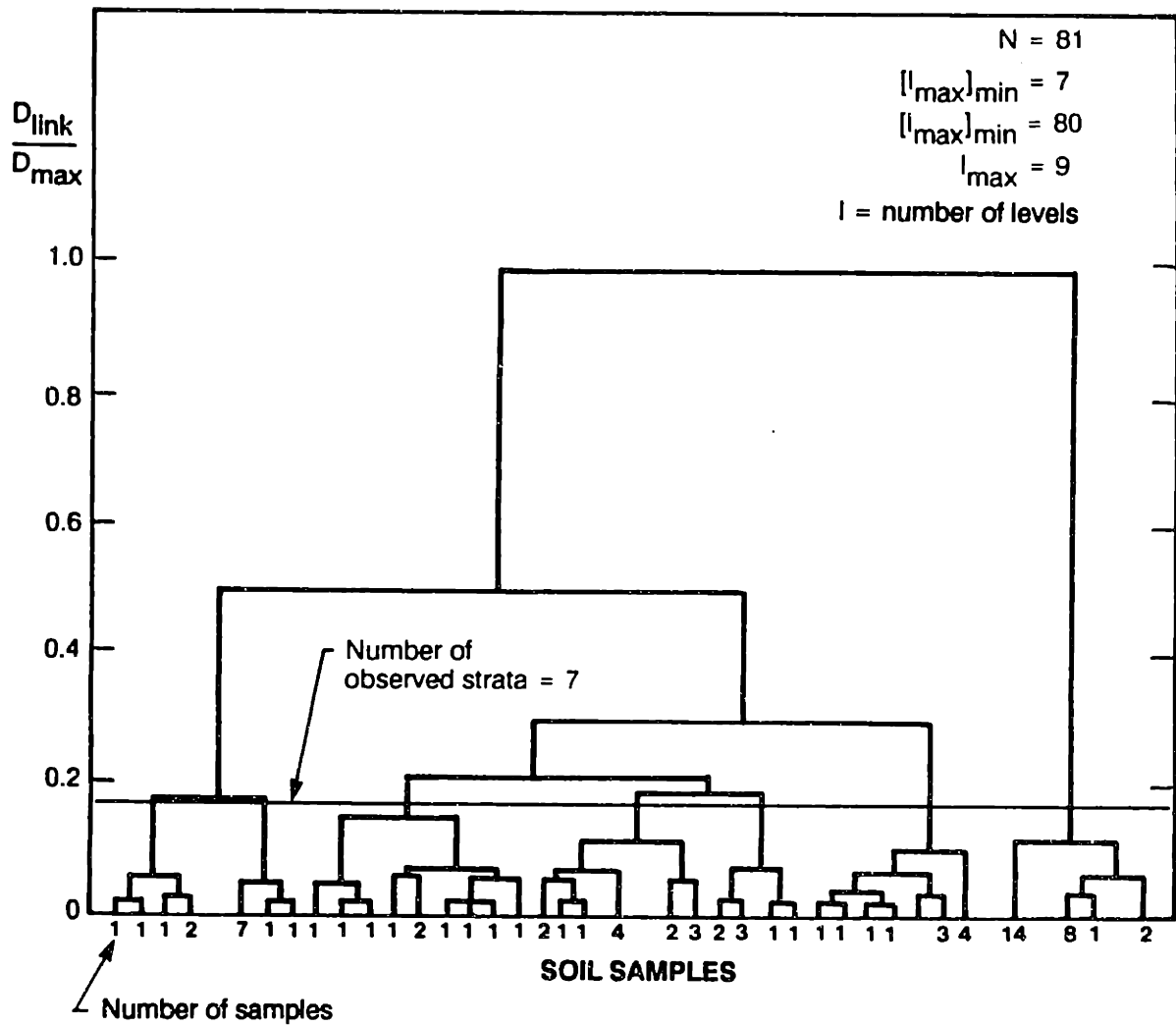
Figure 4.6 - Dendrogram for Profile O, Cambridge Center.
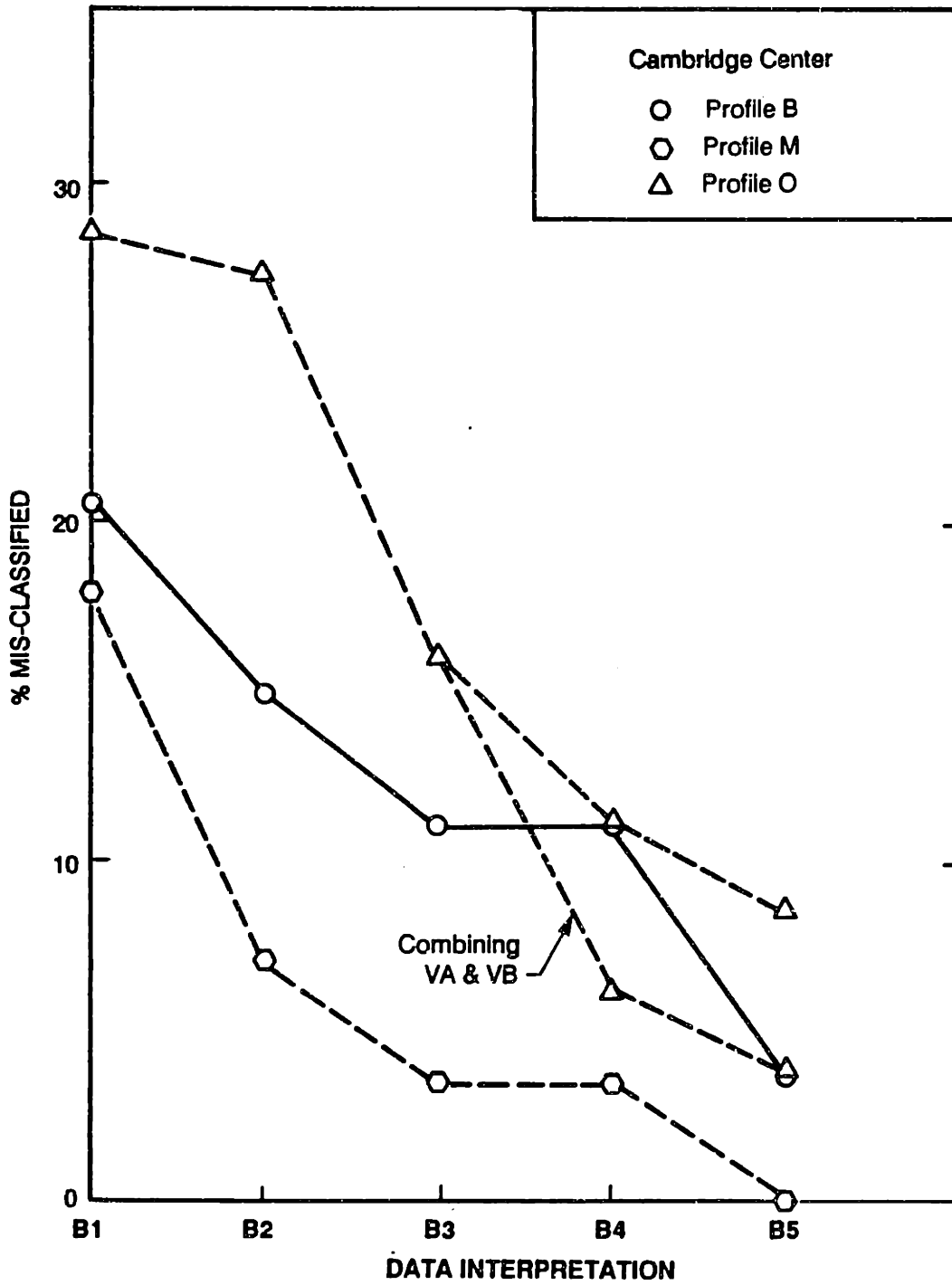
Figure 4.7 - Mis-classification Errors for Various Clustering Analyses.
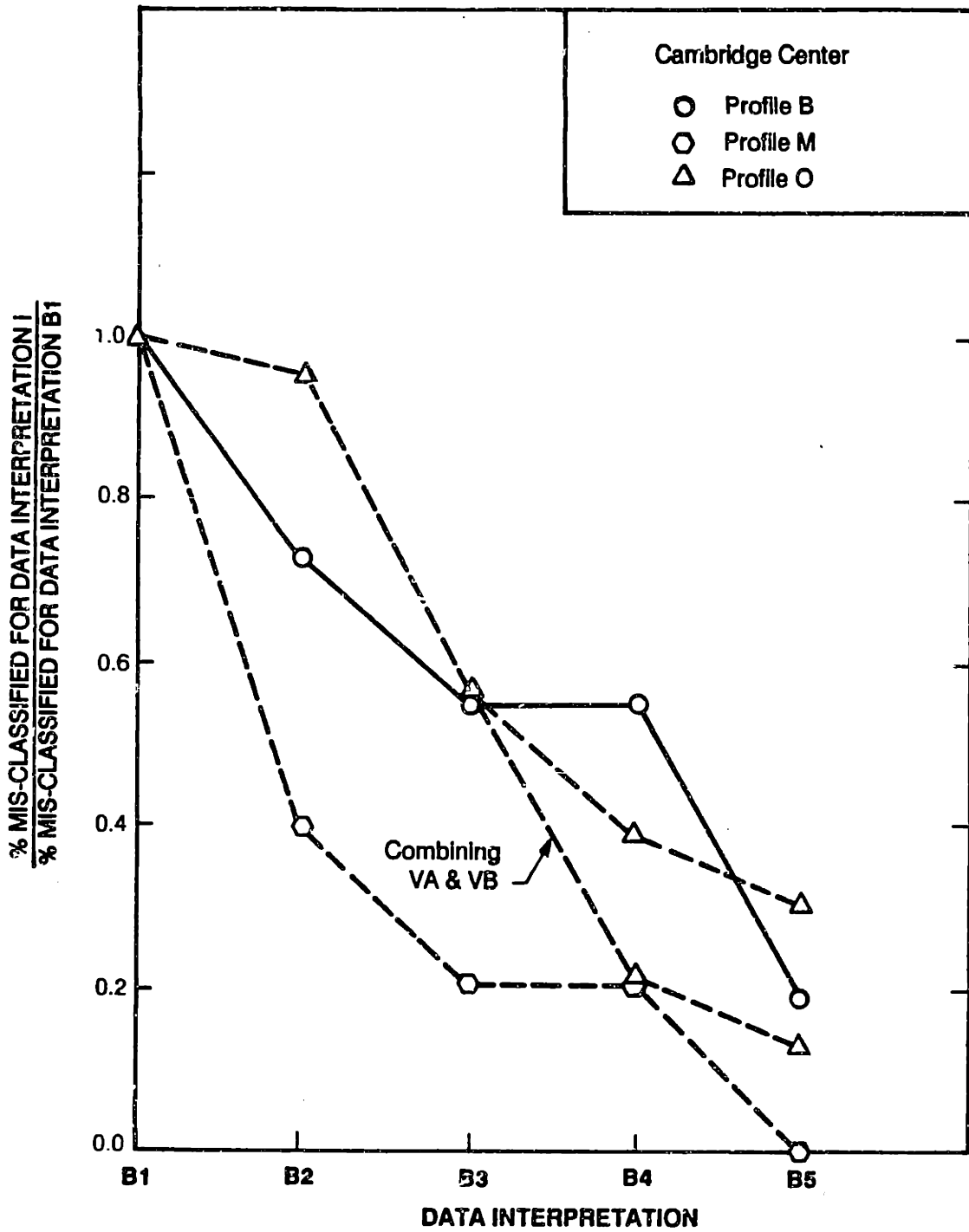
See text for explanation of data interpretations

Figure 4.8 - Relative Mis-classification Errors for Various Clustering Analyses.

Test borings

I

III

IVA

IVB

VB

VB

VB

——— Hand drawn profile line

— — — Regional merging/clustering profile line

20ft

50ft
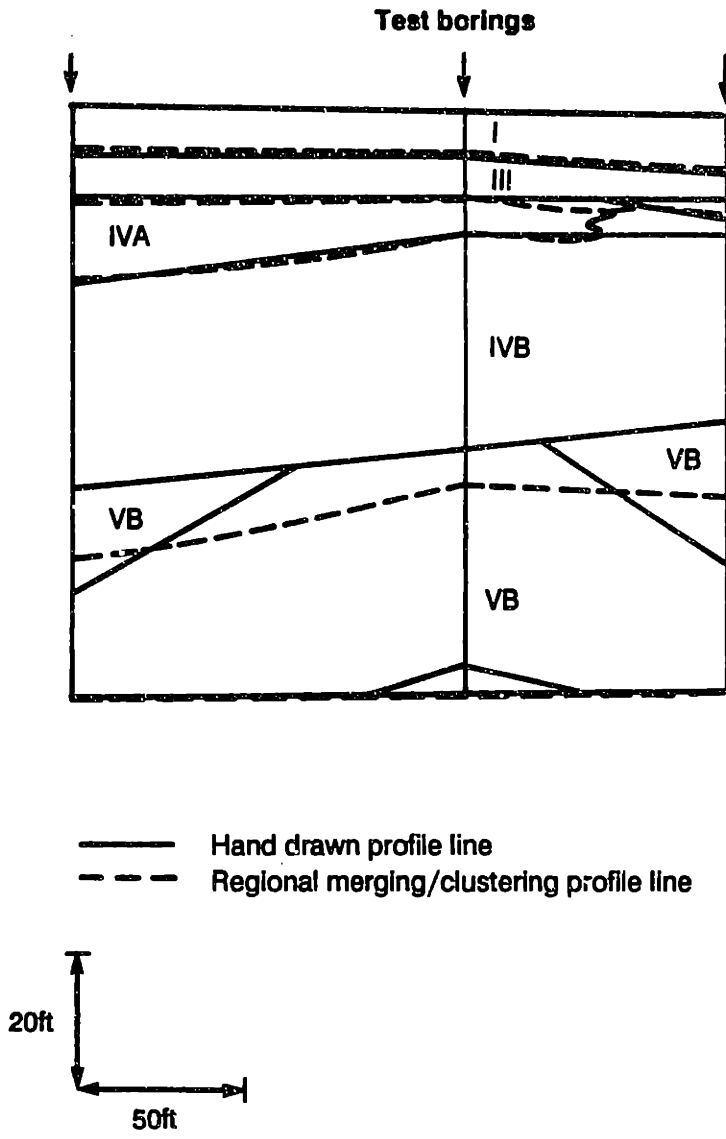
Figure 4.9 - Comparison of Hand Drawn and Clustering Soil Profile, Pro-
file B, Cambridge Center.

Test borings

	5240, *	5240, *	5240, *
	5240, *	3426, 0.17	3426, 0.17
	3426, 0.17	3426, 0.17	3426, 0.17
	2790, 0.17	2790, 0.17	2790, 0.17
		2790, 0.17	2790, 0.17
			2790, 0.17
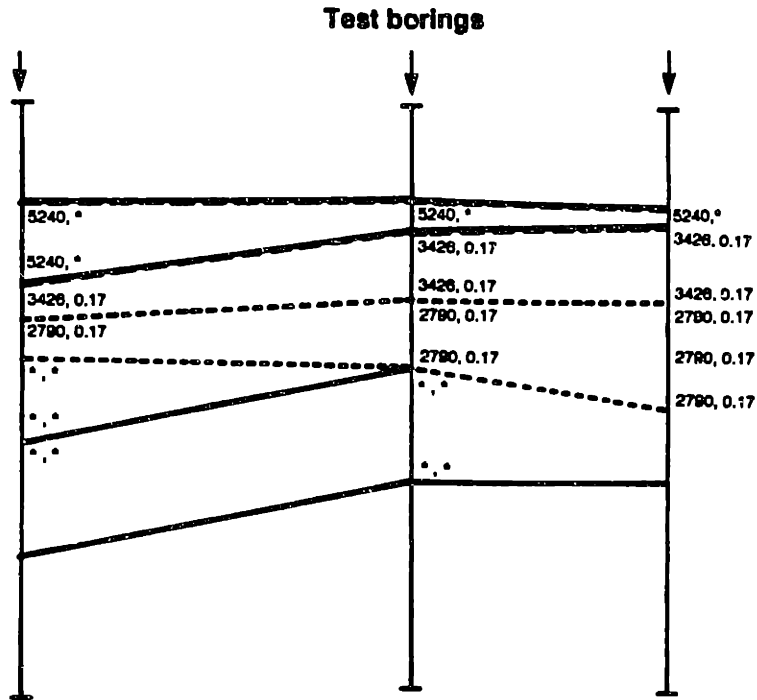
─────── Hand drawn profile line
─ ─ ─ Regional merging/clustering profile line
━ ━ ━ Sub-stratum based on strength clustering

Estimated compressive   Estimated compressibility
strength (psf)   ,   ratio

* - No valid cluster (no estimate)

20ft

50ft
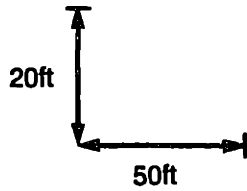
Figure 4.10 - Estimated Soil Properties, Profile B, Cambridge Center.
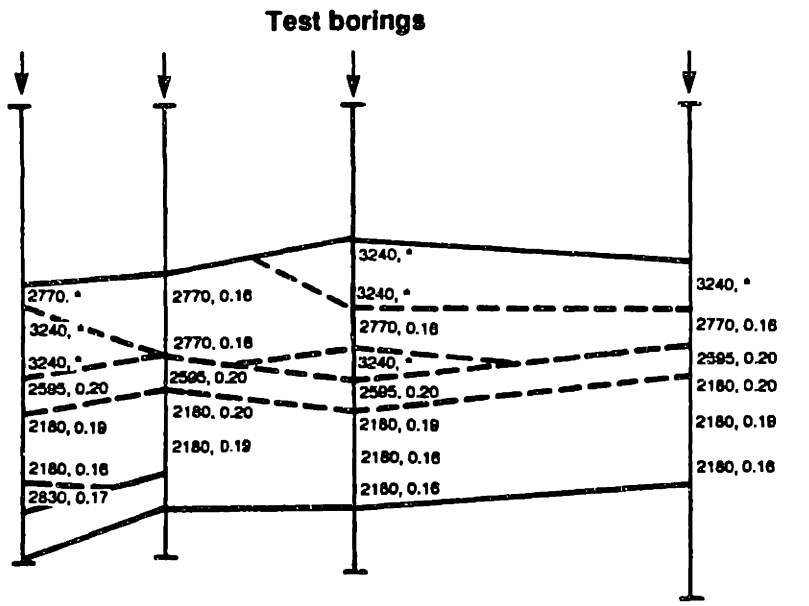
114

Test borings

2770. *

3240, *

3240, *

2595, 0.20

2180, 0.19

2180, 0.16

2830, 0.17

2770, 0.16

2770, 0.16

2595, 0.20

2180, 0.20

2180, 0.19

3240, *

3240, *

2770, 0.16

3240, *

2595, 0.20

2180, 0.19

2180, 0.16

2180, 0.16

3240, *

3240, *

2770, 0.16

2595, 0.20

2180, 0.20

2180, 0.19

2180, 0.16

—————— Hand drawn profile line
— — — Regional merging/clustering profile line

Estimated compressive   Estimated compressibility
strength (psf)   ,   ratio

* - No valid cluster (no estimate)

20ft

50ft
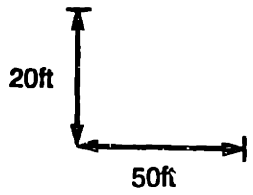
Figure 4.11 - Estimated Soil Properties, Profile M, Cambridge Center.

115

Test borings

	5240, *		3600, *		
	3600, *	3600, *		3600, *	3600, *
2620, 0.16	2620, 0.16		2620, 0.16		2020, *
2600, 0.18	3600, *		3600, *		2810, 0.18
2600, 0.20	2600, 0.18,		2600, 0.18		
2810, 0.13	2600, 0.20		2600, 0.20		2600, 0.20
	2810, 0.13				2180, 0.20

————— Hand drawn profile line

— — — Regional merging/clustering profile line

Estimated compressive   Estimated compressibility
strength (psf)   ,   ratio

* - No valid cluster (no estimate)

20ft

50ft
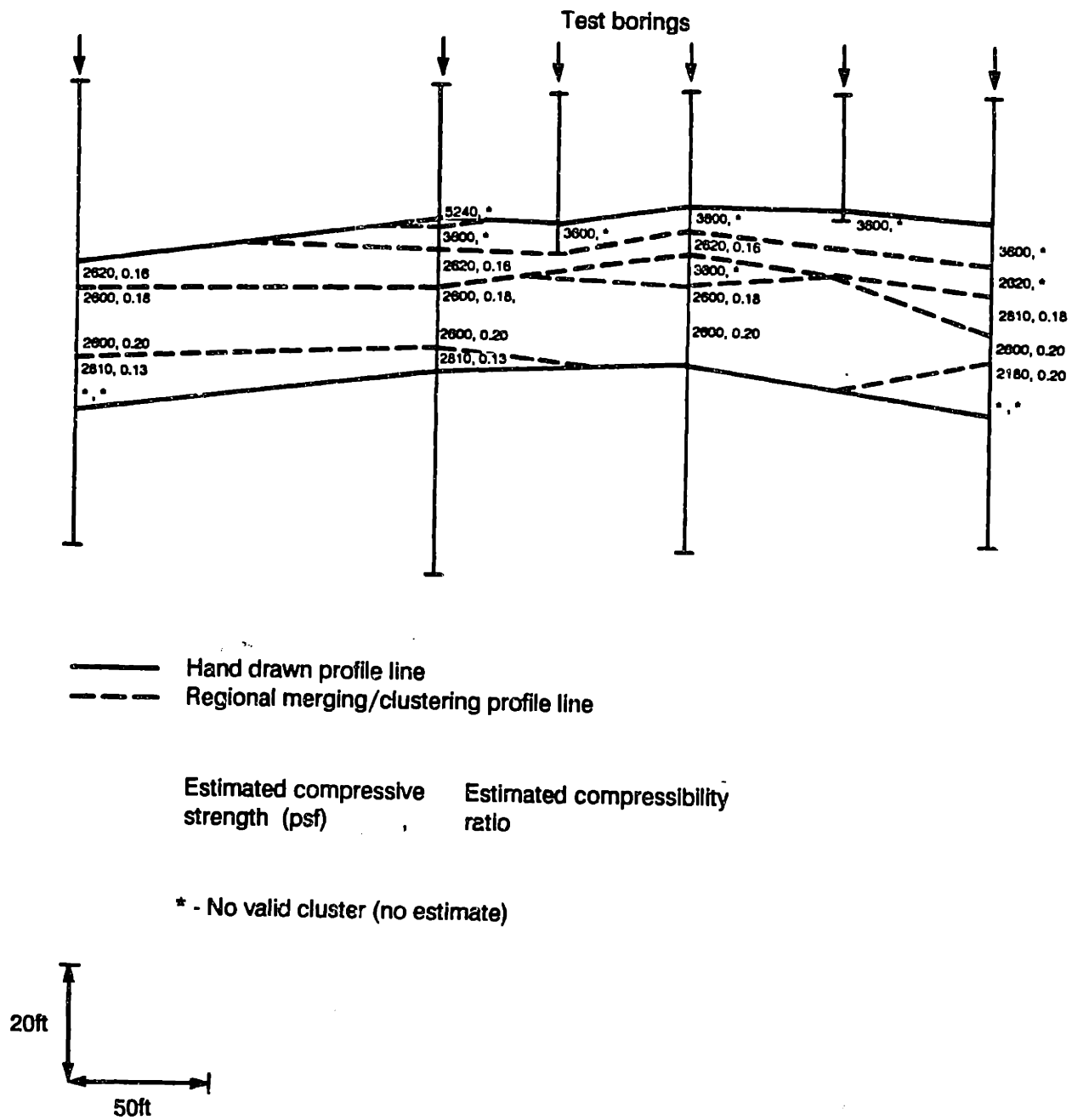
Figure 4.12 - Estimated Soil Properties, Profile O, Cambridge Center.

116

Figure 4.13 - Mis-classification Errors for Various Regional Merging Analyses.
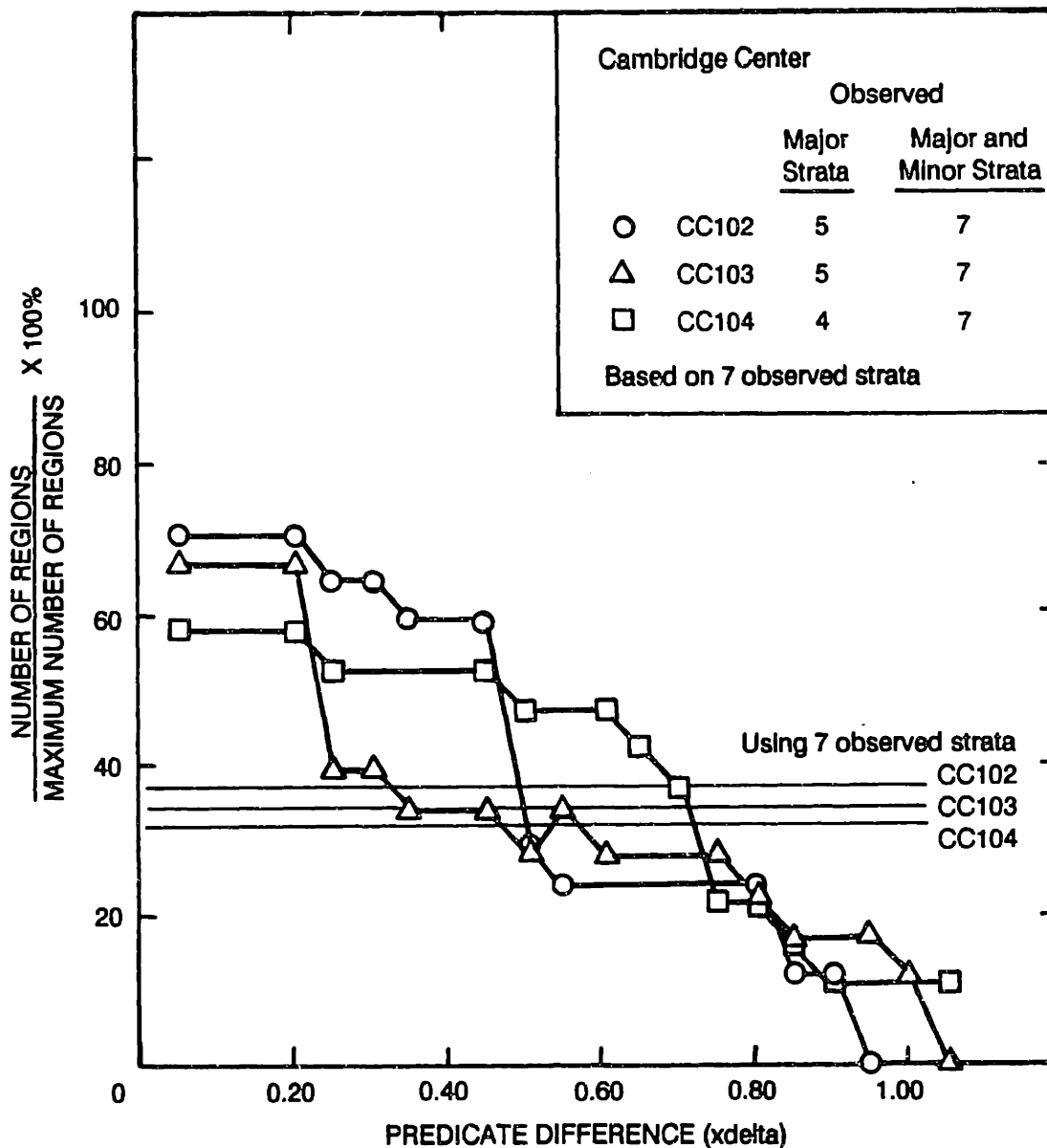
Figure 4.14 - Relative Number of Regions for Various Regional Merging Predicate Differences, Cambridge Center.
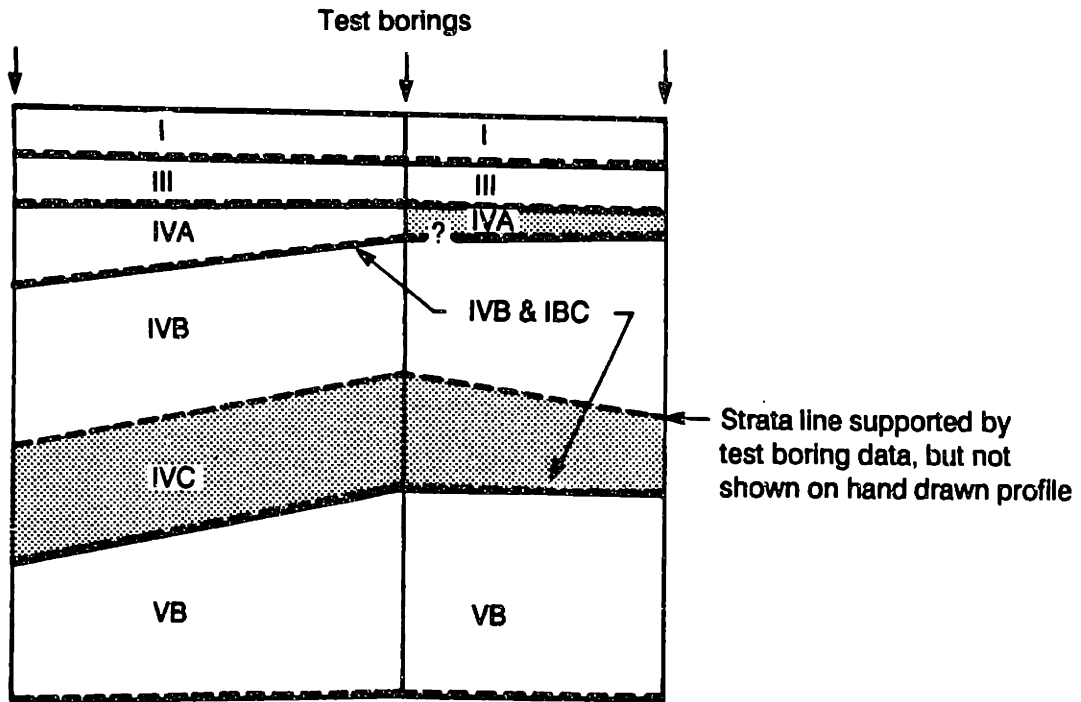
Test borings

I

III

IVA

? IVA

IVB

IVB & IBC

IVC

Strata line supported by
test boring data, but not
shown on hand drawn profile

VB

VB

——— Hand drawn profile line
-- -- -- Regional merging/clustering profile line (xdelta = 0.26)
▓▓▓ Areas of difference

20ft

50ft
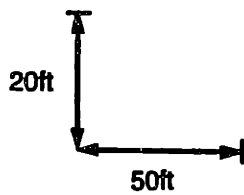
Figure 4.15 - Regional Merging Profile (predicate difference — 0.26),
Profile B, Cambridge Center.
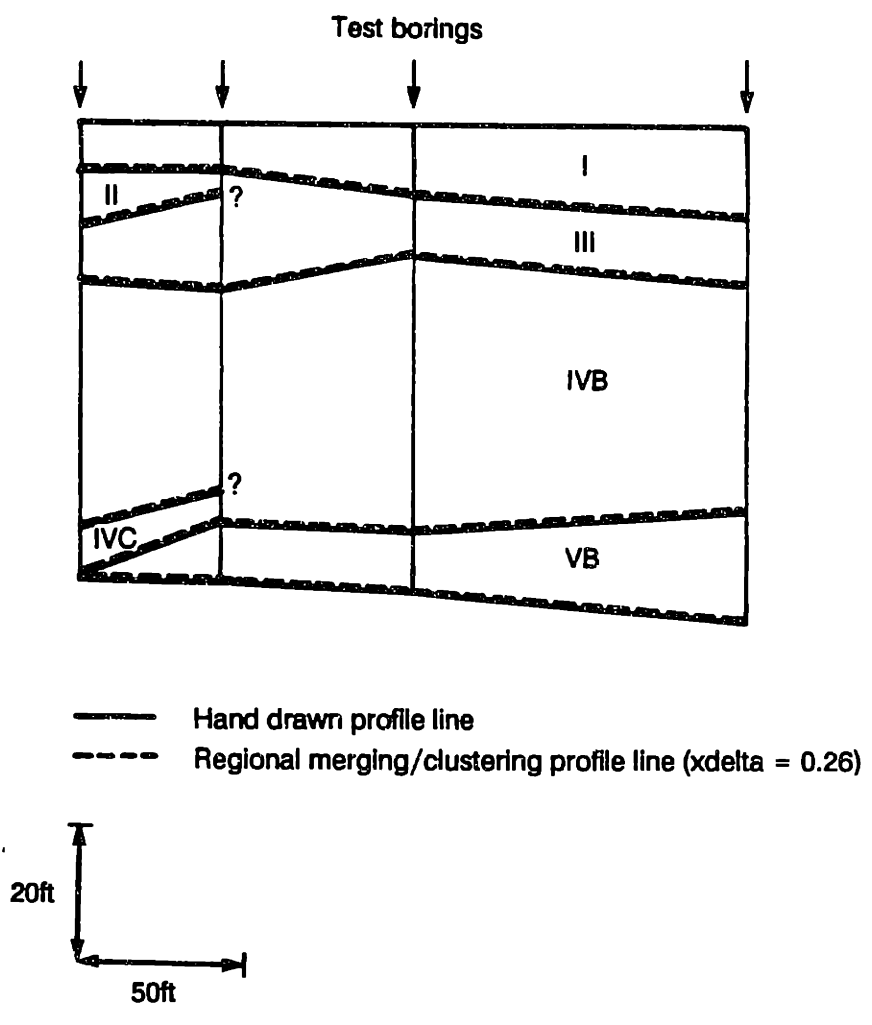
Figure 4.16 - Regional Merging Profile (predicate difference - 0.26),
Profile M, Cambridge Center.

Test borings

Not identified as stratum
in log or hand drawn profile

Not well supported
(visual description of
1 sample only)

IVA

IVB

IVC

I

II

III

VB

VA

VA

VA

VB

VB

VB

───── Hand drawn profile line
── ── Regional merging/clustering profile line (xdelta = 0.26)
▓▓▓▓▓ Areas of difference

20ft

50ft
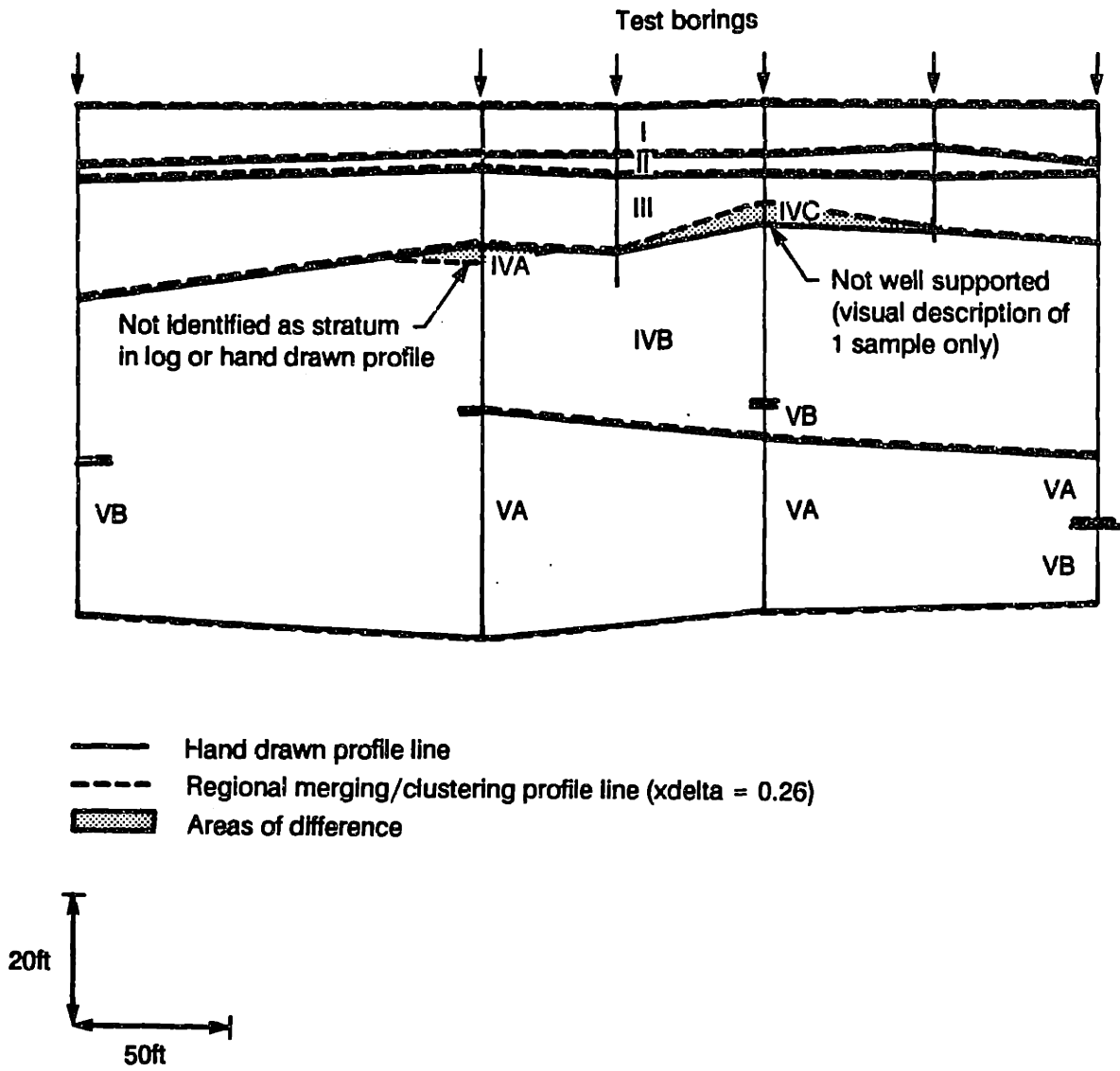
Figure 4.17 - Regional Merging Profile (predicate difference - 0.26),
Profile O, Cambridge Center.

121

Profile B, Cambridge Center

○   Regional Merging (B1*)
△   Clustering
□   Regional Merging/Clustering (Estimated cut)
◨   Regional Merging/Clustering (Optimal cut)
◐   Regional Merging (B4*)

(0.26)   Predicate difference

% OF TOTAL AREA IN AVERAGE REGION
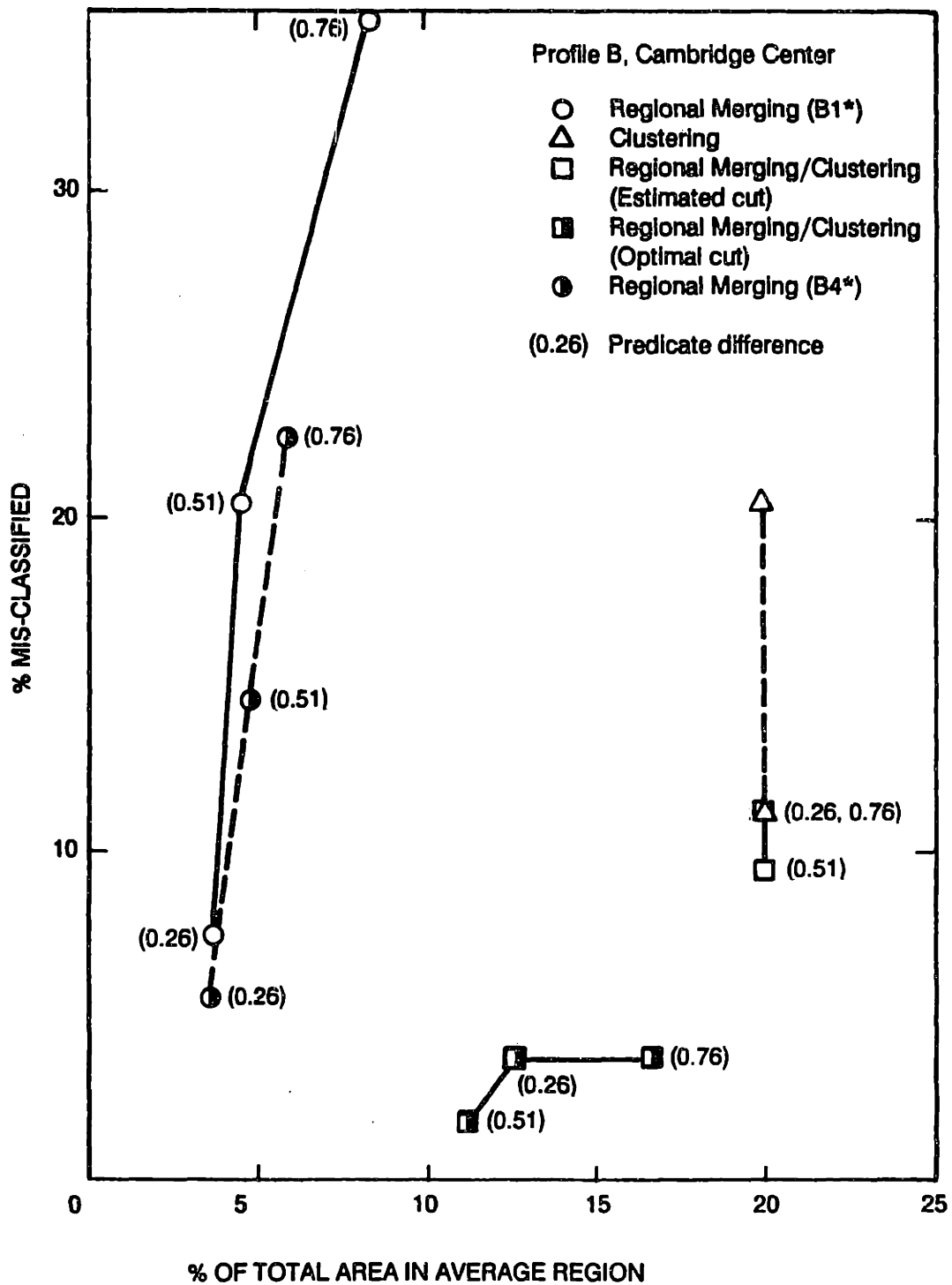
*See text for explanation of data interpretations

Figure 4.18 - Mis-classification Error and Average Region Size for Various Soil Data Preprocessing Methods, Profile B, Cambridge Center.
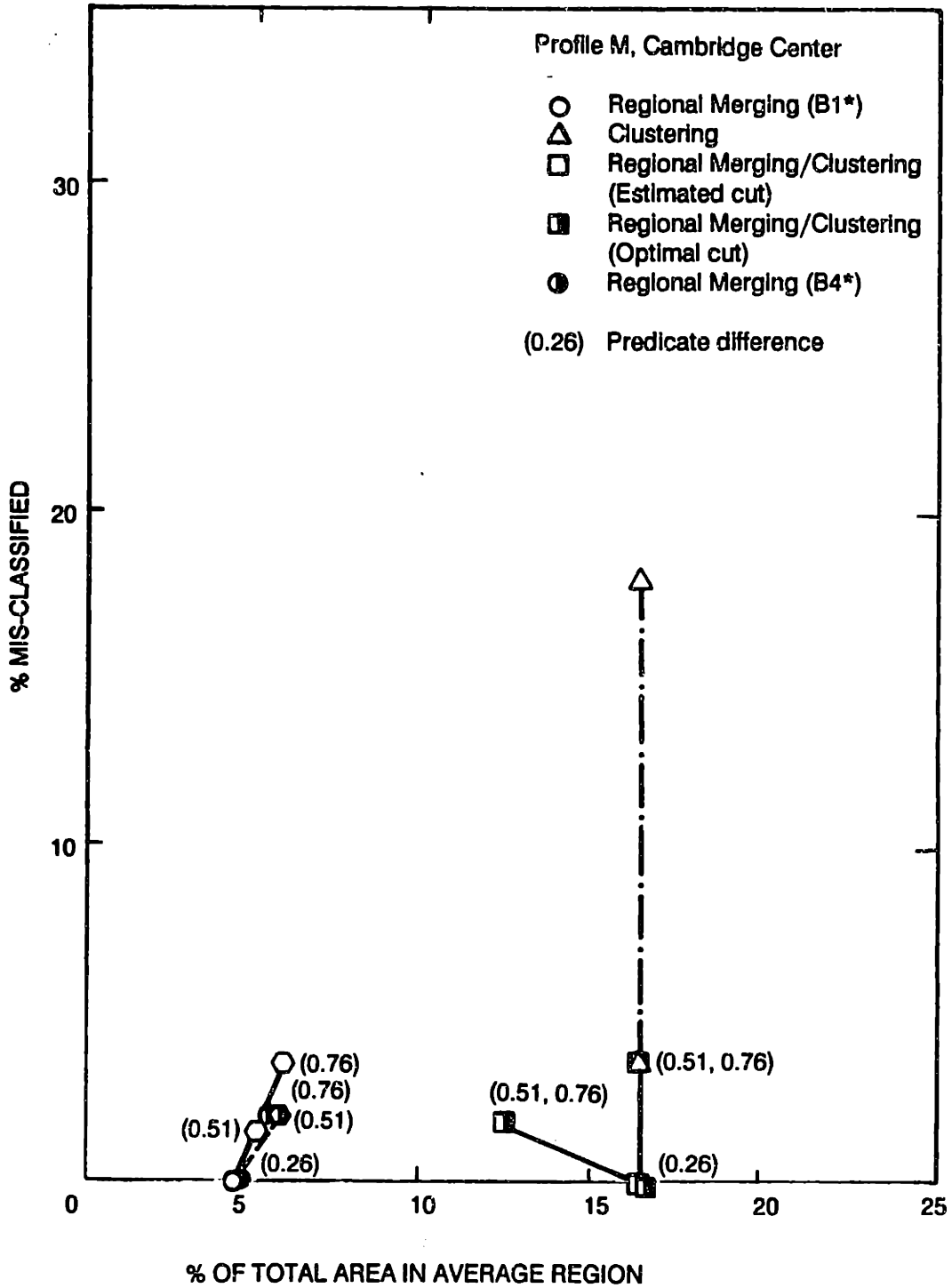
Figure 4.19 - Mis-classification Error and Average Region Size for Various Soil Data Preprocessing Methods, Profile M, Cambridge Center.
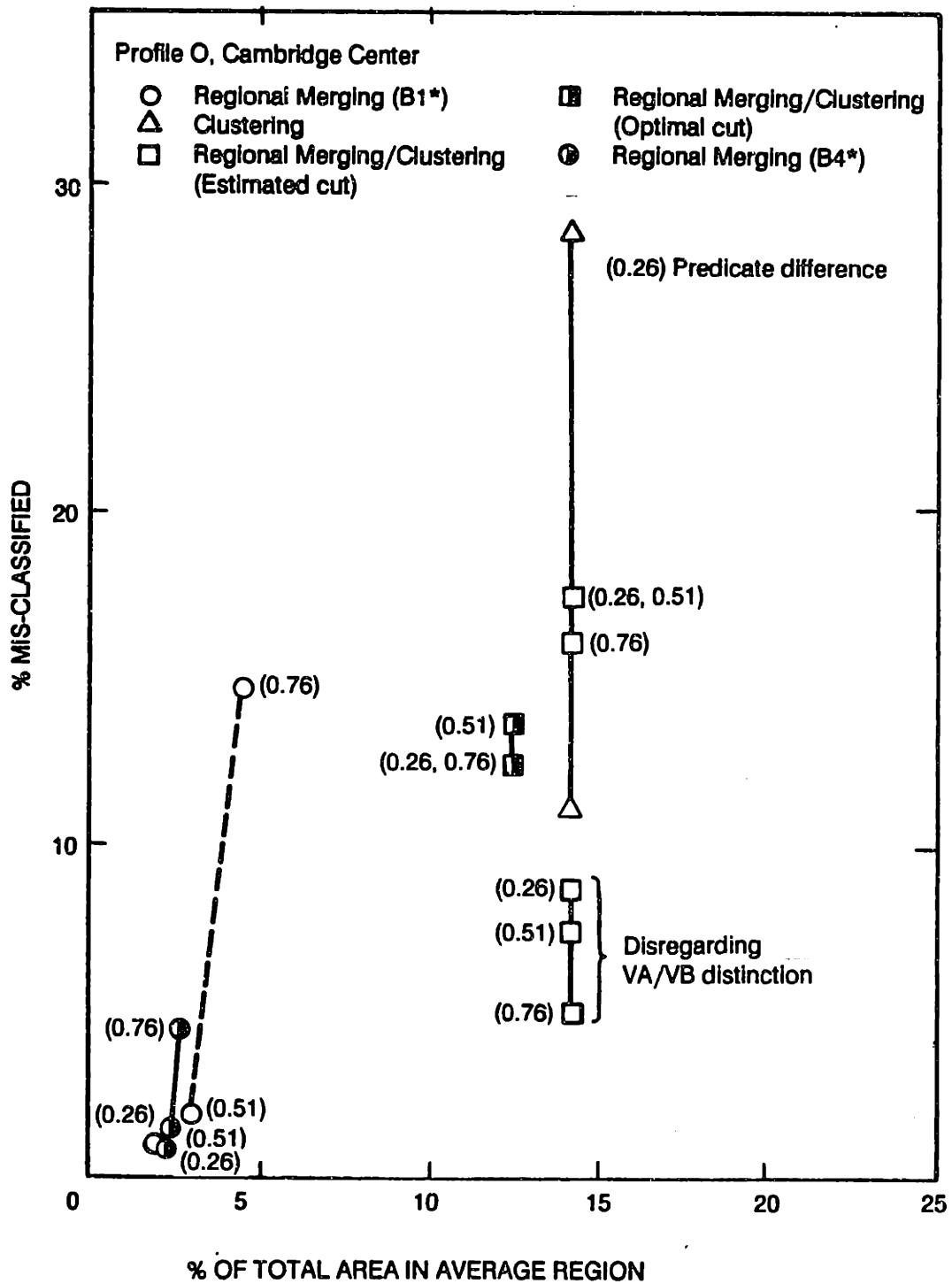
Figure 4.20 - Mis-classification Error and Average Region Size for Various Soil Data Preprocessing Methods, Profile O, Cambridge Center.

CHAPTER 5

SURFACE MODELING

5.1 Introduction

The purpose of this chapter is to review existing analytical techniques which may be appropriate for use in surface modeling, to consider the application of selected techniques to single and multiple surface modeling, and to summarize the advantages and disadvantages of the techniques when applied specifically to soil strata interfaces.

5.2 Objectives

Prior to assessing various modeling techniques, it is helpful to state the desirable properties of an "ideal" surface model, and to discuss the ramifications of compromising these properties. Desirable properties for the development of soil stratigraphy surfaces are as follows:

Continuous Model:

The surface model should be continuous without unexplained discontinuities.

"Honor" Data Points:

The surface model should honor the known data points. Honoring the data points in its strictest definition means that the surface must pass through the strata change data points. In some of the literature, honoring the data points is interpreted to mean that the interpolated contours must be such that the data points fall within a proper contour interval.

"Close Proximity" Data Points:

The number of data points that are used to estimate a surface value at an unknown tested location is a major variable in the surface modeling process. The analytical techniques, described below, vary considerably in the number of data points used in point estimation, and also, in the weight given to the points considered. In soil stratigraphy evaluation it is important that the horizontal dimensions of the zone of influence

around a point to be estimated are consistent with the anticipated distance of significant geologic change. For example, obviously the influence zone of the top of a relatively flat lacustrine deposit is greater than that of a highly eroded, and thus, irregular deposit.

Minimal Estimation Variance:

It is never possible to identify the "real" surface which is being modeled. However, it is desirable to develop a surface model which will have a minimal estimation variance when compare at known locations on the actual surface.

Computational Efficiency:

The practicality of the analytical techniques has been greatly enhanced by the decreasing cost of computer computation resources. Therefore, although computational efficiency was at one time an important consideration, it is now a relatively minor objective.

5.3 Single Surface

5.3.1 Introduction

The logical initial step in the development of subsurface stratigraphy models, after an assessment of the local geology, is to develop models of the soil strata interfaces as single surfaces ignoring for the time being any interdependence between the strata. The Back Bay case history data described in Appendix A was analyzed using the interpolation techniques described in Chapter 3 and below, to develop models of the soil strata as single surfaces.

5.3.2 Interpolation Techniques

Based on the review of existing interpolation techniques (described in Chapter 3), the following techniques were selected and applied to the Back Bay test boring data for the purpose of modeling the single surfaces:

1. Trend Surface Analysis

2. Kriging

3. Delaunay Triangulation

The interpolation techniques were applied to the Back Bay test boring information for the tops of the following soil strata: organic soils, marine sand, Boston Blue clay, glacial till and rock. The remainder of this section is a summary of the analytical techniques used to model these single surfaces.

Trend Surface Analysis:

Trend surface analysis for first through fourth degree least squares polynomial surfaces was performed. Partial results of the fourth degree regression analyses are shown in Figure 5.1. The plots in Figure 5.1 demonstrate the ability of trend surface analysis to produce very smooth, visually appealing contours. However, it must be remembered that the geometric shape of the trend surface model is set by the degree of the regression polynomial, and that the regression process determines the polynomial coefficients that minimize the square of the deviations at the data points.

All of the data points contribute to the least squares regression coefficients, and subsequently to the estimation of any interpolation point. The level of influence for any given data point is referred to as the "leverage", which is in part a function of the distance of the data point from the spatial center of the data (Hoaglin and Welsch, 1978; Unwin and Wrigley, 1987). The leverages of the data points in the trend surface regressions were analyzed. Figure 5.2 is a typical plot of the resulting leverages. Since the data point distribution is approximately rectangular, the leverage increases with the di: ance from the spatial center of the data. Typically, it is recommended that data points with a leverage exceeding twice the average be reviewed for data accuracy (Unwin and Wrigley, 1987).

As part of the trend surface analysis, the goodness-of-fit coefficient was calculated for the Back Bay data. The calculated goodness-of-fit coefficients are summarized in Figure 5.3. The calculated values range from 0.03 to 0.9. Relatively high values (0.3 to 0.9 depending on the degree of the polynomial) were calculated for the tops of the marine sand, glacial till and rock strata. Moderately low values (0.03 to 0.40) were obtained for the tops of the organic soils and the Boston Blue Clay.

Assessing goodness-of-fit coefficients is an exercise in sound judgement since third and fourth degree polynomials will commonly provide high fits (0.8), and randomly generated data sets within the range of the actual data can result in goodness-of-fit values of 0.5 to 0.6 (Davis, 1986).

Conclusions concerning the trend surface analysis of the top of soil strata data for the Back Bay case history are as follows:

1. The goodness-of-fit for the marine sand, glacial till and rock is higher than for the organic soils and Boston Blue Clay (for fourth degree polynomials, approximately 0.9 vs. 0.3 to 0.4).

2. The higher goodness-of-fit coefficients were calculated for the three soil strata with the largest variance in the observed data.

3. All of the trends surface regressions were statistically significant (alpha − 0.05) with the exception of the first and second degree regression for the top of the organic soils (see Appendix A for results).

4. Increasing the degree of the trend surface regression was statistically significant (alpha − 0.05) except for the increase from first to second degree for the organic soils; from second to third degree for the marine sands, glacial till, and rock; and from third to fourth degree for the organic soils (see Appendix A).

5. Depending on the distribution of the data points for a particular stratum, typically 6 to 12% of the data points had leverages in excess of twice the average leverage.

Trend surface analysis was also applied to the strata interface and thickness data from the Cambridge Center case history. The results of this analysis are summarized in Appendix B.

Figure 5.4 is a comparison of the results for fourth degree trend surface analysis of both case histories. The basic conclusion drawn from Figure 5.4 is that for those cases where the goodness-of-fit is greater than 0.5, the trend surface models of the Back Bay data were better. When the goodness-of-fit value was less than 0.5, which really indicates the lack of any significant fit, neither site was consistently modeled better.

Considering the modeling objectives discussed above, trend surface analysis, as demonstrated by these two case histories, has several strengths and weaknesses. On the positive side, trend surface analysis results in a continuous model that is computed efficiently by selecting model parameters that minimize the squared residuals. However, the surface model does not honor the original data points, and contrary to the concept of "close proximity" data points, the model at any point is based on consideration of all the data points. Another disadvantage of trend surface analysis is that the general shape of the surface is set by the polynomial order selected by the user (see Figure 3.3).

Kriging:

Kriging analysis of the soil strata interfaces was performed using the method of estimating the order of the intrinsic random function and the generalized covariance. This process was accomplished using a modified version of the computer program AKRIP developed by Kafritsas and Bras (1981).

As discussed in Chapter 3, the determination of the structural model described in Kafritsas and Bras (1981) is based on the research by Delfiner (1976). The process involves: 1) identification of the order of the intrinsic random function; 2) determination of the coefficients of

the general covariance model that are appropriate for the order of the intrinsic random function; and 3) selection of the "best" generalized covariance model from those identified in 2.

A slightly modified version of the computer program AKRIP was used to evaluate the soil strata interface data from the Back Bay case history. Plots of the estimated surfaces and the variance of the estimates are shown in Figures 5.5 through 5.9 (see Appendix B for additional results).

Compared to the trend surface models of the same data (Figure 5.1), the kriging estimates of the strata surfaces show considerably more irregularity and relief. Of the strata tops modeled, the two models for the top of the glacial till appear visually to be most similar. The kriging estimate of the variance about the estimated surface can be used as a measure of the level of uncertainty in the model. The variance is generally less than 10 for the organic soils, marine sands, and Boston Blue Clay. However, the variance is greater than 60 for most of the glacial till and rock models.

Once again, the kriging model can be compared to the model objectives presented in the introduction to this chapter. The kriging model is continuous, honors the data points, uses "close proximity" data points, and minimizes the estimation variance. Also, using the program AKRIP, the kriging model can be computed efficiently. Therefore, the kriging model satisfies all the objectives of the surface model.

Delaunay triangulation:

Delaunay triangulation can be used as an interpolation technique (Watson and Philip, 1984a) since it creates a piece-wise planar surface model. However, intuitively Delaunay triangulation models do not satisfy the surface model objectives stated above with the exception of honoring the data points and using "close proximity" data points. These are important objectives; however, since Delaunay triangulation modeling results in a discontinuous model (piecewise planar), without consideration of minimal estimation variance, and requires a reasonable amount of computation, it

obviously satisfies fewer objectives than kriging. Therefore, Delaunay triangulation was not used directly as an interpolation method in this research.

Delaunay triangulation methods were used, however, for slightly different purposes. Delaunay triangulation has been used in this research as a means of representing the hand methods currently used in practice. This assumption was made because the triangulation methods honor the original data and are based on the straight line interpolation of local data only.

Where used in this research, Delaunay triangulation was accomplished using a computer program developed as part of the research and based on the algorithm in ACORD (Watson, 1982). Although the Delaunay triangulation technique was not used as an interpolation method, it was used for the development of surface models and profiles as discussed in the remaining sections of Chapter 5 and Chapter 6.

5.3.3 Comparison of Interpolation Techniques

The previous section presents the results of applying selected analytical techniques to the development of single surface models. In order to compare the results of the various techniques in more detail, a single soil interface (top of rock in the Back Bay case history) was selected for further study.

The top of rock data for the Back Bay case history was selected for several reasons including the relatively large variation in the observed elevations (El. -80.7 to -154.9), and the number of observations (77) which while relatively large was still considered to be a manageable number for hand contouring.

The top of rock data was analyzed using two approaches. First, all 77 of the available data points (see Figure 5.10) were used to develop single surface models of the top of rock as described in the previous section. The models were developed using trend surface analysis, kriging, and Delaunay triangulation techniques. Second, the total data set (77 points) was randomly divided in approximate halves such that 40 points

were used to develop models using the same techniques, and then the resulting models were used to estimate values at the remaining 37 data locations.

Using the various developed models, estimates of the top of rock were made at the location of the 37 data points deleted from the original data set. Residuals were then calculated for each data point location for each of the models to complete a relative comparison. Where appropriate, residuals were also calculated at the 40 original data locations.

The residuals for the analytical procedures (trend surface analysis, kriging, and Delaunay triangulation) are summarized in Figure 5.11 and Table 5.1.

Conclusions regarding the residuals are as follows:

1. The Delaunay triangulation and kriging procedures honor the data points completely and, therefore, there are no data point residuals. The trend surface analysis, based on a least squares fit, minimizes the square of the residuals at the data points. The 4th degree least squares regression for the top of rock results in a mean residual of 2.2×10^{-17} ft. and a standard deviation of 5.23 ft. The standard deviation of the data residuals for lesser degree regressions ranged from 14.58 to 8.92 ft. The standard deviation for the 1st degree trend surface (14.58 ft.) approaches the standard deviation of the top of rock data (18.22 ft.) disregarding any spatial relationship.

2. The residuals at the interpolated points had larger absolute value means and standard deviations than the residuals at the data points. The Delaunay triangulation method had the lowest absolute value mean residual (0.64 ft.), followed in order by the kriging method (1.00 ft.) and 4th degree trend surface method (1.44 ft.). The standard deviations of the estimate residuals were 5.71 ft. for kriging, 6.67 ft. for 4th degree trend surface, and 7.52 ft. for the Delaunay triangulation method.

3. The standard deviation of the residuals for trend surface models decreased as the degree of the regression polynomial increased. The mean residual varied from 1.23 to 1.44 ft. for first through fourth degree surface models.

Dahlberg (1975) compared the relative performance for contouring data by hand and computer. Dahlberg concluded that computer generated contouring is technically correct, but may pass over details that were perceived to be important by the individuals doing the hand contouring. However, he observed also that the computers were not subject to the biases of man.

In order to assess hand contouring performance and compare it to other interpolation methods, nine individuals were given the same 40 top of rock data points (shown in Figure 5.10) and asked to develop 10 ft. interval contours of the top of rock (see Appendix A for the hand drawn contour plans).

The hand-drawn contour plans were used for two purposes. Using straight line interpolation, residuals at the 40 data points were calculated for each contour plan. Since the hand drawn contour lines differed in their lateral extent and typically did not extend beyond the convex hull sur-rounding the data points, residuals could be calculated for 20 to 27 of the original 40 data points. The mean data point residuals varied from -0.003 to 0.48 ft. with standard deviations from 0.93 to 1.57 ft. (see Table 5.2).

Residuals at the 37 interpolated points were calculated using straight line interpolation and each of the nine hand-drawn contour plans. Due to the lateral limits of the hand-drawn contours, estimates could be obtained for only 24 to 31 of the interpolation points. The mean of the residuals varied from -0.18 to 1.90 ft. and the standard deviation ranged from 5.20 to 8.02 ft. (see Table 5.2).

Observations concerning the hand-drawn contour plans and the results of the analysis of data and interpolated points are as follows:

133

1. The hand-drawn contour plans honor the data points reasonably well, as indicated by the residual mean and standard deviation (median values of 0.20 ft. and 1.09 ft. respectively).

2. The residuals at interpolated points are considerably greater than at the data points. Both the mean and standard deviation of the interpolated point residuals are approximately five times those of the data point residuals.

3. The hand-drawn contour plans appear to have been typically developed using linear interpolation between selected subsets of the original data. This observation is inferred from the worksheets provided by the individuals doing the contouring.

4. A visual review of the hand-drawn contour plans indicates that with one exception the final contours had been smoothed to provide parallel contours. This indicates that the individuals expect that although the raw data may not exhibit parallel contours, that the real surface is composed of parallel contours.

The residuals from the various estimating techniques were further analyzed to permit comparison of the individual hand-drawn contour plans to the analytical techniques. Figure 5.11 presents the results of this comparison as a plot of the mean and standard deviation of the residuals for the various techniques and the data and estimated points. Table 5.3 was prepared to compare the mean and standard deviation from the individual hand-drawn contours to those obtained for the same interpolated points using the analytical techniques.

Of the nine hand-drawn contour plans three (#2, 5 and 8) have mean residuals less than those for kriging, trend surface analysis and Delaunay triangulation for the same interpolation points. Only one hand-drawn contour plan (#9) has a lower standard deviation for the interpolated points than the analytical techniques.

Correlation coefficients were calculated for the interpolated point residuals for all the estimation techniques (see Table 5.4). The coefficients indicate the following:

1. All of the correlation coefficients between the residuals for the hand-drawn contour plans and the trend surface analyses increase as the degree of the regression increases. However, the coefficients for the 4th degree regressions and hand-drawn contours are typically between 0.7 and 0.8.

2. The correlation coefficients between the hand-drawn contour residuals are typically greater than 0.9 with the exception of those associated with #5 which are in the range of 0.68 to 0.95 (median of 0.79).

3. The correlation between the kriging residuals and the hand-drawn contour residuals are in the range of 0.88 to 0.99 (median of 0.95) with the exception of #5 with a value of 0.76 .

4. The correlation coefficients between the kriging residuals and the Delaunay triangulation residuals and the 4th degree trend surface residuals are 0.99 and 0.84 respectively. The latter value is comparable to the coefficient of 0.82 between the Delaunay triangulation residuals and the 4th degree trend surface residuals.

Based on the comparison of the various interpolation techniques using the top of rock data in the Back Bay area, the conclusions are as follows:

1. The interpolation technique with the lowest residual standard deviation (5.71 ft.) is the kriging method.

2. The mean of the residuals for all the techniques was less than 1.5 ft., which is typically within the uncertainty of the strata change information reported in a test boring log.

3. The interpolation technique with the next lowest residual standard deviation (based on the observed median value of 6.36 ft.) is the hand-drawn contour method.

4. The kriging and Delaunay triangulation methods honor the data points completely, while the hand-drawn contours nearly honor the data points with a residual standard deviation of 1.09 ft. (based on the median value).

5.4 Developed Profiles

5.4.1 Introduction

The interpolation methods described above were applied to the Back Bay case history data to produce stratigraphic profiles based upon interpolation estimates of the various soil strata interfaces. The profiles were developed by producing models of each of the soil interfaces and then plotting the intersection of the model surface with a vertical profile plane.

5.4.2 Comparison of Developed Sections

Profiles A and B (shown in Figures 5.12 through 5.15) were produced using the kriging, Delaunay triangulation, trend surface, and hand profiling techniques for modeling the soil strata interfaces. In this analysis hand profiles were created using computer code to find test borings within 100 feet of the profile plane, and to project the located test borings into the plane. The strata interfaces were then drawn by connecting the strata change elevations in adjacent test borings. In each case the strata interfaces were modeled as continuous single surfaces.

The profiles in Figures 5.12 and 5.14 demonstrate the tendency of the hand profiling methods to exaggerate the vertical relief along a surface. Even though the Delaunay triangulation surface is based upon the same data points, the apparent vertical relief in the profile is much greater in the hand drawn profile. This exaggeration is due to the practice of translating the adjacent data points into the profile plane without any change in the elevation value. Therefore, visually the resulting profile appears to have a greater vertical relief across a shorter distance. The top of the organic soils, glacial till and rock, in particular, appear to have considerably more relief.

136

The smooth profiles of the trend surface models are evident in Figures 5.13 and 5.15. It is interesting to compare the smooth trend surfaces, which do not honor the data points, to the more irregular kriging surfaces which do honor the data points.

The profiles demonstrate two problems that occur when using single surface continuous models to model soil stratigraphy. First, even though the test boring data indicate that the marine sand stratum is discontinuous, the stratum has been modeled as continuous. This is attributed to the convenience of continuous surface mathematical models. Second, as demonstrated in Figure 5.15, the kriging model results in the top of rock above the top of the glacial till. This is disturbing from the geology perspective. Although, there were several test borings where glacial till was not observed, it is generally expected that glacial till will be observed continuously above the rock in this area. Therefore, rock above glacial till, represents a geologic incompatibility in the stratigraphic model.

Resolution of the discontinuous/continuous and geologic incompatibilities is addressed in Chapter 6.

5.5 Summary

The research presented in this chapter reviewed existing analytical techniques for surface modeling, and it is concluded that kriging methods should be used for the modeling of single surfaces for the assessment of soil stratigraphy. The comparison of kriging to hand contouring of a selected data set demonstrated that the hand contouring solutions were fairly accurate, but that the kriging methods resulted in slightly lower residuals and an estimate of the variance of the estimated surface. However, when applied to multiple surfaces using actual case history data, the kriging methods create continuous models of discontinuous strata, and result in overlapping soil strata interfaces.

Table 5.1 - Summary of Residuals for Interpolation Methods, Top of Rock, Back Bay.

	Data Points n(max) - 40			Interpolated Points n(max) - 37		
	No. of Pts., n	Mean (ft)	Stand. Dev. (ft)	No. of Pts., n	Mean (ft)	Stand. Dev. (ft)
Trend Sur-face degree - 1	40	0.0005	14.58	37	1.40	14.36
degree - 2	40	0.00025	9.85	37	1.23	8.27
degree - 3	40	0.00025	8.92	37	1.42	8.57
degree - 4	40	2.2×10^{-17}	5.23	37	1.44	6.67
Delaunay Triangula.	40	0	0	37	-0.64	7.52
Kriging	40	0	0	37	1.00	5.71

Table 5.2 - Summary of Residuals for Hand Contouring, Top of Rock, Back Bay.

Individual (# data pts, # inter. pts)	Data Points n(max) — 40		Interpolated Points n(max) — 37	
	Mean (ft)	Standard Deviation (ft)	Mean (ft)	Standard Deviation (ft)
1 (20,29)	0.48	0.93	1.90	8.02
2 (23,31)	0.25	1.01	0.08	6.39
3 (27,26)	0.01	1.17	1.73	5.94
4 (27,30)	0.23	1.00	1.06	6.27
5 (22,24)	0.00	1.16	0.03	6.47
6 (21,24)	0.21	1.19	1.49	7.02
7 (25,30)	0.20	1.00	0.88	6.60
8 (24,29)	0.09	1.09	-0.18	6.14
9 (27,28)	0.04	1.57	1.20	5.20
Median (24,29)	0.20	1.09	1.06	6.39

Table 5.3 - Summary of Residuals for Estimated Points, Top of Rock, Back Bay.

	No. of Pts.	Mean (ft)	Stand. Dev. (ft)	Delaunay Tri.	Trend Surface (4th)	Kriging
		Residual		**Mean/Stand. Dev. Using Same Sample Subset**		
Delaunay Tri.	37	-0.64	7.52	- -	1.44 6.67	1.00 5.71
Trend Surface (4th degree)	37	1.44	6.67	-0.64 7.52	- -	1.00 5.71
Kriging	37	1.00	5.71	-0.64 7.52	1.44 6.67	- -
Hand Contour #1	29	1.90	8.02	0.99 6.12	1.03 5.74	0.67 5.90
#2	31	0.08	6.39	0.83 5.95	1.33 5.75	0.63 5.70
#3	26	1.73	5.94	1.45 5.95	1.68 5.88	0.98 5.84
#4	30	1.06	6.27	0.06 6.68	0.61 6.89	0.97 5.53
#5	24	0.03	6.47	1.50 5.54	1.29 5.67	1.31 5.79
#6	24	1.49	7.02	1.58 6.28	1.27 5.87	1.21 6.12
#7	30	0.88	6.60	1.16 5.98	1.03 5.64	0.82 5.74
#8	29	-0.18	6.14	1.09 6.07	1.02 5.74	0.81 5.84
#9	28	1.20	5.20	1.23 5.88	1.56 5.75	1.01 5.69

Table 5.4 - Correlation of Residuals at Estimated Points, Top of Rock, Back Bay.

	DLT	TS4	KR	HC-1	HC-2	HC-3	HC-4	HC-5	HC-6	HC-7	HC-8	HC-9
DLT	1	.82	.99	.90	.96	.99	.95	.75	.97	.95	.88	.97
TS4	.82	1	.84	.71	.70	.81	.72	.79	.80	.75	.80	.84
KR	.99	.84	1	.88	.95	.99	.95	.76	.97	.95	.88	.97
HC-1	.90	.71	.88	1	.93	.89	.79	.76	.92	.94	.85	.87
HC-2	.96	.70	.95	.93	1	.95	.94	.77	.98	.97	.90	.95
HC-3	.99	.81	.99	.89	.95	1	.94	.75	.96	.93	.87	.95
HC-4	.95	.72	.95	.79	.94	.94	1	.68	.92	.90	.86	.94
HC-5	.75	.79	.76	.76	.77	.75	.68	1	.84	.81	.95	.86
HC-6	.97	.80	.97	.92	.98	.96	.92	.84	1	.98	.94	.99
HC-7	.95	.75	.95	.94	.97	.93	.90	.81	.98	1	.92	.95
HC-8	.88	.80	.88	.85	.90	.87	.86	.95	.94	.92	1	.96
HC-9	.97	.84	.97	.87	.95	.95	.94	.86	.99	.95	.96	1

DLT, Delaunay Triangulation   TS4, Trend Surface (4th degree)
KR, Kriging   HC-1, Hand Contouring (Individual 1)
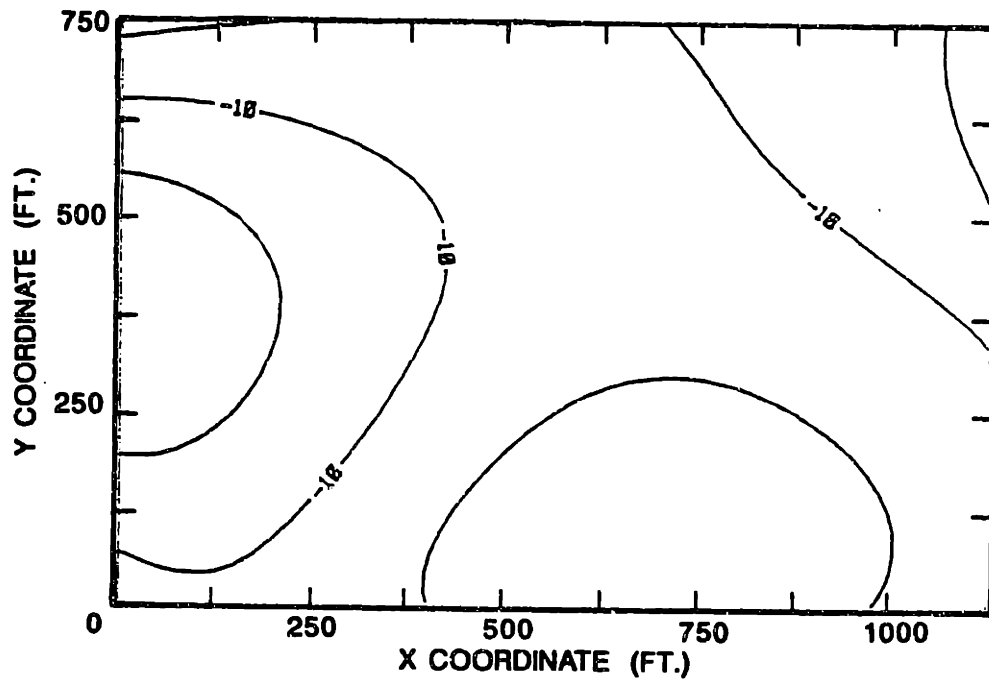
(a) Top of Organic Soils,
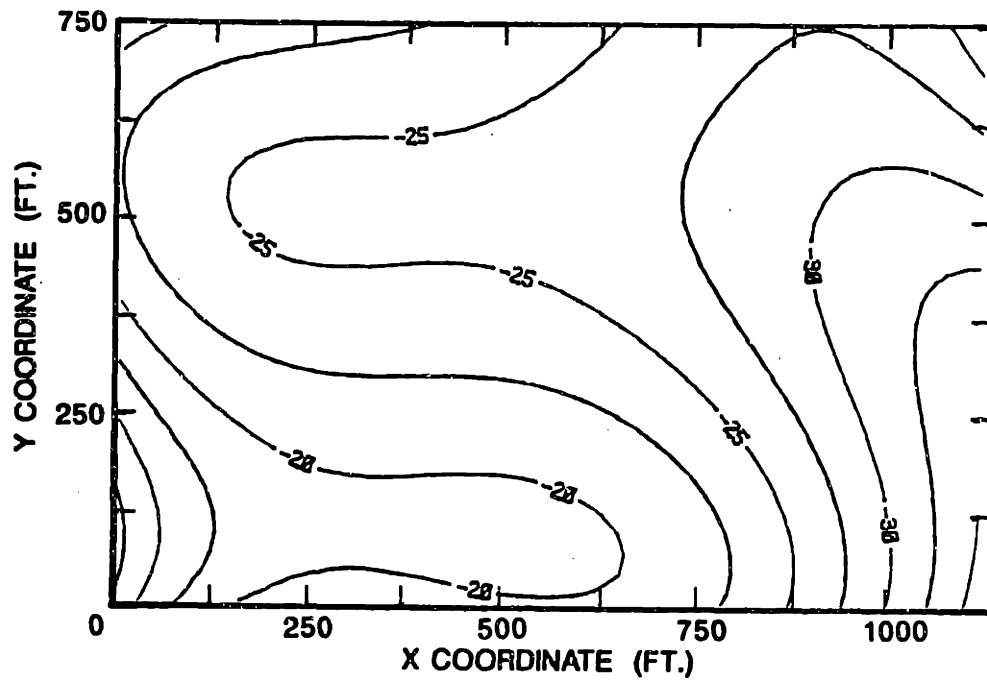
(b) Top of Marine Sands,

Figure 5.1 - 4th Degree Trend Surface Models, Back Bay.

142
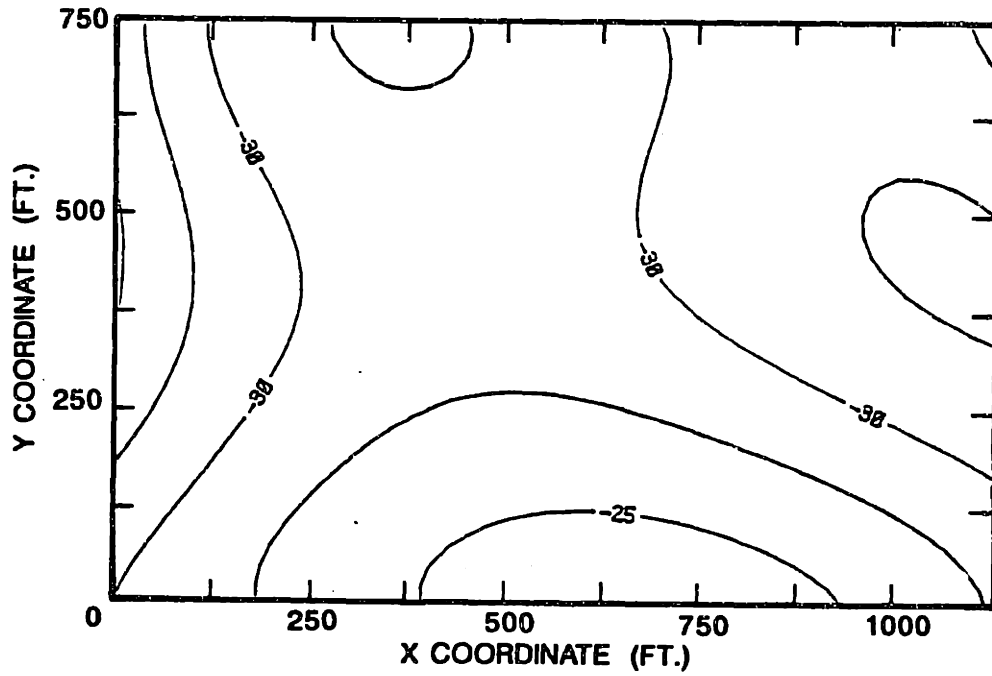
(c) Top of Boston Blue Clay,
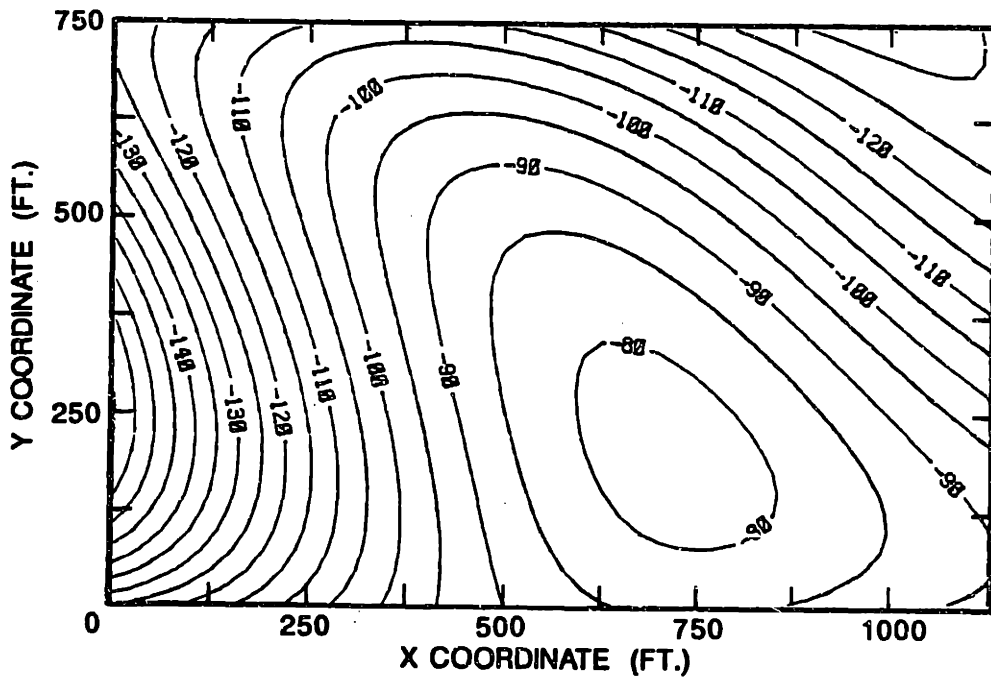
(d) Top of Glacial Till,

Figure 5.1 - Continued.

143
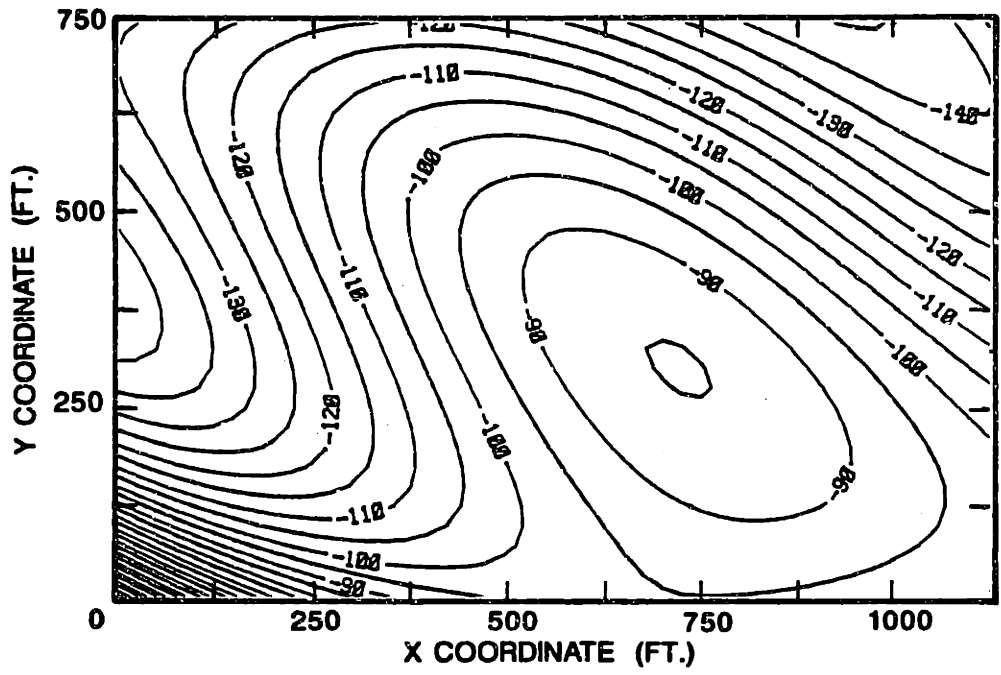
(e) Top of Rock.

Figure 5.1 - Continued.
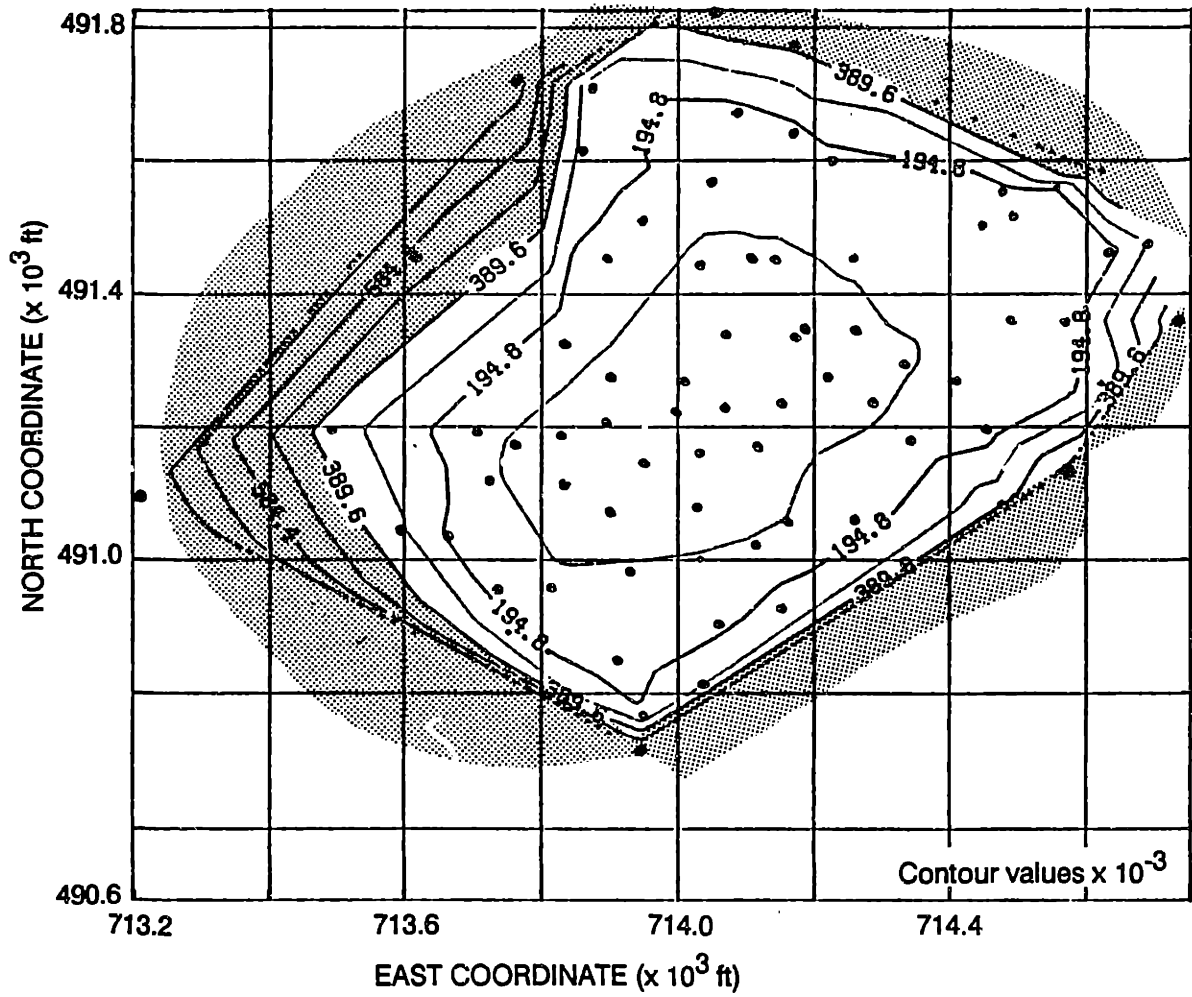
Figure 5.2 - Contours of Leverages, 4th Degree Trend Surface Model of Top of Rock, Back Bay.
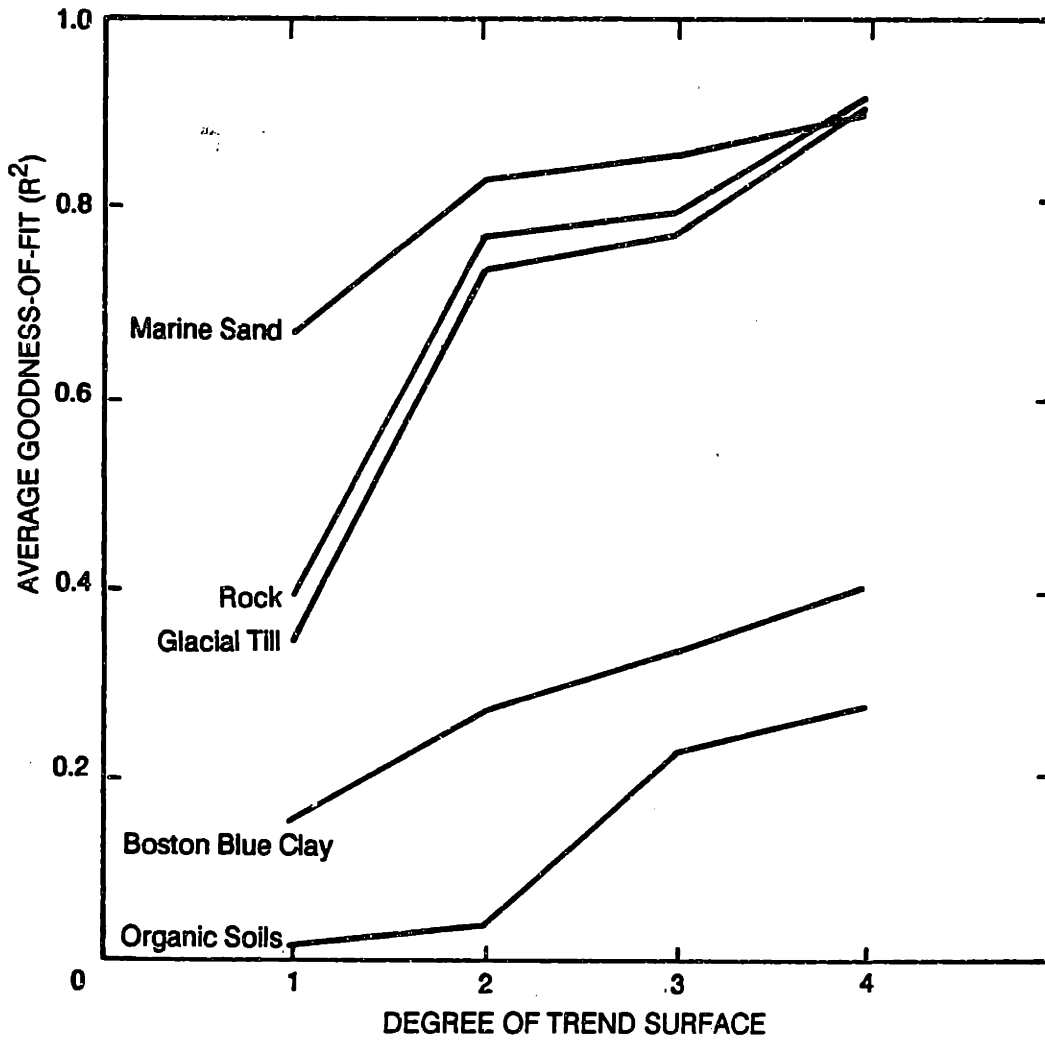
Figure 5.3 - Summary of Trend Surface Goodness-of-Fit Coefficients, Strata Tops, Back Bay.
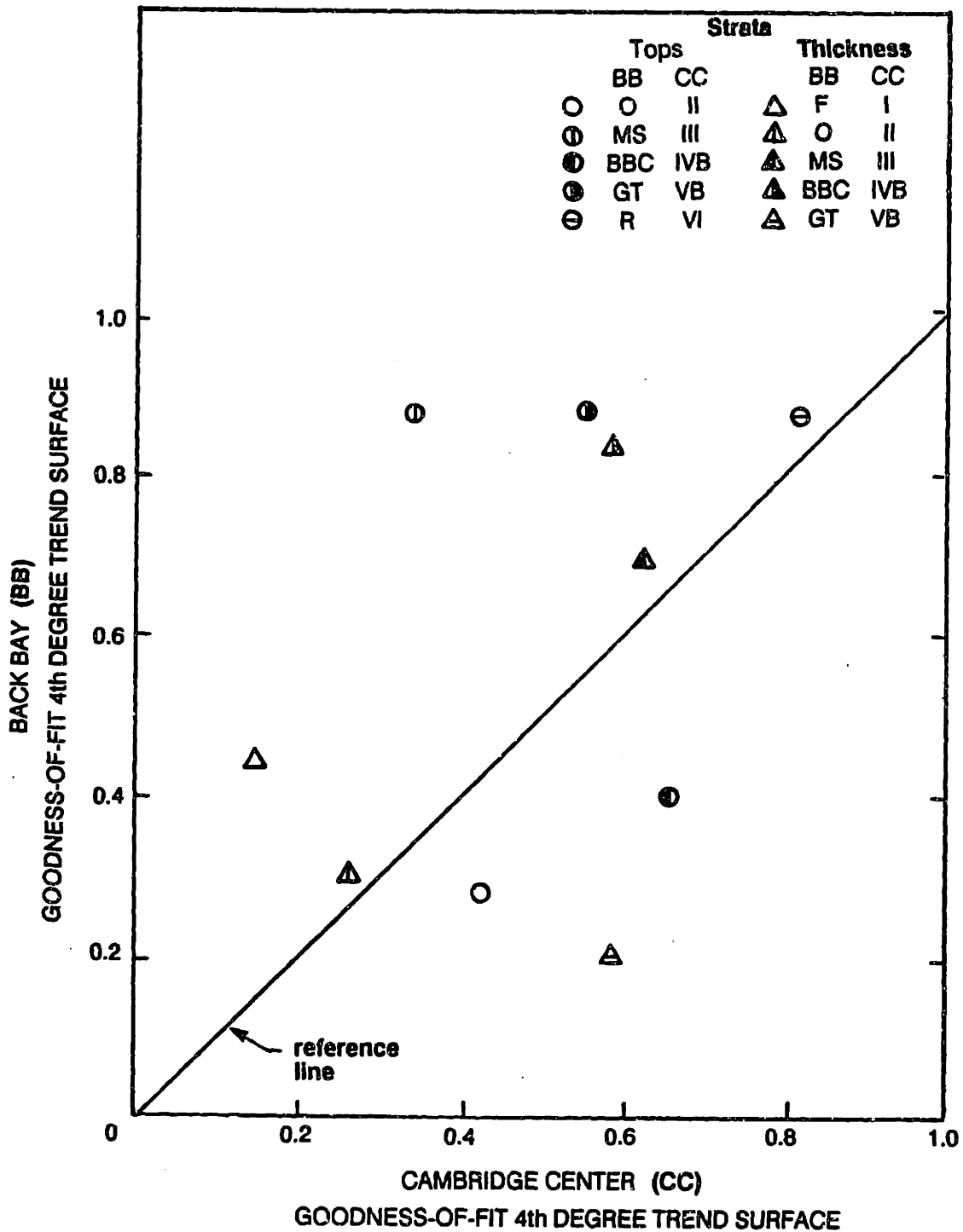
Figure 5.4 - Comparison of Goodness-of-fit Coefficients, Strata Interface and Thicknesses, Back Bay and Cambridge Center (see Appendices A and B for strata designations).
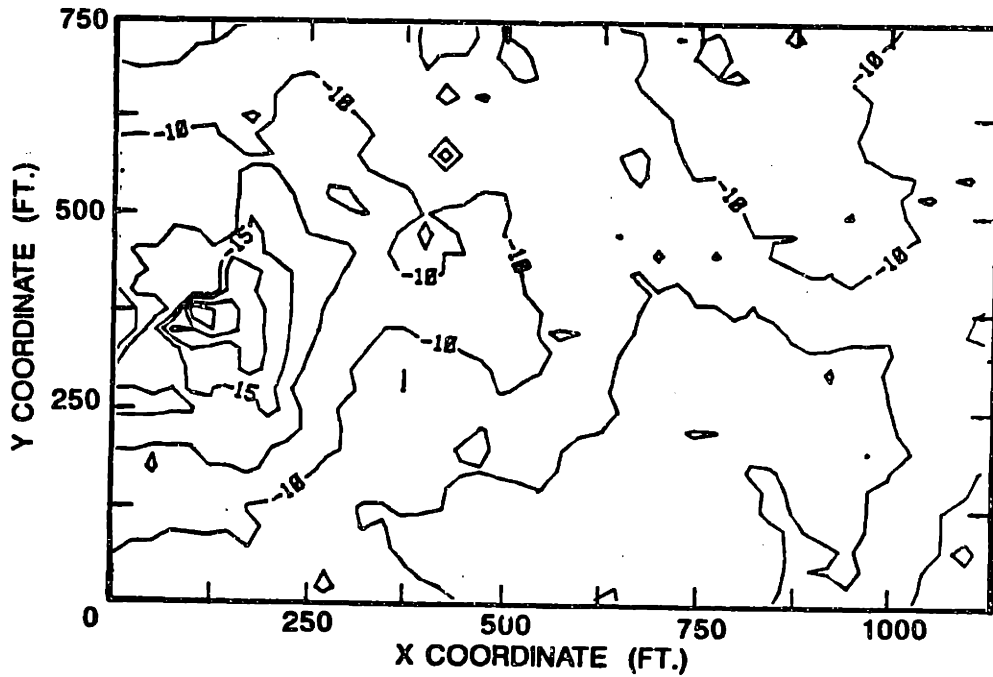
(a) Kriging Estimate of Top of Organic Soils,
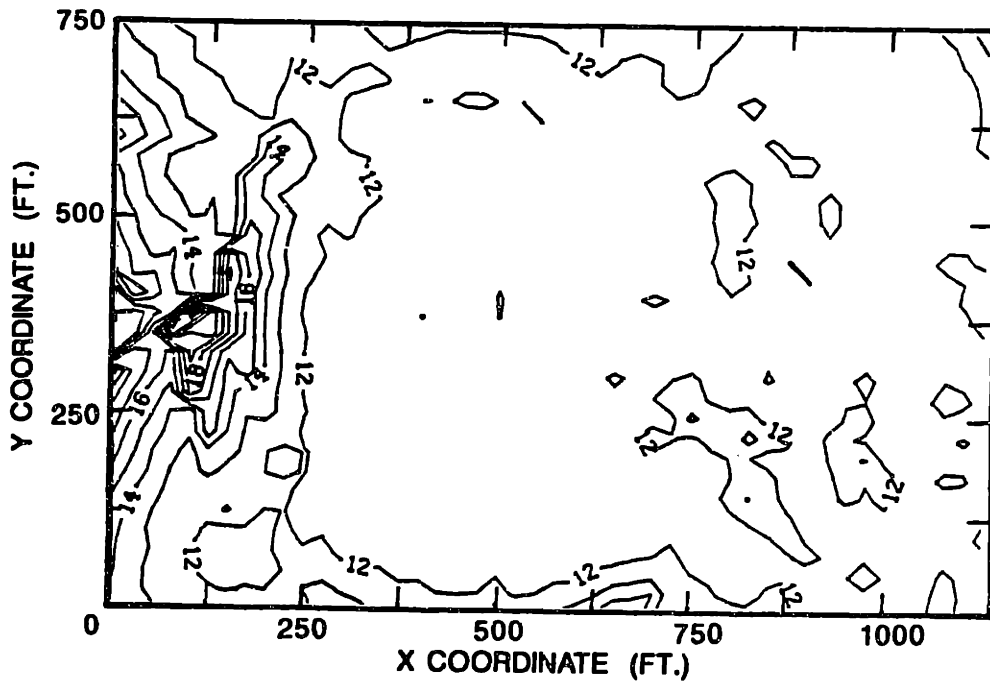
(b) Kriging Estimate of the Variance About the Estimated Surface.

Figure 5.5 - Kriging Analysis of the Top of Organic Soils, Back Bay.

148
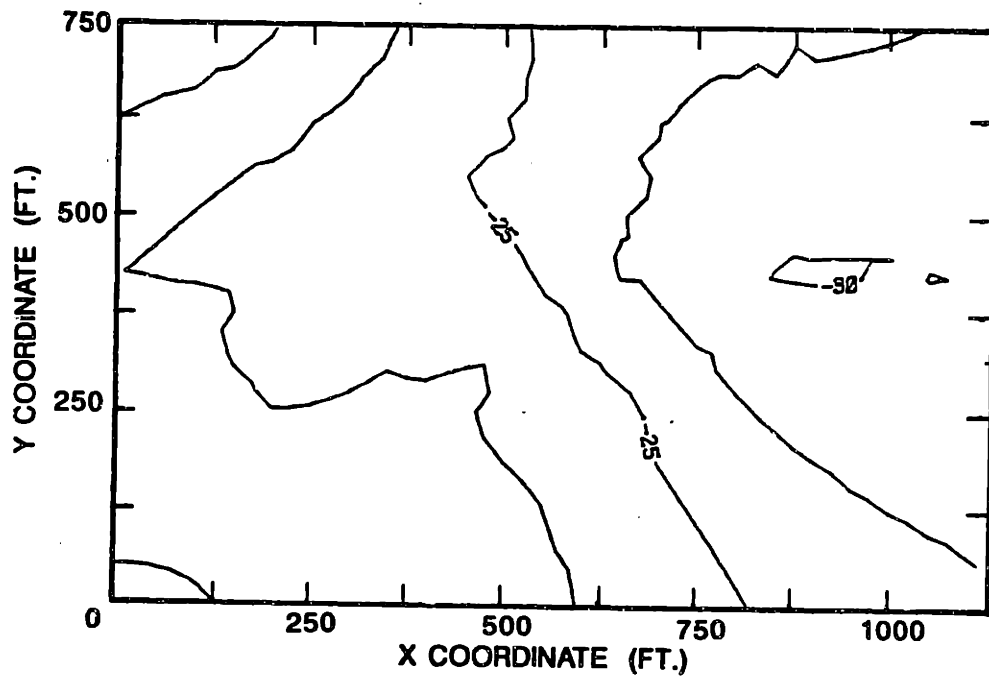
(a) Kriging Estimate of Top of Marine Sands,
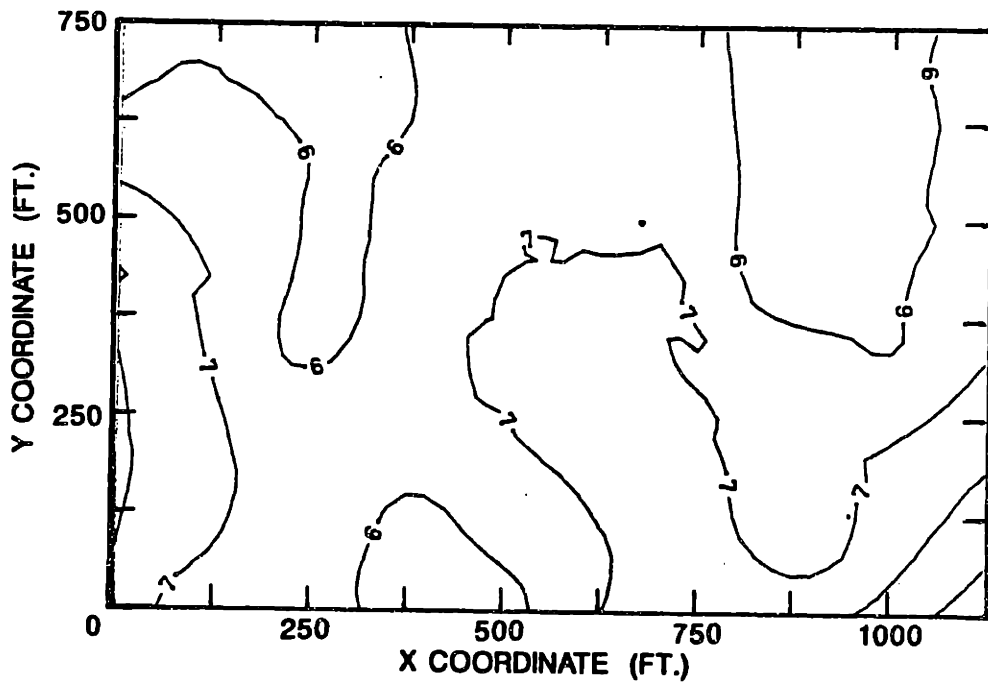
(b) Kriging Estimate of the Variance About the Estimated Surface.

Figure 5.6 - Kriging Analysis of the Top of Marine Sands, Back Bay.
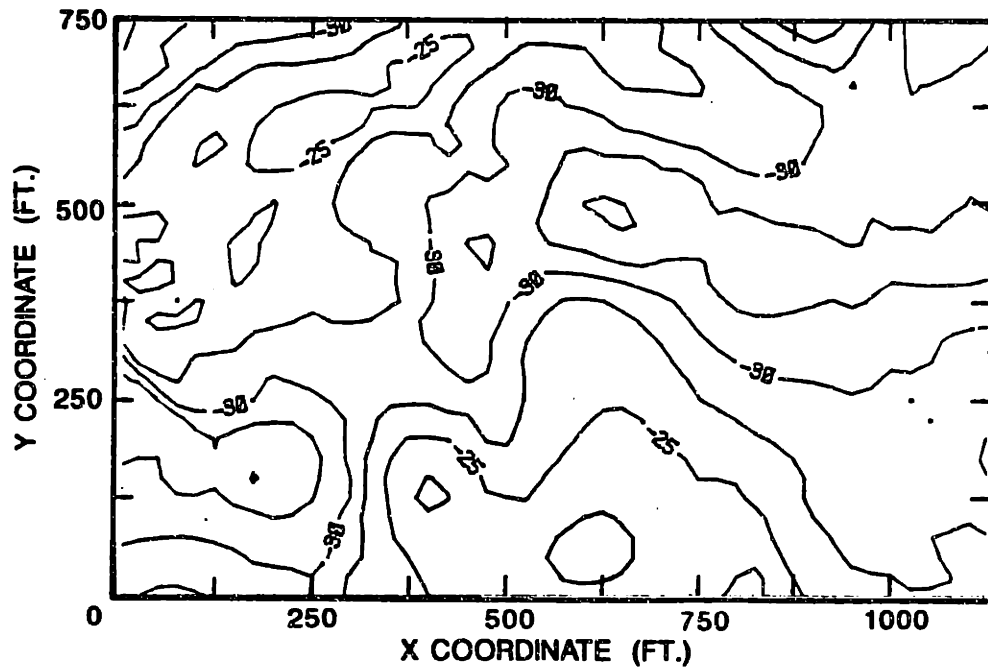
(a) Kriging Estimate of Top of Boston Blue Clay,
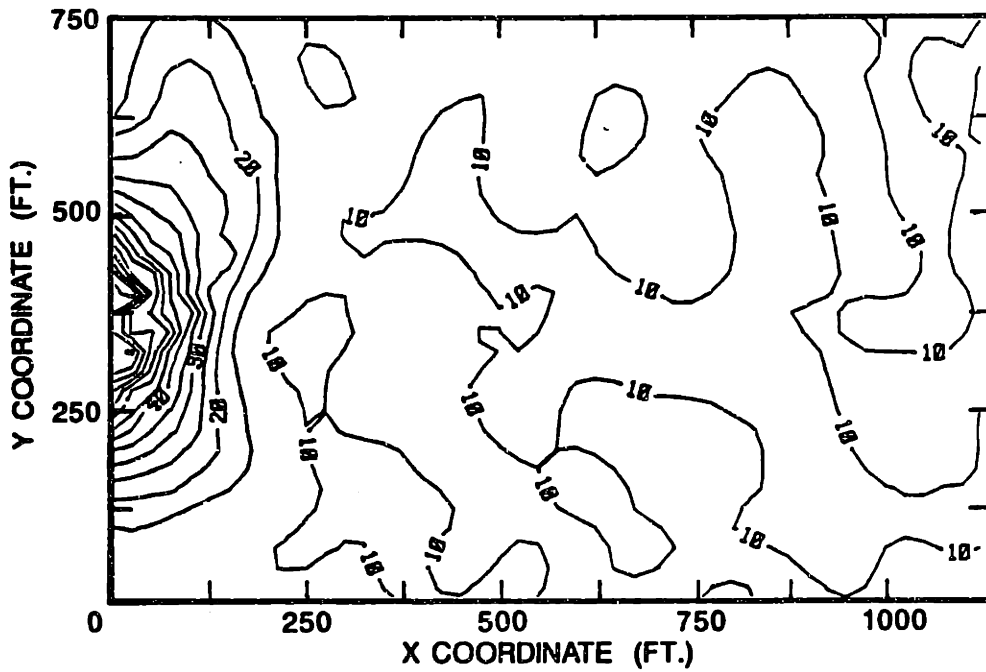
(b) Kriging Estimate of the Variance About the Estimated Surface.

Figure 5.7 - Kriging Analysis of the Top of Boston Blue Clay, Back Bay.
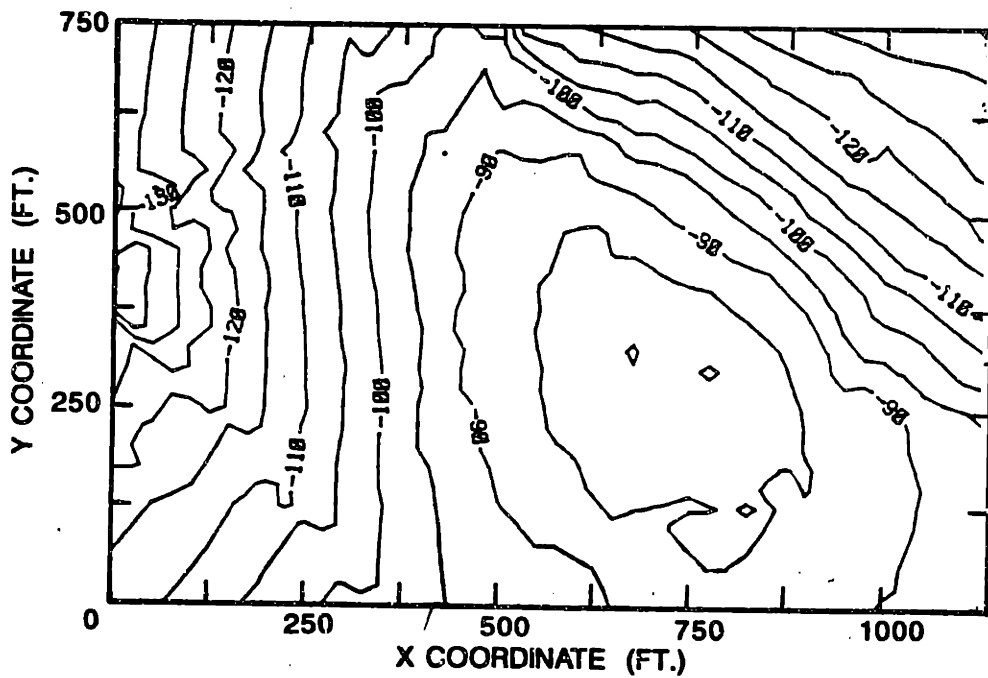
(a) Kriging Estimate of Top of Glacial Till,
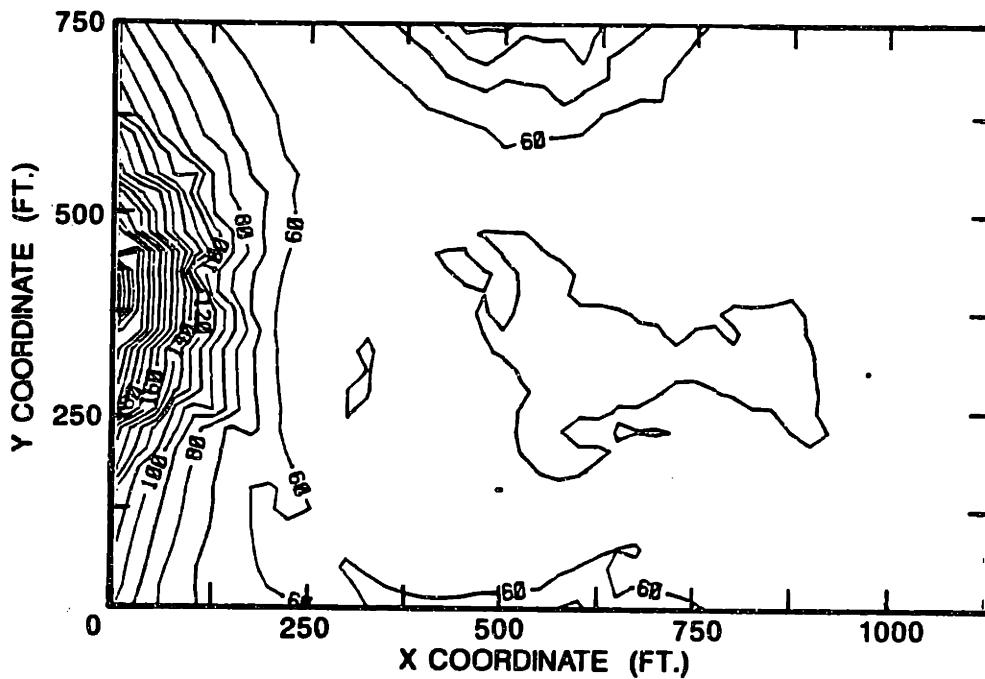
(b) Kriging Estimate of the Variance About the Estimated Surface.

Figure 5.8 - Kriging Analysis of the Top of Glacial Till, Back Bay.
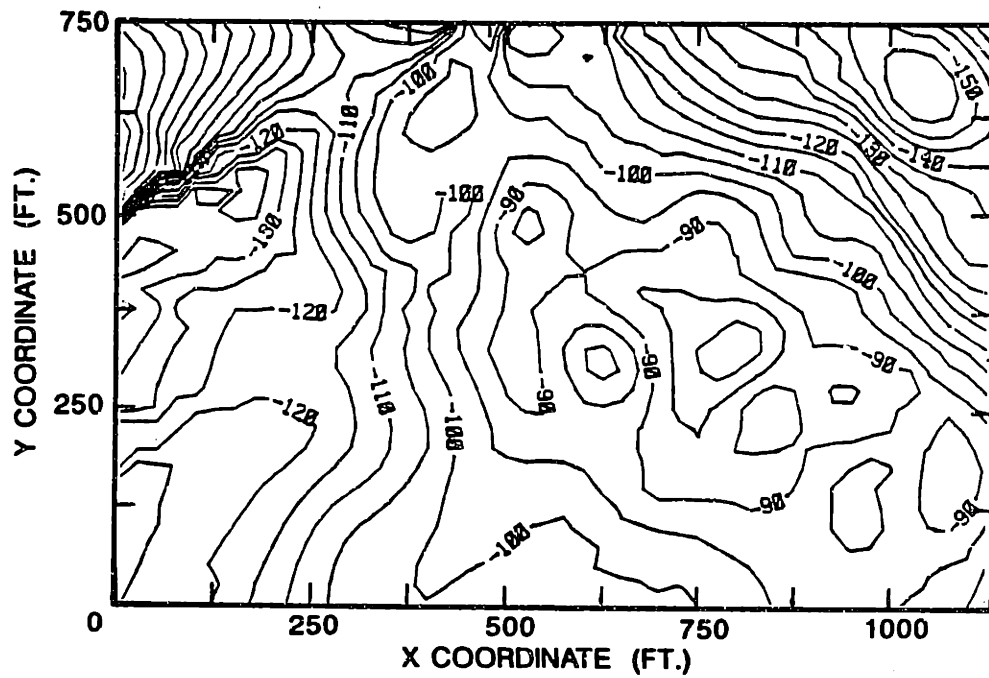
(a) Kriging Estimate of Top of Rock,
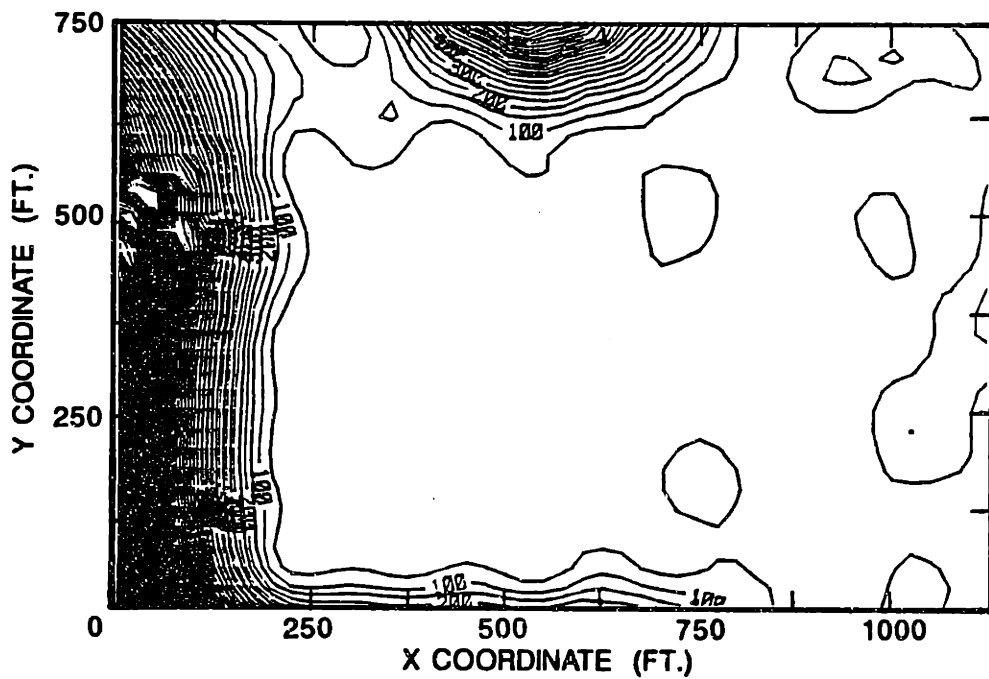
(b) Kriging Estimate of the Variance About the Estimated Surface.

Figure 5.9 - Kriging Analysis of the Top of Rock, Back Bay.
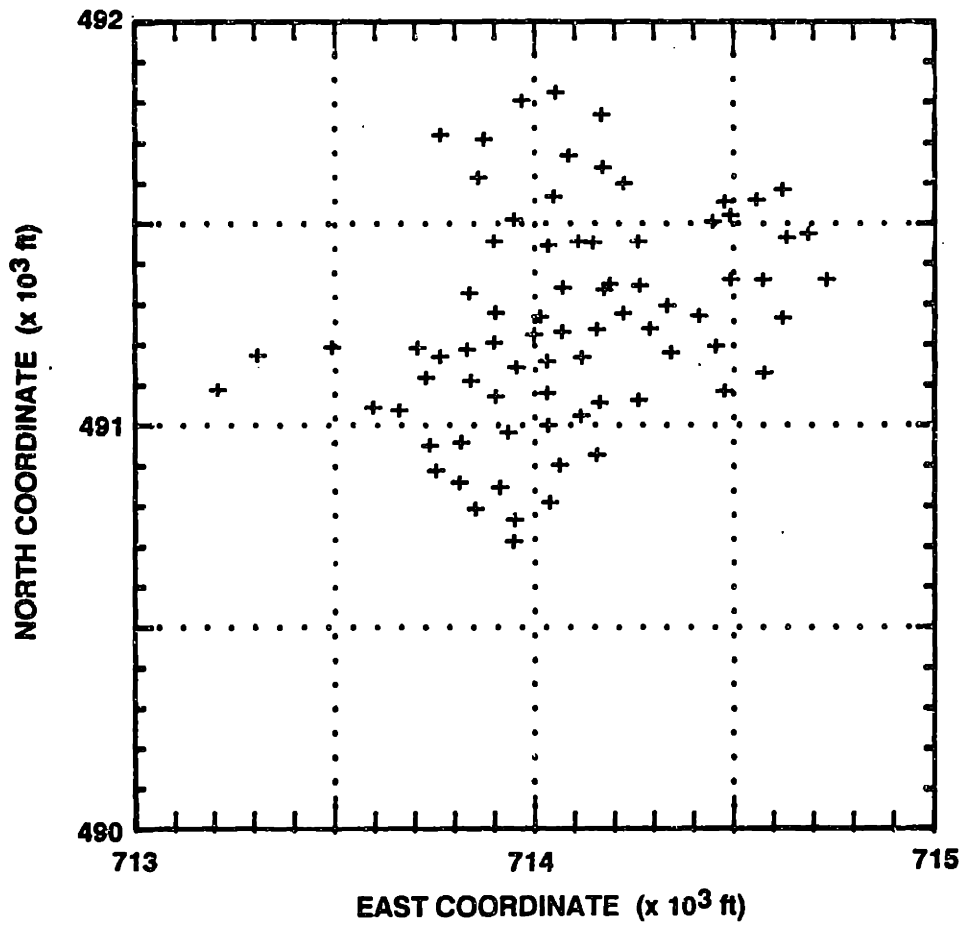
Figure 5.10 - Locations of the Top of Rock Data (77 pts.), Back Bay.

153
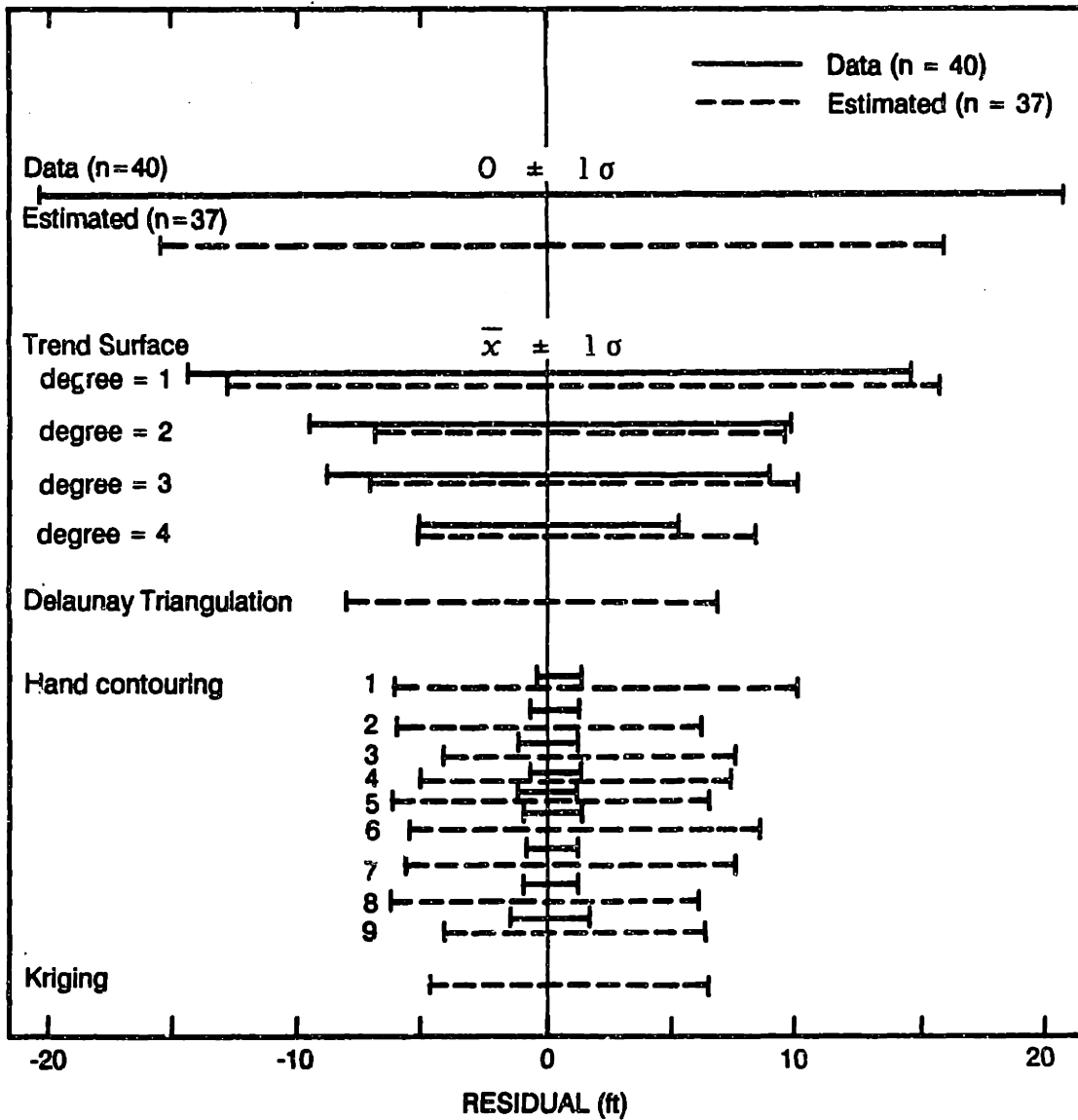
Figure 5.11 - Comparison of Residuals of Data and Estimated Points for Various Analytical Techniques, Top of Rock, Back Bay.

154
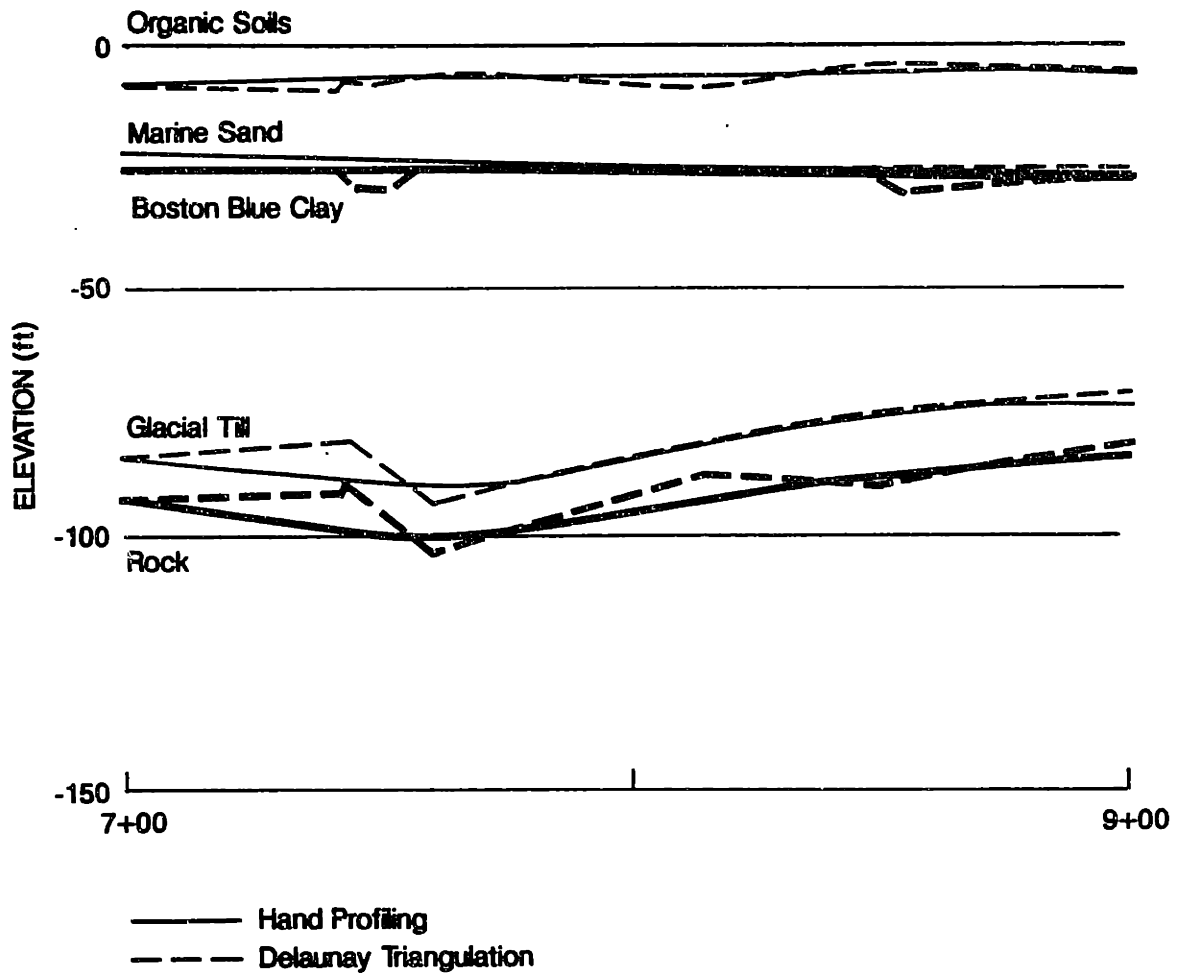
Figure 5.12 - Comparison of Hand Profiling and Delaunay Triangulation
Profiling, Profile A, Back Bay.
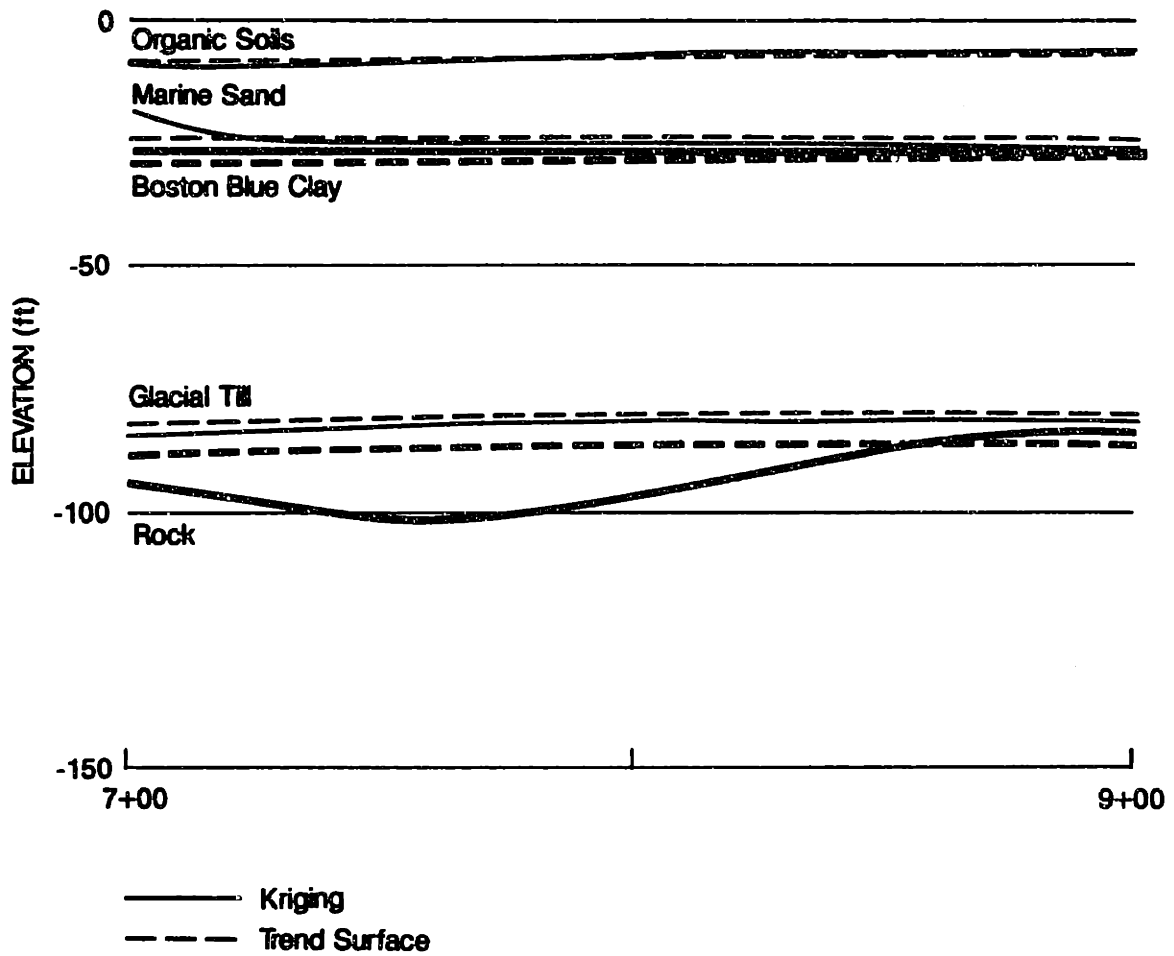
Figure 5.13 - Comparison of Kriging Profile and Trend Surface (4th degree) Profile, Profile A, Back Bay.

156
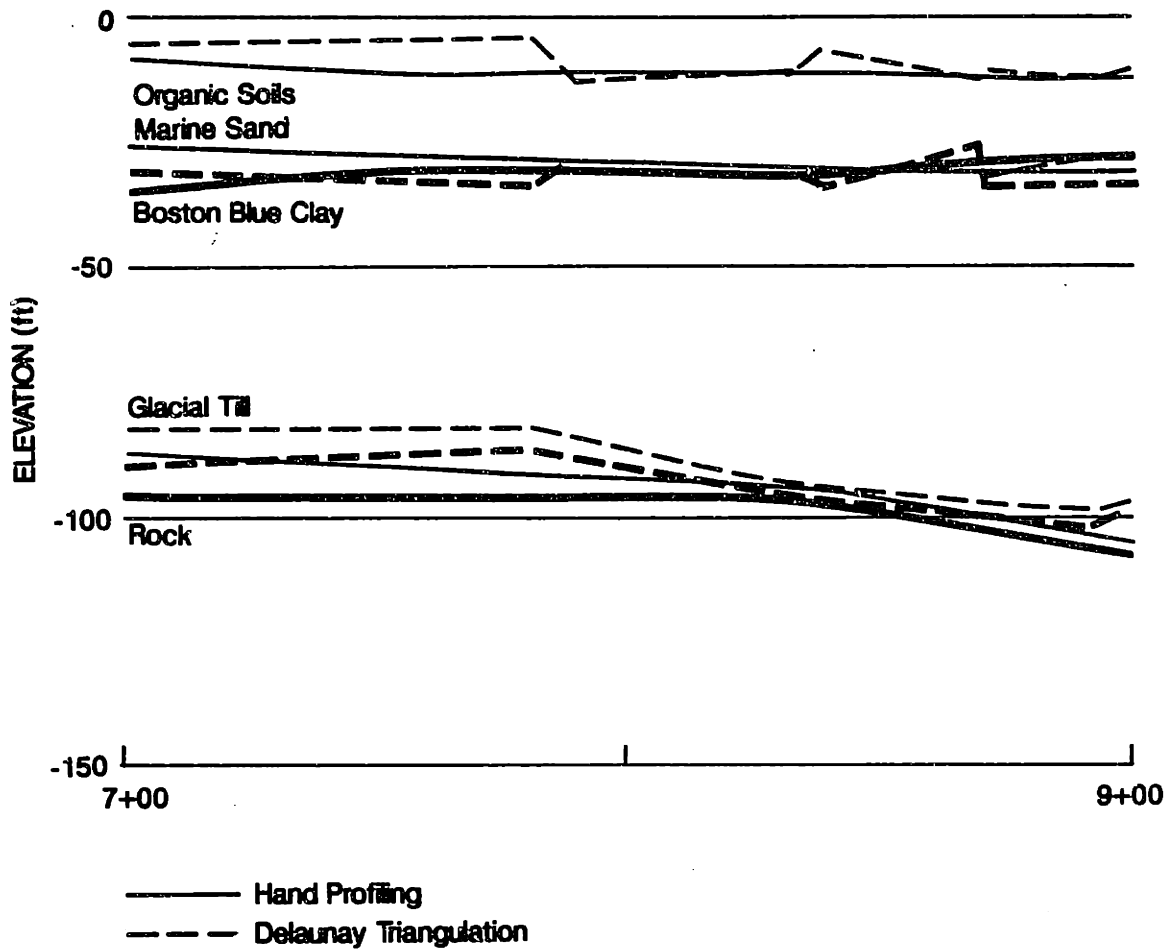
Figure 5.14 - Comparison of Hand Profiling and Delaunay Triangulation
Profiling, Profile B, Back Bay.
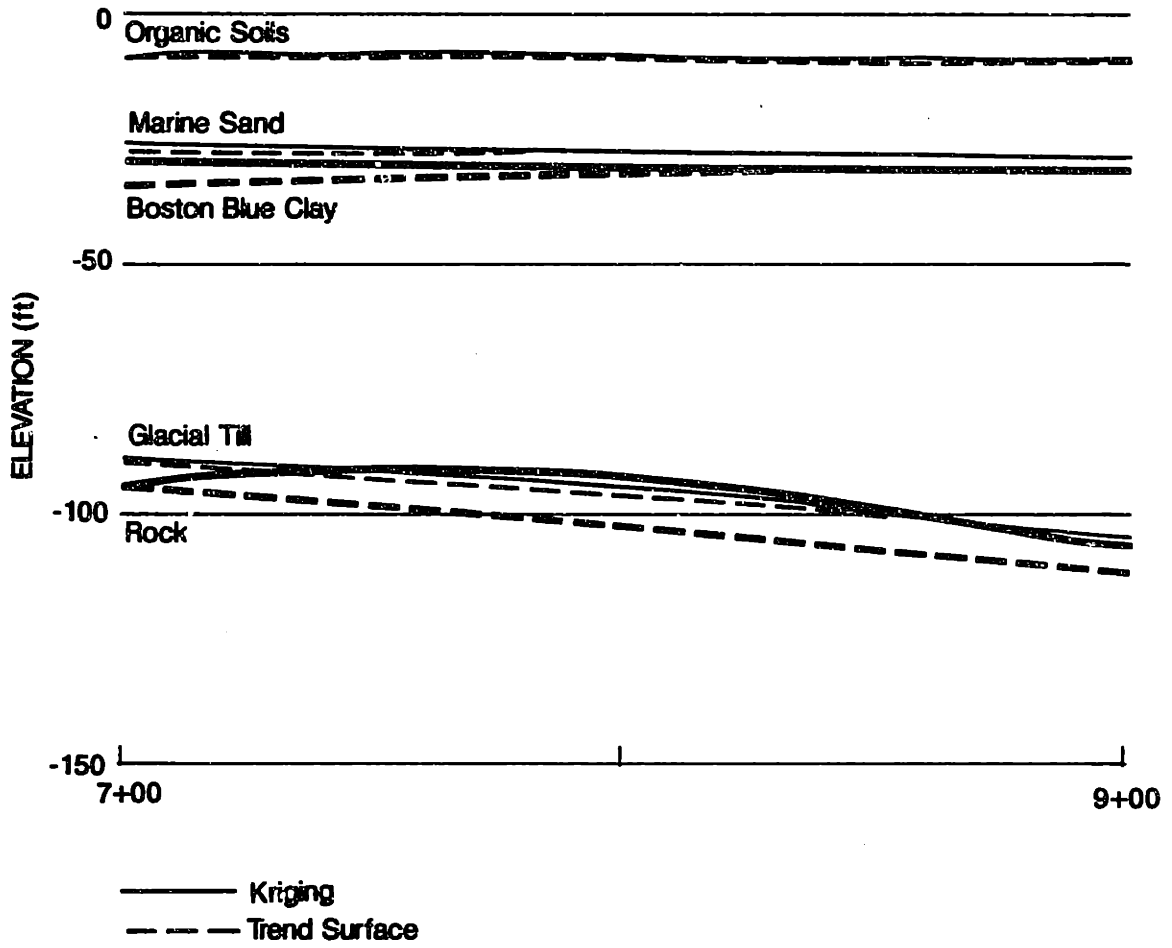
Figure 5.15 - Comparison of Kriging Profile and Trend Surface (4th degree) Profile, Profile B, Back Bay.

CHAPTER 6

PROFILING

6.1 Introduction

Profiling is the practice of developing a cross section showing the sub-surface soil and rock conditions. The profiles are developed to assist with the geotechnical design and also, to evaluate overall design and construction issues. The number of profiles developed is influenced by among other things the apparent complexity of the subsurface conditions, the perceived influence of the subsurface conditions on the overall design, and the budget for analysis. Generally, a limited number of profiles are developed along critical orientations.

The objectives of the research on profiling are to assess the applicability of existing probability-based mapping techniques to soil profiling, and develop computer techniques for probabilistic soil profiling. Additional objectives for profiling are to develop methods for incorporating strata discontinuities and the engineer's subjective judgement into stratigraphic models.

This chapter presents a discussion of soil profile development as it is done in practice, computerized techniques developed as part of this research for improvement of the process, and two case history applications of the improved techniques.

6.2 Methods Used in Practice

6.2.1 Description of Methods

Soil profiles are usually developed by the following steps with some minor variations:

1) The orientation of the profile in plan is selected;

2) Test borings in the area of the profile plane are identified;

3) The test borings to be included in the profile are

159

selected; and

4) The profile is developed by projecting the selected test borings into the profile plane.

These steps are shown in Figure 6.1 and discussed in the following section. In practice variations in the process include, among others, the distance and direction that the test borings are projected.

6.2.2 Limitations of Methods

It should be noted that in the process of developing the profile the test borings are projected varying directions and distances into the profile plane without any indication of the projection direction or distance. Once projected into the profile plane, all the test borings are treated with equal weight regardless of the projection direction or distance. Examples of the possible ramifications of the common methods for plotting soil profiles are shown in Figure 6.2.

Once all of the test borings have been plotted in the profile plane, the strata change elevations indicated in the test boring logs are used to identify the continuous strata. These strata changes are then connected using straight lines between the test borings. Discontinuous strata are handled in methods completely at the discretion of the geotechnical engineer. Common methods for indicating discontinuous strata include the use of dashed lines, question marks, or non-connected strata lines.

Another common feature of soil profiles is a scale distortion to exaggerate the vertical changes in the stratigraphy. Scales of 1:5 (V:H) are common for soil profiles. Typical examples of hand drawn profiles have been presented previously in Figures 4.1 through 4.3.

The remaining sections of this chapter will discuss research performed to develop computerized methods for developing soil profiles and assessing soil stratigraphy.

6.3 Stratigraphy Models

6.3.1 Introduction

One possible method for the improvement of the current practice of soil profiling is to first model the soil strata interfaces as single surfaces, and then superimpose the single surfaces to create a model of the soil stratigraphy. This section presents the development and analysis of stratigraphy models based upon kriging estimators of the individual surfaces.

6.3.2 Definition of Models for Back Bay

The two classes of information available for the development of the stratigraphy models are the observed strata change elevations, and the observed soil stratum thicknesses. It is possible to model any strata interface using the observed interface observations. As an alternative, the interface could be modeled by subtracting the observed strata thickness from the observed interface above the one being modeled. Figure 6.3 shows several alternative methods of modeling the same surface. It is possible to develop any number of models by considering combinations of the strata change elevations and strata thicknesses.

Jones et al. (1986) present a discussion of the merits of using stratum thickness in the stratigraphy models. Probably the most convincing argument can be made in the case of discontinuous strata. If the observed strata interface is used for the model, it will be continuous even in those areas where test borings did not encounter the discontinuous soil stratum. If the stratum thickness is modeled instead of the interface, the true value should be 0 in areas where the stratum was not observed. In fact, modeling of the stratum thickness should result in areas with predicted thickness less than 0. When using stratum thickness in the model, it seems appropriate to use the zero contour as the lateral limit of the soil stratum (see Figure 6.4).

The Back Bay case history data was used to study the effects of model definition on the predicted models. Five alternative models (see Figure 6.5) were developed and used to estimate the soil conditions at known points (test boring locations). These models were developed for various reasons. Model 1 is based on kriging the observed soil interface elevations to estimate the soil stratigraphy. Model 2 is based solely on observed strata thicknesses without any consideration of the observed interface elevations. Kriging Models 3 through 5 represent several intermediate alternatives with some of the interfaces based on actual observations and others based on adding or subtracting observed stratum thicknesses for observed interfaces.

Additional models could have been developed and evaluated; however, the following section shows that the models were basically equivalent with only minor differences.

6.3.3 Comparison of Models

Before presenting the results of the model comparisons, methods of comparing stratigraphic models will be discussed. Several methods of comparing the observed conditions to those estimated by a model were considered. Eventually, the factors were reduced to those shown in Figure 6.6 and discussed below.

A brief discussion of the factors follows:

> Total Agreement Ratio (TAR): This factor is the ratio of the agreement lengths for all strata to the overall length of the test boring. By definition the TAR is greater than or equal to 0 and less than or equal to 1. If any of the strata are relatively thick in comparison to the test boring length, it is likely that the total agreement ratio will be high. Similarly, if the strata are relatively thin, it is possible that a small offset in the stratigraphic model could result in a relatively low total agreement ratio. It should also be noted that by definition the TAR may be biased toward high values for short test borings.

162

Stratum Agreement Ratio (SAR): This factor is defined as the ratio of the length of agreement in a particular stratum to the observed thickness of the stratum. By definition the SAR must be greater than or equal to 0 and less than or equal to 1.

Stratum Thickness Ratio (STR): This factor is defined as the ratio of the model stratum thickness to the observed stratum thickness for those strata that are fully penetrated at a particular test boring location. This factor is thus greater than or equal to 0. A high STR may be due to a very thin observed stratum or a very high estimate of the stratum thickness.

Stratum Interface Residual (SIR): The stratum interface residual is the mathematical difference between the model estimate of the top of a particular stratum and the observed top of the same stratum. By definition there are no restrictions on the value of the SIR.

Obviously, the factor or factors to be used in a given situation will depend on the purpose for developing the model. If the objective is to estimate the thickness of a critical stratum, then the total agreement ratio would be of less importance than the stratum agreement ratio. Similarly, if the purpose of the model was to estimate the top of a critical stratum, the most important factor would be the stratum interface residual.

Subsurface stratigraphy is partially known at the test boring locations. Each of the test boring logs includes strata change elevations. Obviously strata changes below the bottom of the test boring are unknown. Therefore, in order to compare models it is necessary to compare estimates of the soil conditions at the known locations and within the penetrated depth of the test borings.

This was accomplished by jackknifing the test boring locations such that a single test boring was removed from the total data set which was then used to estimate the conditions at the eliminated test boring location. By repeating the process until each of the test boring locations had been

individually removed, it was possible to evaluate the models as well as the surface modeling techniques. It is possible to repeat the jackknifing deleting more than a single point each time. However, this was not considered to be merited based on the results of the single elimination discussed below.

There are many methods (see Chapter 5) for modeling single surfaces. Based on the results presented in Chapter 5, two methods, kriging and Delaunay triangulation, were selected for use in the stratigraphy models. Kriging methods were chosen because kriging estimators have desirable properties as discussed in Chapter 5 and performed best in the analysis presented in Chapter 5. Delaunay triangulation was chosen as a computerized method that closely simulates hand methods; therefore allowing an efficient comparison between the "best" analytical modeling method and "hand" methods.

The models shown in Figure 6.5 were evaluated. Each model was evaluated using kriging to estimate the necessary strata tops and thicknesses. Model 1 was also evaluated using Delaunay triangulation to estimate the strata tops.

The jackknifing procedure was performed using the case history data and the models shown in Figure 6.5 to compare the stratigraphic models. Summary statistics of the comparison factors were also calculated (see Table 6.1 for typical results).

The TAR was used to compare the actual overall performance of the models. A summary of the TAR values for the Kriging Models 1 through 5 and Delaunay Triangle Model 1 is presented in Table 6.1. The Kriging models are compared for all the data points available (156). In addition, summary statistics are presented for the Kriging Models 1 and 5 and Delaunay Triangle Model 1 for those interior points which the Delaunay triangle model could predict.

The mean TAR values are nearly identical for the models considered, rang-
ing from 0.717 to 0.750. The lowest mean value (0.717) is Kriging Model
2, which is based on the subtraction of the estimated stratum thicknesses
from the ground surface. The lower mean can be attributed to the fact
that this model is additive in the estimation variance for each subse-
quently lower stratum. Since the strata thicknesses are estimated by
kriging and then used to estimate the top of each stratum, it is expected
that the performance of the model, particularly on the lower strata,
would be suspect. This expectation was supported by the SIR analysis
where Kriging Model 2 had consistently high mean and standard deviation
values compared to the other models.

The second lowest mean TAR is for the Delaunay Triangle Model 1. Since
the model is triangle based, the interpolated values are based on the
three nearest neighbors only without any influence by the remaining
points. Therefore, it is expected that a triangulation-based model would
on the average not perform as well as kriging models which in this analy-
sis included consideration of the ten nearest data points.

The kriging models, with the exception of Model 2 discussed above, have
almost identical mean TAR values. The slight differences in the means
are most likely due to the subtle differences in the models and the ten-
dency of the model differences to average out over the samples consid-
ered.

It is important to note that the mean TAR values for the models in Table
6.1 range from 0.717 to 0.750 meaning that these models, on the average,
only agree along about three quarters of the test boring length. How-
ever, as stated above, the TAR values may be biased by thin soil strata.

The models were also compared with respect to the STR and SIR values.
Summary statistics for кriging Models 1 and 5, and Delaunay Triangle
Model 1 are presented in Tables 6.2 and 6.3.

Each of the models in Table 6.2 tends to over estimate the stratum thicknesses as indicated by the mean STR values ranging from 1.017 to 1.863. Each of the three models is reasonably successful modeling the thickness of the fill, organic soils and Boston Blue Clay. However, the kriging models, with mean STR values ranging from 1.017 to 1.058, are on the average better models than the Delaunay triangle model with values from 1.036 to 1.084. With each of the three models the higher STR values occur with the thinner strata (marine sands and glacial till). For these strata the mean STR values range from 1.194 to 1.863. Although the mean STR values appear reasonable for many strata, the maximum and range values indicate that in the worst case the models can over estimate the stratum thickness by as much as 34 to 2039 %.

The mean SIR values are all acceptably close to zero. However, the standard deviations, maximums and ranges are all relatively high indicating that although the average performance is acceptable, the point by point performance is poor. It should be noted, however, that even with the relatively poor performance that the standard deviation of the glacial till and rock SIR values is less than half of the standard deviation of the observed strata top values.

Since many of the summary statistics differ only slightly, the results of the model comparisons are more correctly presented by ranking the various models for each eliminated test boring location and then comparing the ranks after each point has been eliminated. The ranking comparisons were performed for the Total Agreement Ratio, the absolute value of the Stratum Interface Ratio, and the absolute value of 1 minus the Stratum Thickness Ratio. The modifications were made to the SIR and STR values in order to account for the true optimal values of 0 and 1, respectively.

The results of the ranking comparisons are indicated in Table 6.4. The ranking relationships are relative and should be judged accordingly. The fact that a given model ranks better than another gives no information concerning the absolute performance of either model, or the difference in actual performance between the two models.

Although the ranking of the model performance identifies the "best" performing model relatively, it is important to consider the actual values of the ratios and factors also. As discussed previously, the mean Total Agreement Ratio for these models was approximately 0.75, which indicates that they are not particularly good models.

Partial results of the model analysis are presented in Figures 6.7 through 6.9. The results of the "better" models have been presented to provide an indication of the performance of these models.

Figure 6.7 is a plot of the Kriging Model 5 Total Agreement Ratio versus the individual point numbers. The plot provides a good visual impression of the performance of the model with respect to individual points. Initially it appears in Figure 6.7 that the deeper test borings would tend to result in higher Total Agreement Ratio values, due in part to the relatively large thickness of the Boston Blue Clay. However, the correlation coefficient between the Total Agreement Ratio and the test boring depth was found to be -0.56, indicating a moderate inverse relationship. This relationship could be due to poor performance of the models with respect to estimating the glacial till and rock strata (see discussion below).

Figures 6.8 and 6.9 are plots of the TAR values for the Kriging Models 1 and 5, and Delaunay Triangle Model 1 and Kriging Model 1, respectively. These figures demonstrate the relationship of the TAR values for the model comparisons. Figure 6.8 with less scatter around the reference diagonal demonstrates the close agreement of the two kriging models (Models 1 and 5). Figure 6.9 with more scatter around the diagonal illustrates the weaker relationship between the Delaunay triangle and kriging versions of Model 1. Note in Figure 6.9 that there are four outlier points where the kriging version of the model was considerably better than the Delaunay triangle version.

Another way to compare these three models is using the correlation coefficient (see Table 6.5). The correlation coefficients indicate that there are very strong linear relationships between the TAR values for all three models. The relationship between the Kriging Models 1 and 5 is exceptionally strong.

Relatively small differences were observed in the TAR values for Kriging Models 1 and 5, and Delaunay Triangle Model 1 with the exception of the four outlier values that are also observed in Figure 6.9. These outliers are good examples of the ability of the kriging models, which in this analysis considered the ten nearest data points, to make better estimates than the Delaunay triangle model which is limited to consideration of the three nearest neighbors.

Plots of the STR and SIR values for the various strata were prepared as part of the analysis. The plots, which are not included herein, provide good visual impressions of the overall performance of the Kriging Model 5. One observation is that the model performs better on the thicker soil strata with respect to the STR values. The SIR values are relatively large, and depending on the purpose of the stratigraphic modeling, may be unacceptable.

One very significant observation of the models is the difference in how discontinuous strata are considered. Kriging Model 5, which was the "best" performer, used a continuous kriged surface to model the top of the marine sand, a stratum that is discontinuous. Therefore, Model 5 contains significant errors of indicating the presence of the marine sand stratum at test boring locations which indicated its absence. This is a very serious deficiency with these models that are based on continuous surface modeling. Other kriging models such as Models 2, 3 and 4 compensated for discontinuity where the estimated thickness of the marine sand was less than 0. However, when considering the global TAR, these models did not perform as well as Model 5. This is partially attributed to the relative thickness of the marine sand.

The general conclusions which are drawn from the model analyses are as follows:

1. The models as presented perform on the average at about 75% with respect to the Total Agreement Ratio.

2. Of the models considered, the Kriging Model 5 performed best based on a 1 X 1 ranking comparison of the TAR, STR and SIR values. However, the actual performance of the Kriging Models 1 and 5 was for all practical purposes the same. The Delaunay Triangle Model 1 performed almost as well as either of the kriging models with four exception points.

3. The ranking and actual performance comparisons demonstrated that the "best" model depended on which strata interface or stratum thickness was being used as the criterion. Therefore, model selection should be based upon the ultimate objective.

4. Even though the Kriging Model 5 was considered the "best" performer, this model, which includes a continuous model of the discontinuous marine sand stratum, is intuitively unacceptable. This model will result in errors of absence/presence with respect to the marine sand stratum.

6.3.4 Summary

The soil stratigraphy models presented in this section demonstrate an initial effort at soil stratigraphy modeling. The models demonstrated that kriging models performed slightly better than Delaunay triangle based models. However, the models have demonstrated a generally unacceptable level of success with respect to being able to predict soil conditions at known locations. In particular the models have demonstrated difficulty with presence/absence errors, which are very significant errors in the practice of geotechnical engineering, and the models are still based upon the superimposing of single surfaces without any expression of the interaction between the surfaces.

6.4 Probabilistic Profiles

6.4.1 Introduction

The soil stratigraphy models of the previous section were developed using kriging analysis of the soil strata interfaces and thicknesses. It was concluded, however, that the models still lacked quantitative expression of the level of uncertainty. This section addresses implementation of the level of uncertainty into multiple surface stratigraphic models.

6.4.2 Multiple Surfaces as Random Variables

Section 6.3 presents modeling of soil interfaces as functions of the observed soil strata interfaces and thicknesses. Section 6.3 concluded that the kriging models, at least for the case history considered, performed slightly better than the Delaunay triangle based model which approximates the current hand methods of assessing soil stratigraphy.

If the strata interfaces and thicknesses are considered to be independent random variables, it is possible, as shown below, to create probabilistic soil profiles which will indicate the level of uncertainty in the soil strata. Before discussing the specific problem of soil stratigraphy, an introduction of random variable concepts is helpful.

Consider a line on which the locations of two points, X and Y, are known. The points divide the line into three segments (ignoring the case when the points are coincident). It is then possible to define the three segments deterministically knowing the locations X and Y. If the locations, X and Y, are statistically independent random variables with known normal distributions, it is possible to define the three segments probabilistically.

The three line segments defined by the locations of X and Y are:

Segment 1: $\{i < X, \ i < Y\}$

Segment 2: $\{X \leq i < Y\}$

Segment 3: $\{i > X, \ Y \leq i\}$

Assuming that locations X and Y are statistically independent with known normal distributions:

$$X \sim N(\mu_x, \sigma_x^2)$$

$$Y \sim N(\mu_y, \sigma_y^2)$$

then ignoring the possibility of the points being coincident and assuming that Y is always greater than X, the probability of any location, i, belonging to each of the three line segments can be estimated as:

$$P(i \in Segment\ 1) \quad = \quad P(i < X) \cdot P(i < Y)$$

$$P(i \in Segment\ 1) \quad = \quad \Phi\left(\frac{i - \mu_x}{\sigma_x}\right) \cdot \Phi\left(\frac{i - \mu_y}{\sigma_y}\right)$$

$$P(i \in Segment\ 2) \quad = \quad P(X \leq i) \cdot P(i < Y)$$

$$P(i \in Segment\ 2) \quad = \quad \left[1 - \Phi\left(\frac{i - \mu_x}{\sigma_x}\right)\right] \cdot \Phi\left(\frac{i - \mu_y}{\sigma_y}\right)$$

$$P(i \in Segment\ 3) \quad = \quad P(i > X) \cdot P(Y \leq i)$$

$$P(i \in Segment\ 3) \quad = \quad \left[1 - \Phi\left(\frac{i - \mu_x}{\sigma_x}\right)\right] \cdot \left[1 - \Phi\left(\frac{i - \mu_y}{\sigma_y}\right)\right]$$

Making the same assumptions concerning independence and known distributions of the random variables, an approach similar to the one dimensional example can be applied to two surfaces in space. These surfaces divide space into three regions. Note that the constraint that surface X must be above surface Y was imposed. The result of this constraint is that a potential fourth region, the space below surface Y over surface X, has been eliminated. This means that the probabilities of the three regions will not sum to 1 without normalization by their sum.

The three regions defined by surfaces X and Y for any elevation, a, are as follows:

Region 1: $\quad \{a > X, \quad a > Y\}$

Region 2: $\{Y < a \leq X\}$

Region 3: $\{a < X, \quad a \leq Y\}$

Assuming that surfaces X and Y are statistically independent with known normal distributions:

$$X \sim N(\mu_x, \sigma_x^2)$$

$$Y \sim N(\mu_y, \sigma_y^2)$$

Then the probability of any elevation, a, belonging to each of the three regions can be estimated as:

$$P(a \in Region\ 1) \quad = \quad P(a \geq X) \cdot P(a \geq Y)$$

$$P(a \in Region\ 1) \quad = \quad \Phi\left(\frac{a - \mu_x}{\sigma_x}\right) \cdot \Phi\left(\frac{a - \mu_y}{\sigma_y}\right)$$

$$P(a \in Region\ 2) \quad = \quad P(a \leq X) \cdot P(Y < a)$$

$$P(a \in Region\ 2) \quad = \quad \left[1 - \Phi\left(\frac{a - \mu_x}{\sigma_x}\right)\right] \cdot \Phi\left(\frac{a - \mu_y}{\sigma_y}\right)$$

$$P(a \in Region\ 3) \quad = \quad P(a < X) \cdot P(a \leq Y)$$

$$P(a \in Region\ 3) \quad = \quad \left[1 - \Phi\left(\frac{a - \mu_x}{\sigma_x}\right)\right] \cdot \left[1 - \Phi\left(\frac{a - \mu_y}{\sigma_y}\right)\right]$$

Using the same methodology, it is possible to extend the equations above to consider any number of surfaces continuing to impose constraints with respect to the vertical sequence of the surfaces.

As discussed in Chapter 3, the kriged surfaces result in estimates of the surface value at any point in space and an estimate of the variance of the estimate about that surface. Assuming that the location of the true surface is normally distributed about the estimated surface with a variance equal to the estimated variance, it is possible to use kriged surfaces to subdivide space into regions similar to this approach.

172

In addition to subdividing space using the kriged surfaces, estimates of the probability of any point belonging in any of the regions can be calculated since the mean and variance of the surface is estimated by kriging at any x,y location. Using the probabilities obtained by this approach, a probabilistic profile can be created using the procedure presented in the following section.

6.4.3 Examples of Probabilistic Profiles

The creation of probabilistic profiles is based upon the assumptions of the preceding section. The main assumptions are that the true surfaces being modeled are normally distributed about the kriged estimate of the surface, and that a geologic sequence can be imposed on the surfaces.

Figure 6.10 shows contours of the probabilities of the six soil strata for the Back Bay Profile B (mod.). Typically, the individual soil profiles exhibit regions with low probabilities and regions with considerable transition in the probabilities. The probabilities are double-sided for the interior strata and single-sided for the upper (fill) and lower strata (rock). The contours are not parallel due to the change in the estimated variance about the estimated surface in space.

By essentially overlaying the individual soil types, a probabilistic profile can be created. The probabilistic profile can be interpreted in several ways. Figures 6.11 and 6.12 are examples of interpretations of the probabilistic profiles. Figures 6.11 and 6.12 show the regions in the profile where the individual soil type probabilities exceed 0.1 and 0.5 respectively.

Figure 6.11 shows regions where there are two and three soil types with probabilities greater than 0.1. The major regions are in the area of the organic soils/marine sand/Boston Blue Clay and the Boston Blue Clay/glacial till/rock. A minor region is in the area of the fill/organic soils. The two soil type regions are continuous while the three soil type regions are discontinuous.

173

Figure 6.12, where the criteria is probabilities greater than 0.5, indicates regions where there is less uncertainty about the classification. Note in Figure 6.12 that there are regions where the maximum soil type probability is less than 0.5.

6.4.4 Overlap and Discontinuity Problems with Probabilistic Profiles

The probabilistic profiles are a major step toward expressing level of uncertainty in the soil profile. However, there are two significant problems with the probabilistic profiles as discussed to this point. To demonstrate these problems, a "best estimate" profile (see Figure 6.13) can be developed by assigning the soil type at any location to the soil type with the maximum probability at that location.

The "best estimate" in Figure 6.13 indicates that the marine sand stratum is continuous, and also that the rock stratum occurs above glacial till. The first condition is incorrect based on comparison with actual test borings close to the plane of the profile. The second condition is geologically unacceptable. Therefore, although the probabilistic profile is a means of expressing uncertainty in the profile, there are still the common problems of using a continuous model to model a discontinuous stratum and of strata overlap resulting in unacceptable profiles that were also encountered in Chapter 5 (see Figure 5.15).

6.4.5 Summary

Probabilistic profiles as presented in this section represent a major step toward incorporating an quantitative expression of uncertainty into soil profiles. This is a significant advancement to the common practice of soil profiling. In addition to this advancement, extensions of these concepts could be applied to a variety of geotechnical engineering problems. For example, using these same concepts, it is possible to model stratum thickness probabilistically. Therefore, for instance, probabilistic estimates of excavation volumes or foundation pile lengths could be developed with a rational basis. These techniques would be

particularly helpful in estimating quantities and costs for the excavation of contaminated materials where a deterministic estimate may be prohibitively expensive.

6.5 Probabilistic Relaxation Profiles

6.5.1 Introduction

Probabilistic profiles, which are based on kriging continuous surfaces, attempt to model a discontinuous stratum as a continuous stratum. This problem is inherent to the use of any continuous model. Ideally, the modeling would be done with a mathematically restrained model that would result in a discontinuous model surface. The only reference found in the literature to this approach was Henley (1981). Henley also discusses briefly an approach to the problem of multiple surface interpolation. In the absence of a mathematical model for discontinuous surfaces, an alternative approach is to modify the probabilistic profile in a rational manner to resolve the identified problems of discontinuity and overlap.

As discussed in Chapter 3, probabilistic relaxation is an image enhancement technique for decreasing the level of uncertainty in an array of pixels. The process is based on the initial classification probabilities at each location and a compatibility matrix, which is in effect a set of constraints. Probabilistic relaxation is an iterative process which is repeated until the level of uncertainty in the image is reduced to a satisfactory level.

This section presents the application of probabilistic relaxation to the resolution of the overlap and discontinuity conditions encountered in the probabilistic profiles. Before examining applications to actual soil profiles, the following section presents a preliminary assessment of the probabilistic relaxation process using contrived data.

6.5.2 Assessing Influence of Compatibility Matrix

The initial assessment of the probabilistic relaxation technique consisted of observing the effects of various compatibility matrices on the

estimated posterior probabilities. The effects of the various compatibility matrices can be assessed by the rate and direction of expansion of the P_{ij} contours with successive iterations (see Chapter 3 for an explanation of terms).

Four initial prior probability matrices and four compatibility matrices (shown in Figures 6.14 and 6.15, respectively) were used to assess the general effects of the compatibility matrices. The results of the application of probabilistic relaxation using the initial probability matrices and the compatibility matrices are shown in Figures 6.16 through 6.19 as plots of the estimated probability after the fifth and tenth iteration. The plots demonstrate that the effect of the compatibility matrix is significant on the direction of the expansion of the posterior probabilities. The four initial compatibility matrices demonstrate noticeable different expansion directions, especially for the Trial 1 data set.

For the trial compatibility matrices where the maximum value was always +1, the effect of the compatibility matrix is minimal with respect to the rate of expansion for the posterior probabilities. If the maximum value as less than +1 and varied between the compatibility matrices, it is anticipated that a more noticeable effect on the rate of expansion would be observed.

The rate of increase in the posterior probabilities, based on comparison of the fifth and tenth iterations, is such that typically the estimated probability will increase from the initial value of 0.50 to greater than 0.95 in five iterations. For any given iteration the transition from 0.50 to greater than 0.95 occurs across typically 3 to 5 nodes.

Boundary effects are relatively minimal as demonstrated by the Trail 2 and Trial 3 data sets.

6.5.3 Combined Effects of Compatibility Matrix and Prior Probabilities

The next assessment of probabilistic relaxation techniques was to consider the effects of the compatibility matrix $(c(i,j:h,k))$ and initial probabilities $(P_{ij}^{(0)})$ for several basic "typical" geotechnical profiles.

176

Two of the profiles are shown in Figures 6.20 and 6.21. These profiles were chosen as examples of geometric relationships which are often encountered in soil stratigraphy. The objective in this analysis was to use different initial probabilities and compatibility matrices and assess the ability of probabilistic relaxation methods to predict the "true" maps.

Input variables included the prior probabilities and the compatibility matrices. The assumed prior probabilities ranged from 0.25 to 0.40. Use of 0.25 assumes no prior information ($P(1) - P(2) - P(3) - P(4) - 0.25$) and thus, the initial probabilities were equal across the maps. If values higher than 0.25 were assumed, the higher values were assigned based on the assumption of four equal thickness strata (see Figures 6.20 and 6.21). If a value greater than 0.25 was assumed for a stratum, the initial probabilities of the other three soil types were set to be equal so that the sum of the initial probabilities at each point was 1.

The "true" maps were sampled by simulating three test borings in each map. The test borings were equally spaced as indicated in Figures 6.20 and 6.21. The soil conditions in the test boring columns were assumed to be known so the soil types were given probabilities of either 1 or 0 based on the actual soil types in the "true" map columns.

Two compatibility matrices were used to estimate the "true" maps. The first compatibility matrix, referred to as the isotropic matrix, was composed of values of +1 for consideration of the same soil type at any neighboring cell as at the central cell. All other elements in the isotropic compatibility matrix were -1. The second compatibility matrix used was based upon complete knowledge of the entire "true" map. In this case, the compatibility matrix for each soil type was based on the following equation:

Equation 6.1:

$$c(i \in j, h \in k) = P \frac{(i \in j, h \in k)}{P(i \in j) P(h \in k)}$$

where

$i = the$ central cell,

$j, k = soil$ types,

$h = a$ neighboring cell.

The calculated "true" map compatibility matrices differed substantially from the assumed isotropic matrices. The off-diagonal elements of the calculated matrices were very close to the assumed -1 values in the isotropic matrices. However, the diagonal elements, which were assumed to be +1 in the isotropic matrices, were substantially lower. The average values for the diagonal elements for soil types 1, 2, 3 and 4 for the map in Figure 6.20 were 0.55, 0.42, 0.76 and 0.55, respectively. By comparison the average values for the map in Figure 6.21 were 0.33, 0.89, 0.64 and 0.55.

The results of the application of probabilistic relaxation to "typical" geotechnical profiles are shown in Figures 6.20 and 6.21. The high mis-classification error for the isotropic compatibility matrix with the assumed 0.25 prior probabilities is directly attributed to the effects of no prior information. When the initial probabilities are all equal (0.25), points away from the actual data points, where one of the proba-bilities is 1.0 and the others are 0.0, require several iterations for the known points to affect the classification.

Use of the isotropic compatibility matrix resulted in consistently lower mis-classification error than use of the compatibility matrix calculated from the "true" map. Mis-classification error after sufficient itera-tions to overcome initial mis-classification was typically 2 to 6% with the isotropic compatibility matrix compared to 10 to 60% for the "true" map compatibility matrix.

Mis-classification error for the isotropic compatibility matrix was less than would occur if the "true" map spatial frequencies were used to esti-

mate the final map. This is attributed to the tendency of the isotropic compatibility matrix to cause the probabilities to grow outward from the data points, similar to Trial Data 4 in Figure 6.19.

With the "true" map compatibility matrix the mis-classification error was greater than if the "true" map spatial frequencies were used to estimate the final map.

The mis-classification error is directly proportional to the prior probabilities for the isotropic compatibility matrix and inversely proportional for the "true" map compatibility matrix. The isotropic compatibility matrix performs best when the prior probabilities are equal. This is attributed to the ability of the isotropic compatibility matrix to expand from the geometry of the known data points and to reflect that geometry into the regions with lower initial probabilities. The "true" map compatibility matrix has values of lower magnitudes (i.e., closer to 0), and is less successful in reflecting the data geometry into the full map.

For the example data sets with 10 cells between the data columns, it took 5 to 8 iterations for the mis-classification error to stabilize with the isotropic compatibility matrix. The number of iterations required corresponds directly with the number of iterations required to "close" the spacing between the data columns.

Entropy is not a good indicator of mis-classification error since entropy decreases with successive iterations as the posterior probabilities increase regardless of the mis-classification error.

6.5.4 Comparison Between the Switzer Model and Probabilistic Relaxation

Probabilistic relaxation was used to estimate final probabilities for Maps 2 and 3 that were used by Nucci (1979) and Lee (1982). These maps (see Figures 6.22 and 6.23) were selected by Nucci and Lee to assess the capability of the Switzer model to estimate two state probabilities using discrete points (random and regular grid) and transect lines, respectively. These maps, and others, were chosen specifically by Nucci and

179

Lee because they appeared to be nearly isotropic with respect to the distribution of the two states that also were nearly equal in their spatial frequency.

Nucci (1979) and Lee (1982) used the maps to study the ability of Switzer type models to predict two-state, isotropic maps. Nucci (1979) studied the maps using random and grid sampling patterns with various sampling intensities to study the performance of the Switzer model in general and to assess the resulting differences in the model parameters. In each case, Nucci assumed that the spatial frequency of the two states was known.

Lee (1982) studied the application of a Switzer model based method to the estimation of state between parallel sampling lines or transect lines. Lee's model used the information from the transect lines to improve the estimates of state between the lines. Lee used the actual state frequency observed along the length of a particular sampling line for the spatial frequency in the model. This is a significant departure from the assumption of spatial isotropy used by Nucci.

Probabilistic relaxation was applied to the maps in Figures 6.22 and 6.23 by digitizing the maps in a 66 x 66 grid and analyzing the resulting cellular map. The grid spacing was selected to agree with that used by Lee. Using the same transect lines as Lee, the mis-classification error was calculated for probabilistic relaxation iterations using both the isotropic and, in some cases, "true" map compatibility matrices.

The results of the estimation methods are summarized in Figures 6.24 and 6.25. Conclusions regarding the mapping methods, based on the analysis performed and indicated by Figures 6.24 and 6.25, are as follows:

1. The magnitude of the mis-classification error decreases for the randomly spaced points and regularly gridded points using Nucci's Switzer type model, transect lines using probabilistic relaxation, and transect lines using Lee's Switzer type model.

2. The mis-classification error for the transect lines using probabilistic relaxation with the isotropic compatibility matrix and prior probabilities of 0.5 is approximately 150% of the error for the same data using the Lee transect line model based on the Switzer model. However, it should be noted that the Lee model does not use the spatial frequency for the entire map, but calculates spatial frequencies for each map segment (area between transect lines) using the observed frequency on the two line transects which border the map segment to be estimated.

3. The mis-classification error for all four mapping methods decreases as the relative distance between data points decreases.

4. Plots of the $P_{ij}^{(r+1)}$ for Map 3 show the regions of relatively high probabilities with relatively narrow transition zones between states.

5. Unlike Lee's model where P_{ij} dropped to the spatial frequency very quickly moving perpendicular to the transect line, the probabilistic relaxation model predicts high probabilities between the transect lines with successive iterations.

6.5.5 Definition of the Compatibility Matrix

6.5.5.1 Introduction

The analysis of the contrived sections and the actual geology maps demonstrated that the performance of the isotropic compatibility matrices is better than the actual map compatibility matrices. The isotropic matrices consistently resulted in lower mis-classification errors. This is attributed to the tendency of the higher compatibility matrix elements to expand the regions around the actual data points. The actual map compatibility matrices with their lower element values have not demonstrated the ability to expand the regions.

The definition of the compatibility matrix is relatively easy in the case of the contrived data or the two-state geology maps. However, definition of the compatibility matrix for refinement of a probabilistic profile is another matter.

Conceivably, an isotropic compatibility matrix could be used. However, there is no basis in the data for the selection of such a matrix. The definition of the compatibility matrix could be left to the engineer. The engineer is often aware of the general stratigraphic sequence and could define general compatibilities and incompatibilities. However, the definition of the more subtle elements would be totally arbitrary.

Before probabilistic relaxation methods can be applied to the refinement of probabilistic profiles, it is necessary to define the compatibility matrix in a rational, repeatable form. This definition should be based upon the image enhancement research, but should also incorporate geology and geotechnical engineering concepts.

Soil stratigraphy issues, unlike the typical image enhancement problems, are three dimensional. Therefore, the definition of the compatibility matrix should also incorporate three dimensional considerations.

The following sections describe a method developed as part of this research to rationally define the compatibility matrix based on the information obtained in the test borings.

6.5.5.2 General Considerations

Development of the compatibility matrix definition should include three dimensional consideration of the available geometry and geology information. The three dimensional consideration means that the number of neighbors to a cell is increased to 26 (see Figure 6.26) compared to 8 in two dimensions. The inclusion of three dimensional considerations will require a significant increase in the number of calculations. This will be discussed in more detail in the case history applications.

182

The developed compatibility matrix is based upon Equation 6.1, repeated here.

Equation 6.1:

$$c(i \in j, h \in k) = P \frac{(i \in j, h \in k)}{P(i \in j) P(h \in k)}$$

where

i = the central cell,

j, k = soil types,

h = a neighboring cell.

In image enhancement the numerator of Equation 6.1 is often evaluated using the "best estimate" probabilities in the map or image. However, that approach implies a certain level of confidence in the original image. The definition developed here is based on the test boring data, not an extension of that data such as a probabilistic profile.

The joint probability in the numerator can be estimated using the available strata interface and thickness information, considering three dimensional geometry. The individual probabilities in the denominator can be estimated using the test boring information regarding relative strata thickness directly. The following sections discuss the development of the compatibility matrix definition.

6.5.5.3 Consideration of Available Data

The basis of the compatibility matrix is to define the relative compatibility of soil types based on the observed spatial relationships. Conceptually, the soil strata interface surfaces have a major influence on the spatial relationships between soil types. Therefore, the definition of the compatibility matrix should include consideration of the geometry of the interface surfaces.

183

Test borings provide data regarding strata surfaces in the form of strata change elevations. Ideally, the definition of the compatibility matrix should include these observations with a limited amount of interpretation. Based on the discussion in Chapter 3, the surface modeling methods with the least amount of interpretation are those that are triangle based. These methods are attractive for other reasons. Mainly that the piecewise planar surfaces are easily quantifiable for computer use as compared to continuous surfaces.

Each of the planes separates space into two regions, those on either side of the infinite plane. These regions in the area of the triangle are, in fact, regions of different soil types. Considering the three dimensional array of cells shown in Figure 6.26, the planes which could separate the center cell from each of the neighboring cells can be defined by a range of strike and dip angles assuming that the condition of soil type J being above soil type K is always maintained.

The relationship of the acceptable ranges of strike and dip for the dividing planes is summarized in Figure 6.27. Note that the definition of acceptability is based on the relationship of soil type J over soil type K, and the geometry of the cell arrangements. Since the vertical scale in profiles is usually exaggerated to 1H:5V, this factor has been included in defining the ranges of acceptability.

The available strata interface information can be summarized by performing the Delaunay triangulation, and then calculating the dip vector for each of the triangles. Delaunay triangulation was chosen due to its favorable properties discussed in Chapter 3. The dip vectors can be summarized in a polar plot. Figure 6.28 is a typical dip vector polar plot for the information from the Back Bay and Cambridge Center case histories. The dip vector plots for the case histories are discussed in more detail below.

184

In order for the center cell to be soil type J and any other cell to soil type K, two conditions must be met. First, the soil interface J/K must pass between the two cells. Second, soil type J must be penetrated. The consideration of the soil strata interfaces has addressed the first condition. The strata thickness data can be used to consider the second condition.

The test borings provide information about the observed stratum thickness for any stratum that is encountered. The compatibility matrix definition presented here is restricted to using full penetration data. Partial penetration data, which is discussed in Chapter 5, could be implemented into the definition.

The critical thickness with respect to the full penetration of soil type J is a function of the interface geometry, the cells being considered, and the observed soil type J stratum thickness (see Figure 6.29). Note that the definition of the probability is location independent. This was specifically chosen because the ultimate goal is a global definition of the compatibility matrix, as opposed to a regional or location dependent definition.

The analytical methodology presented in Figures 6.27 through 6.29 can be used to define a joint probability if the assumption is made that the interface geometry and stratum thickness considerations are independent. In that case the joint probability is the product of the individual probability of the interface geometry and stratum thickness considerations. Transitions from soil type J to L or others are handled using the same methods.

The individual probabilities of the soil types in the denominator were estimated by using the relative proportions of the fully penetrated stratum thicknesses from the test boring data.

6.5.6 Probabilistic Relaxation Profiles - Back Bay

6.5.6.1 Definition of the Compatibility Matrix

Probabilistic profiles of the Back Bay and Cambridge Center case histories were studied to evaluate the definition of the compatibility matrix and the performance of probabilistic relaxation.

The compatibility matrix was defined as described in the previous section. The image enhancement literature (Peleg and Rosenfeld, 1978; Fekete et al., 1981; Rosenfeld and Kak, 1982; DiZenzo, 1983; Kittler and Illingworth, 1985) includes discussion of methods of scaling the compatibility matrix such that the range is from -1 to +1. The normal procedure is to take the logarithm of the probability ratio in Equation 6.1, and then truncate the results such that the desired range is accomplished. At this point it should be noted that in image enhancement the truncation level appears to be arbitrary.

Due to the relatively low probability of the marine sand and glacial till strata, the probability ratios were comparatively high so it was necessary to adjust the values to achieve the range from -1 to +1. The image enhancement approach was applied with variations in the level of truncation. Varying the truncation limit results in a significant change in the compatibility matrix. Any logarithm terms above or below the truncation limits are in effect set to +1 or -1, and those terms within the limits are scaled accordingly. Therefore, as the truncation limit is reduced, the tendency of the elements in the compatibility matrix is to approach an isotropic condition (all +1's for the same soil type and all -1's elsewhere). This process is discussed in the following section with examples of the results.

6.5.6.2 Example Profiles

Profile 5 was chosen from the Back Bay case history for an evaluation of the definition of the compatibility matrix and the application of probabilistic relaxation to the probabilistic profile. This profile was cho-

sen because it exhibits the conditions of overlapping strata and continuous models of discontinuous strata. Initially, a probabilistic profile (using the methods discussed in Section 6.4) was developed for Profile 5 and for two planes paralleling Profile 5, but offset 25 feet in either direction. Probabilistic profiles were developed for the three planes so that three dimensional probabilistic relaxation could be studied, as well as, two dimensional.

A cellular map of the Profile 5 probabilistic profile is shown in Figure 6.30. Also shown in Figure 6.30 are the known conditions at test boring locations that are closer to the plane of Profile 5 than either of the other two planes. These test boring columns are in essence known; however, it must be remembered that the test borings have been shifted into the nearest plane and therefore, the "true" conditions in the plane may be different than the known conditions.

Probabilistic relaxation was applied to probabilistic Profile 5 using various truncation levels in the definition of the compatibility matrix. The various compatibility matrices were then applied to both Profile 5 alone (a two dimensional problem), and the three probabilistic profiles together (a three dimensional problem) with Profile 5 in the middle. The results of the two dimensional application will be presented first.

One of the objectives of probabilistic relaxation is to refine the probabilistic profile. Ideally, the refinement process will result in a decrease in soil types with overlaps or that are discontinuous, and a corresponding increase in the compatible soil types. Therefore, one of the first performance checks is to observe the tendency of the soil types to either expand or contract. Figure 6.31 shows the effects of the various truncation values on the expansion and contraction of the areas of the soil types in Profile 5 after 100 iterations of probabilistic relaxation.

Of particular interest is the performance of the marine sand and glacial till strata. The marine sand demonstrates a very consistent tendency to reduce its area within the range of truncation values analyzed. The glacial till exhibits a very strong propensity to expand with a corresponding decrease in the adjacent Boston Blue Clay and the rock. Note that these are the two strata (marine sand and glacial till) with the lowest probability of occurrence based on the test borings, and therefore, the smallest denominator in the probability ratio (Equation 6.1). It is expected then that these strata would reflect the effects of the truncation value most since the probability ratios are truncated significantly.

The performance of the glacial till is particularly interesting. Due to the nearly equal probabilities of the Boston Blue Clay, glacial till and rock, truncation values larger than +1 result in a tremendous increase in the glacial till. This is attributed to the condition that at larger truncation values, the glacial till is given compatibility values of +1 for both the Boston Blue Clay and the rock. Therefore, the probabilities of the glacial till rise considerably. Of interest also is the sensitivity of the glacial till to the truncation value. Even though it expands tremendously with values in excess of +1, it also contracts with values less than +1.

The marine sand performs differently than the glacial till for two reasons. First, due to its discontinuity as observed in the test borings and observed stratum thickness, the estimated probabilities for the marine sand are relatively low, so that with probabilistic relaxation iterations the marine sand probabilities decrease and it is replaced by other soil types. Secondly, the relationship of the tendency to expand is not nearly as strong as the glacial till due to the absence of the marine sand in many locations.

An assessment of the compatibility matrix definitions and the process of probabilistic relaxation applied to soil profiling must include comparison of the results to the "true" profile. However, unlike the probabil-

ity mapping research by others (Nucci, 1979; Lee, 1982), the "true" map is unknown in the soil profiling application except for the test boring data which includes some uncertainty as well. In order to check the results of probabilistic relaxation, it was assumed that the "true" conditions are those observed in the test borings, which have in turn been translated into the nearest profile plane. Since the soil conditions in the plane may differ from the adjacent test borings, it is impossible to calculate the actual mis-classification errors. However, use of the test borings for calculation of the apparent mis-classification errors is the best alternative. Before discussing the comparisons, however, it is necessary to discuss the types and severity of those errors.

There are two types of errors that occur in mis-classification. First, and by far more serious, are errors of absence/presence. These are errors of either predicting the presence of a soil type which was not encountered in the test borings or the absence of an observed soil type. These errors have potentially severe consequences on typical geotechnical engineering analysis such as slope stability or settlement analysis. In critical applications, these errors could lead to the unnecessary expenditure of site characterizations resources. The second type of error is elevation error. These are errors in the predicted elevation of a soil strata interface. In most cases the consequences of elevation errors are much less than for presence/absence errors.

Both presence/absence and elevation errors may occur as a result of the cellular nature of the probabilistic profiles and probabilistic relaxation techniques. For the analysis presented here, the cells are 5 ft. high and 25 ft. wide (1V:5H).

Figure 6.32 is a summary of the mis-classification errors for the two dimensional analysis performed on Profile 5 using various compatibility matrices and compared to the adjacent test borings. The figure shows plots of the total mis-classification error and the presence/absence error in terms of both the number of mis-classified cells and the percentage of the cells in the test borings that were mis-classified. The

189

difference between the total and presence/absence errors is the elevation error. The errors are shown for both 20 and 100 iterations of probabilistic relaxation with compatibility matrices based on a range of truncation values.

All three errors (total, presence/absence, and elevation) are minimal at a truncation value of +1. Higher truncation values lead to a considerable increase in error, particularly in the more serious presence/absence error. In most cases the error for 100 iterations is greater than that at 20 iterations. Based on this information, it appears that it is not necessary to perform more than 20 iterations. This same conclusion will be drawn later when considering other parameters such as entropy and the rate of change in the probabilities. This conclusion is consistent with image enhancement literature (Rosenfeld and Kak, 1982; Fekete et al., 1981) which recommends using approximately 10 iterations or so.

The results of probabilistic relaxation with the optimal truncation value (+1) are a 50% reduction in the presence/absence error and a 10% reduction in the elevation error. The reduction in presence/absence error is particularly significant.

Profile 5 was also analyzed as a three dimensional case. In this application three planes with Profile 5 as the interior one were analyzed concurrently using the same compatibility matrix for all three. Compared to the two dimensional case with a maximum of 8 neighbors, the three dimensional case with a maximum of 26 neighbors requires a corresponding increase in the number of calculations.

Figure 6.33 presents a summary of the mis-classification error as a function of the compatibility matrix truncation value for the three dimensional analysis. Similar to the two dimensional case, it is possible to reduce the presence/absence error by 25% and the elevation error by 10% by choosing the proper truncation value. In this case that value appears to be 0.9.

Similar to the two dimensional analysis results, the errors after 100 iterations are generally higher than after 20 iterations. Although, the three dimensional difference is less than that observed when using two dimensions.

Another measure of the effects of probabilistic relaxation is the average entropy of the image or map as a function of the relaxation iterations. Figure 6.34 is a plot of the average entropy in Profile 5 versus the number of iterations for the compatibility matrix based on the optimal truncation values for both two and three dimensional analysis. The probabilistic relaxation with the optimal truncation value compatibility matrices resulted in nearly identical reduction in the initial entropy, which is the same for both cases. It should be noted also that the average entropy was reduced by about 85% of the initial value in the first 20 iterations. The subsequent 80 additional iterations only lowered the average entropy another 10%. The entropy data demonstrate that the probabilities have increased considerably in the first 20 iterations, and that only relatively minor changes occur in subsequent iterations.

Average entropy was calculated for each of the compatibility matrices for 100 iterations of probabilistic relaxation of Profile 5 for both two and three dimensional cases. The results are presented in Figure 6.35. The results show that the average entropy is less for three dimensional analysis after 20 iterations, but that the average entropy is about the same after 100 iterations.

Another method for assessing the benefits of additional iterations is to review the average rate of change in the probabilities. The average rate of change for the probabilistic relaxation of Profile 5 using the optimal two and three dimensional compatibility matrices is shown in Figure 6.36. The average rate is two orders of magnitude less after about 40 iterations, and then decreases by less than an order of magnitude over the next 60 iterations.

191

The results of probabilistic relaxation with the optimal two and three dimensional compatibility matrices are presented in Figure 6.37 in the form of cell maps after 20 iterations. The cell maps, along with the analysis presented in this section, demonstrate that both the two and three dimensional probabilistic relaxation analysis have resulted in a significant improvement of the original probabilistic profile.

6.5.7 Probabilistic Relaxation Profiles - Cambridge Center

The Back Bay test boring data (see Table A.4) indicates that the geologic sequence is nearly the same with the exceptions of the discontinuous marine sand and the glacial till, which was not observed at several locations. By contrast, the Cambridge Center test boring data (see Table B.3) indicates considered irregularity in the geologic sequence.

It is expected that application of probabilistic relaxation methods will be less successful on the Cambridge Center profiles. The major reasons for this are that the soil strata are interbedded (see Appendix B), and therefore, the conditions are not consistent with the assumptions in Sections 6.4 and 6.5.5 concerning the geologic sequence used to develop the definitions of the probabilistic profiles and compatibility matrix.

Probabilistic relaxation analysis was performed on Profiles B, M and O in the Cambridge Center case history using the same methods described in Section 6.5.6. However, as anticipated, the results indicate no improvement in the presence/absence, elevation or total mis-classification errors. The lack of improvement is attributed to the variable geologic sequence in the Cambridge Center area.

6.6 Summary

Chapter 6 presents the application of existing surface modeling and probability mapping methods to soil stratigraphy assessment, and the development of new probabilistic relaxation methods. The existing surface modeling methods result in conditions (continuous models of discontinuous strata, and strata overlap) which are unacceptable for soil stratigraphy

models. The existing probability mapping techniques, with their limitations to two colors and assumed isotropic conditions, do not satisfactorily address the soil stratigraphy conditions and issues.

The research results demonstrate that the developed probabilistic relaxation methods can significantly decrease the presence/absence, elevation and total mis-classification errors if the site geologic sequence is consistent with the assumptions used to develop the approach.

Table 6.1 - Summary Statistics for the Total Agreement Ratio (TAR) for
Selected Stratigraphic Models.

SUMMARY STATISTICS FOR TOTAL AGREEMENT RATIO (TAR)					
Stratigraphic Model	No. of Pts.	Mean	Stand. Dev.	Median	Range
Kriging - Model 1	156	0.750	0.185	0.826	0.651
Kriging - Model 1	140	0.750	0.186	0.824	0.651
Kriging - Model 2	156	0.717	0.197	0.785	0.793
Kriging - Model 3	156	0.743	0.194	0.811	0.719
Kriging - Model 4	156	0.750	0.185	0.819	0.661
Kriging - Model 5	156	0.749	0.185	0.818	0.647
Kriging - Model 5	140	0.749	0.186	0.814	0.647
Delaunay Tri. - Model 1	140	0.732	0.199	0.804	0.754

Table 6.2 - Summary Statistics of Stratum Thickness Ratio (STR) for Krig-
ing Models 1 and 5, and Delaunay Triangle Model 1, Back Bay.

SUMMARY STATISTICS FOR STRATUM THICKNESS RATIO (STR)					
KRIGING MODEL 1	No. of Pts.	Mean	Stand. Dev.	Max.	Range
Fill	156	1.040	0.279	2.812	2.426
Organic Soils	156	1.058	0.303	2.356	1.895
Marine Sands	38	1.194	1.226	4.909	4.909
Boston Blue Clay	81	1.031	0.123	1.366	0.630
Glacial Till	72	1.583	2.460	20.394	20.394

SUMMARY STATISTICS FOR STRATUM THICKNESS RATIO (STR)					
KRIGING MODEL 5	No. of Pts.	Mean	Stand. Dev.	Max.	Range
Fill	156	1.040	0.279	2.813	2.426
Organic Soils	156	1.058	0.303	2.356	1.895
Marine Sands	38	1.194	1.226	4.909	4.909
Boston Blue Clay	81	1.017	0.121	1.343	0.633
Glacial Till	72	1.421	1.584	12.286	12.106

SUMMARY STATISTICS FOR STRATUM THICKNESS RATIO (STR)					
DELAUNAY TRIANGLE MODEL 1	No. of Pts.	Mean	Stand. Dev.	Max.	Range
Fill	140	1.039	0.297	2.860	2.565
Organic Soils	140	1.084	0.349	2.464	2.011
Marine Sands	32	1.863	2.215	9.340	9.340
Boston Blue Clay	69	1.036	0.132	1.406	0.617
Glacial Till	64	1.328	1.285	8.220	8.095

Table 6.3 - Summary Statistics of Stratum Interface Residual (SIR) for Kriging Models 1 and 5, and Delaunay Triangle Model 1, Back Bay.

SUMMARY STATISTICS FOR STRATUM INTERFACE RESIDUAL (SIR)					
KRIGING MODEL 1	No. of Pts.	Mean	Stand. Dev.	Max.	Range
Organic Soils	156	0.038	4.020	12.69	24.95
Marine Sands	37	0.127	2.717	7.30	11.74
Boston Blue Clay	157	-0.031	3.386	10.72	20.75
Glacial Till	76	0.044	7.687	22.66	49.72
Rock	77	0.226	8.431	25.54	57.29

SUMMARY STATISTICS FOR STRATUM INTERFACE RESIDUAL (SIR)					
KRIGING MODEL 5	No. of Pts.	Mean	Stand. Dev.	Max.	Range
Organic Soils	156	0.039	4.020	12.69	24.95
Marine Sands	37	0.127	2.717	7.30	11.74
Boston Blue Clay	157	-0.031	3.386	10.72	20.75
Glacial Till	76	-0.496	7.925	19.73	49.66
Rock	77	-0.725	8.378	18.20	51.01

SUMMARY STATISTICS FOR STRATUM INTERFACE RESIDUAL (SIR)					
DELAUNAY TRIANGLE MODEL 1	No. of Pts.	Mean	Stand. Dev.	Max.	Range
Organic Soils	140	-0.073	4.182	13.02	25.27
Marine Sands	25	-0.194	2.530	6.41	10.27
Boston Blue Clay	141	-0.021	3.547	11.11	21.71
Glacial Till	66	0.377	7.359	27.59	41.71
Rock	67	0.114	8.171	29.06	58.56

Table 6.4 - Summary of Model Comparisons Based on 1 X 1 Ranking of Selected Agreement Ratios and Residuals. (/ indicates that by model definition models are identical for that particular stratum)

Comparison Factor	Model No. In Order of Decreasing Performance ->				
TAR (total boring)	5	1	4	3	2
|SIR| (stratum top)					
Organic Soils	1/4/5	3	2	-	-
Marine Sands	1/5	3/4	2	-	-
Boston Blue Clay	1/3/4/5	2	-	-	-
Glacial Till	3/5	1/4	2	-	-
Rock	3/5	1/4	2	-	-
|1-STR| (stratum thick.)					
Fill	5	2	3	4	1
Organic Soils	4	1/2/5	3	-	-
Marine Sands	2	5	3	4	1
Boston Blue Clay	5	4	1/2	3	-
Glacial Till	2	3/5	4	1	-

Table 6.5 - Correlation Coefficient Matrix for Total Agreement Ratios for Selected Stratigraphic Models.

Correlation Coefficient Matrix for TAR			
	Delaunay Tri. - Model 1	Kriging - Model 1	Kriging - Model 5
Delaunay Tri. - Model 1	1.000	0.846	0.839
Kriging - Model 1	0.846	1.000	0.994
Kriging - Model 5	0.839	0.994	1.000
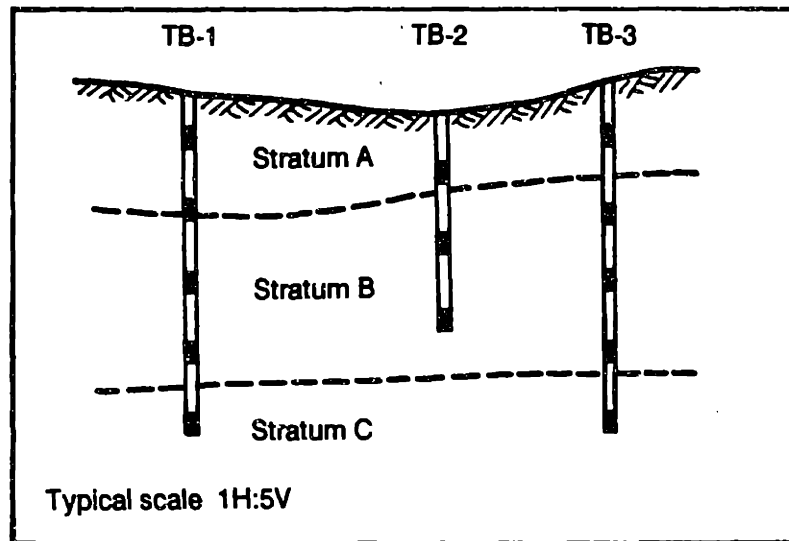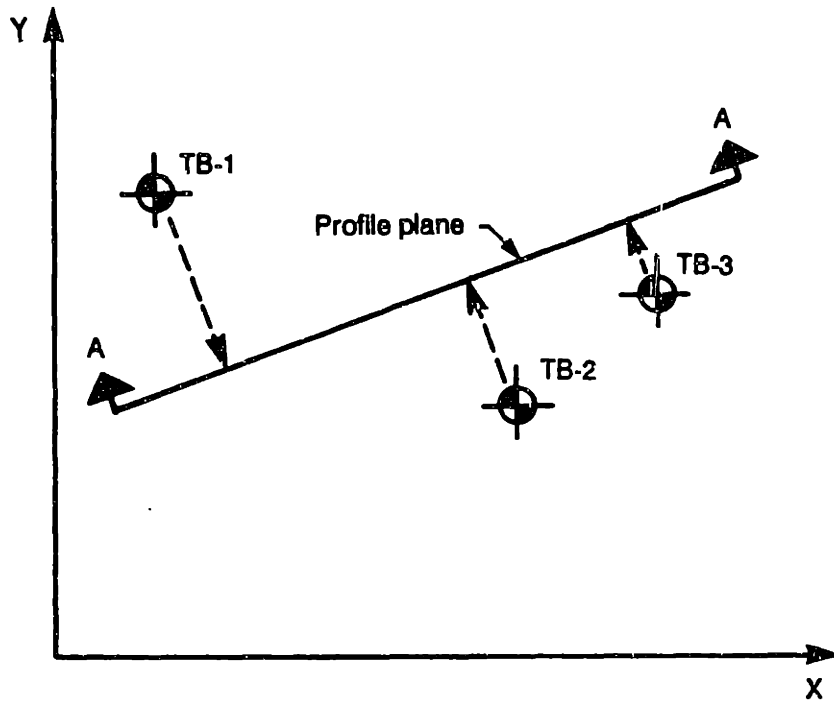
Figure 6.1 - General Procedure for Developing Soil Profiles.
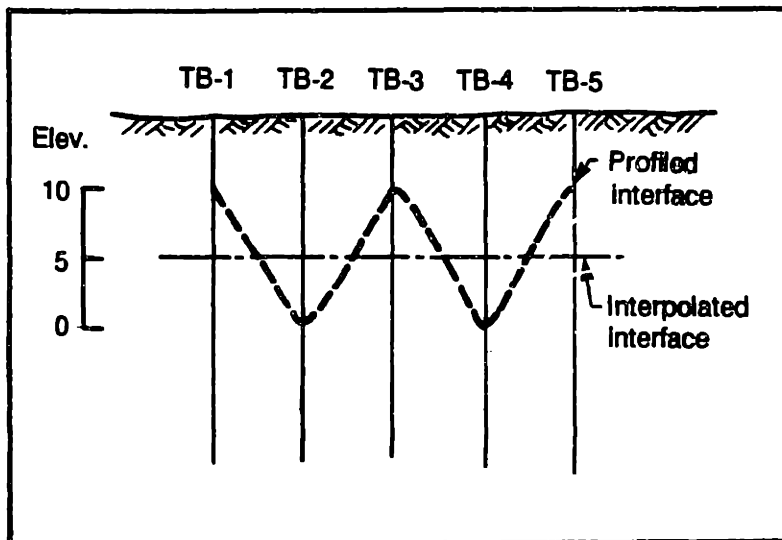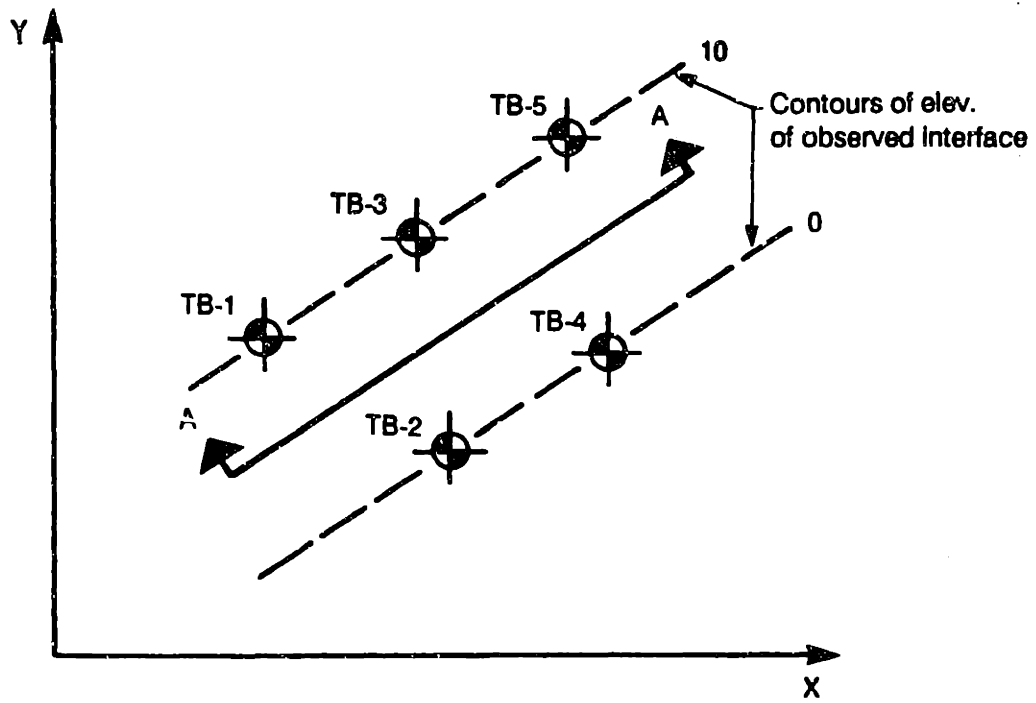
Figure 6.2 - An Example of Problems with Common Soil Profiling Methods.

(a) True conditions,

(b) Model 1: Single surface,
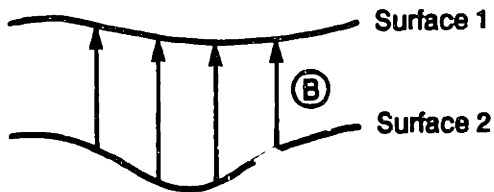
(c) Model 2: Modeled Surface 2 +
Modeled Stratum Thickness B,
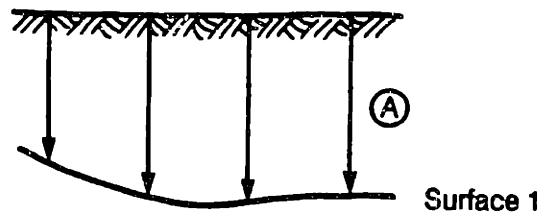
(d) Model 3: Ground Surface -
Modeled Stratum Thickness A.

Figure 6.3 - Examples of Alternative Methods for Modeling a Soil Stratum
Interface.

201
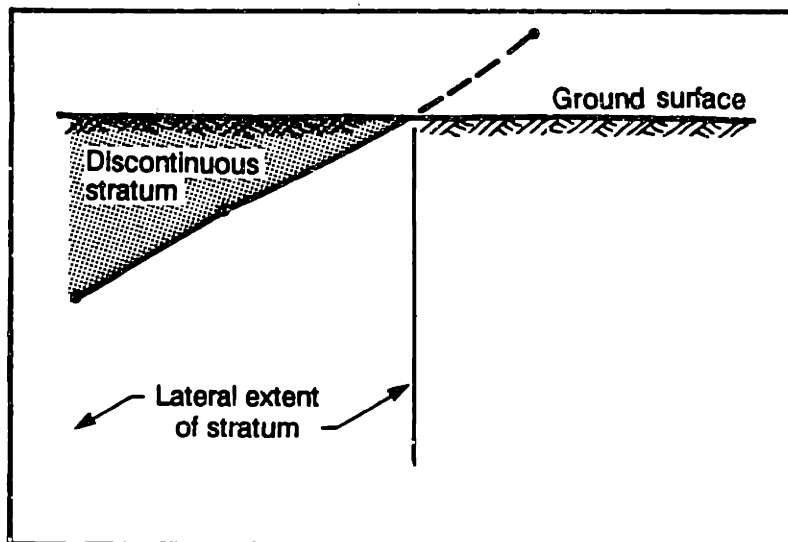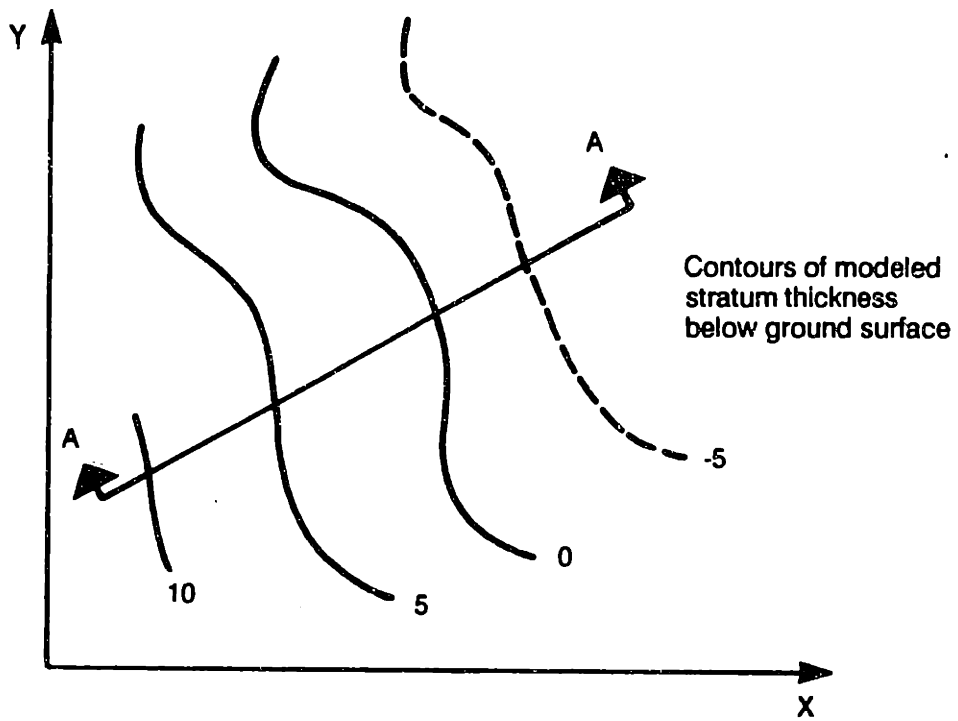
Figure 6.4 - Example of a Model Using Thickness of a Discontinuous Stratum

| | Model 1 | Model 2 | Model 3 | Model 4 | Model 5 |

Ground Surface

Fill

Organic Soils

Marine Sand

Boston Blue Clay

Glacial Till

Rock

Interface modeled using interpolation method and observed interface elevations

Interface modeled by subtracting modeled stratum thickness from modeled overlying interface

Interface modeled by adding modeled stratum thickness to modeled underlying interface

Figure 6.5 - Models of the Back Bay Soil Stratigraphy.
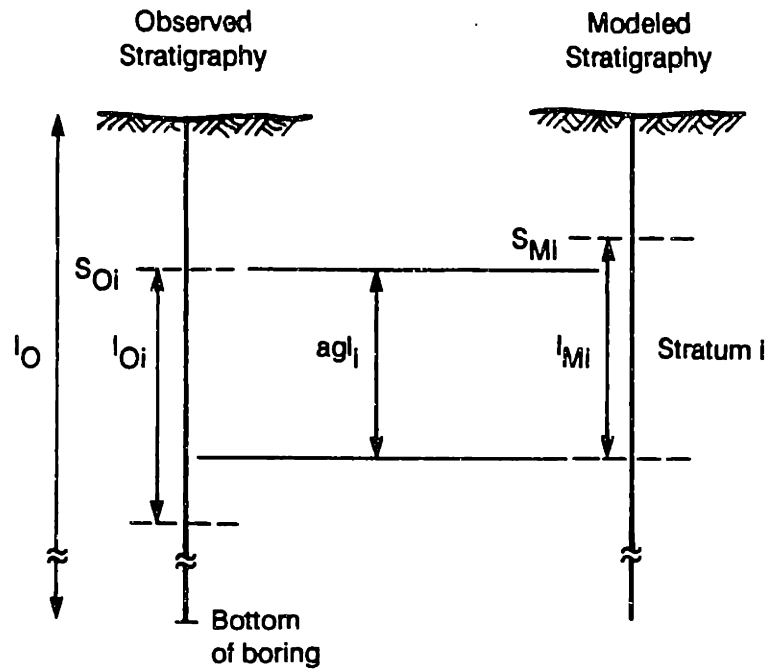
$$\text{Total Agreement Ratio, } TAR = \frac{\sum\limits_{i=1}^{j} agl_i}{\sum\limits_{i=1}^{j} l_{oi}}$$

$j = $ total number of observed strata

$0 \leq TAR$

$$\text{Stratum Agreement Ratio, } SAR = \frac{agl_i}{l_{oi}}$$

$0 \leq SAR \leq 1$

$$\text{Stratum Thickness Ratio, } STR = \frac{l_{mi}}{l_{oi}}$$

$0 \leq STR \leq +\infty$

$$\text{Stratum Interface Residual, } SIR = S_{mi} - S_{oi}$$

$-\infty \leq SIR \leq +\infty$

Figure 6.6 - Factors for Comparison of Estimated Stratigraphy to Observed Stratigraphy.
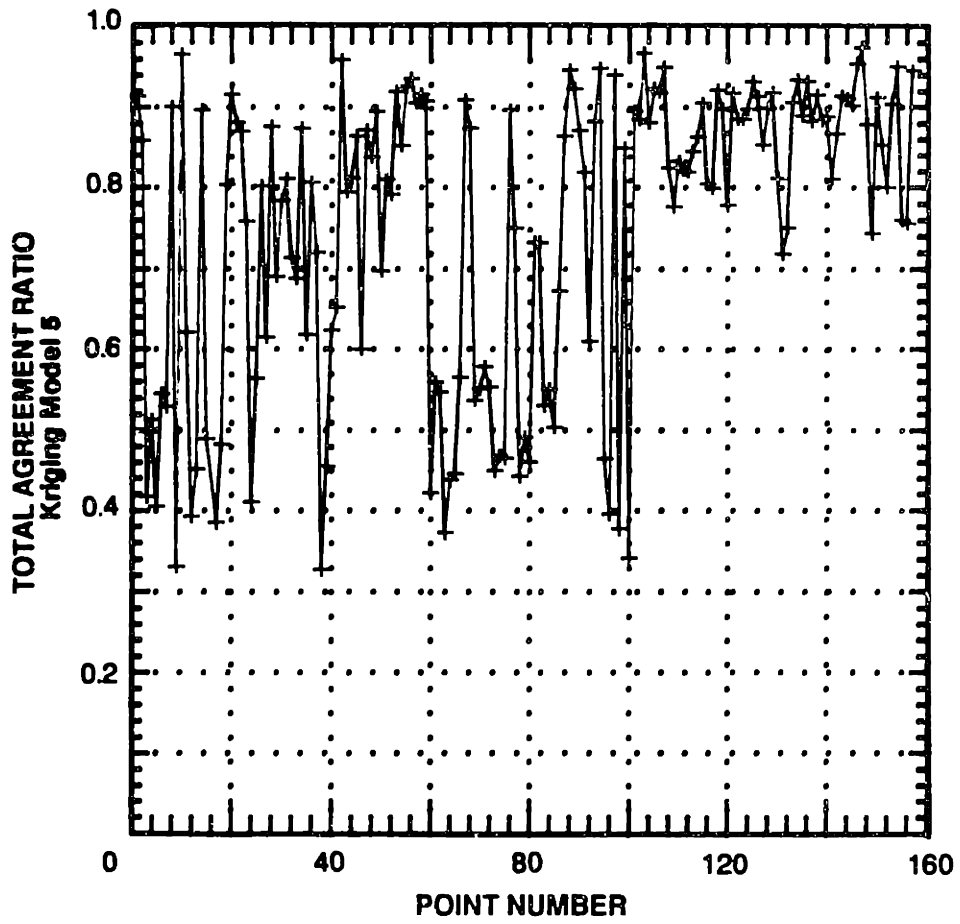
Figure 6.7 - Total Agreement Ratio for Kriging Model 5, Back Bay.
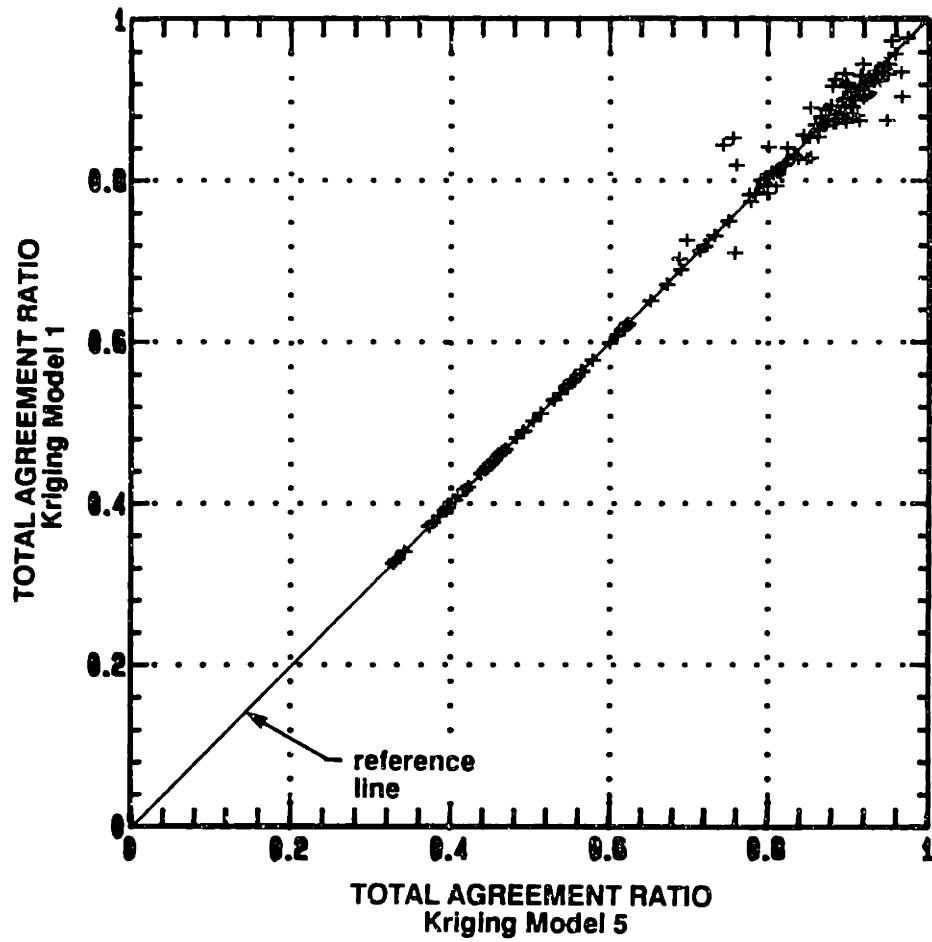
Figure 6.8 - Comparison of Total Agreement Ratio for Kriging Model 1 and Kriging Model 5, Back Bay.
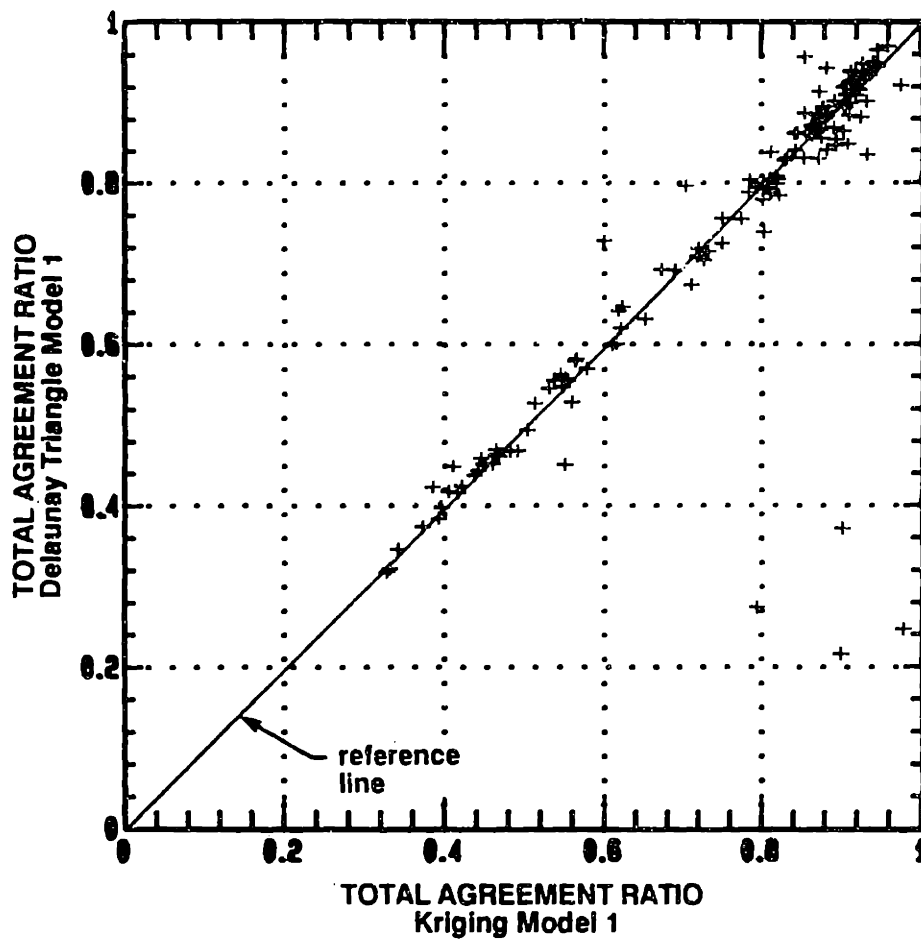
Figure 6.9 - Comparison of Total Agreement Ratios for Delaunay Triangle
Model 1 and Kriging Model 1, Back Bay.
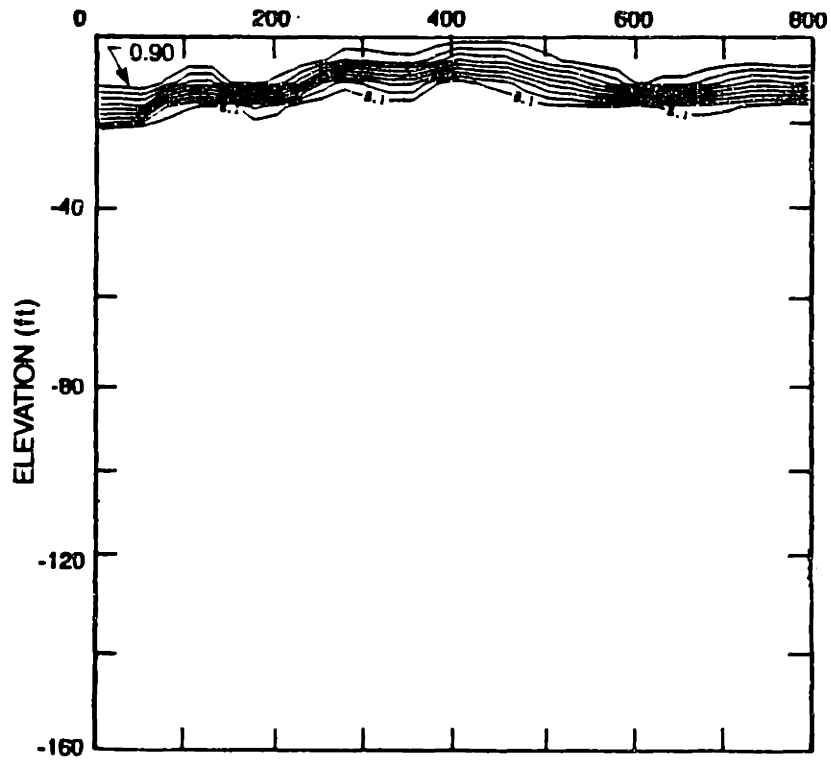
(a) Fill,
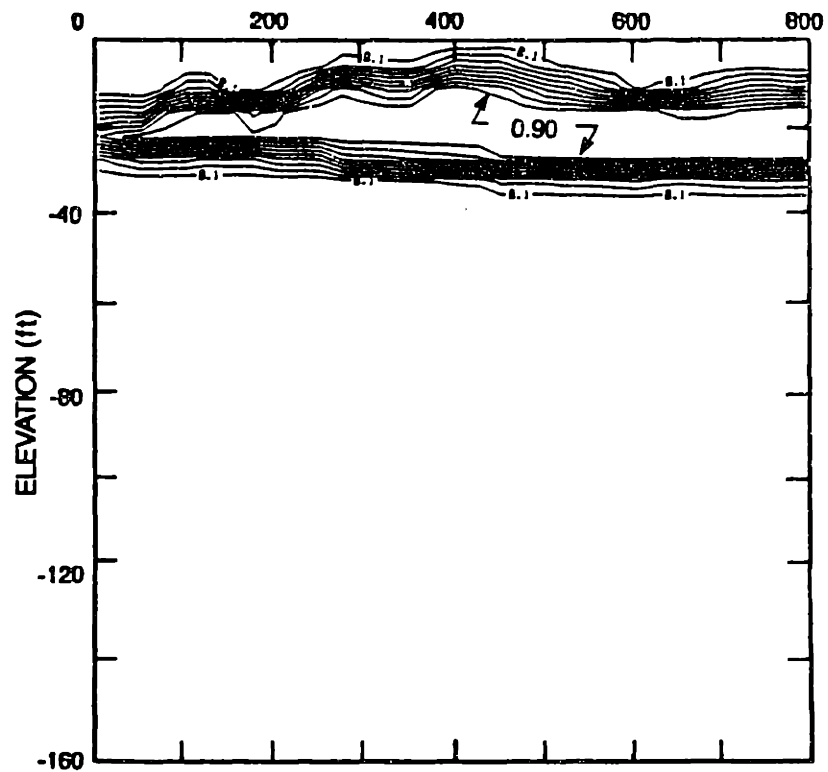
(b) Organic Soils,

Figure 6.10 - Probabilistic Profile Contours of the Probability Individual Strata, Back Bay Profile B (mod.).

208
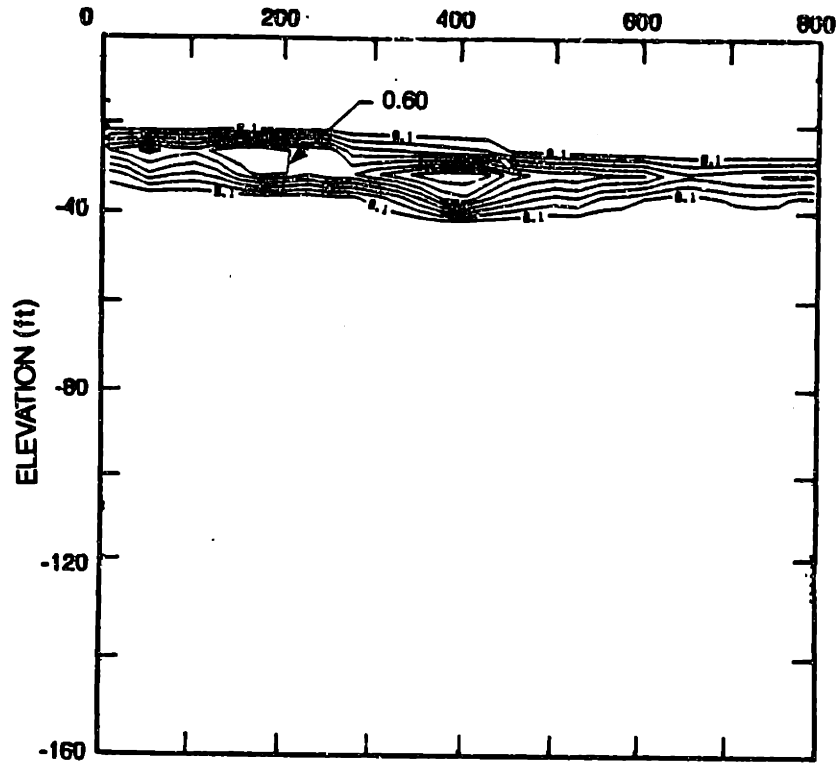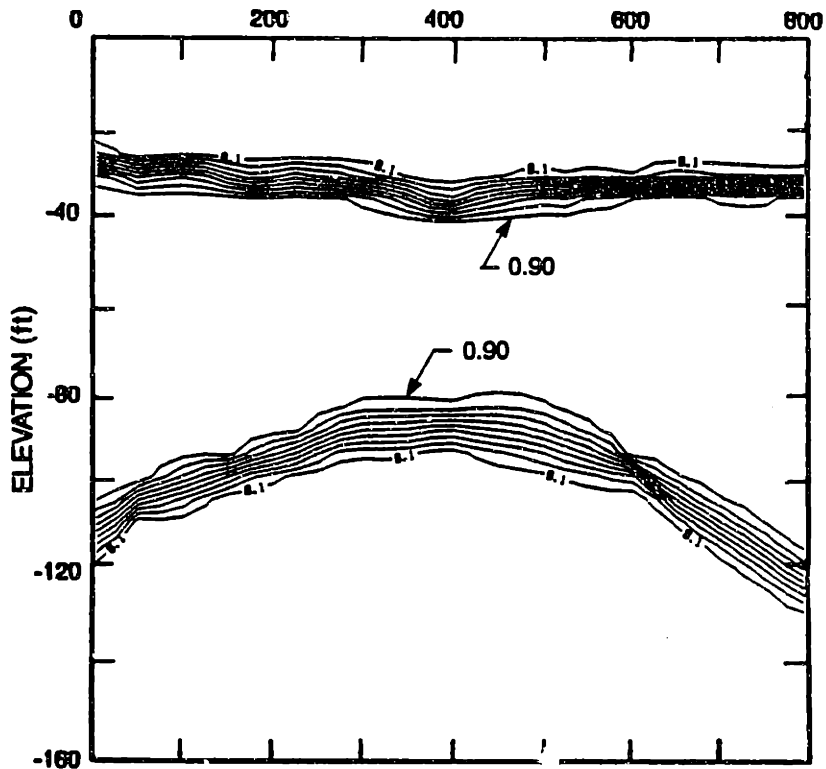
(c) Marine Sand,

(d) Boston Blue Clay,

Figure 6.10 - Continued.
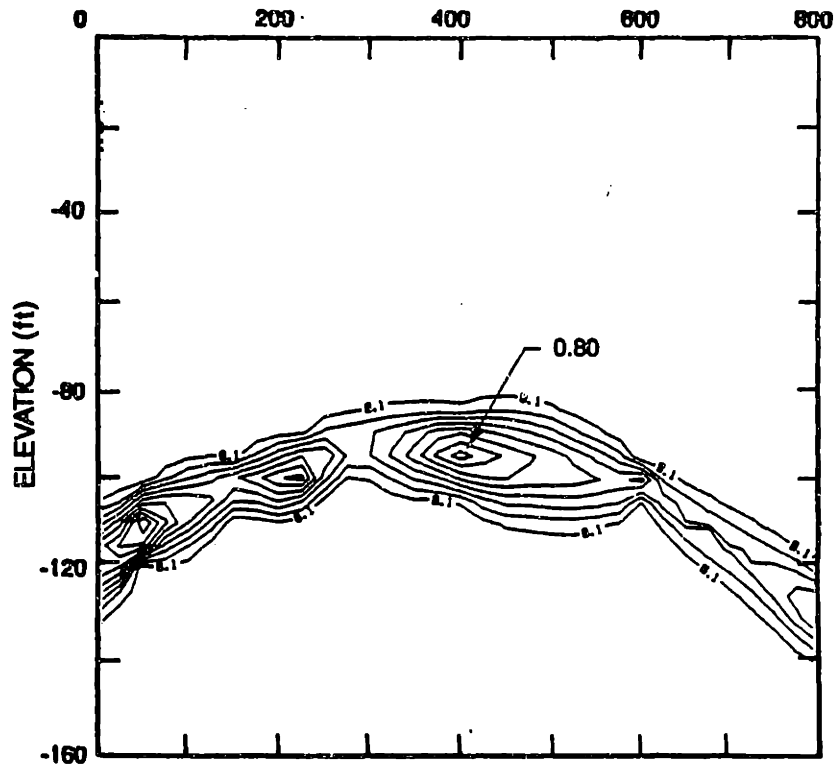
(e) Glacial Till,
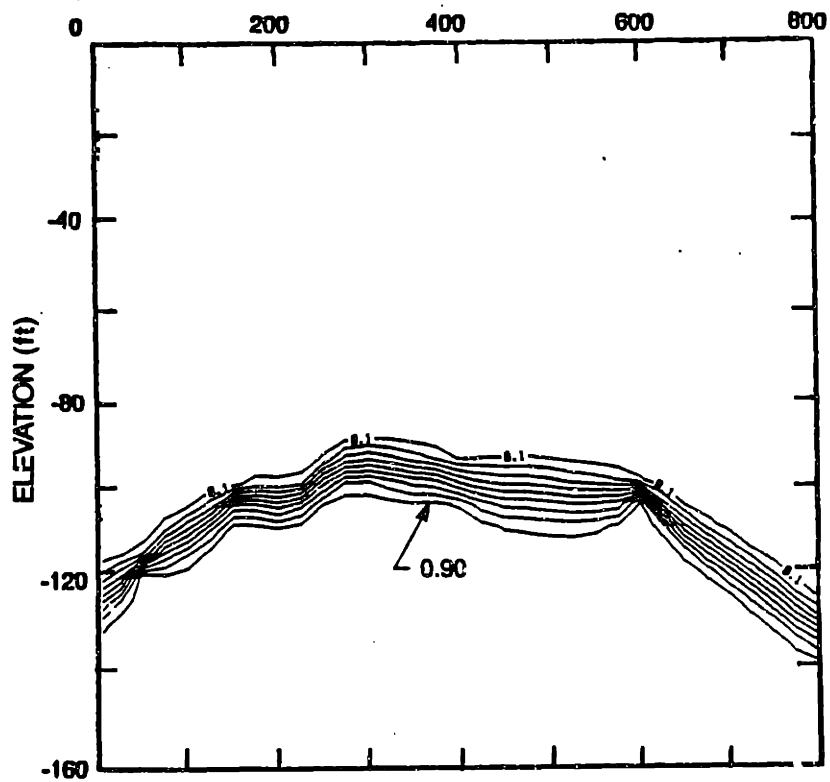
(f) Rock.

Figure 6.10 - Continued.

STATION (ft)
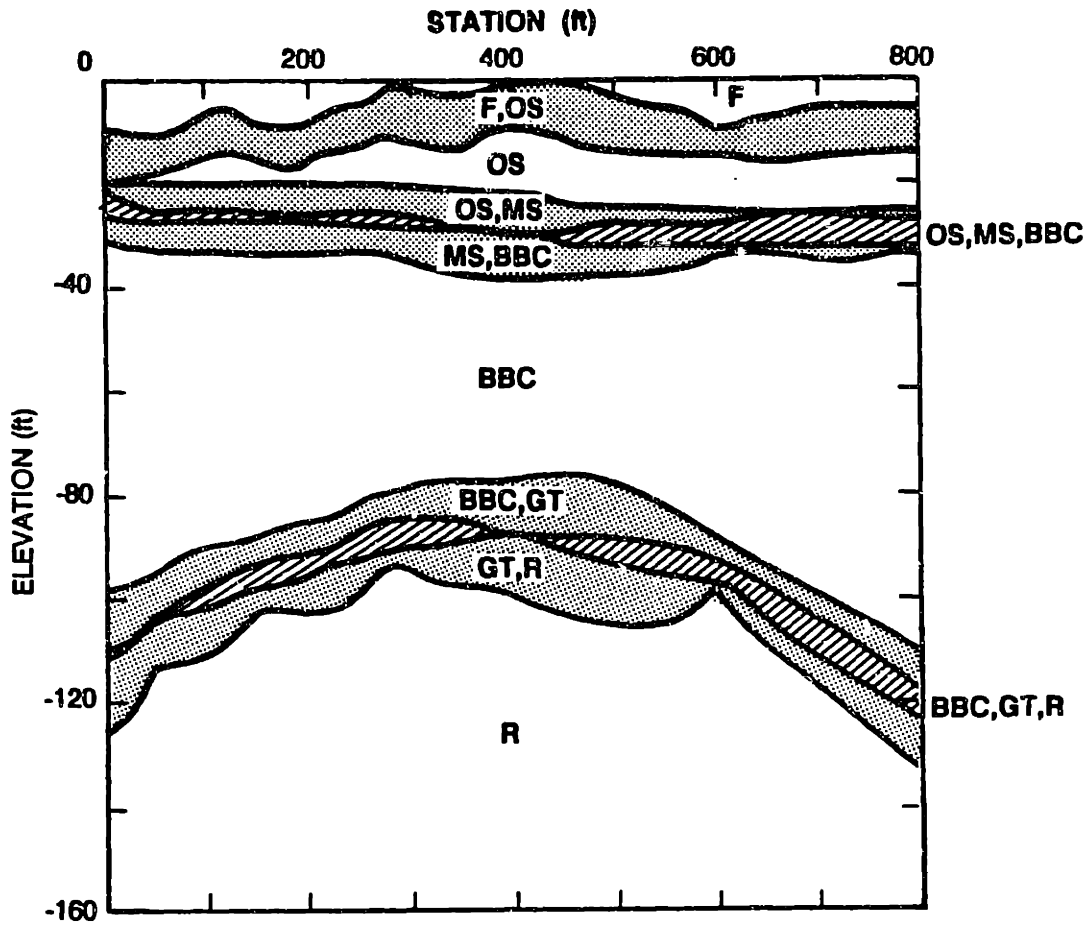
F - Fill
OS - Organic soil
MS - Marine sand
BBC - Boston Blue Clay
GT - Glacial till
R - Rock

☐ P(i) > 0.10

▨ P(i) > 0.10, P(j) > 0.10

▧ P(i) > 0.10, P(j) > 0.10, P(k) > 0.10

Figure 6.11 - Probabilistic Profile of P(i) $\geq$ 0.1 for Profile B (mod.), Back Bay.

STATION (ft)
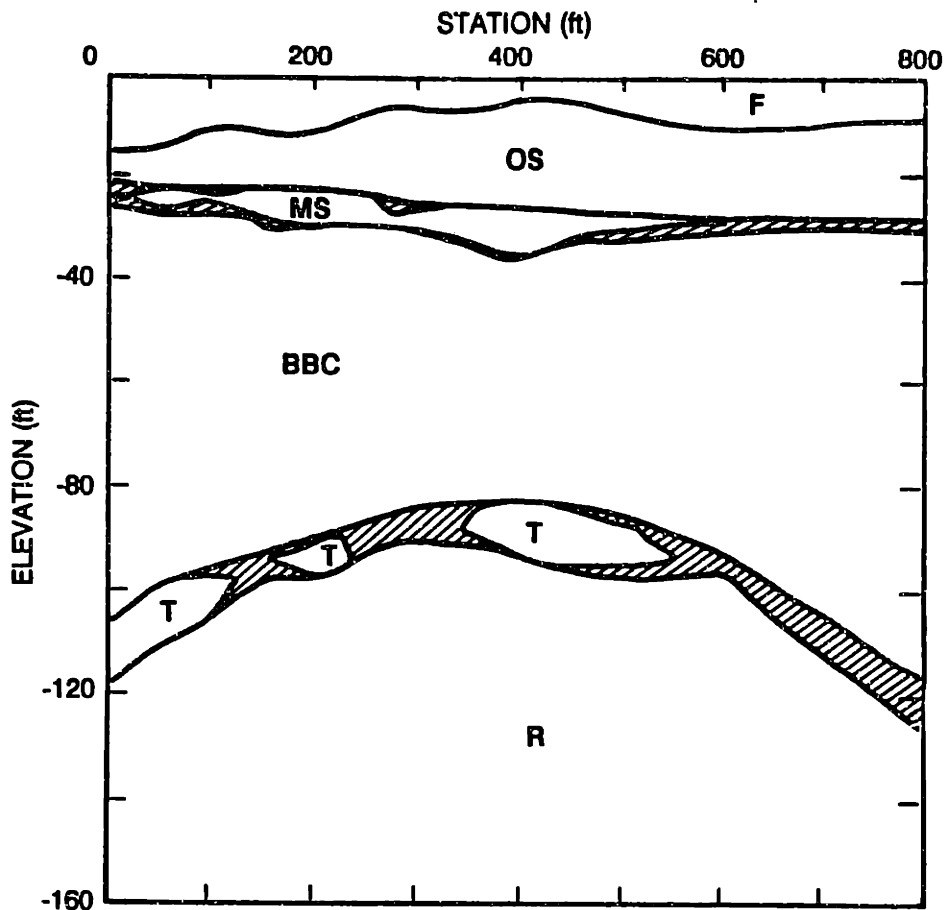
F - Fill
OS - Organic soil
MS - Marine sand
BBC - Boston Blue Clay
GT - Glacial till
R - Rock

☐ P(i) > 0.50
▨ P(all soil types) < 0.50

Figure 6.12 - Probabilistic Profile of P(i) ≥ 0.5 for Profile B (mod.), Back Bay.

ELEVATION
(ft)

Top of Organic Soils

Top of Marine Sands

Top of Boston Blue Clay

Top of Rock

Top of Glacial Till

Top of Organic Soils

Top of Marine Sands

Top of Boston Blue Clay

Top of Glacial Till

Top of Rock
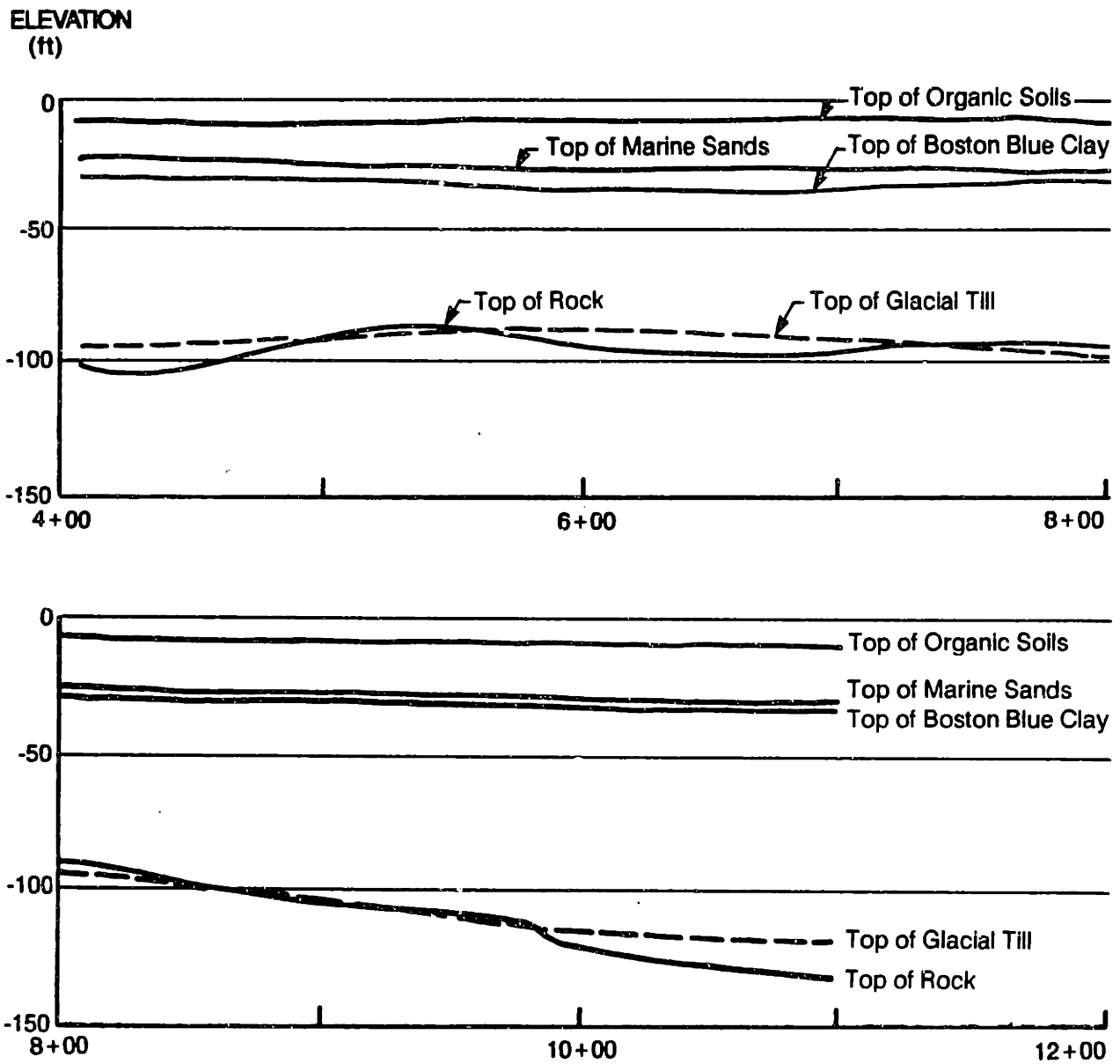
Figure 6.13 - "Best Estimate" Probabilistic Profile for Profile B (mod.),
            Back Bay.
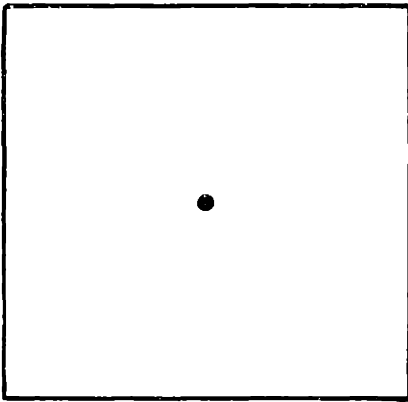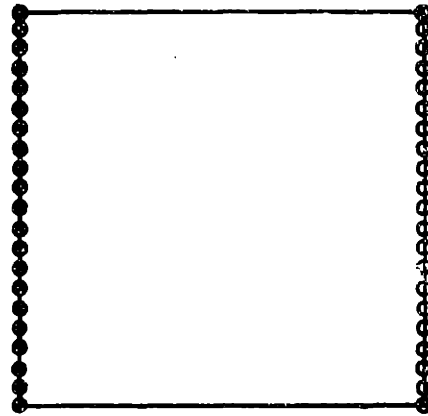
(a) Trial Data 1,   (b) Trial Data 2,
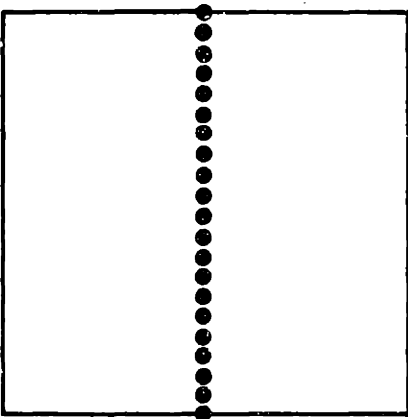
(c) Trial Data 3,   (d) Trial Data 4.
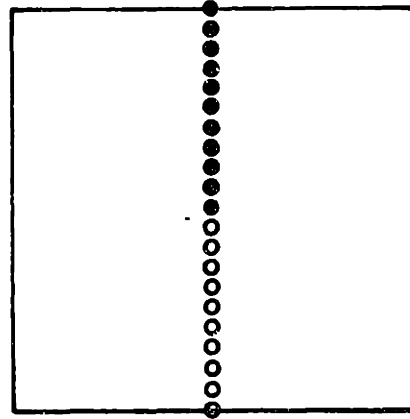
o   Initial P(1) – 0, P(2) – 1
●   Initial P(1) – 1, P(2) – 0
At all other nodes P(1) – P(2) ᴏ 0.50
All data arrays are 21 X 21 grids.

Figure 6.14 - Initial Trial Data Arrays.

Matrix I (c=1, n=1):

+1	+1	+1
+1	c=1 n=1	+1
+1	+1	+1

Matrix I (c=1, n=2):

-1	-1	-1
-1	c=1 n=2	-1
-1	-1	-1

Matrix I (c=2, n=1):

-1	-1	-1
-1	c=2 n=1	-1
-1	-1	-1

Matrix I (c=2, n=2):

+1	+1	+1
+1	c=2 n=2	+1
+1	+1	+1

(a) Matrix I,

Matrix II (c=1, n=1):

-1	-1	-1
-1	c=1 n=1	+1
-1	+1	+1

Matrix II (c=1, n=2):

-1	-1	-1
-1	c=1 n=2	-1
-1	-1	-1

Matrix II (c=2, n=1):

-1	-1	-1
-1	c=2 n=1	-1
-1	-1	-1

Matrix II (c=2, n=2):

-1	-1	-1
-1	c=2 n=2	+1
-1	+1	+1

(b) Matrix II,

Matrix III (c=1, n=1):

-1	-1	-1
0	c=1 n=1	-1
+1	0	-1

Matrix III (c=1, n=2):

-1	-1	-1
-1	c=1 n=2	-1
-1	-1	-1

Matrix III (c=2, n=1):

-1	-1	-1
-1	c=2 n=1	-1
-1	-1	-1

Matrix III (c=2, n=2):

-1	-1	-1
0	c=2 n=2	-1
+1	0	-1

(c) Matrix III,

Matrix IV (c=1, n=1):

-1	+1	-1
+1	c=1 n=1	+1
-1	+1	-1

Matrix IV (c=1, n=2):

-1	-1	-1
-1	c=1 n=2	-1
-1	-1	-1

Matrix IV (c=2, n=1):

-1	-1	-1
-1	c=2 n=1	-1
-1	-1	-1

Matrix IV (c=2, n=2):

-1	+1	-1
+1	c=2 n=2	+1
-1	+1	-1

(d) Matrix IV.

c is state being considered at center   +1 compatible
n is state of neighbor   0 no influence
                                         -1 incompatible

Figure 6.15 - Trial Compatibility Matrices.
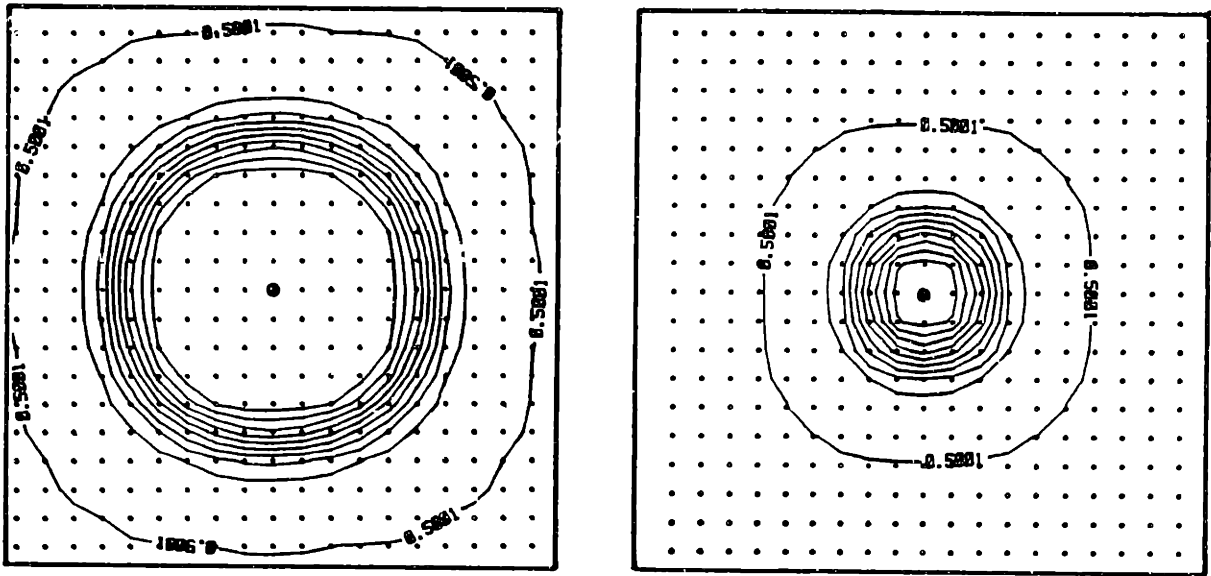
(a) Compatibility Matrix I (5 (l) and 10 (r) iterations),
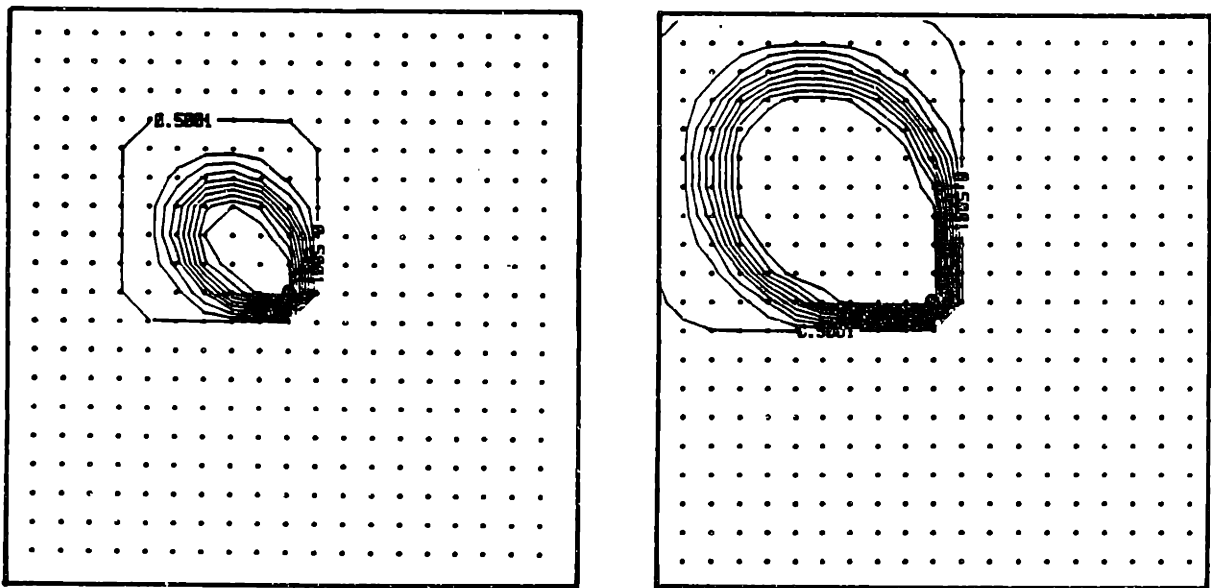
(b) Compatibility Matrix II (5 (l) and 10 (r) iterations),

Figure 6.16 - Contours of P(1) in Increments of 0.005 from 0.50001 to 1.0 for Probabilistic Relaxation of Trial Data 1.
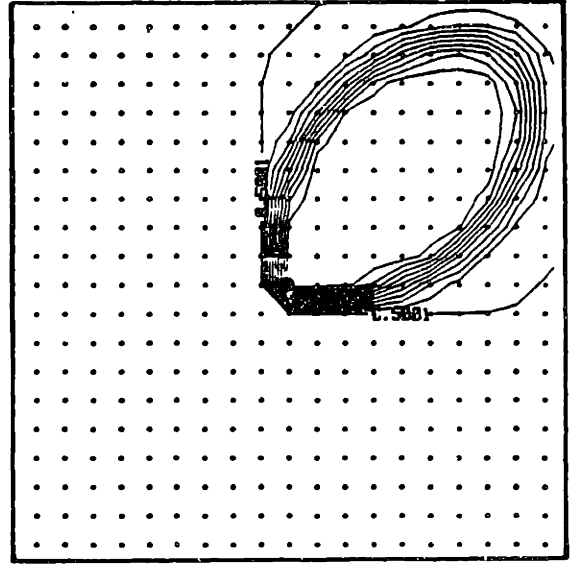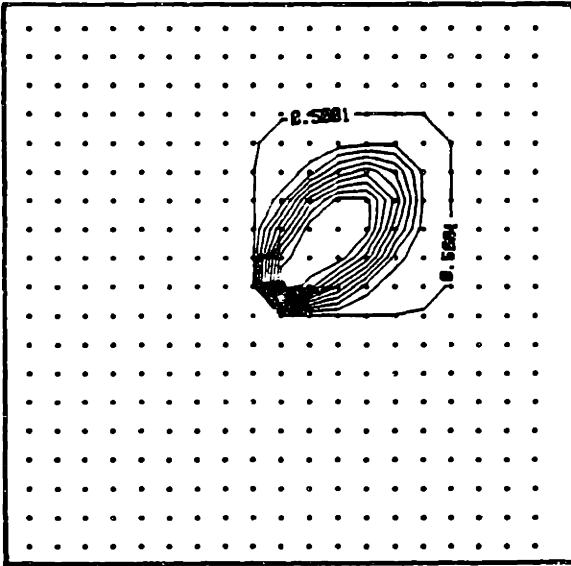
(c) Compatibility Matrix III (5 (l) and 10 (r) iterations),
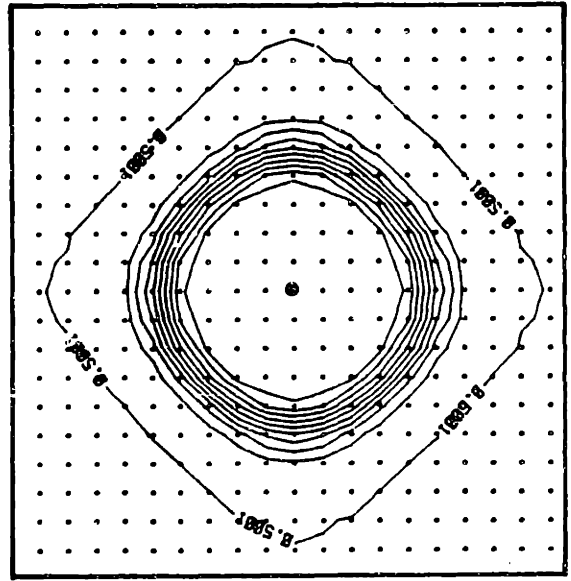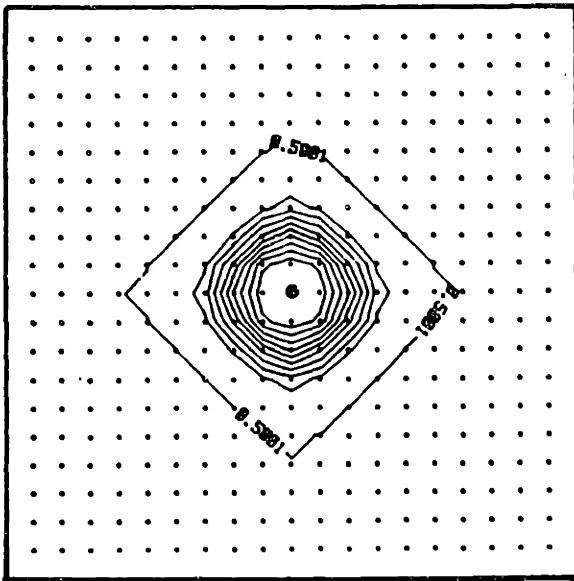
(d) Compatibility Matrix IV (5 (l) and 10 (r) iterations),

Figure 6.16 - Continued.
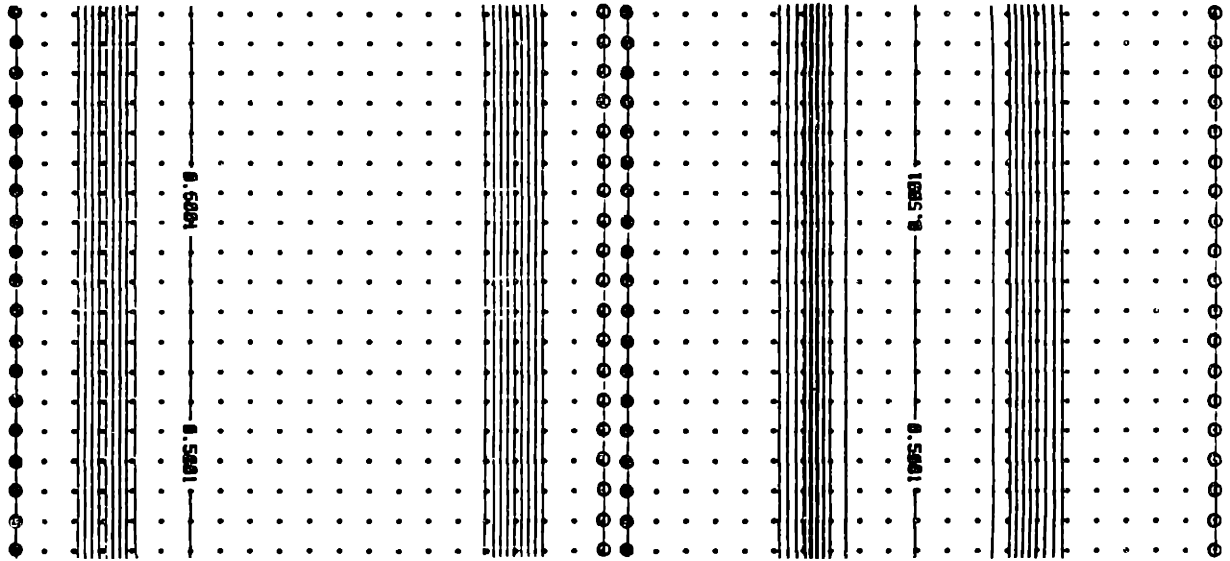
(a) Compatibility Matrix I (5 (l) and 10 (r) iterations),
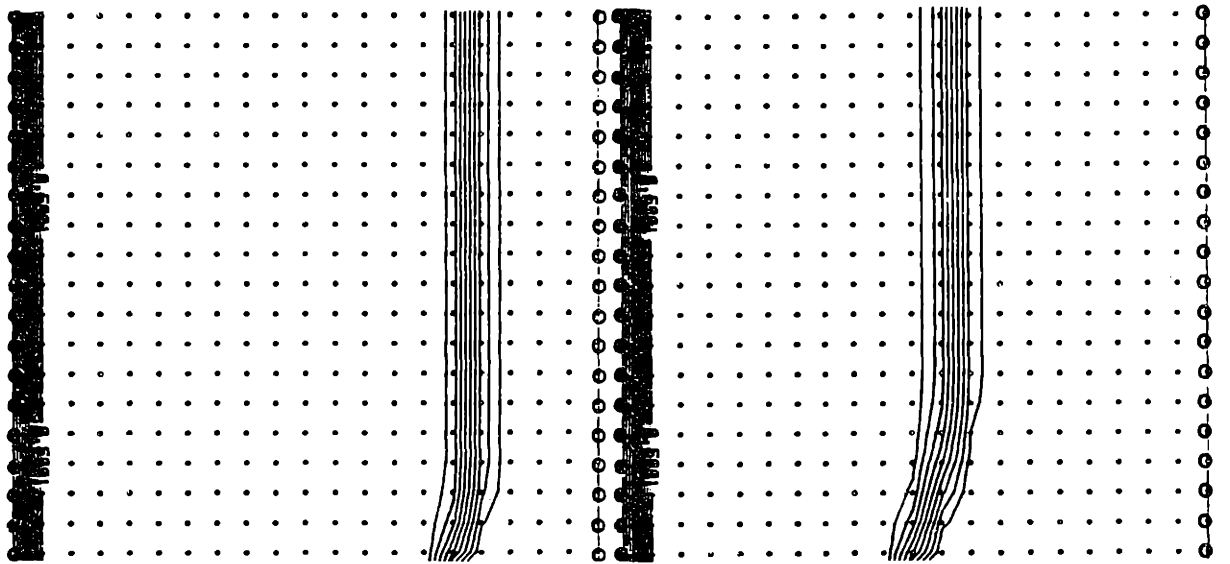
(b) Compatibility Matrix II (5 (l) and 10 (r) iterations),

Figure 6.17 - Contours of P(1) in Increments of 0.005 from 0.50001 to 1.0 for Probabilistic Relaxation of Trial Data 2.
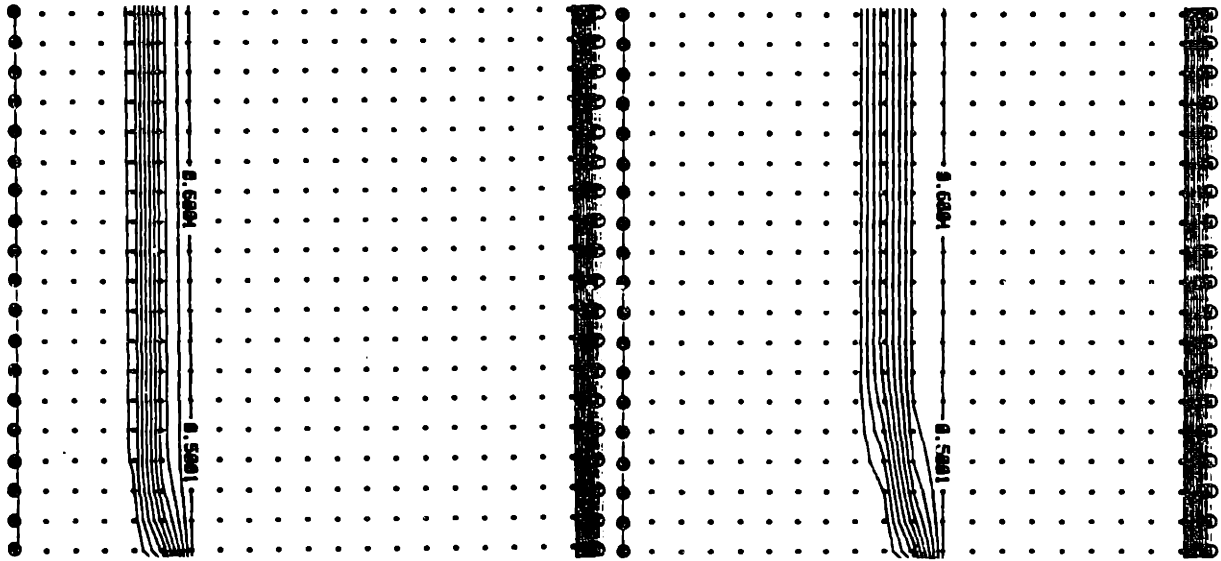
218

(c) Compatibility Matrix III (5 (1) and 10 (r) iterations),
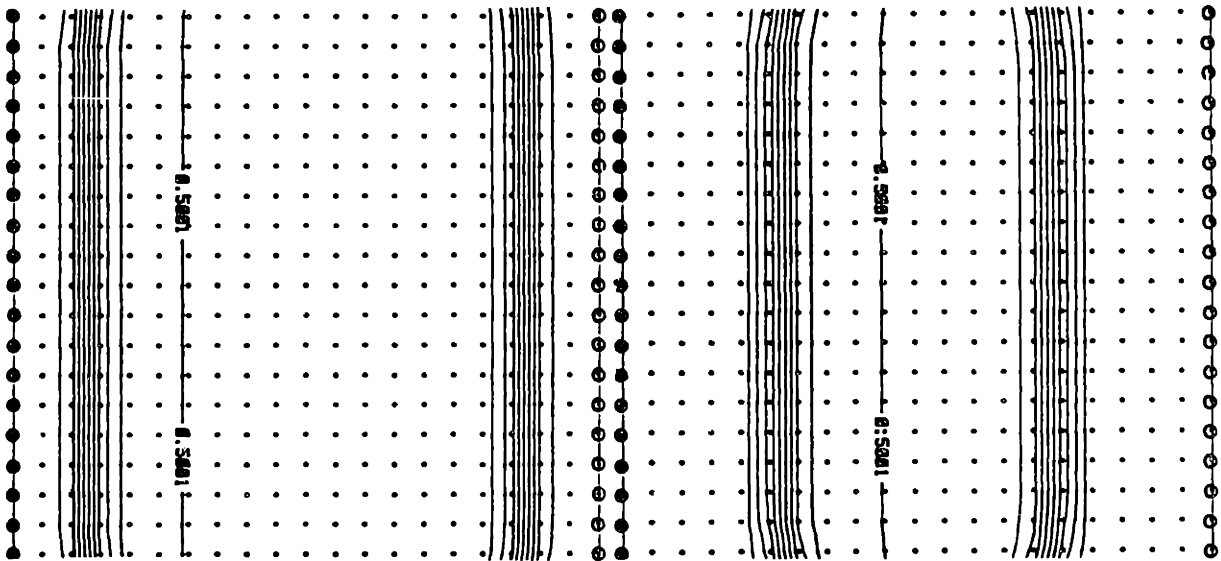
(d) Compatibility Matrix IV (5 (1) and 10 (r) iterations),

Figure 6.17 - Continued.
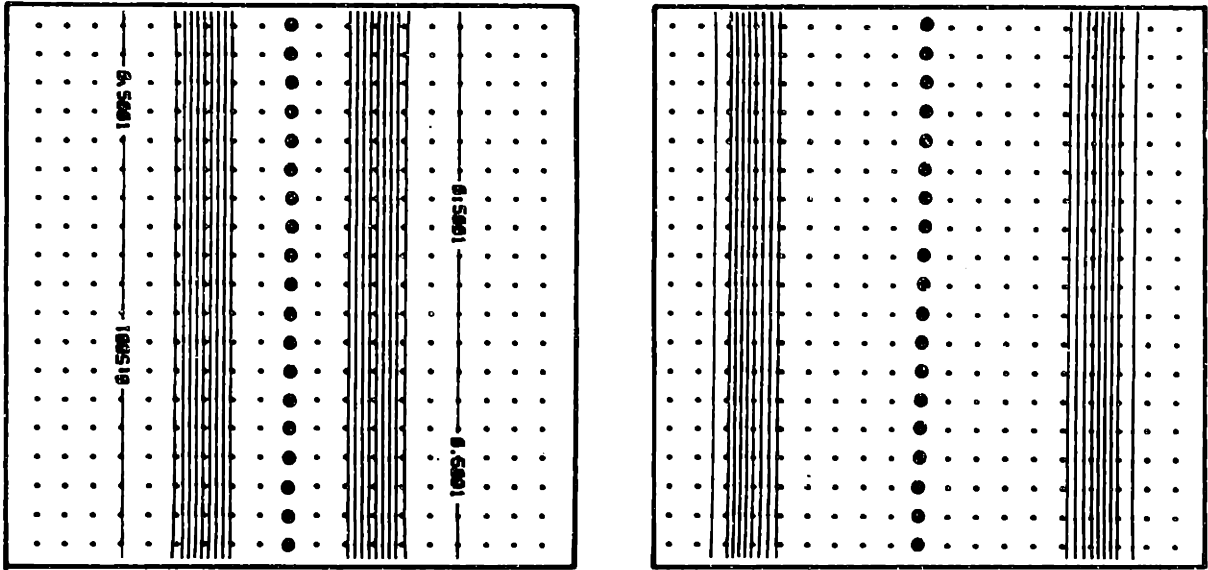
(a) Compatibility Matrix I (5 (l) and 10 (r) iterations),
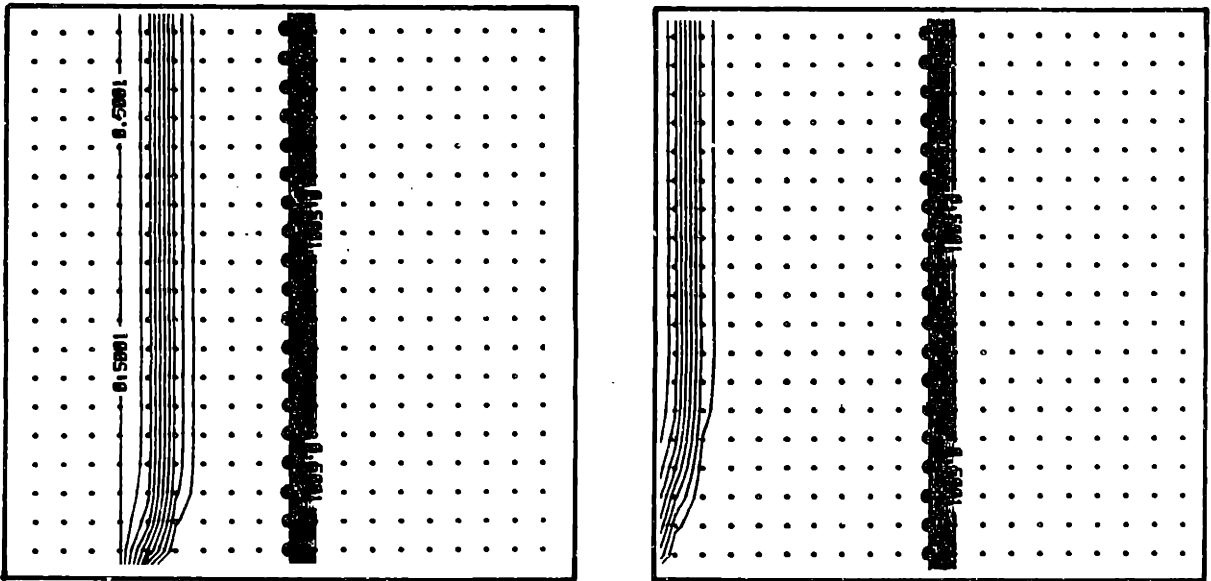
(b) Compatibility Matrix II (5 (l) and 10 (r) iterations),

Figure 6.18 - Contours of P(1) in Increments of 0.005 from 0.50001 to 1.0
for Probabilistic Relaxation of Trial Data 3.
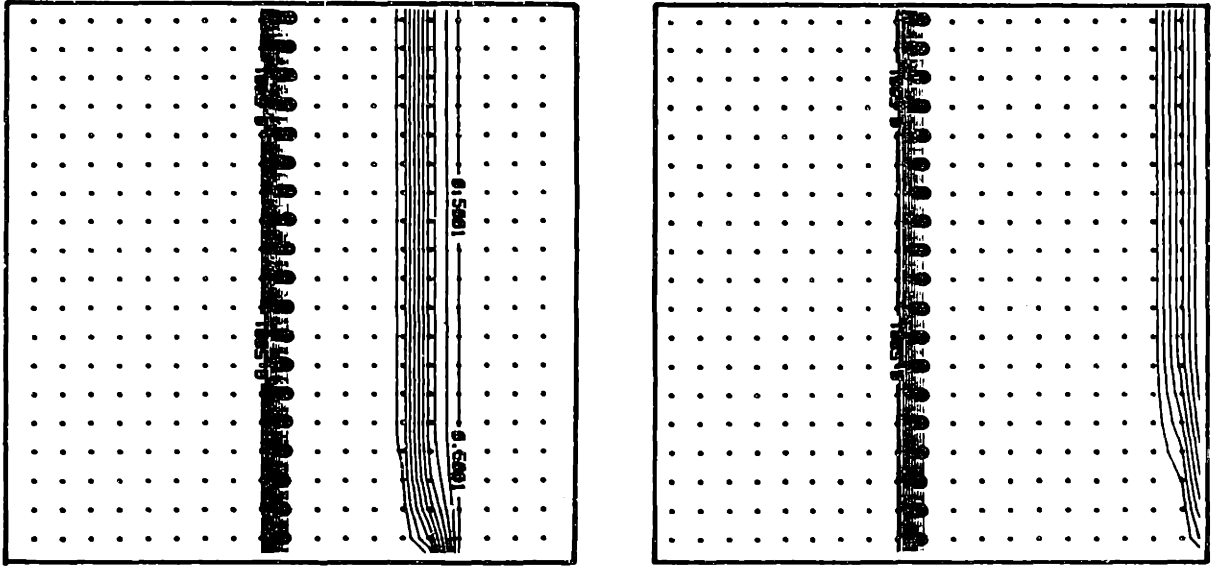
(c) Compatibility Matrix III (5 (l) and 10 (r) iterations),
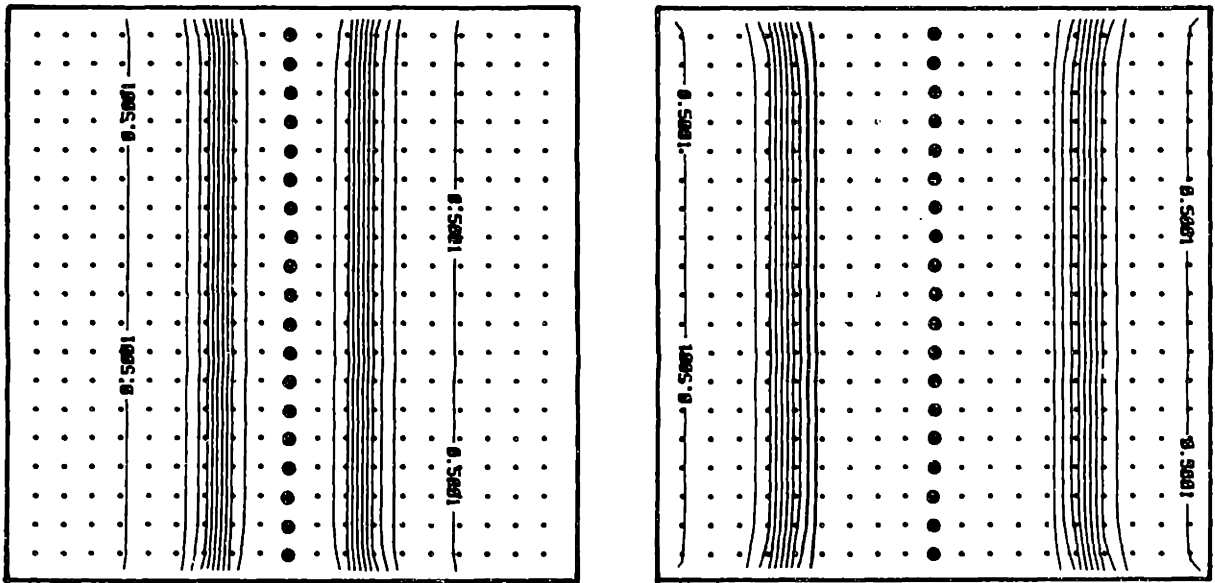
(d) Compatibility Matrix IV (5 (l) and 10 (r) iterations),

Figure 6.18 - Continued.
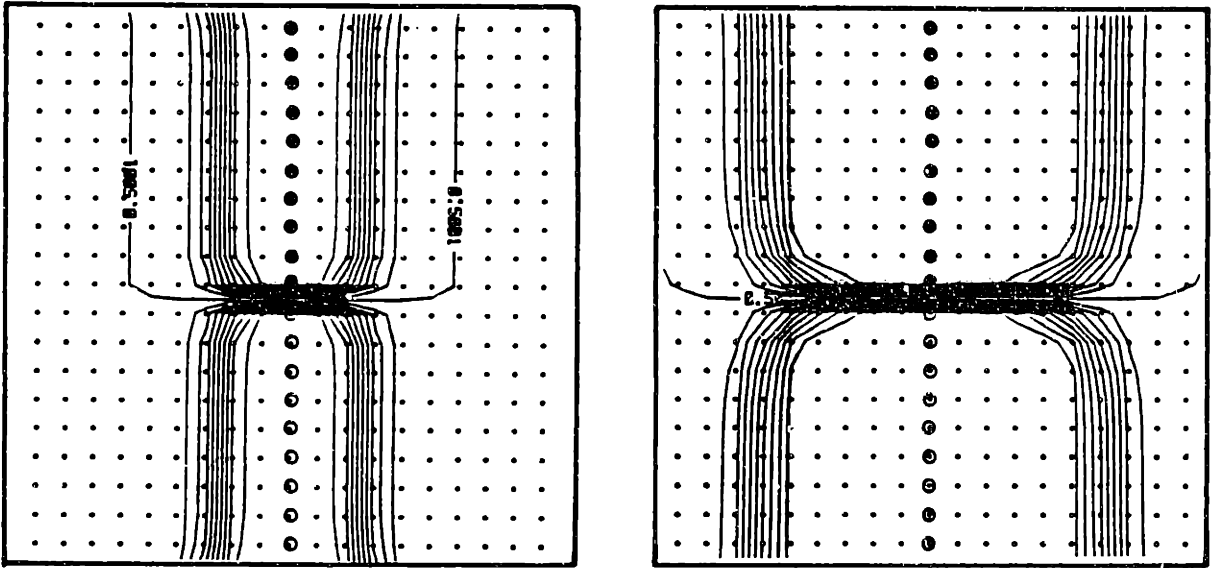
(a) Compatibility Matrix I (5 (l) and 10 (r) iterations),
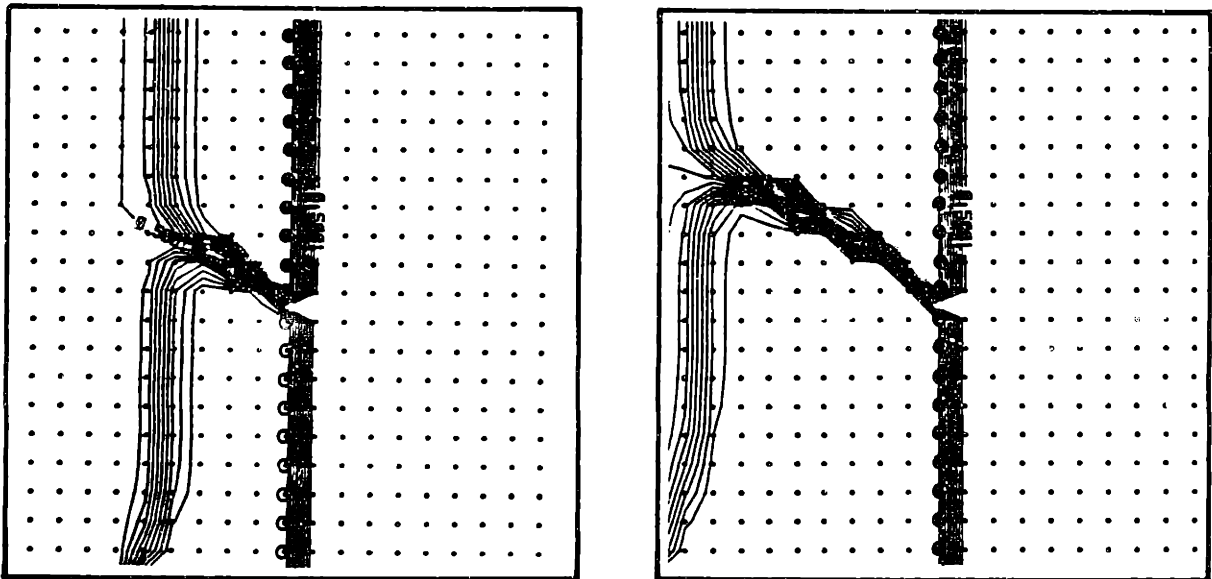
(b) Compatibility Matrix II (5 (l) and 10 (r) iterations),

Figure 6.19 - Contours of P(1) in Increments of 0.005 from 0.50001 to 1.0
for Probabilistic Relaxation of Trial Data 4.
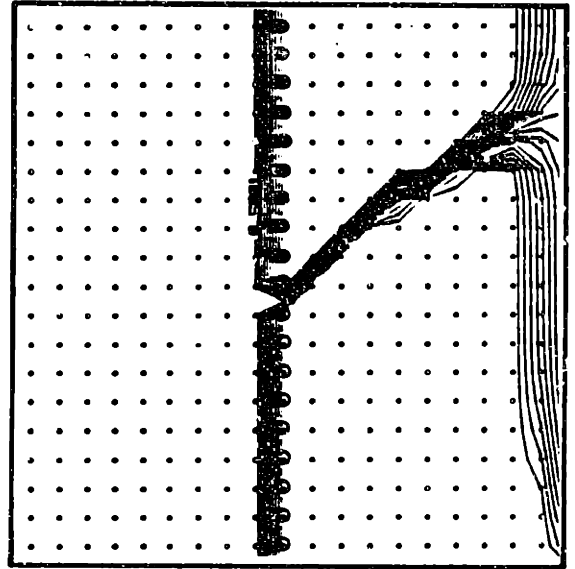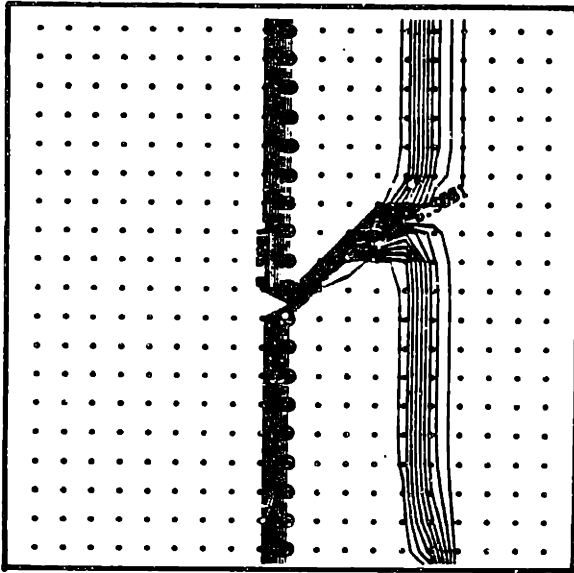
(c) Compatibility Matrix III (5 (1) and 10 (r) iterations),
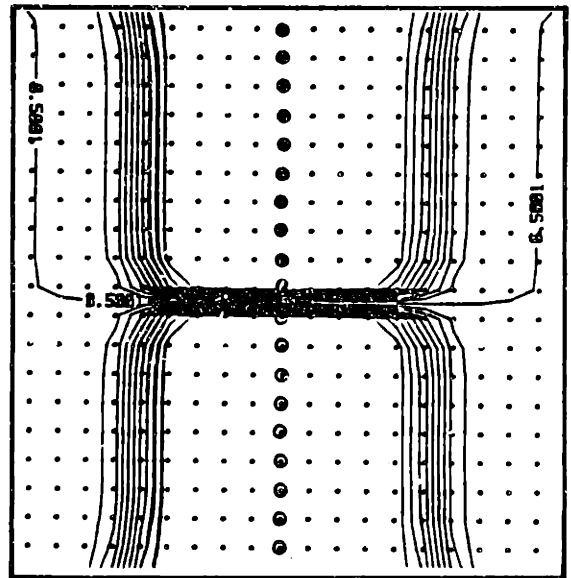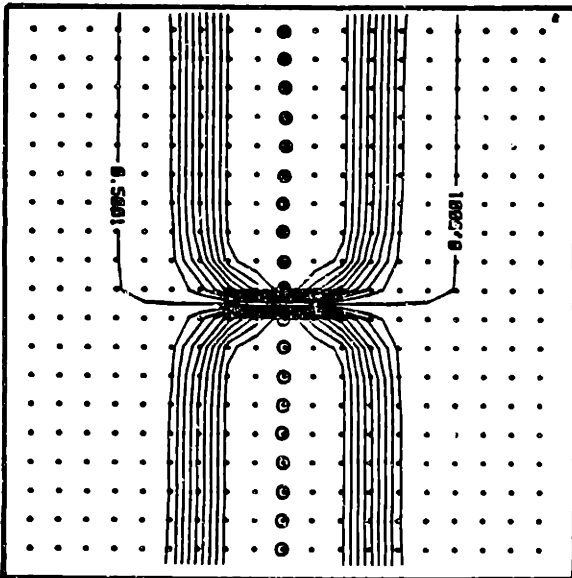
(d) Compatibility Matrix IV (5 (1) and 10 (r) iterations),

Figure 6.19 - Continued.
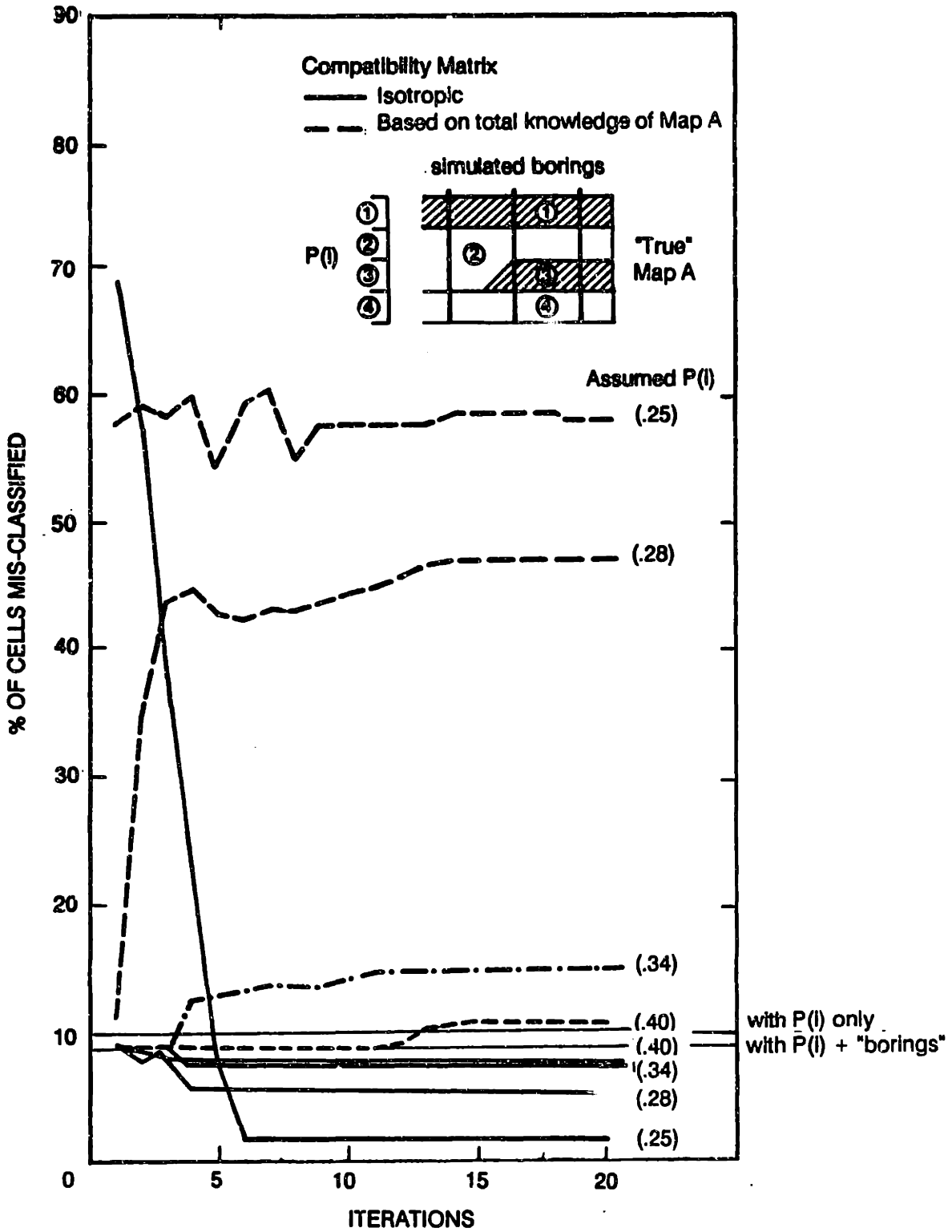
Figure 6.20 - Summary of Probabilistic Relaxation Results for Contrived Map A.
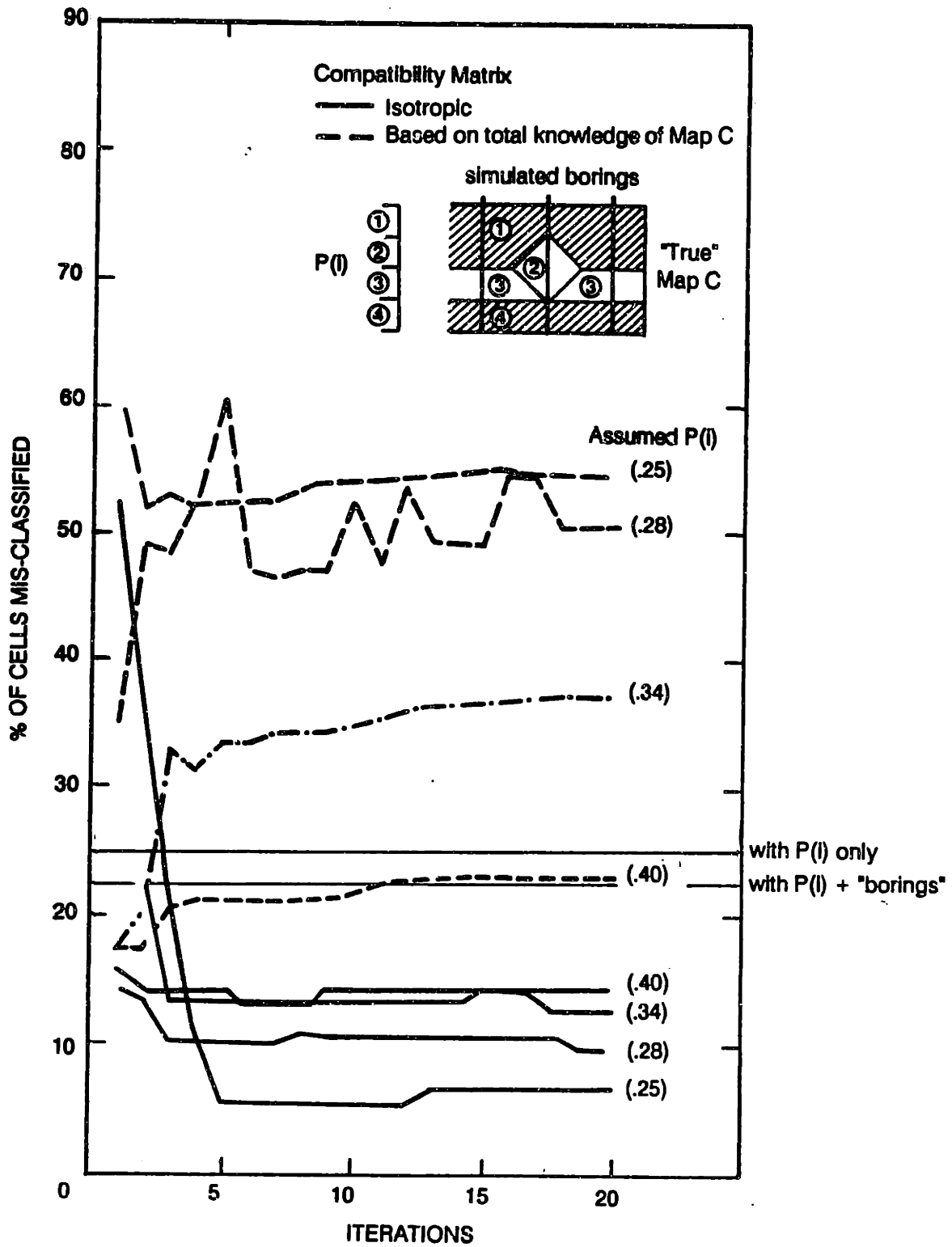
Figure 6.21 - Summary of Probabilistic Relaxation Results for Contrived
Map C.
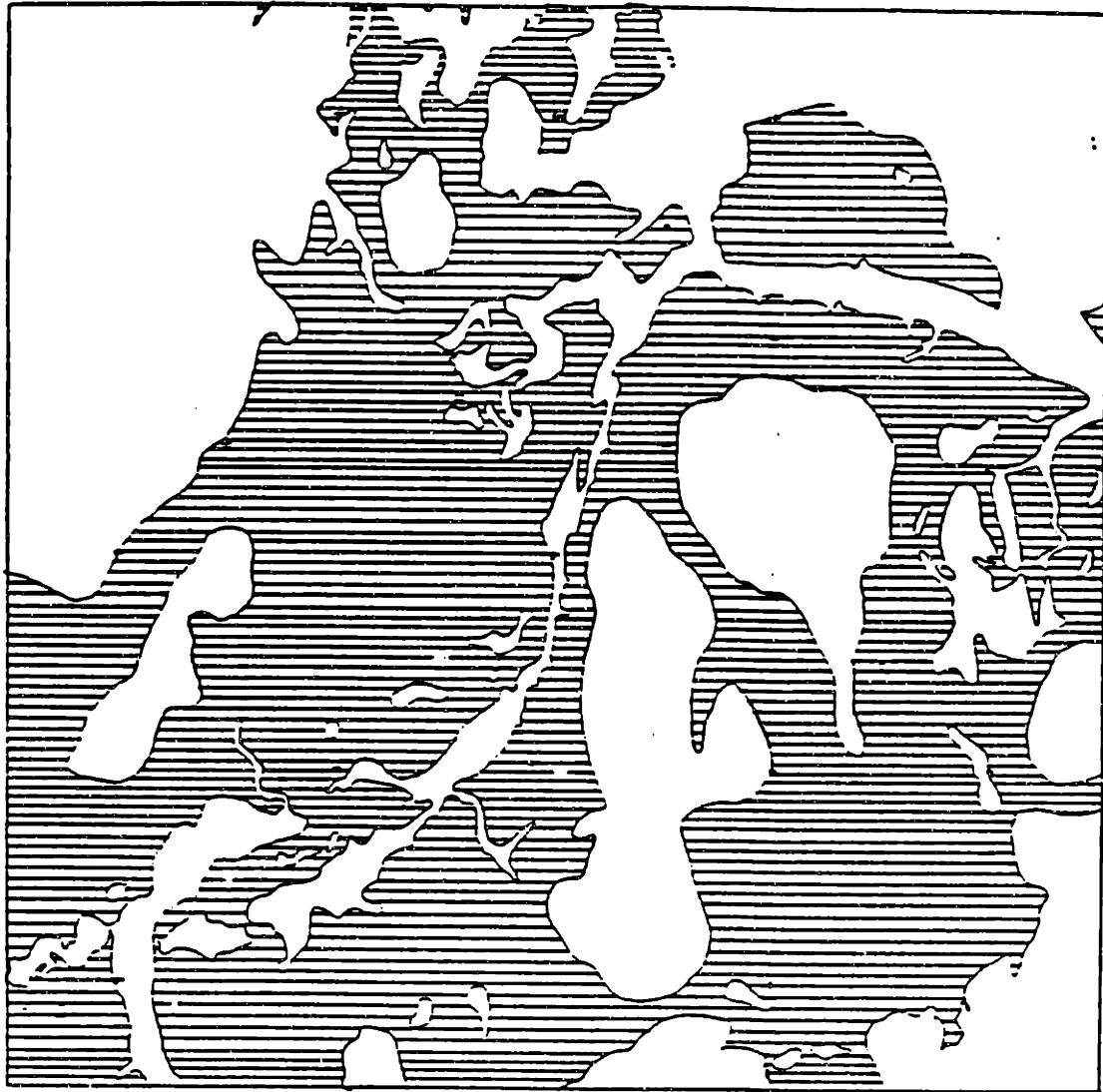
Figure 6.22 - Map 2 (Geology of the Bridgewater Quadrangle, MA USGS Map GQ-127; Lee, 1982).
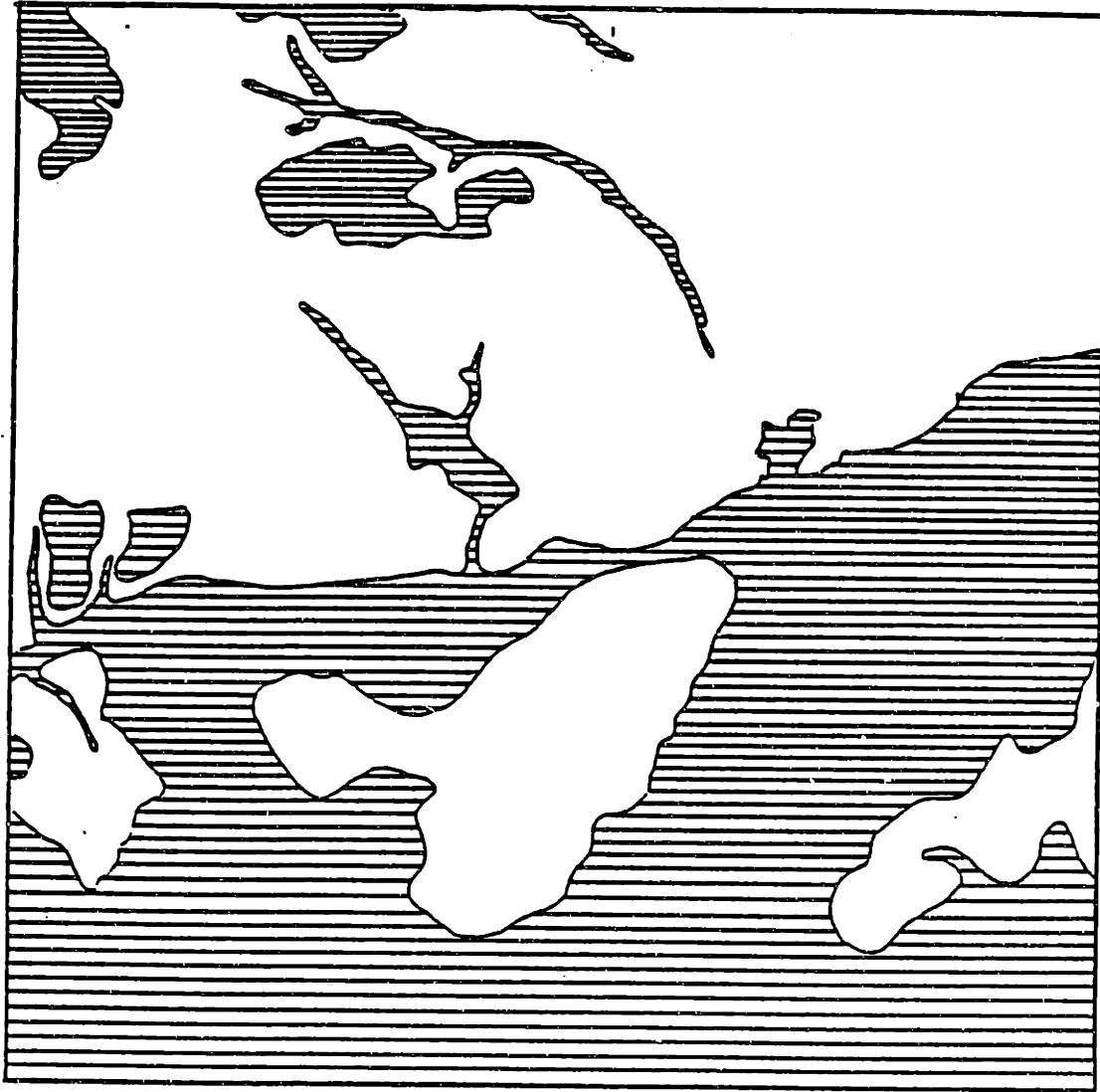
Figure 6.23 - Map 3 (Pre-Quaternary Geology of the Brown's Mill Quad-
rangle, NJ, USGS Map GQ-264; Lee, 1982).

227
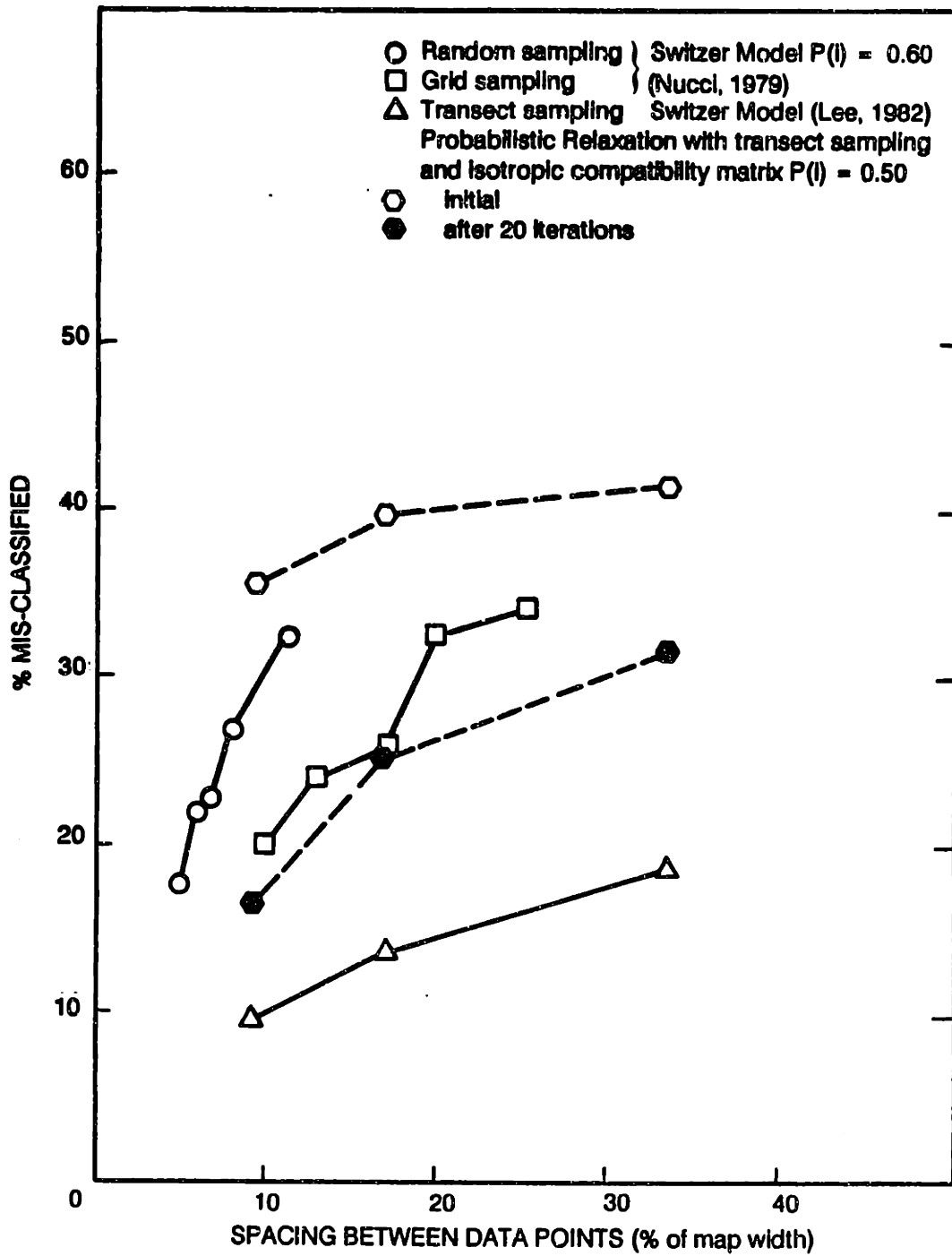
Figure 6.24 - Comparison of Probabilistic Mapping Methods for Map 2.
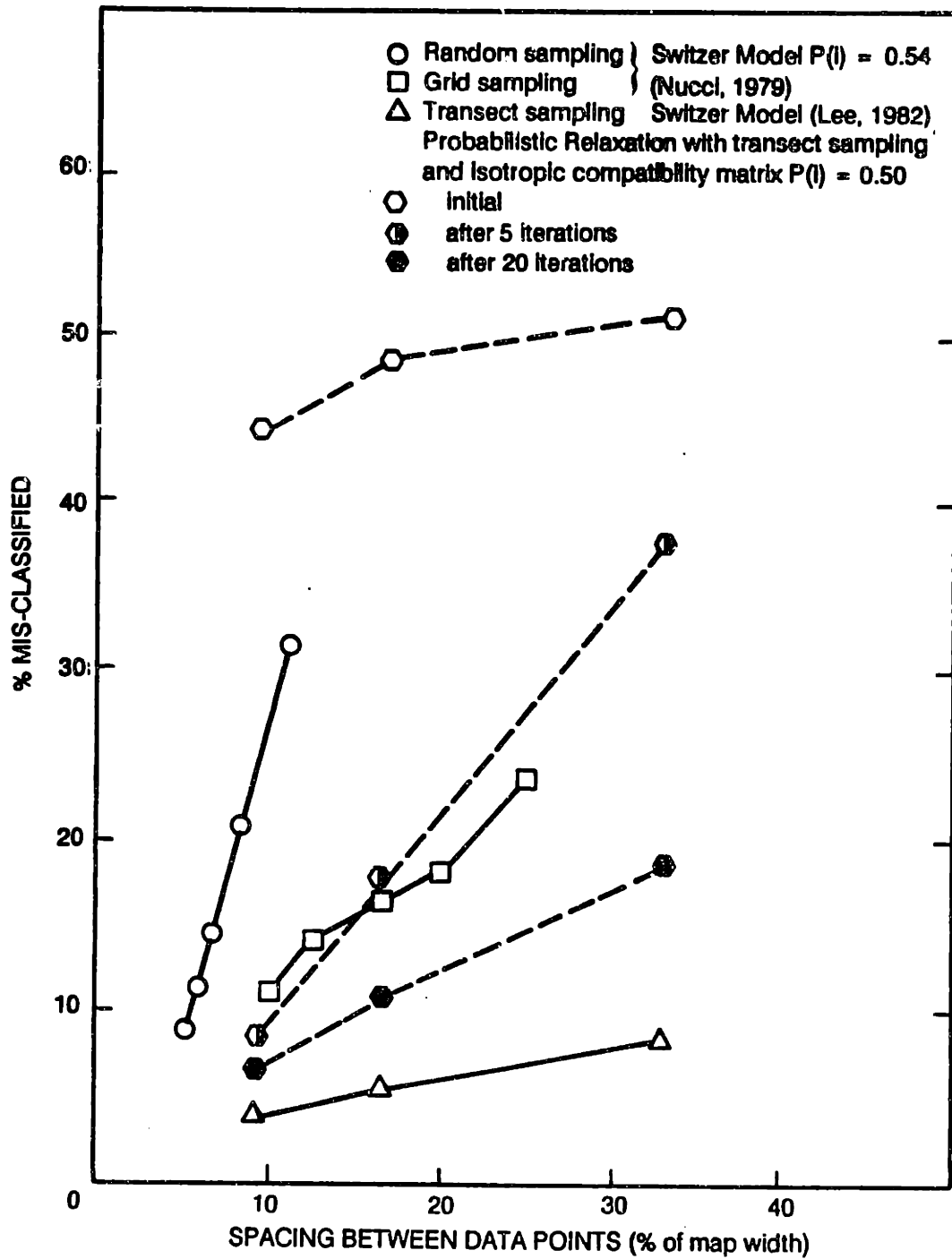
Figure 6.25 - Comparison of Probabilistic Mapping Methods for Map 3.

229
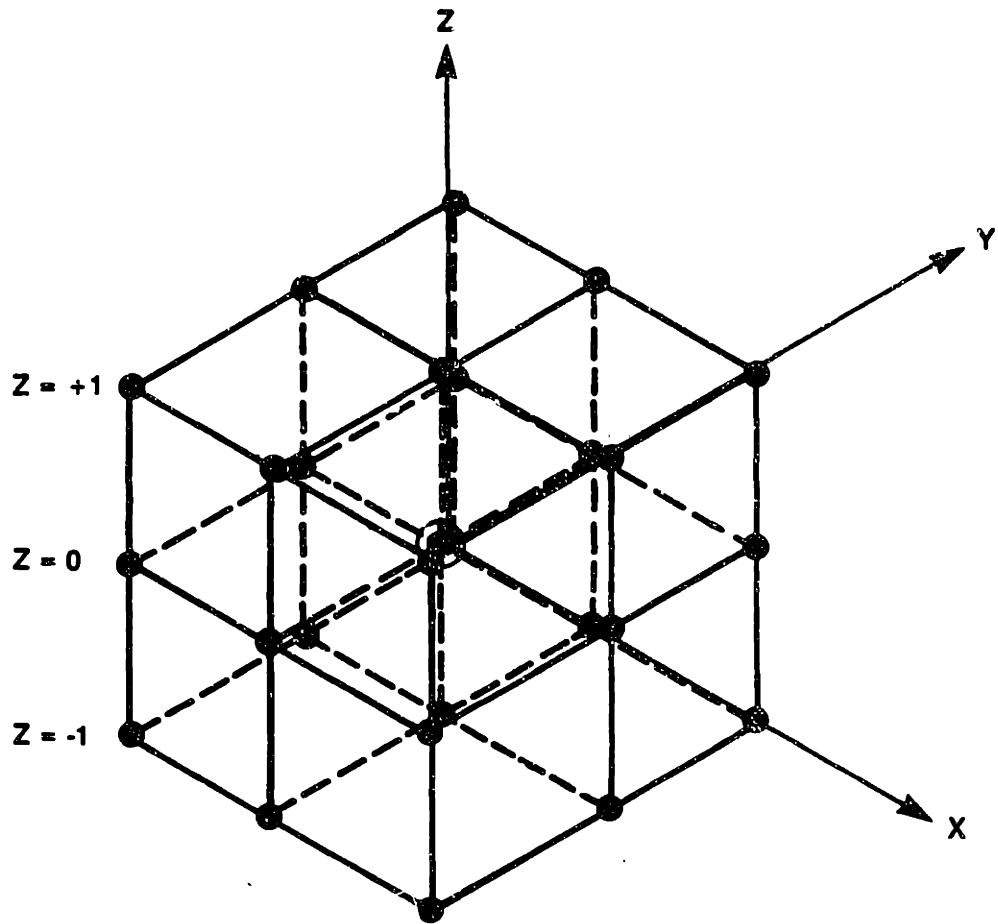
Figure 6.26 - Three Dimensional Cell Arrangement.

Z = +1

(293-338) [A-90]	(338-23) [A-90]	(23-68) [A-90]
(248-293) [A-90]	none	(68-113) [A-90]
(203-248) [A-90]	(158-203) [A-90]	(113-158) [A-90]

Z = 0

(293-338) [0-90]	(338-23) [0-90]	. (23-68) [0-90]
(248-293) [0-90]	none (central point)	(68-113) [0-90]
(203-248) [0-90]	(158-203) [0-90]	(113-158) [0-90]

Z = -1

(293-338) [0-A] (113-158) [0-90]	(338-23) [0-A] (158-203) [0-90]	(23-68) [0-A] (203-248) [0-90]
(248-293) [0-A] (68-113) [0-90]	(0-360) [0-90]	(68-113) [0-A] (248-293) [0-90]
(203-248) [0-A] (23-68) [0-90]	(158-203) [0-A] (338-23) [0-90]	(113-158) [0-A] (293-338) [0-90]

( ) Range of strike angles
[ ] Range of dip angles
A = True angle between center point and node

Figure 6.27 - Acceptable Strike/Dip Conditions for 26 Neighboring Cells with Soil Type J above Soil Type K.
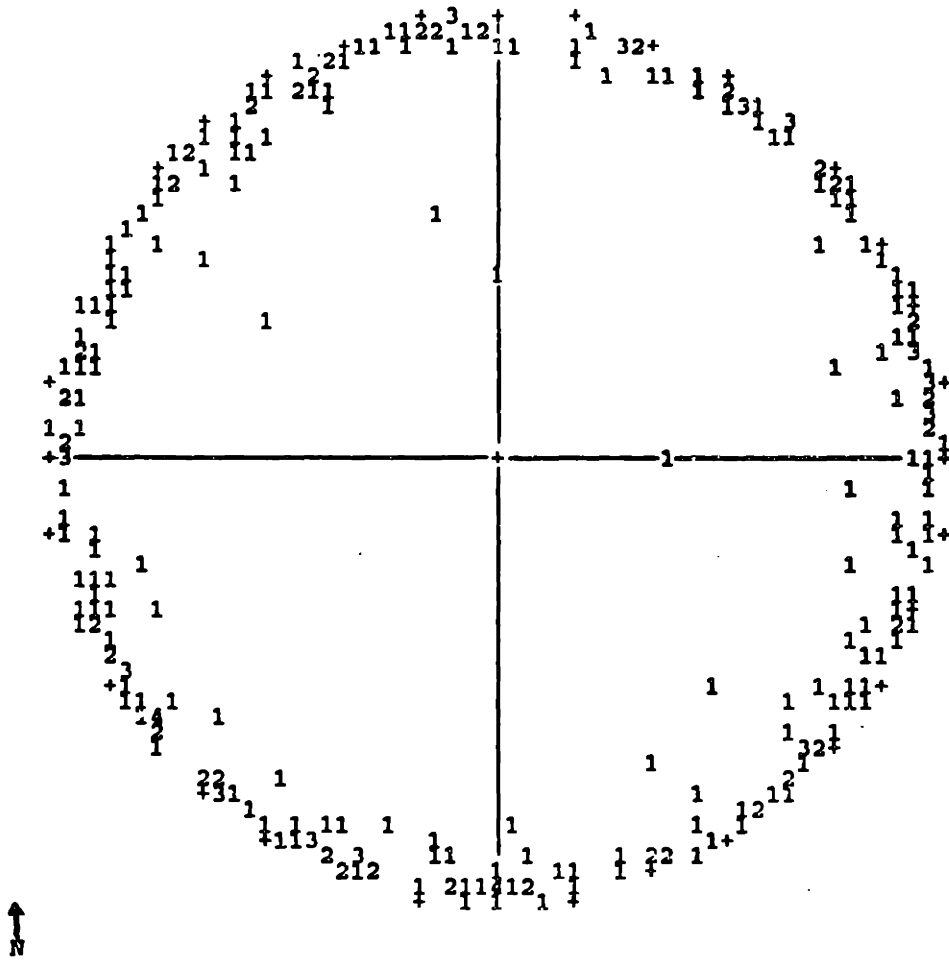
Figure 6.28 - Typical Equal Area Net Plot of Dip Vectors for Delaunay
Triangles (Top of Organic Soils, Back Bay).

P(penetrating soil type J) =
P(observed stratum thickness < $t_{critical}$)

J

γ_{avg}

K

A

B

$t_{critical}$

γ_{avg} = average dip angle of observed strata interface triangles in appropriate strike range

P(x)

$t_{critical}$

Observed Stratum Thickness
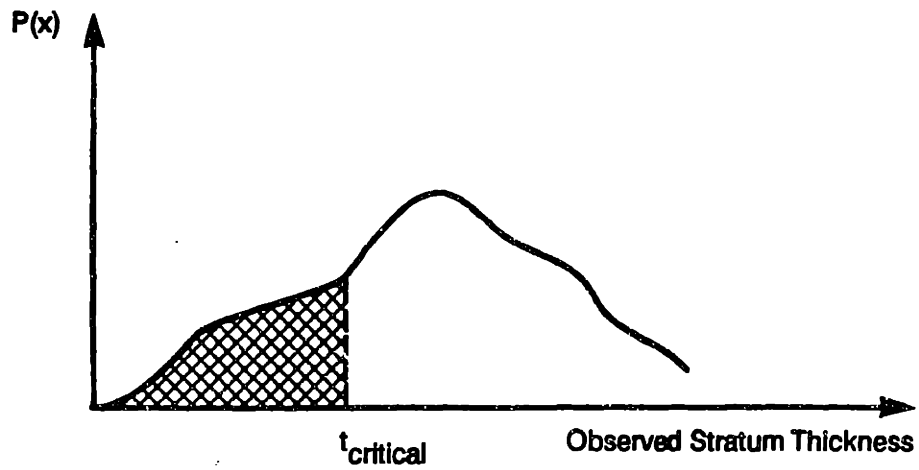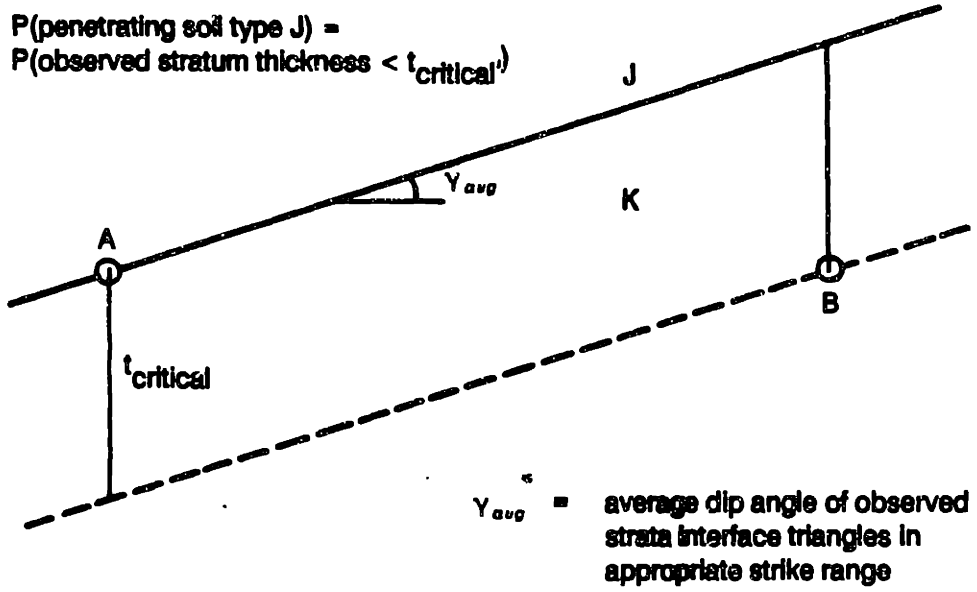
Figure 6.29 - Definition of Critical Thickness for Stratum Thickness Considerations.

233
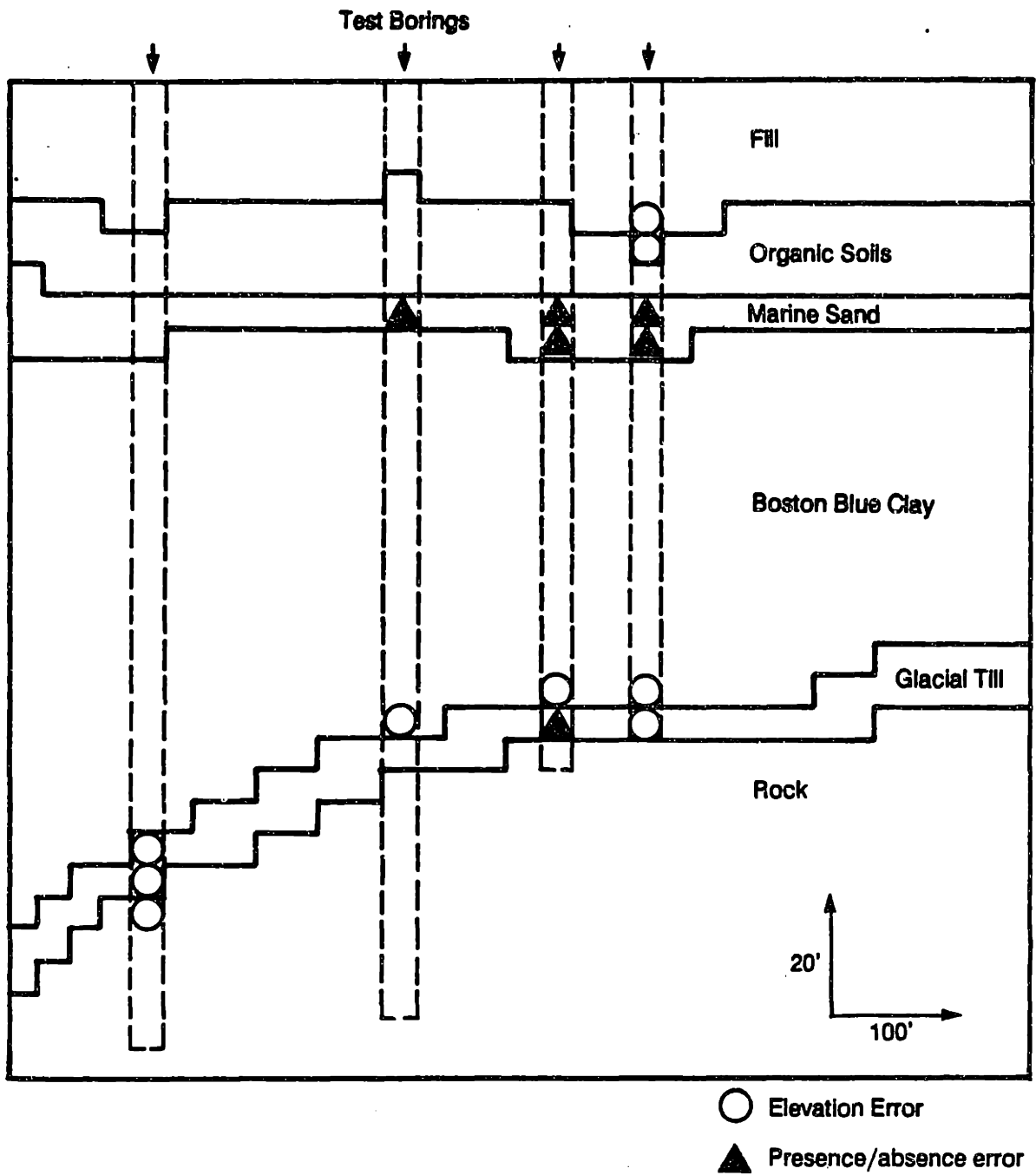
Figure 6.30 - Cellular Map of Initial Probabilistic Profile, Profile 5, Back Bay.
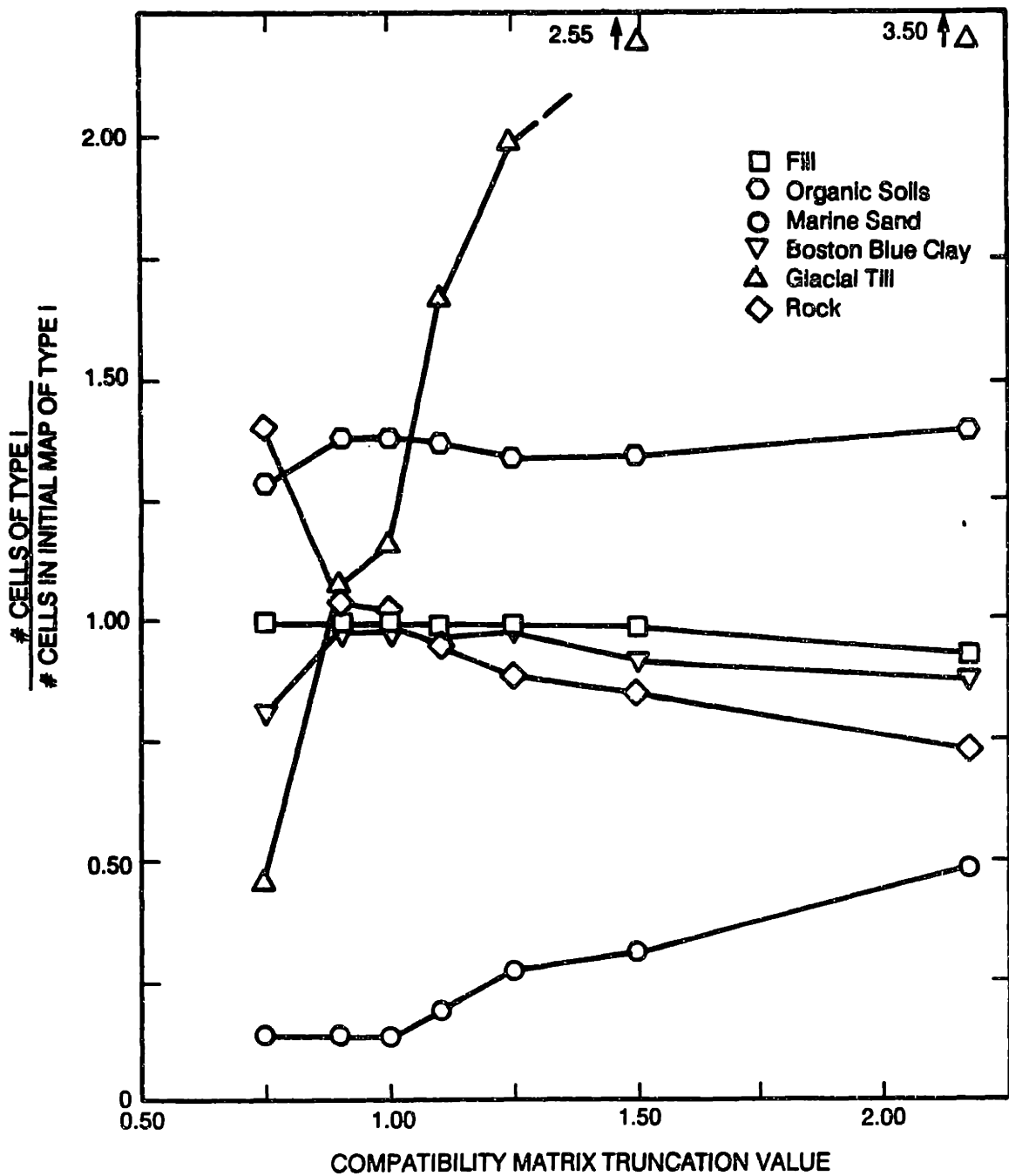
Figure 6.31 - Ratio of Soil Type Cells for Various Compatibility Matrix
Truncation Values, Two Dimensional Analysis After 100 Iter-
ations, Profile 5, Back Bay.
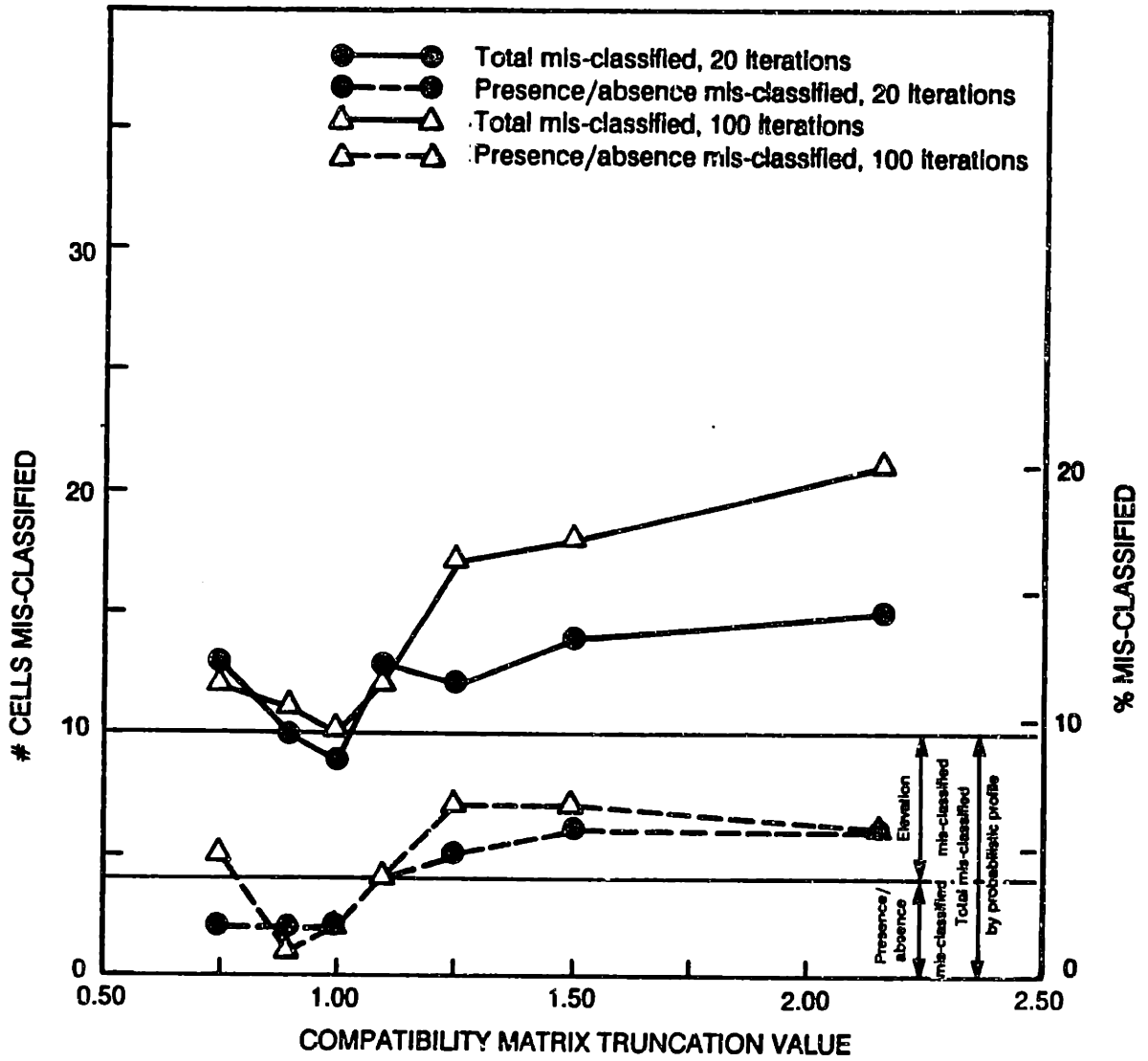
Figure 6.32 - Mis-Classification Error Summary for Various Compatibility
Matrix Truncation Values, Two Dimensional Analysis After 20
and 100 Iterations, Profile 5, Back Bay.

236
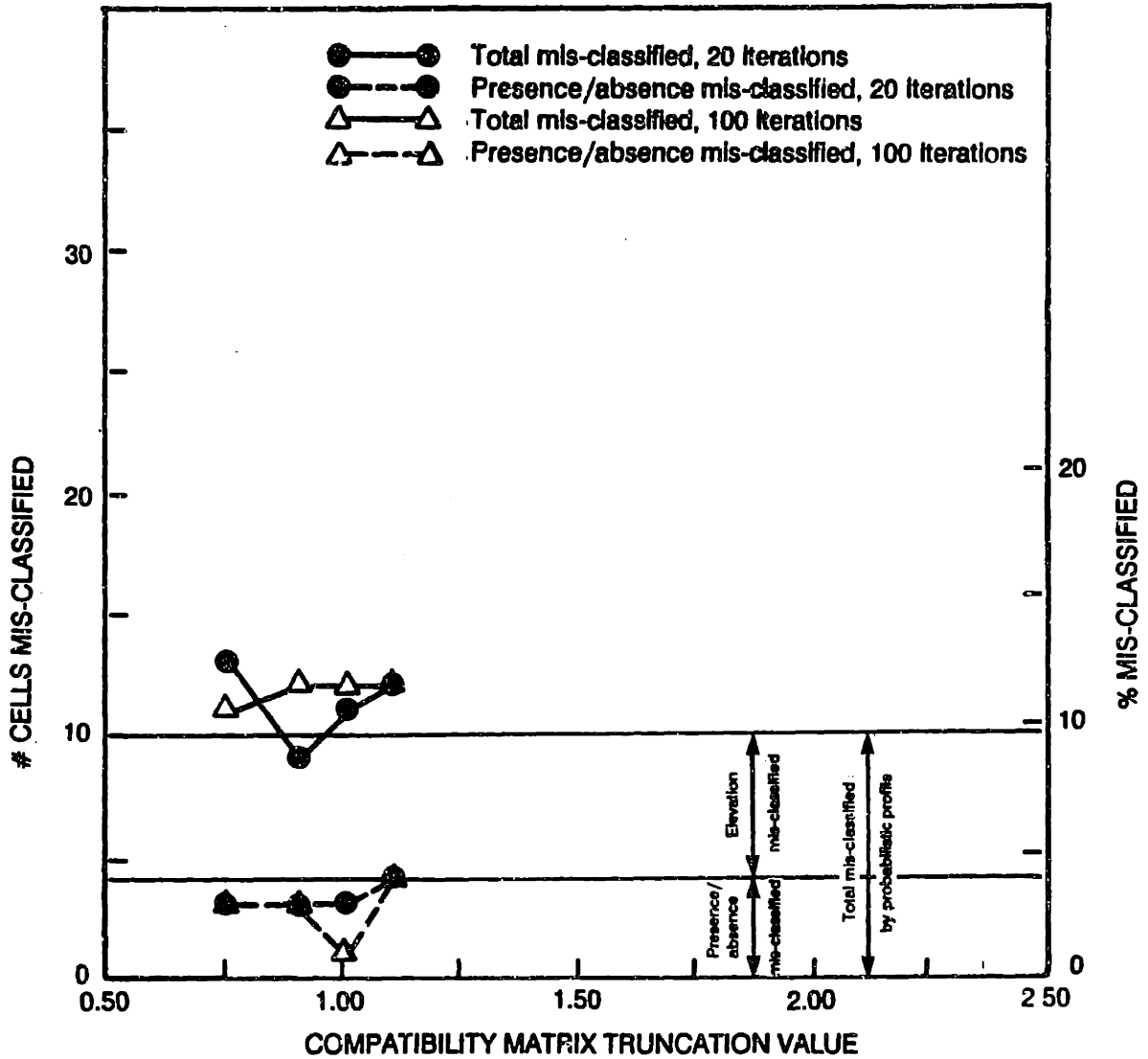
Figure 6.33 - Mis-Classification Error Summary for Various Compatibility
Matrix Truncation Values, Three Dimensional Analysis After
20 and 100 Iterations, Profile 5, Back Bay.

The figure contains the following legend and equations:

2D analysis with compatibility matrix truncated at +1.0
3D analysis with compatibility matrix truncated at +0.9

$$H(i,m) = -\sum_{j=1}^{k} P_i^m L_j \ln(P_i^m L_j)$$

$$H(m) = \frac{1}{N} \sum_{i=1}^{N} H(i,m)$$

Y-axis: AVERAGE ENTROPY AT END OF ITERATION = $\frac{H(m)}{H(o)}$ / INITIAL AVERAGE ENTROPY

X-axis: ITERATIONS
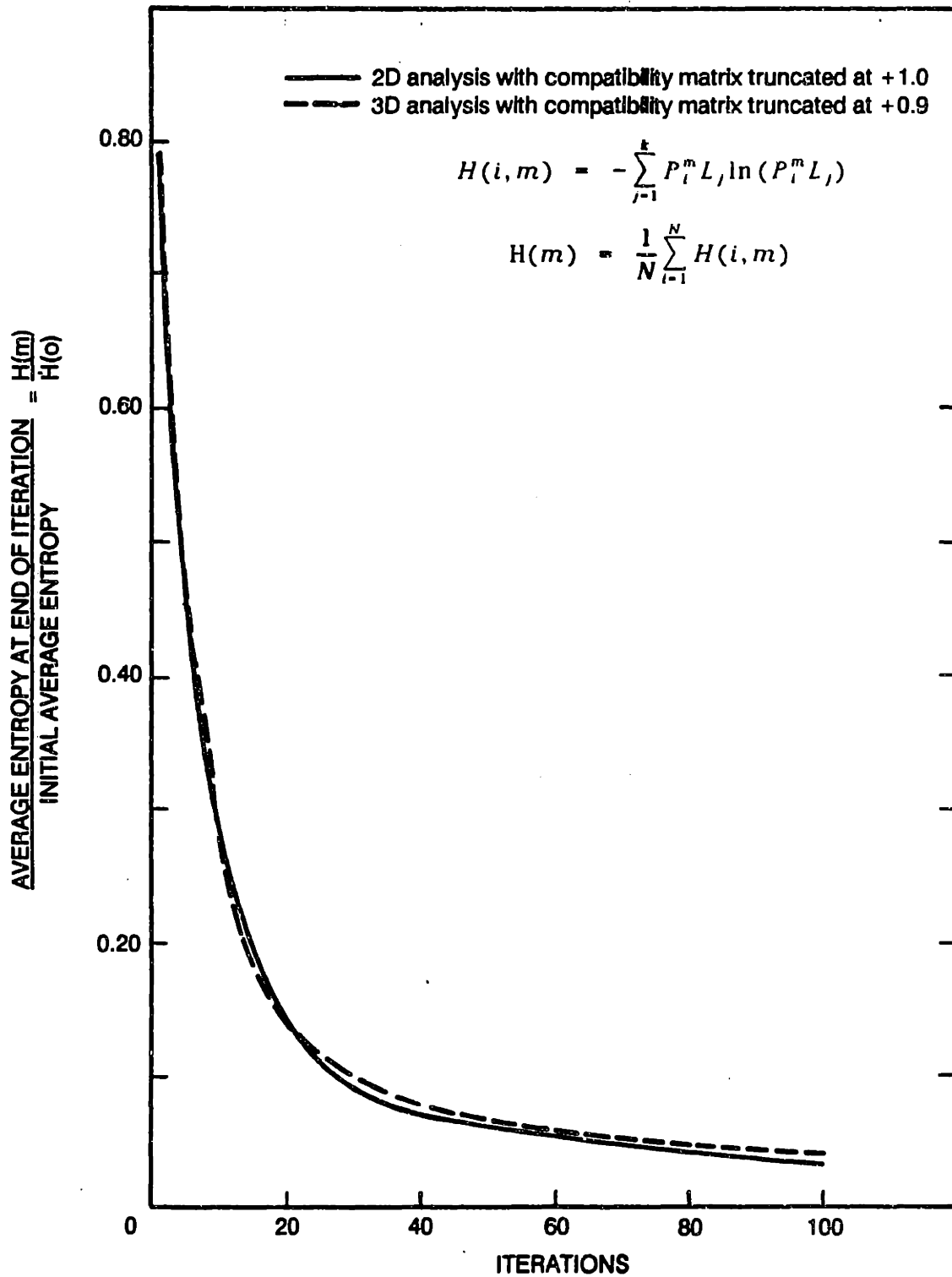
Figure 6.34 - Average Entropy as Percentage of Initial Entropy versus Number of Iterations, Probabilistic Relaxation of Profile 5, Back Bay.
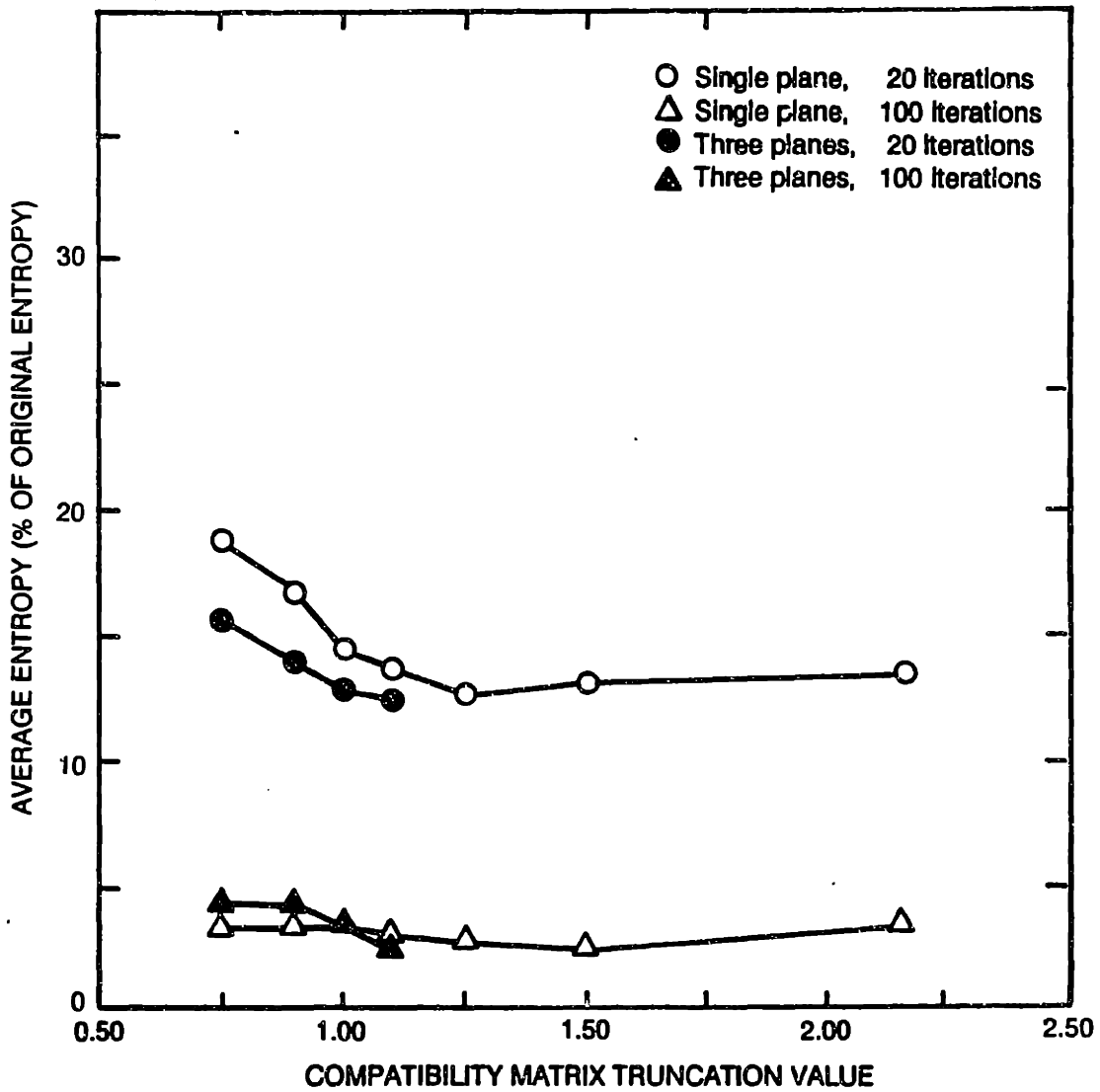
Figure 6.35 - Summary of Average Entropy for Various Compatibility Matrix Truncation Values, Two and Three Dimensional Analysis After 20 and 100 Iterations, Profile 5, Back Bay.

Legend:
- 2D analysis with compatibility matrix truncated at +1.0
- 3D analysis with compatibility matrix truncated at +0.9

$$R(m) = \frac{1}{N}\sum_{i=1}^{N}\left[\sum_{j=1}^{K}(P_i^m(L_j) - P_i^{(m-1)}(L_j))^2\right]^{\frac{1}{2}}$$
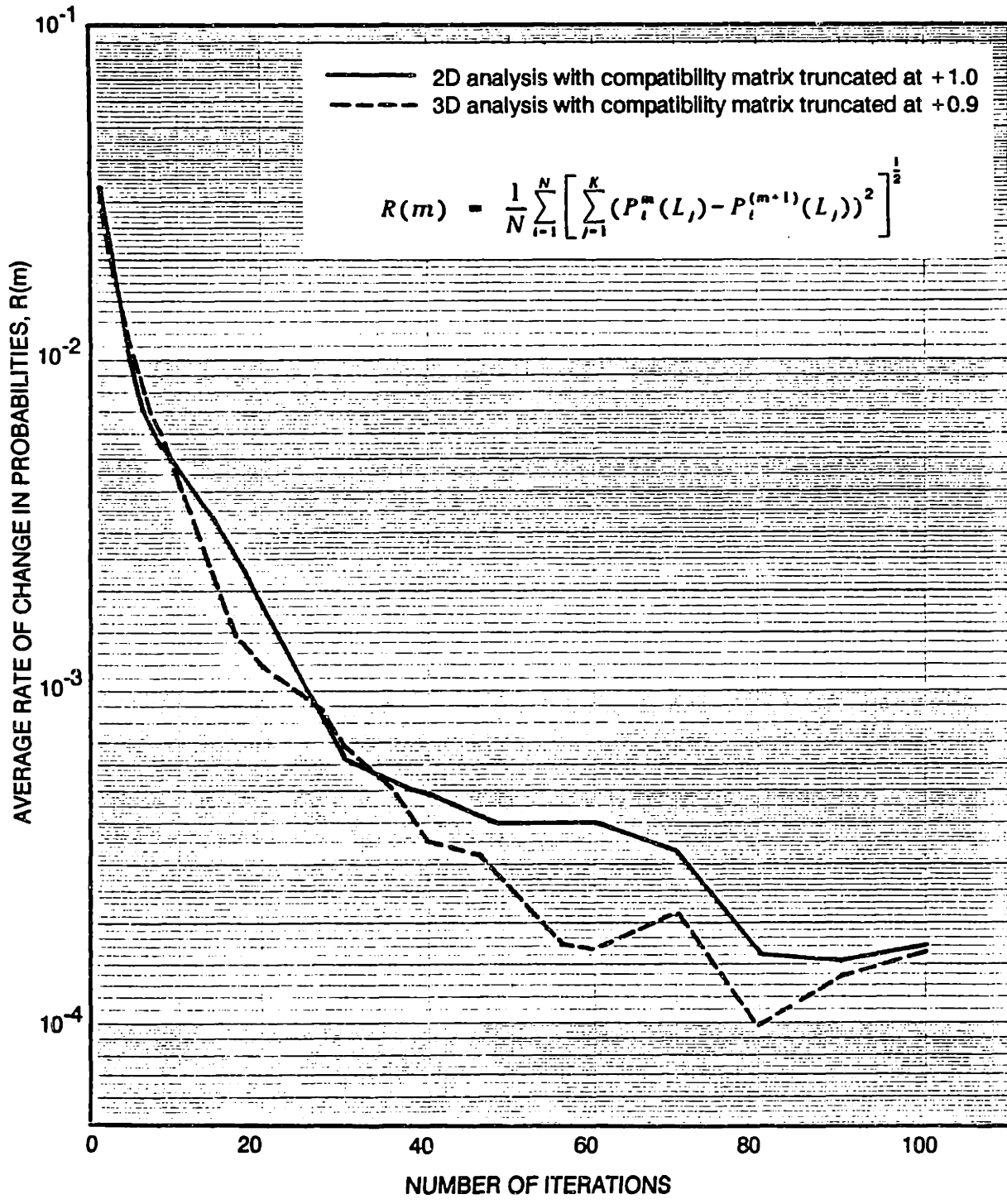
Figure 6.36 - Average Rate of Change in Probabilities versus Number of Iterations, Probabilistic Relaxation of Profile 5, Back Bay.

240
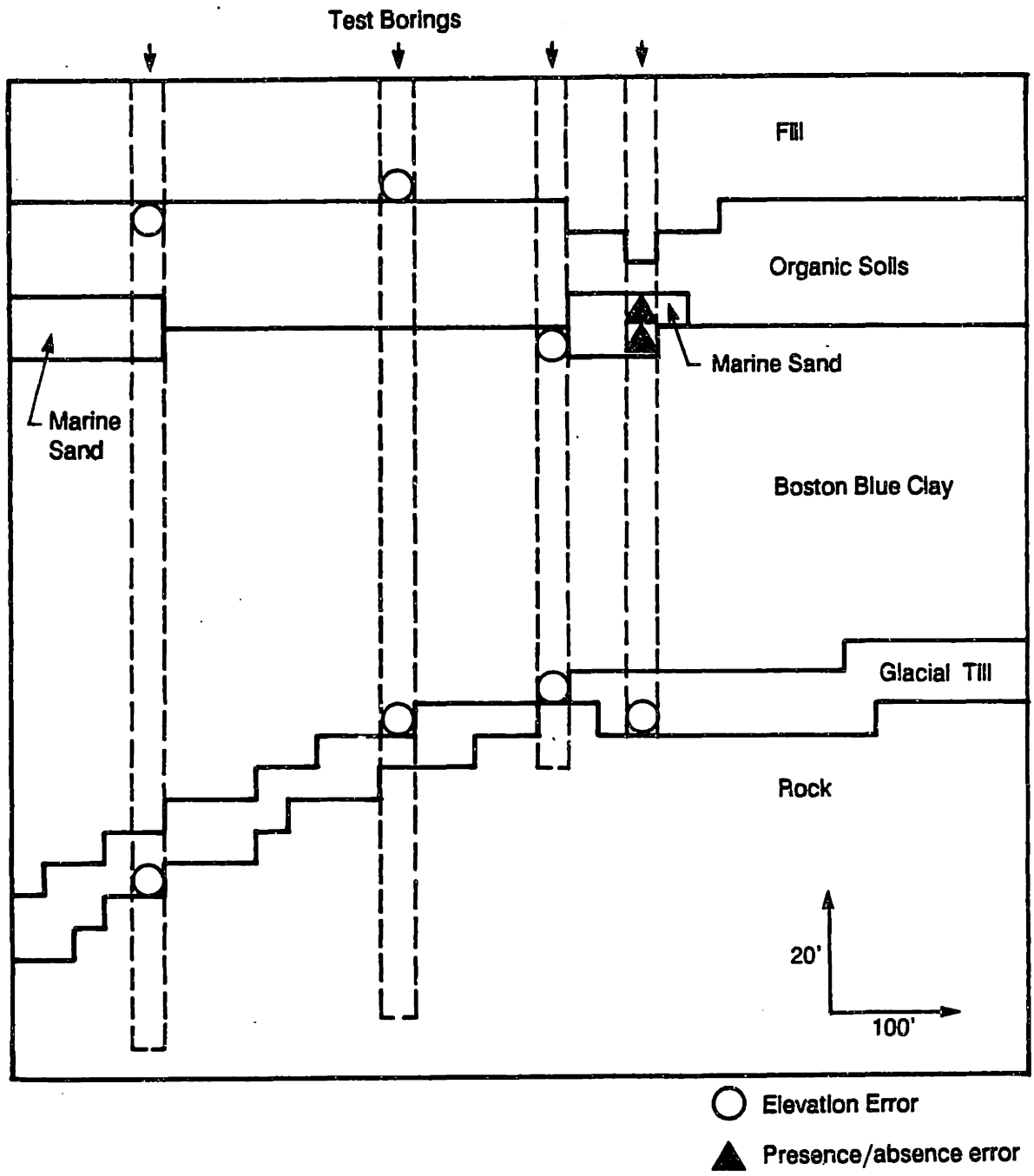
Figure 6.37 - Cellular Map After Probabilistic Relaxation: a) Two dimensional analysis with optimal compatibility matrix and 20 iterations,

241
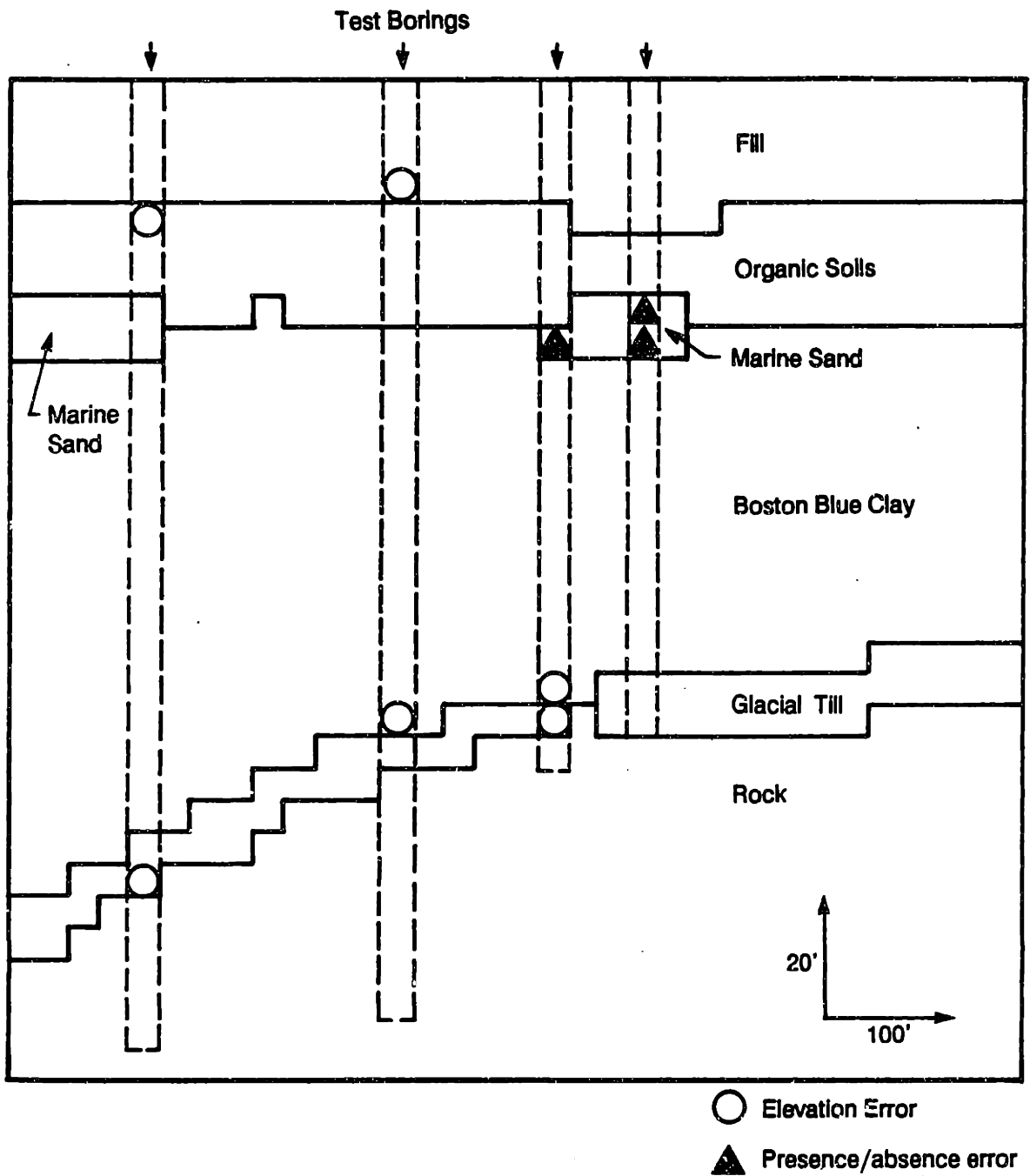
Figure 6.37 (continued) - b) Three dimensional analysis with optimal compatibility matrix and 20 iterations.

CHAPTER 7

CONCLUSIONS

7.1 Surface Modeling

Existing surface modeling algorithms were reviewed with respect to their applicability to soil profiling. Selected analytical techniques were applied to a case history data set for a single surface to assess their comparative performance. Also included in the comparison were nine hand drawn contour plans. The results of the comparison indicated that the kriging method (using generalized covariances) produced the surface model with the lowest mean residual; however, the hand drawn contours had only slightly higher mean residuals.

Single surface modeling techniques, including kriging, trend surface analysis, Delaunay triangulation, and a computerized version of current hand techniques, were applied to case history data. The results demonstrated that multiple surface models, using combinations of single surface models, exhibit unacceptable results with respect to strata overlap and continuous models of discontinuous strata.

7.2 Profiling

Probability-based mapping techniques were reviewed and assessed with respect to their applicability to soil profiling. The methods reviewed were the Switzer model (nearest neighbor) and published variations, which are two color techniques based on assumptions including map isotropy. The Switzer model and known variations were considered unsuitable for soil profiling due to, among other things, the isotropy limitations.

Clustering and regional merging techniques were applied as soil data preprocessing methods using visual description information. Both techniques were applied separately and the results were compared to hand drawn profiles. A combination of the methods, merging samples within single test borings and then clustering the resulting regions, demonstrated that

243

soil profiles, including determination of design soil properties, could be developed efficiently and that the results were comparable to hand drawn profiles.

Probabilistic profiles were developed treating the single surface models as random variables and assuming the geologic sequence is known. It has been demonstrated that probabilistic profiles, illustrating the level of uncertainty in the profiling, can be developed based on kriging analysis of the individual strata interface. Since the kriging models are continuous, the probabilistic profiles may result in continuous models of discontinuous strata depending on the strata thicknesses and other factors. In case history applications, the probabilistic profiles also exhibited localized strata overlap.

Probabilistic relaxation methods were applied to the probabilistic profiles to resolve the strata overlap and discontinuity issues. The application of probabilistic relaxation methods significantly improved the probabilistic profiles, including removal of strata overlap and transforming continuous models of selected strata into discontinuous models.

The surface modeling and profiling methods were applied to two case history data sets. The results demonstrate improvements in surface modeling and profiling methods including development of computerized profiles incorporating the available information, probability-based methods modified for the purpose, and also, subjective engineering input.

7.3 Future Research

This research has established fundamental approaches to the development of a framework for incorporating available information, subjective engineering input, and probability-based analytical methods into the geometric modeling of soil stratigraphy. The results of the research are very encouraging; however, there are opportunities for future research.

Specifically, future research should extend the methods presented here by incorporating geologic knowledge (regional geology, geomorphology, etc.) into the definition of the compatibility matrix used for probabilistic relaxation. Incorporation of geologic knowledge into site characterization has always been a difficult and highly subjective process. However, the probabilistic relaxation methods developed and applied in this research provide a framework for the incorporation of this knowledge.

Future research should also include relaxing the assumptions of the geologic sequence used here, such that modifications of the same methods can be applied to sites with more variable geologic sequences. This research has demonstrated the applicability of the methods to soil profiling on selected sites (i.e., those with reasonably consistent geologic sequence). Future research should broaden the applicability of the methods through relaxation of the assumptions.

REFERENCES

Aldrich, Jr., H. P., (1970), "Back Bay Boston - Part 1," *Journal of the Boston Society of Civil Engineers*, Vol. 57, No. 1, pp. 1-33.

Anderson, A. J. B., (1971), "Numeric Examination of Multivariate Soil Samples," *Mathematical Geology*, Vol. 3, No. 1, pp. 1-14.

Aurenhammer, F. and Edelsbrunner, H., (1984), "An Optimal Algorithm for Constructing the Weighted Voronoi Diagram in the Plane," *Pattern Recognition*, Vol. 17, No. 2, pp. 251-257.

Baecher, G. B., (1972), "Site Exploration, A Probabilistic Approach," Thesis submitted in partial fulfillment for the Degree of Doctor of Philosophy, Massachusetts Institute of Technology.

Belsley, D. A., Kuh, E. and Welsch, R. E., (1980), Regression Diagnostics: Identifying Influential Data and Sources of Collinearity, John Wiley & Sons, New York, 292 p.

Birks, H. J. B., and Gordon, A. D., (1985), Numerical Methods in Quarternary Pollen Analysis, Academic Press, Orlando, 377 p.

Chung, C. F., (1984), "Use of the Jackknife Method to Estimate Autocorrelation Functions (or Variograms)," Geostatistics for Natural Resources Characterization, Part 2, Verly, G. et al. (eds.), D. Reidel Publishing Company, pp. 55-69.

Clark, I., (1979), Practical Geostatistics, Applied Science Publishers, Ltd., London, 129 p.

Cliff, A. D., and Ord, J. K., (1975), "The Choice of a Test for Spatial Autocorrelation," Display and Analysis of Spatial Data, Davis, J. C. and McCullagh, M. J. (eds.), J. W. Arrowsmith Ltd., Bristol, Great Britain, pp. 54-77.

Dahlberg, E. C., (1975), "Relative Effectiveness of Geologists and Computers in Mapping Potential Hydrocarbon Exploration Targets," *Mathematical Geology*, Vol. 7, No. 5/6, p. 373-394.

Davis, J. C., (1973), Statistics and Data Analysis in Geology, John Wiley & Sons, Inc., New York, 550 p.

_____, (1986), Statistics and Data Analysis in Geology, Second Edition, John Wiley & Sons, Inc., New York, 646 p.

Davis, M. W. and Culhane, P. G., (1984), "Contouring Very Large Data Sets Using Kriging," Geostatistics for Natural Resources Characterization, Part 2, Verly, G. et al. (eds.), D. Reidel Publishing Company, pp. 599-619.

Delfiner, P., (1976), "Linear Estimation of Non-stationary Spatial Phenomena," Advanced Geostatistics in the Mining Industry, NATO ASI Series C: Mathematical and Physical Sciences, Vol. 24, Guarascio et al. (eds.), D. Reidel, Dordrecht Holland, pp. 49-68.

Deo, N., (1974), Graph Theory with Applications to Engineering and Computer Science, Prentice-Hall, Inc., Englewood Cliffs, New Jersey.

DiZenzo, S., (1983), "Advances in Image Segmentation," *Image and Vision Computing*, pp. 196-210.

Dowd, P. A., (1984), "The Variogram and Kriging: Robust and Resistant Estimators," <u>Geostatistics for Natural Resources Characterization, Part 2</u>, Verly, G. et al. (eds.), D. Reidel Publishing Company, pp. 91-106.

_____, (1985), "A Review of Geostatistical Techniques for Contouring," <u>Fundamental Algorithms for Computer Graphics</u>, Earnshaw, R. A. (ed.), pp. 483-530.

Duda, R. O., and Hart, P. E., (1973), <u>Pattern Recognition and Scene Analysis</u>, John Wiley & Sons, New York, 482 p.

Einstein, H. H., (1984), personal communication and class notes, Massachusetts Institute of Technology.

Erikson, C. M., (1985), "Supplementary Techniques for Determining Soil Profiles," Submitted in partial fulfillment of the requirements for the degree of Master of Science, Massachusetts Institute of Technology, 136 p.

Fekete, G., Eklundh, J-O., and Rosenfeld, A., (1981), "Relaxation: Evaluation and Applications," *IEEE Transactions on Pattern Analysis and Machine Intelligence*, Vol. PAMI-3, No. 4, pp. 459-469.

Fortune, S., (1987), "A Sweepline Algorithm for Voronoi Diagrams," *Algorithmica*, Vol. 2, pp. 153-174.

Gilbert, E. N., (1962), "Random Subdivisions of Space into Crystals," *Annals of Mathematical Statistics*, No. 33, pp. 958-972.

Goodall, D. W., (1966), "A New Similarity Index Based on Probability," *Biometrics*, No. 22, pp. 882-907.

Gower, J. C., (1971), "A General Coefficient of Similarity and Some of Its Properties," *Biometrics*, No. 27, pp. 857-871.

Green, P. J. and Sibson, R., (1978), "Computing Dirichlet tesselations in the plane," *The Computer Journal*, Vol. 21, No. 2, pp. 168-173.

Grimm, E. C., (1987), "CONISS: A FORTRAN 77 Program for Stratigraphically Constrained Cluster Analysis by the Method of Incremental Squares," *Computers & Geosciences*, Vol. 13, No. 1, pp. 13-35.

Harbaugh, J. W., and Merriam, D. F., (1968), <u>Computer Applications in Stratigraphic Analysis</u>, John Wiley & Sons, New York, 282 p.

Henley, S., (1981), <u>Nonparametric Geostatistics</u>, John Wiley & Sons, New York, 145 p.

Hoaglin. D. C. and Welsch, R. E., (1978), "The Hat Matrix in Regression and ANOVA," *The American Statistician*, Vol. 32, No. 1, pp. 17-22.

Hodder, I., and Orton, C., (1976), <u>Spatial Analysis of Archeology</u>, Cambridge University Press, Cambridge, England.

Howell, J. A., (1983), "A FORTRAN 77 Program for Automatic Stratigraphic Correlation," *Computers & Geoscience*, Vol. 9, No. 3, pp. 311-327.

Huijbregts, C. J., (1975), "Regionalized Variables and Quantitative Analysis of Spatial Data," *Display and Analysis of Spatial Data*, Davis, J. C. and McCullagh, M. J. (eds.), J. W. Arrowsmith Ltd., Bristol, Great Britain, pp. 38-53.

Jones, T. A., Hamilton, D. E., and Johnson, C. R., (1986), *Contouring Geologic Surfaces with the Computer*, Van Nostrand Reinhold Company, Inc., New York, 314 p.

Kafritsas, J. and Bras, R. 1., (1981), "The Practice of Kriging," Report No. 263, Ralph M. Parsons Laboratory, Department of Civil Engineering, Massachusetts Institute of Technology, 107 p.

Kittler, J. and Illingworth, J., (1985), "Relaxation Labelling Algorithms - A Review," *Image and Vision Computing*, Vol. 3, No. 4, pp. 206-216.

Krumbein, W. C., (1976), "Probabilistic Modelling in Geology," *Random Processes in Geology*, Merriam, D. F. (ed.), Springer-Verlag, New York, pp. 39-54.

Lee, S. L., (1982), " Uses of Acoustic Profiling Information in Reducing Uncertainties in Sub-Seabottom Exploration," Submitted in partial fulfillment of the requirements for the degree of Master of Science in Civil Engineering, Massachusetts Institute of Technology.

Lee, D. T. and Schachter, B. J., (1980), "Two Algorithms for Constructing a Delaunay Triangulation," *International Journal of Computer and Information Sciences*, Vol. 9, No. 3, pp. 219-242.

Matheron, G., (1965), "Les Variables regionalisees et leur estimation: Masson et Cie," Editeurs, Paris, 305 p.

_____, (1970), "The Theory of Regionalized Variables and its Applications," *Cah. Centre Morphol. Math.*, 5.

_____, (1971), "The theory of regionalized variables and its applications," Les Cahiers du Centre de Morphologie Mathematique, Ecole Nationale Superieure des Mines, Paris, 211 p.

_____, (1973), "The Intrinsic Random Functions and Their Applications," *Advances in Applied Probability*, No. 5, pp. 439-468.

_____, (1976), "Le Choix des Modeles en Geostatistique," *Advanced Geostatistics in the Mining Industry*, Guarascio et al. (eds.), NATO ASI Series C: Mathematical and Physical Sciences, Vol. 24, D. Reidel, Dordrecht Holland, pp. 3-10.

_____, (1979), "Le Krigeage Universel," *Cha. Centre Morphol. Math.*, 1.

Matuszak, D. R., (1972), "Stratigraphic Correlation of Subsurface Geologic Data by Computer," *Mathematical Geology*, Vol. 4, No. 4, pp. 331-343.

McCullagh, M. J., (1981), "Creation of Smooth Contours Over Irregularly Distributed Data Using Local Surface Patches," *Geographical Analysis*, Vol. 13, No. 1, pp. 51-63.

Meijering, J. L., (1953), "Interface area, edge length, and number of vertices in crystal aggregates with random nucleation," Philips Research Reports, No. 8, pp. 270-290.

Merriam, D. F., (1971), "Computer Applications in Stratigraphic Problem Solving in Decision Making in the Mineral Industry," *Can. Inst. Min. Met.*, Vol. 12, p 139-147.

Miles, R. E., (1970), "On the Homogeneous Planar Poisson Point Process," *Mathematical Biosciences*, Vol. 6, pp. 85-127.

Muir, J. W., Hardie, H. G. M., Inkson, R. H. E., and Anderson, A. J. B., (1970), "The classification of profiles by traditional and numerical methods," *Geoderma*, Vol. 4, No. 1, pp. 81-90.

Nucci, L. R., (1979), "An Analysis of the Rate of Error in Two Color Maps," Submitted in partial fulfillment of the requirements for the degree of Master of Science, Massachusetts Institute of Technology.

Olea, R. A., (1975), "Optimum Mapping Techniques Using Regionalized Variable Theory," Number Two Series on Spatial Analysis, Kansas Geological Survey, Lawrence, Kansas, 137 p.

_____, (1982), "Systematic Approach to Sampling of Spatial Functions," Doctoral degree thesis, University of Kansas, Lawrence, Kansas, 276 p.

_____, (1984), "Systematic Sampling of Spatial Functions," Number Seven, Series on Spatial Analysis, Kansas Geological Survey, Lawrence, Kansas, 57 p.

Omre, H., (1984), "The Variogram and Its Estimation," Geostatistics for Natural Resources Characterization, Part 2, Verly, G. et al. (eds.), D. Reidel Publishing Company, pp. 107-125.

_____, (1987), "Bayesian Kriging - Merging Observations and Qualified Guesses in Kriging," *Mathematical Geology*, Vol. 19, No. 1, pp. 25-39.

Pavlidis, T., (1977), Structural Pattern Recognition, Springer-Verlag, New York, 302 p.

Peleg, S. and Rosenfeld, A., (1978), "Determining Compatibility Coefficients for Curve Enhancement Relaxation Processes," *IEEE Transactions on Systems, Man, and Cybernetics*, Vol. SMC-8, No. 7, pp. 548-555.

Pielou, E., (1977), Mathematical Ecology, Wiley-Interscience, New York.

Preparata, F. P. and Shamos, M. I., (1985), Computational Geometry - An Introduction, Springer-Verlag, New York, 390 p.

Puente, C. E. and Bras, R. L., (1986), "Disjunctive Kriging, Universal Kriging, or No Kriging: Small Sample Results with Simulated Fields," *Mathematical Geology*, Vol. 18, No. 3, pp. 287-305.

Rayner, J. H., (1965), "Multivariate Analysis of Montmorillinite," *Clay Minerals*, Vol. 6, pp. 59-70.

_____, (1966), "Classification of Soils by Numerical Methods," *Journal of Soil Science*, Vol. 17, No. 1, pp. 79-92.

Rehak, D. R., (1985), "An Electronic Workbench for Geotechnical Site Characterization," Proceedings, Fourth International OMAE Symposium, ASME, Dallas, Texas, pp. 570-581.

Rendu, J.-M., (1978), An Introduction to Geostatistical Methods of Mineral Exploration, South African Institute of Mining and Metallurgy Monograph Series, Geostatistics 2, Northern Cape Printers, Ltd., Kimberley, South Africa, 84 p.

Ripley, B. D., (1977), "Modelling Spatial Patterns," *Journal of the Royal Statistical Society*, Vol. 39, No. 2, pp. 172-212.

_____, (1981), Spatial Statistics, John Wiley & Sons, New York, 252 p.

Rosenfeld, A., and Kak, A. C., (1982), _Digital Picture Processing_, Academic Press, New York.

Sabin, M. A., (1985), "Contouring the State-of-the-Art," _Fundamental Algorithms for Computer Graphics_, Earnshaw, R. A. (ed.), pp. 411-483.

Sackin, M. J., Sneath, P. H. A., and Merriam, D. F., (1965), ALGOL Program for Cross-association of Non-numeric Sequences Using a Medium Sized Computer, Kansas Geol. Survey Sp. Dist. Publ., Vol. 23, 36 p.

Shaw, B. R., (1977), "Evaluation of Distortion of Residuals in Trend Surface Analysis by Clustered Data," _Mathematical Geology_, Vol. 9, No. 5, pp. 507-517.

Sneath, P. H. A., and Sokal, R. R., (1973), _Numerical Taxonomy_, W. H. Freeman and Company, San Francisco, 573 p.

Solow, A. R., (1986), "Mapping by Simple Indicator Kriging," _Mathematical Geology_, Vol. 18, No. 3, pp. 335-352.

Switzer, P., Mohr, M., and Heitman, R. E., (1964), Statistical Analyses of Ocean Terrain and Contour Plotting Procedures, Project Trident Technical Report No. 1440464, A. D. Little, Inc., Cambridge, MA, 81 p.

Switzer, P., (1965), "A Random Set Process in the Plane with a Markovian Property," _The Annals of Mathematical Statistics_, Vol. 36, No. 4, pp. 1859-1863.

_____, (1967), "Reconstructing Patterns from Sample Data," _The Annals of Mathematical Statistics_, Vol. 38, pp. 138-155.

_____, (1976), "Applications of Random Process Models to the Description of Spatial Distributions of Qualitative Geologic Variables," _Random Processes in Geology_, Springer-Verlag, New York, pp. 124-134.

Tipper, J. C., (1979), "Surface Modelling Techniques," Number Four, Series on Spatial Analysis, Kansas Geological Survey, Lawrence, Kansas, 108 p.

Unwin, D. J. and Wrigley, N., (1987), "Towards a General Theory of Control Point Distribution Effects in Trend-Surface Models," _Computers & Geosciences_, Vol. 13, No. 4, pp. 351-355.

Upton, G. and Fingleton, B., (1985), _Spatial Data Analysis by Example, Volume I - Point Pattern and Quantitative Data_, John Wiley & Sons, New York, 410 p.

Waterman, M. S. and Raymond, R., Jr., (1987), "The Match Game: New Stratigraphic Correlation Algorithms," _Mathematical Geology_, Vol. 19, No. 2, pp. 109-127.

Watson, G. S., (1972), "Trend Surface Analysis and Spatial Correlation," Fenner, P. (ed.), Quantitative Geology: The Geological Society of America, Spec. Paper 146, pp. 39-46.

Watson, D. F., (1982), "ACORD: Automatic Contouring of Raw Data," _Computers & Geoscience_, Vol. 8, No. 1, pp. 97-101.

Watson, D. F. and Philip, G. M., (1984a), "Triangle Based Interpolation," _Mathematical Geology_, Vol. 16, No. 8, pp. 779-795.

_____, (1984b), "Systematic Triangulations," *Computer Vision, Graphics, and Image Processing*, Vol. 26, pp. 217-223.

Whitten, E. H. T., (1975), "The practical use of trend-surface analyses in the geological sciences, in Davis, J. C., and McCullagh, M. J., (eds.), *Display and Analysis of Spatial Data*, John Wiley & Sons, London, pp. 282-297.

Zupan, J. (1982), *Clustering of Large Data Sets*, John Wiley & Sons, London, 122 p.

APPENDIX A

BACK BAY CASE HISTORY

A.1 Introduction

Over a hundred years ago a tidal estuary in Boston was filled by man to create additional land for development. This area, locally known as Back Bay, is shown in Figure A.1. A detailed account of the development of Back Bay and the subsurface soil conditions was presented by Aldrich (1970).

The Back Bay area covers an area of approximately 600 acres which have been used for development since the early 1800's. Today some of the tallest, as well as the oldest, buildings in Boston are located within the Back Bay area. The Back Bay area has been a very active development area since the early 1950's. Many of the building sites have been occupied by several structures through time.

For the purposes of this research, a portion of the Back Bay area was selected as a case history site due to the relative wealth of test boring data available. Figure A.1 shows the area of Boston known as the Back Bay and the general area of the portion chosen for the following case history.

A.2 Subsurface Conditions

The geology and subsurface soil conditions of the Back Bay area are well documented by Aldrich (1970). A very brief summary of the rock and sub-surface soil conditions, as reported by Aldrich, follows.

The upper bedrock in the Back Bay area is the Cambridge Slate which belongs to the Boston Bay Group. Although the Cambridge Slate is slaty in places, the slaty cleavage is locally absent. As a result the rock is locally called "argillite".

Glacial till was deposited by the overlying glaciers which covered the bedrock during the Pleistocene. Locally the thickness of glacial till varies from a couple of feet to more than a 100 feet in the general Boston area, and about 30 feet in the Back Bay. The glacial till is an unsorted mixture of cobbles and boulders grading to silt and clay, which is very dense in place.

A stratum of sand and gravel overlies the glacial till throughout much of the Back Bay. This stratum is believed to be glacial outwash deposits.

Clay, locally known as Boston Blue Clay (BBC), overlies the outwash deposits. BBC is a medium plasticity silty clay deposited in a quiet marine environment in the general Boston area. In the Back Bay area the thickness of BBC typically ranges from 50 to 125 ft. with maximum observed thickness of 180 ft. Locally BBC may contain sand lenses and occasional boulders. Although the original surface of the BBC was probably relatively flat, changes in the sea level resulted in weathering and erosion which altered the surface of the deposit.

In parts of the Back Bay area BBC is overlain by sand and gravel outwash deposits which were deposited by readvancing glaciers. The outwash deposits are not continuous across the Back Bay area. Generally, the deposits exist in the northwest portion with increasing thickness toward the west, and are absent in the eastern portion of the Back Bay area.

Following the glaciers, organic soils (fresh water peat, organic silts and salt marsh peat) were deposited across the Back Bay region. The observed thickness of the organic soils is from 5 to 25 ft.

The surficial soil deposit in the Back Bay is the fill placed by colonists for the general purpose of developing the land. The fill is highly variable in composition and density.

A.3 Field Investigations

Test boring logs for borings performed in the case history area were obtained from various sources. The test boring logs were often prepared

by drilling contractors, and the visual descriptions of the subsurface soils varied considerably. The logs were reviewed for general consistency and perceived quality of information. Test boring logs which were judged to be of questionable quality were deleted from the study.

The locations of the selected test borings (see Figure A.2) were obtained as accurately as possible. Although some of the test boring locations were given in state plane coordinates, many of the coordinates were determined by scaling from available test boring location plans.

A.4 Summary Statistics

The soil strata information from the case history test borings was analyzed to determine summary statistics. The summary statistics were calculated for the observed top of the soil strata and the observed thickness of the soil deposits. The results for the observed strata tops and thicknesses are given in Tables A.1 and A.2, respectively.

The summary statistics for the observed top of the soil strata indicate a greater level of uncertainty in the top of the glacial till and rock compared to the other strata. This is primarily reflected by the standard deviations which are four to five times larger for the glacial till and rock surfaces than for the other soil interfaces.

Based on the standard deviation statistics, it appears that the thickness of the Boston Blue Clay is most irregular. However, the coefficient of variation statistics indicate that the marine sand thickness is most variable followed by the glacial till thickness.

In addition to the summary statistics for the observed strata tops and thicknesses, which are non-spatial, a correlation matrix (see Table A.3) was developed to assess general relationships.

The correlation coefficient analysis indicates generally weak relationships with two exceptions. First, the correlation between the east coordinate and the top of the marine sand (-0.95) indicates that there is a strong relationship. The surface of the marine sand apparently slopes

254

generally downward in an easterly direction. The other apparently strong relationship is the top of the glacial till and the top of the rock, where the correlation coefficient is 0.97. This is a very strong relationship, indicating that the two surfaces are generally conformable.

The ratio of the coordinates was included in the correlation coefficient analysis in order to assess general trends in directions other than the four principal directions (north, south, east and west). The correlation coefficients for several of the strata tops, particularly the glacial till and rock, were higher for the ratio. This indicates that the general trend of the surfaces is closer to one of the minor directions (northeast, southeast, southwest or northwest) than one of the principal directions.

A.5 Transition Matrix

Using the test boring data, a transition matrix was developed based on an embedded Markov chain approach (Davis, 1986). With an embedded Markov chain, the transition must be between two states (transitions within the same state are not permitted). The calculated transition matrix is presented in Table A.4.

The results of the transition matrix indicate that the stratigraphy in the Back Bay case history is very consistent with respect to state transitions. The maximum transition probability is greater than 0.94 for all transitions with the exception of the organic soils to either marine sand or BBC. The marine sand is the only significant discontinuous stratum. Technically the glacial till is discontinuous, although the low transition probability (0.06) may be partially attributed to the possibility that the glacial till was thin in those locations and either not sampled or observed.

The consistency of the stratigraphy was one factor for selecting the Back Bay case history. The continuous stratigraphy is advantageous for the application of mathematical stratigraphic modeling discussed in Chapters 5 and 6.

A.6 Trend Surface Analysis

The soil stratigraphy data for the 157 test borings in the Back Bay case history were analyzed to fit first through fourth degree polynomial surfaces to the data using least squares regression techniques and the computer programs TRENDS, JRTRENDS, and LSMODEL developed as part of this research.

TRENDS is a computer program which calculates first through fourth order least squares polynomial trend surfaces given irregularly spaced data in the form of x, y, z. TRENDS calculates regression coefficients, estimated values and residuals at the data points, and summary statistics (sum of squares and mean square errors for the regression, deviation and total, and the R^2 goodness of fit coefficient).

JRTRENDS is a modified version of the program TRENDS. JRTRENDS uses the process of jackknifing to sequentially remove a single data point, perform first through fourth degree polynomial regression, and estimate the surface value at the deleted data point. The actual observed value and the regression estimate at the deleted data point are used to calculate a "residual" which is stored in an array. JRTRENDS continues until each of the data points has been removed separately, storing critical summary statistics and the "residual" values in arrays.

LSMODEL is a program developed to use irregularly spaced data in the form x, y, z to develop a least squares regression model of the surface within a specified rectangular area. The program input includes the degree of the polynomial surface to be fit, and data to specify the limits of the rectangle of interest. The program can accommodate axis rotation and translation for the specified triangle. LSMODEL estimates the regression surface values for a specified regular grid in the rectangle. The program substitutes each observed data point for the estimated surface value at the nearest grid node. If there are multiple substitutions at a given grid node, the final value is the observed value for the closest data

point. LSMODEL can be used for the preparation of trend surface models, discussed below, or for the development of regularly spaced data to be used as input into plotting programs.

The program TRENDS was used to evaluate the case history test boring data concerning the observed tops of the soil strata and the thickness of the deposits. The results of the analysis using TRENDS are summarized in Tables A.5 through A.14, which are discussed separately below.

Using the programs TRENDS and LSMODEL, trend surface analyses were performed using the data from the Back Bay case history test borings. Polynomials of first through fourth degree were fit to the strata top and thickness data.

The goodness-of-fit coefficient is often used as a means of evaluating the "success" of an attempt to model a surface using least squares regression techniques. The goodness-of-fit coefficients for the observed strata tops data (shown in Table A.5) range from 0.03 to 0.9. Relatively high values (0.3 to 0.9 depending on the degree of the polynomial) were obtained for the strata top regression for the marine sands, glacial till and rock. Moderate values (0.03 to 0.4) were obtained for the top of the organic soils and BBC.

In addition to the goodness-of-fit coefficients, the results of the trend surface analysis were evaluated using the mean squares for the regressions and deviations. The mean square of the deviation is essentially the variance about the regression line. The mean square of the regression is the variance of the line about its mean. The mean squares for the first through fourth order trend surfaces are summarized in Tables A.7 through A.10.

Using mean squares as estimates of the variance, it is possible to compare the variances using the F distribution. Typically for trend surfaces, the ratio of the variance due to the regression (mean squares of the regression) to the variance due to deviation (mean squares of the

deviation) is used. If the regression is significant, the deviation about the regression will be small compared to the variance of the regression.

The F test is used to compare the variances, and to probabilistically answer whether or not the regression effect is significantly different from a random sample from the same population. It is possible to perform significance tests for both the order of a polynomial and the increase in the order of the polynomial. The results of the significance testing for the trend surface analysis of the observed strata tops and thicknesses are summarized in Tables A.11 through A.14.

Most of the trend surface polynomial orders were significant with alpha of 0.05 with the exception of the first and second order polynomials for the top of the organic soils, and the first through fourth order polynomials for the thickness of the glacial till. It is interesting to note that the goodness-of-fit coefficients for these cases were all less than 0.21, and in most cases were less than 0.05.

The significance tests for the increase in the order of the trend surface polynomials were less consistent than those for the order of the polynomials. The increase in order for the polynomials of the thickness of glacial till were all not significant. Each of the other regressions, except for those of the BBC (tops and thickness) and marine sand (thickness), were also not significant with one increase or another.

The trend surface analysis included an analysis of the leverages of the data points for each of the surface models. Partial results of this analysis are shown in Table A.15. As indicated in the table, typically 10% or more of the data points were in regions where the final leverages exceeded the recommended limit of 2p/n, where p is the number of explanatory terms in the model and n is the number of data points (Unwin and Wrigley, 1987).

A typical plot of the leverages (see Figure 5.2) shows the leverages for the fourth order trend surface model of the top of rock. Similar plots were prepared for trend surface models of first through fourth order for each soil surface. In each case, the points around the perimeter of the case history area had leverage values exceeding the recommended limit of $2p/n$.

Unwin and Wrigley (1987) discuss the effects of the distribution of data points on trend surface models. Their discussion includes references regarding the detrimental edge effects and the effects of spatial clustering. Davis (1973) and others recommend that the area of data collection should be extended beyond the subject area in order to partially overcome the negative edge effects. This practice is not usually easily accomplished in geotechnical engineering studies, due to the need for access to adjacent properties, perceived unnecessary increase in exploration costs, etc. Unwin and Wrigley (1987) also recommend leverage analysis as a means of evaluating the need and location for additional exploration.

The application of leverage analysis to trend surface modeling is interesting on an academic level; however, it should be remembered that the trend surface models do not satisfy the basic objectives of soil interface surface modeling (see Chapter 5).

Jackknifed trend surface models for the observed strata tops were developed for polynomials of order one through four. Summary statistics of the results are presented in Table A.16.

The mean residual values are close to zero and the higher mean residual values occur with the glacial till and rock as expected. However, the magnitude of the standard deviations and the rages of the residuals are high. The standard deviations are higher than the summary statistics, which are non-spatial, for the organic soils, marine sand and BBC. The standard deviations are slightly lower than the summary statistics for

259

the glacial till and rock. In summary, the jackknifed residuals indicate the relatively poor performance of the trend surface models as interpolators.

A.7 Delaunay Triangulation Analysis

The available case history data for the observed top and thickness of the strata was analyzed using Delaunay triangulation. The analysis consisted of jackknifing the data by sequentially deleting a single observation and then estimating the surface elevation or thickness at that location and comparing it with the observation. The results for the Back Bay data are summarized in Tables A.17 and A.18.

The summary statistics for the jackknifed Delaunay triangulation analysis appear to be more satisfactory than those for the jackknifed trend surface analysis. It should be remembered, however, that the Delaunay triangulation method can not estimate values for those points on the exterior convex hull. Therefore, the statistics can not be directly compared with those in Table A.16.

The results of the jackknifed Delaunay triangulation analysis indicate mean residuals close to zero, and standard deviations that are close to or less than those of the non-spatial summary statistics. In the case of the glacial till and rock, the standard deviations are approximately half of those for the non-spatial summary statistics. The ranges of the residuals are less for the jackknifed Delaunay triangulation than for the trend surface analysis. This may be due in part to the local nature of the Delaunay triangulation compared to the global nature of trend surface analysis where every data point influences the polynomial coefficients to some extent.

The results of the jackknifed Delaunay triangulation analysis of strata thickness are similar to those for the strata tops. In general, the performance appears to be better than that for the jackknifed trend surface analysis.

A.8 Kriging Analysis

Kriging analysis was performed on the Back Bay case history data to assess the performance of kriging as an interpolation method. The analysis was based on the use of a modified version of AKRIP by Kafritsas and Bras (1981). Partial results for the analysis are presented below following a brief discussion of the analysis methodology.

As discussed in Chapter 3, Matheron (1973) and Delfiner (1976) express the most common form of the generalized covariances as polynomials of the general form:

Equation A.1:

$$C(h) = b_o + \sum_{j=0}^{K} (-1)^{(j+1)} b_j + 1 |h|^{(2j+1)}$$

The coefficients of the common form of the generalized covariance function are controlled such that C(h) is conditionally positive definite. The conditions for the common values of K (0 to 2) are as follows:

$K = 0$

$$C(h) = b_o - b_1 |h|$$

$$b_o \geq 0, \qquad b_1 \geq 0$$

$K = 1$

$$C(h) = b_o - b_1 |h| + b_2 |h|^3$$

$$b_0 \geq 0, \quad b_1 \geq 0, \quad b_2 \geq 0$$

$K = 2$

$$C(h) = b_o - b_1 |h| + b_2 |h|^3 - b_3 |h|^5$$

$$b_o \geq 0, \quad b_1 \geq 0, \quad b_3 \geq 0, \quad b_2 \geq -2\sqrt{(b_1 b_3)}$$

The Back Bay case history data for the observed top of soil strata and observed thickness of soil strata was analyzed using kriging. The analysis was performed using a modified version of AKRIP called KRM (KRiging Model). The modified code removed much of the user interaction, and finds the best generalized covariance model automatically. The only technical change in the code is that the "pure nugget" effect structural model is precluded. This change was made in order to develop a model which can always estimate the variance of the estimate. The structural model coefficients from the analysis using KRM are summarized in Tables A.19 and A.20.

The structural models from the kriging analysis were all zero order intrinsic functions with the exception of the model of the glacial till thickness which was first order. Most of the zero order models did not have a nugget coefficient (b_0). The two exceptions were the models of the top of the marine sand and BBC. These models may have a nugget coefficient, since both surface appear to be reasonably planar when compared to the other surfaces.

Examples of the surface estimates and the estimated variance about those surfaces for the Back Bay strata tops are shown in Figures 5.5 through 5.9.

The kriging analysis of the observed strata top data included jackknifing and calculation of summary statistics for the residuals and the standardized residuals. The results are shown in Tables A.21 and A.22.

The standard deviations of the standardized residuals indicate that the predictive performance of the jackknifed kriging analyses was fairly similar. The higher values for the organic soils, glacial till and rock indicate that there was a broader range and higher uncertainty level in the predictions for these surfaces. The magnitude of the ranges seems high, indicating that at least in isolated cases even the kriging interpolator does not perform as well as hoped.

A.9 Comparison of Interpolation Methods

In a general sense, it is possible to compare the performance of the interpolation methods by comparing the mean and standard deviation of the jackknifed residuals. The ideal interpolator would have a mean and standard deviation of zero.

Figure A.3 is a plot of the residual means and standard deviations of the jackknifed analysis using fourth order trend surface, Delaunay triangulation and kriging methods. Figure A.3 demonstrates the relative performances of the jackknifed interpolation methods on the various soil interfaces. The performance of all the methods was better for the organic soils, marine sand and BBC than for the glacial till and the rock. Based on the mean and standard deviation of the residual, the performance of the kriging method was typically better than that of the trend surface and Delaunay triangulation methods.

A.10 Other Analyses

As discussed in Section 5.3.3, a sub-set of the top of rock data (40 pts.) was hand contoured by nine individuals in order to compare hand methods of surface modeling to analytical methods. The resulting contour plans are shown in Figure A.4.

The Back Bay case history data were analyzed using the methods described in Chapter 6 for probabilistic profiles, stratigraphic models and probabilistic relaxation. The significant results of these analyses are presented in Chapter 6.

Table A.1 - Summary Statistics for the Strata Tops, Back Bay.

	Organic Soils	Marine Sand	Boston Blue Clay	Glacial Till	Rock
No. of Obs., n	156	37	157	76	77
Mean, (El.)	-9.03	-23.88	-29.31	-97.95	-106.10
Stand. Dev., (ft.)	3.72	5.18	4.05	16.80	18.22
Median, (El.)	-8.65	-25.7	-29.5	-94.6	-100.7
Range, (ft.)	20.65	21.85	21.00	80.25	74.70
Coef. of Variation	0.412	0.217	0.138	0.171	0.171

Table A.2 - Summary Statistics for Strata Thickness, Back Bay. ([ ] indicates statistics for non-zero data)

	Fill	Organic Soils	Marine Sand	Boston Blue Clay	Glacial Till
No. of Obs., n	156	156	156 [38]	81	77 [72]
Mean, (ft.)	19.45	18.65	1.70 [6.99]	68.66	7.27 [7.78]
Stand. Dev., (ft.)	7.62	4.72	4.07 [5.63]	16.33	4.60 [4.32]
Median, (ft.)	19.0	18.9	0.0 [5.0]	65.0	7.0 [7.0]
Range, (ft.)	32.0	27.0	21.5 [20.5]	76.0	19.0 [18.5]
Coef. of Variation	0.392	0.253	2.394 [0.805]	0.238	0.633 [0.555]

Table A.3 - Correlation Coefficient Matrix, Back Bay.

	E. Coord.	N. Coord.	ECoord NCoord	Top of Organic Soils	Top of Marine Sands	Top of BBC	Top of Glacial Till	Top of Rock
E. Coord.	1.00	0.57	0.19	-0.45	-0.95	-0.13	0.25	0.32
N. Coord.	0.57	1.00	-0.70	-0.14	-0.48	-0.62	-0.43	-0.34
E. Coord. N. Coord.	0.19	-0.70	1.00	-0.22	-0.25	0.63	0.73	0.69
Top of Organic Soils	-0.45	-0.14	-0.22	1.00	0.65	0.12	-0.41	-0.49
Top of Marine Sands	-0.95	-0.48	-0.25	0.65	1.00	0.09	-0.34	-0.42
Top of BBC	-0.13	-0.62	0.63	0.12	0.09	1.00	0.14	0.15
Top of Glacial Till	0.25	-0.43	0.73	-0.41	-0.34	0.14	1.00	0.97
Top of Rock	0.32	-0.34	0.69	-0.49	-0.42	0.15	0.97	1.00

Table A.4 - Strata Change Transition Matrix, Back Bay.

From\To	Fill	Organic Soils	Marine Sand	BBC	Glacial Till	Rock
Fill	0	1.00	0	0	0	0
Organic Soils	0	0	0.23	0.77	0	0
Marine Sand	0	0	0	1.00	0	0
BBC	0	0	0	0	0.94	0.06
Glacial Till	0	0	0	0	0	1.00
Rock	0	0	0	0	0	0

Table A.5 - Trend Surface Goodness-of-Fit Values, Strata Tops, Back Bay.

	Order of Polynomial			
	1	2	3	4
Organic Soils	0.0273	0.0472	0.2306	0.2831
Marine Sands	0.6229	0.7421	0.7785	0.8746
Boston Blue Clay	0.1475	0.2601	0.3207	0.3970
Glacial Till	0.3393	0.7254	0.7529	0.8802
Rock	0.3765	0.7260	0.7606	0.8744

Table A.6 - Trend Surface Goodness-of-Fit Values, Strata Thickness, Back Bay.

	Order of Polynomial			
	1	2	3	4
Fill	0.1203	0.1430	0.2847	0.4428
Organic Soils	0.1002	0.2597	0.2895	0.3064
Marine Sands	0.2927	0.5402	0.6521	0.6937
Boston Blue Clay	0.2811	0.6957	0.7349	0.8401
Glacial Till	0.0329	0.0670	0.1283	0.2052

Table A.7 - Summary of Mean Squares of Regression for Trend Surface Analysis, Strata Tops, Back Bay.

	Order of Polynomial			
	1	2	3	4
Organic Soils	29.38	20.28	55.09	43.47
Marine Sands	300.34	143.13	83.41	60.24
Boston Blue Clay	188.79	133.14	91.21	72.57
Glacial Till	3590.41	3070.19	1770.46	1330.46
Rock	4226.69	3260.29	1897.64	1402.38

Table A.8 - Summary of Mean Squares of Regression for Trend Surface Analysis, Strata Thickness, Back Bay.

	Order of Polynomial			
	1	2	3	4
Fill	542.09	257.61	284.96	288.14
Organic Soils	173.35	179.74	111.31	75.71
Marine Sands	377.11	278.42	186.73	127.69
Boston Blue Clay	3000.13	2970.34	1743.28	1280.98
Glacial Till	26.43	21.55	22.93	23.57

Table A.9 - Summary of Mean Squares of Deviation for Trend Surface Analysis, Strata Tops, Back Bay.

	Order of Polynomial			
	1	2	3	4
Organic Soils	13.67	13.66	11.33	10.93
Marine Sands	10.69	8.02	7.91	5.49
Boston Blue Clay	14.17	12.54	11.83	10.87
Glacial Till	191.53	83.02	79.22	41.58
Rock	202.92	93.23	86.71	49.50

Table A.10 - Summary of Mean Squares of Deviation for Trend Surface Analysis, Strata Thickness, Back Bay.

	Order of Polynomial			
	1	2	3	4
Fill	51.79	51.47	44.14	35.28
Organic Soils	20.35	17.07	16.84	17.02
Marine Sands	11.91	7.90	6.14	5.60
Boston Blue Clay	196.77	86.62	79.70	51.73
Glacial Till	21.02	21.14	20.93	20.62

Table A.11 - Summary of Test of Significance (Alpha - 0.05) of Regression of Trend Surface Analysis, Strata Tops, Back Bay. (NS - not significant, S - significant)

	Order of Polynomial			
	1	2	3	4
Organic Soils	NS	NS	S	S
Marine Sands	S	S	S	S
Boston Blue Clay	S	S	S	S
Glacial Till	S	S	S	S
Rock	S	S	S	S

Table A.12 - Summary of Test of Significance (Alpha - 0.05) of Regression for Trend Surface Analysis, Strata Thickness, Back Bay. (NS - not significant, S - significant)

	Order of Polynomial			
	1	2	3	4
Fill	S	S	S	S
Organic Soils	S	S	S	S
Marine Sands	S	S	S	S
Boston Blue Clay	S	S	S	S
Glacial Till	NS	NS	NS	NS

Table A.13 - Summary of Test of Significance (Alpha - 0.05) of Increase
in Order of Regression for Trend Surface Analysis, Strata
Tops, Back Bay. (NS - not significant, S - significant)

	Increase in Order of Polynomial		
	1 to 2	2 to 3	3 to 4
Organic Soils	NS	S	NS
Marine Sands	S	NS	S
Boston Blue Clay	S	S	S
Glacial Till	S	NS	S
Rock	S	NS	S

Table A.14 - Summary of Test Of Significance (Alpha - 0.05) of Increase
in Order of Regression for Trend Surface Analysis, Strata
Thickness, Back Bay. (NS - not significant, S - significant)

	Increase in Order of Polynomial		
	1 to 2	2 to 3	3 to 4
Fill	NS	S	S
Organic Soils	S	NS	NS
Marine Sands	S	S	S
Boston Blue Clay	S	S	S
Glacial Till	NS	NS	NS

Table A.15 - Summary of Leverages (Percentage of Points Exceeding 2p/n) of Regression for Trend Surface Analysis, Strata Tops, Back Bay.

	Order of Polynomial			
	1	2	3	4
Organic Soils	6.4%	10.9%	12.2%	12.2%
Marine Sands	0.0%	8.1%	8.1%	8.1%
Boston Blue Clay	5.7%	8.9%	12.7%	12.7%
Glacial Till	7.9%	10.5%	14.5%	14.5%
Rock	7.8%	10.4%	13.0%	13.0%

Table A.16 - Summary of Jackknifed Trend Surface Residuals, Strata Tops, Back Bay.

Stratum	Order of Polynomial	Mean, (ft)	Stand. Dev., (ft)	Max. (ft)	Min. (ft)	Range (ft)
Organic Soils n-156	1	-.0026	3.75	9.82	-11.48	21.29
	2	.0043	3.78	10.00	-11.03	21.04
	3	.0174	3.51	10.34	-9.32	19.67
	4	.0064	3.49	10.96	-9.82	20.79
Marine Sands n-37	1	.0608	3.25	8.80	-5.60	14.40
	2	.0055	2.49	8.49	-3.78	12.27
	3	.4740	3.79	15.33	-4.35	19.68
	4	.9832	5.97	27.44	-9.92	37.37
Boston Blue Clay n-157	1	-.0070	3.81	9.11	-10.25	19.37
	2	-.0067	3.60	10.20	-10.76	20.96
	3	.0052	3.55	8.15	-10.63	18.78
	4	.0305	3.51	8.76	-10.36	19.12
Glacial Till n-76	1	-.2479	14.31	26.01	-32.45	58.46
	2	.1957	10.40	41.79	-22.22	64.01
	3	.8541	14.10	85.84	-24.23	110.29
	4	-1.5022	14.71	19.98	-112.53	131.51
Rock n-77	1	-.2333	14.85	27.57	-37.16	64.73
	2	.0876	10.00	28.98	-32.69	61.67
	3	.2361	10.52	32.07	-30.48	62.55
	4	-.1252	7.51	18.57	-26.37	44.94

Table A.17 - Summary Statistics for Jackknifed Residuals for Delaunay
Triangulation Analysis, Strata Tops, Back Bay.

Stratum	No. of Pts., n	Mean, (ft)	Stand. Dev. (ft)	Range, (ft)	Min. (ft)	Max. (ft)
Organic Soils	141	-0.04	4.18	25.27	-12.25	13.02
Marine Sands	25	-0.19	2.53	10.27	-3.86	6.41
BBC	142	0.00	3.54	21.71	-10.61	11.11
Glacial Till	67	0.45	7.33	41.71	-14.12	27.59
Rock	68	0.00	8.17	58.56	-29.50	29.06

Tab A.18 - Summary Statistics for Jackknifed Residuals for Delaunay
Triangulation Analysis, Strata Thickness, Back Bay.

Stratum	No. of Pts., n	Mean, (ft)	Stand. Dev. (ft)	Range, (ft)	Min. (ft)	Max. (ft)
Fill	141	-0.04	5.94	38.81	-20.82	17.98
Organic Soils	141	0.05	4.45	26.59	-13.09	13.50
Marine Sands	141	-0.10	2.15	14.81	-7.03	7.78
BBC	72	-0.20	8.70	49.91	-30.88	19.03
Glacial Till	68	0.21	4.86	24.21	-11.12	13.09

273

Table A.19 - Summary of Kriging Coefficients, Strata Tops, Back Bay.

Stratum	K	b_0	b_1	b_2	b_3
Organic Soils	0	0	-.1944	-	-
Marine Sands	0	4.2213	-.0105	-	-
BBC	0	2.4706	-.1311	-	-
Glacial Till	0	0	-.4812	-	-
Rock	0	0	-.5774	-	-

Table A.20 - Summary of Kriging Coefficients, Strata Thickness, Back Bay.

Stratum	K	b_0	b_1	b_2	b_3
Fill	0	0	-.4032	-	-
Organic Soils	0	0	-.2480	-	-
Marine Sand	0	0	-.0810	-	-
BBC	0	0	-.6175	-	-
Glacial Till	1	11.838	0	5.4E-06	-

Table A.21 - Summary Statistics for Residuals of Jackknifed Kriging Analysis, Strata Tops, Back Bay.

Stratum	No. of Pts., n	Mean, (ft)	Stand. Dev. (ft)	Range, (ft)	Min. (ft)	Max. (ft)
Organic Soils	156	0.04	4.02	24.95	-12.26	12.69
Marine Sands	37	0.13	2.72	11.74	-4.44	7.30
BBC	157	-0.03	3.39	20.75	-10.03	10.72
Glacial Till	76	0.04	7.69	49.72	-27.06	22.66
Rock	78	0.23	8.43	57.29	-31.76	25.53

Table A.22 - Summary Statistics for Standardized Residuals of Jackknifed Kriging Analysis, Strata Tops, Back Bay.

Stratum	No. of Pts., n	Mean, (ft)	Stand. Dev. (ft)	Range, (ft)	Min. (ft)	Max. (ft)
Organic Soils	156	0.01	1.42	12.16	-5.91	6.25
Marine Sands	37	0.05	1.07	4.82	-1.65	3.18
BBC	157	-0.01	1.03	6.71	-3.25	3.45
Glacial Till	76	0.03	1.17	7.95	-4.41	3.55
Rock	78	0.00	1.33	10.65	-6.61	4.04
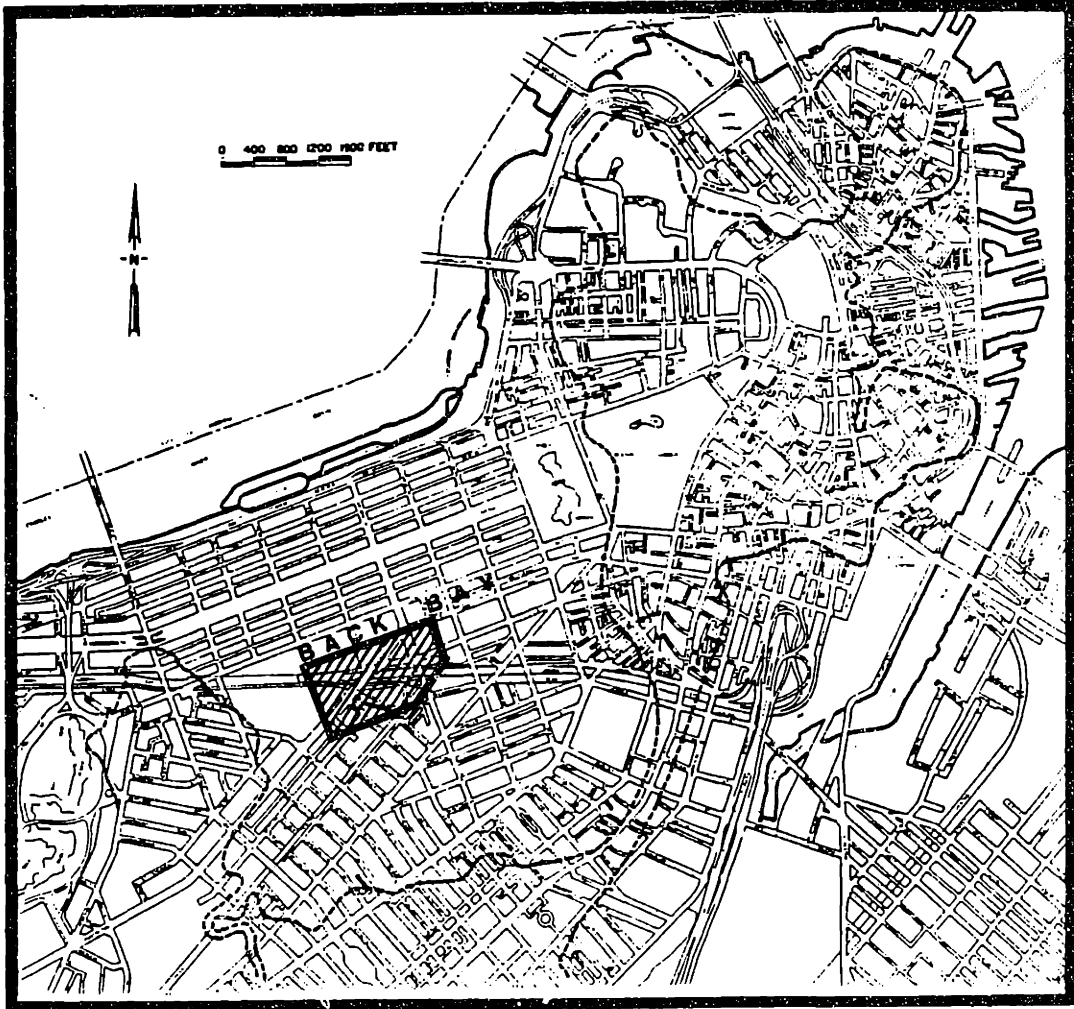
Case History Area

Figure A.1 - The Back Bay Area of Boston (after Aldrich, 1970).
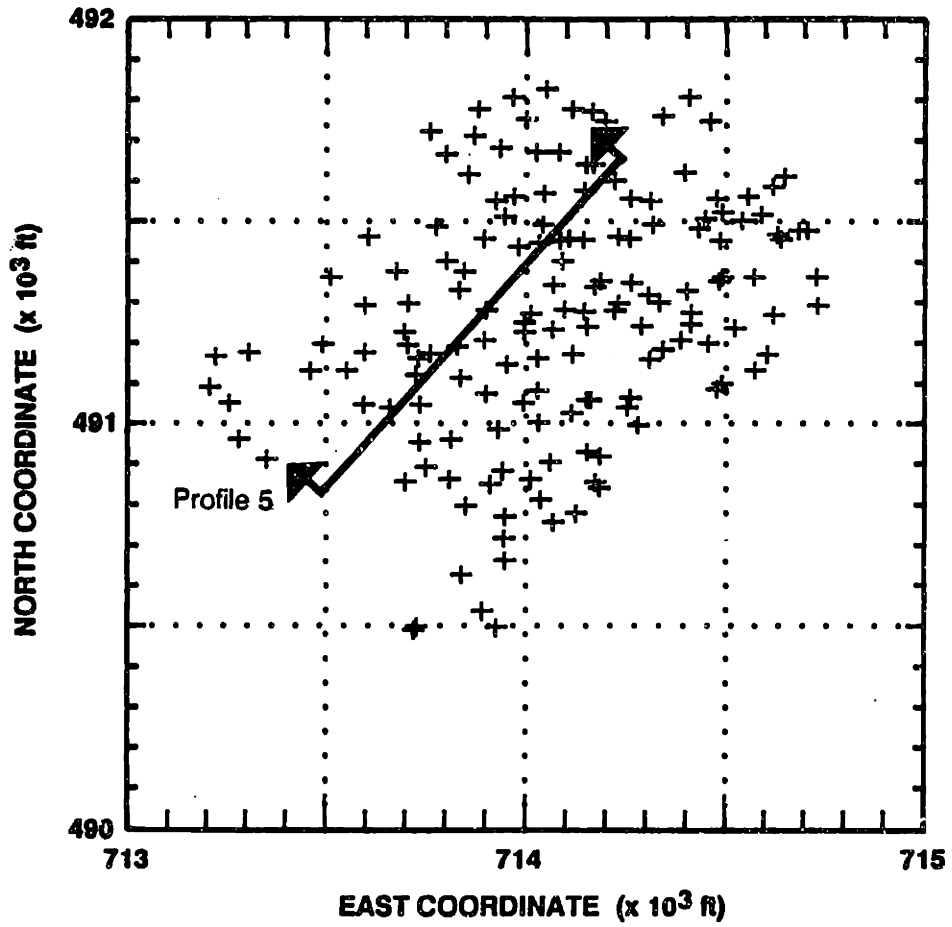
Figure A.2 - Locations of Case History Test Borings (157), Back Bay.
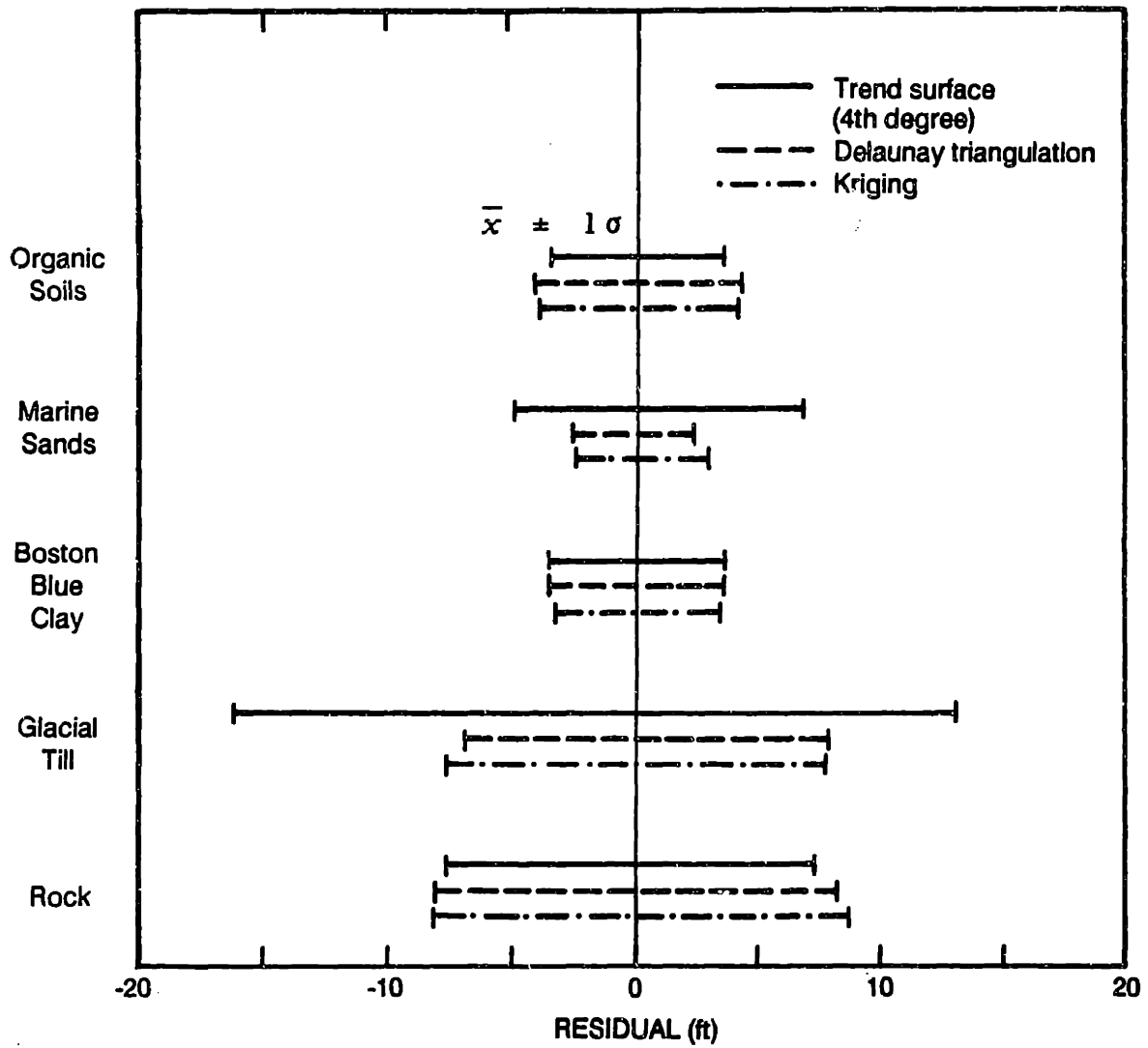
Figure A.3 - Comparison of Jackknifed Residual Means and Standard Deviations, Strata Tops, Back Bay.
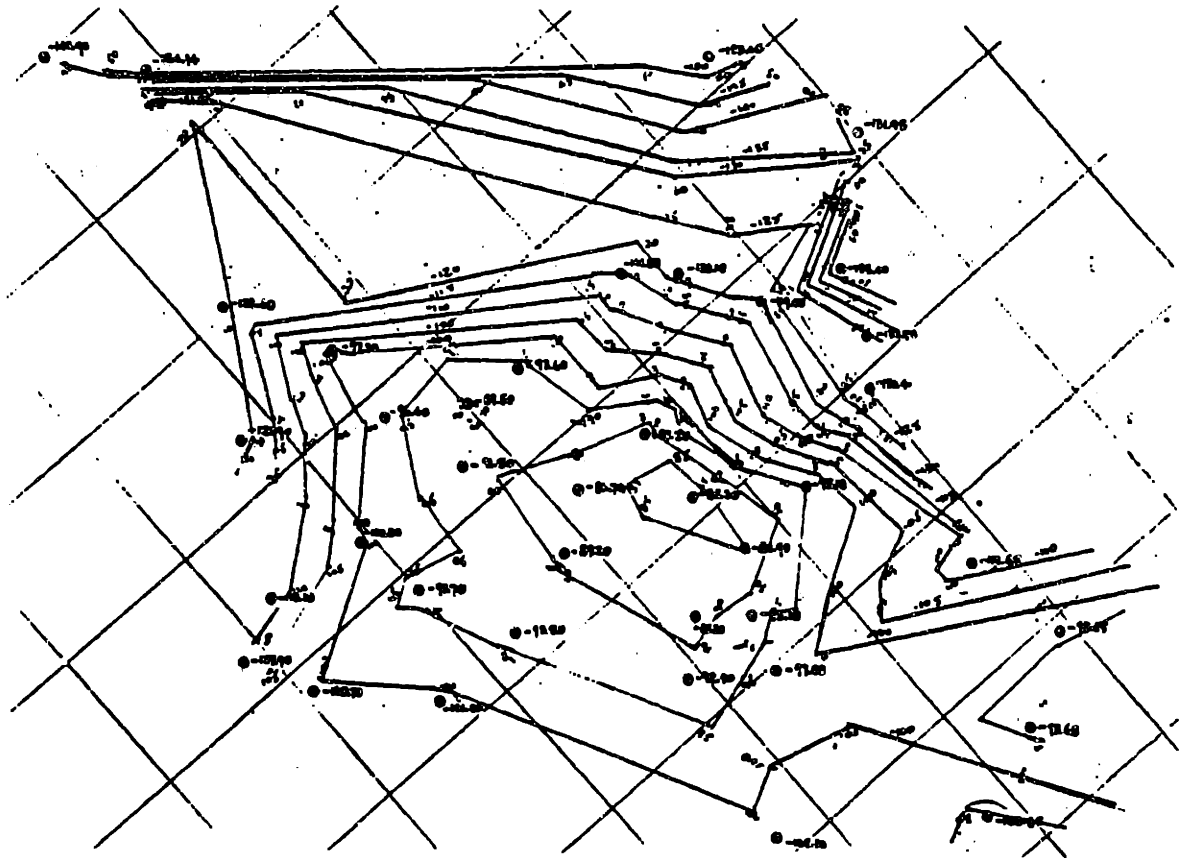
Figure A.4 · Hand Drawn Contours of Top of Rock (40 pts.), Back Bay: (a)
Individual #1,
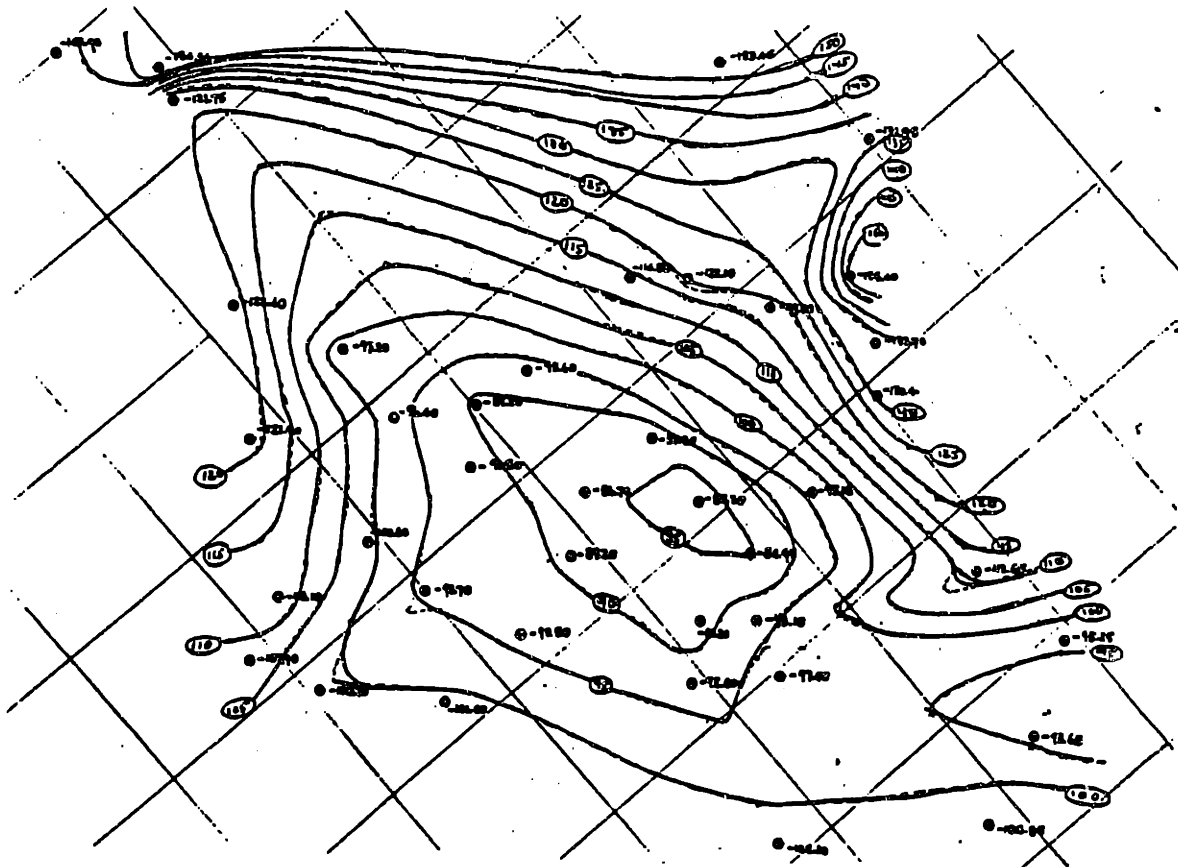
Figure A.4 - Continued. (b) Individual #2,
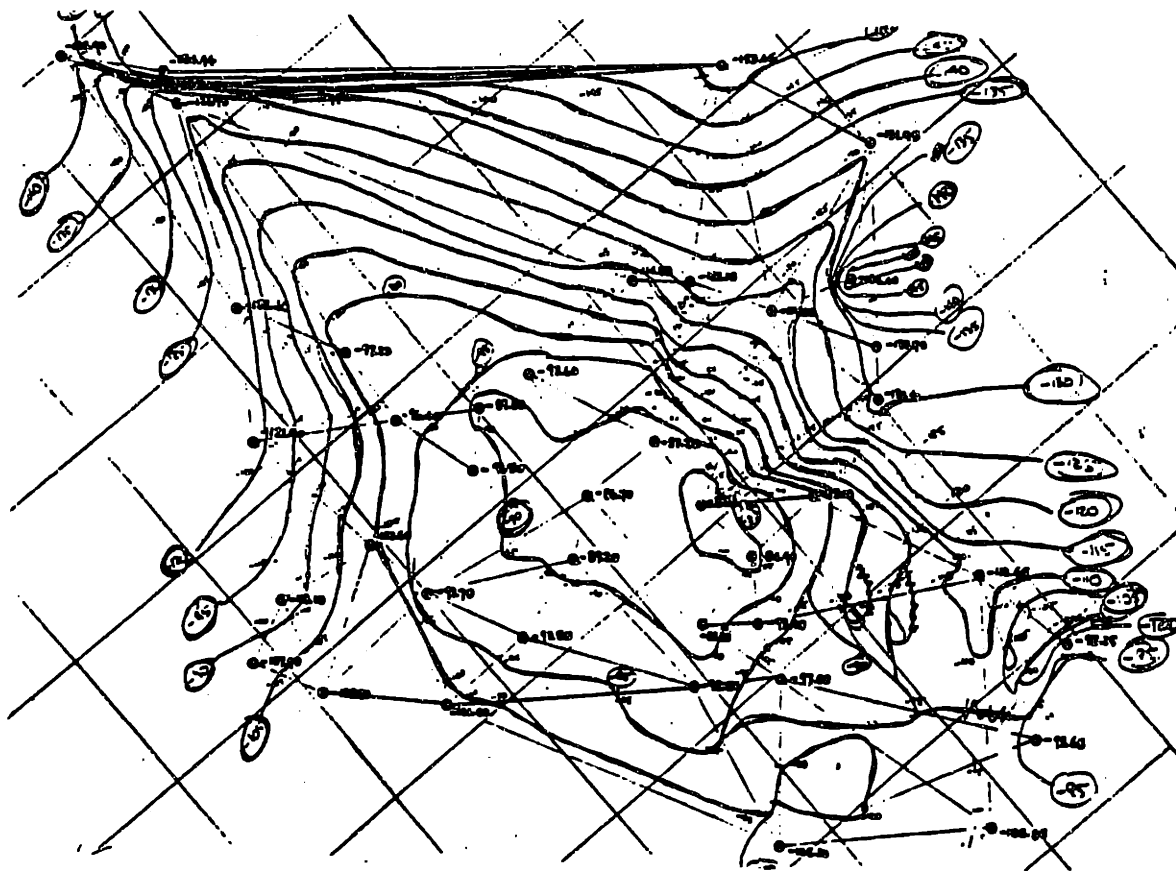
Figure A.4 - Continued.   (c) Individual #3,

Figure A.4 - Continued.   (d) Individual #4,
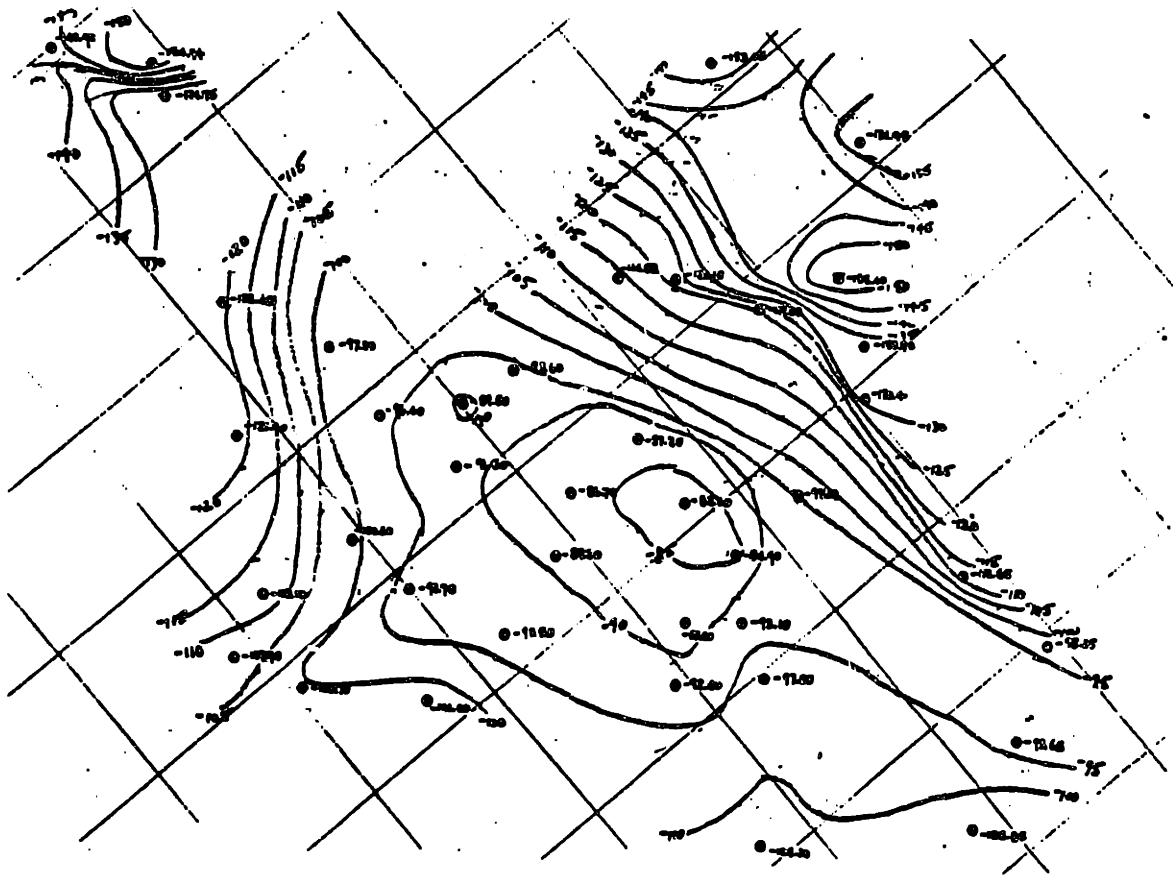
Figure A.4 - Continued.   (e) Individual #5,
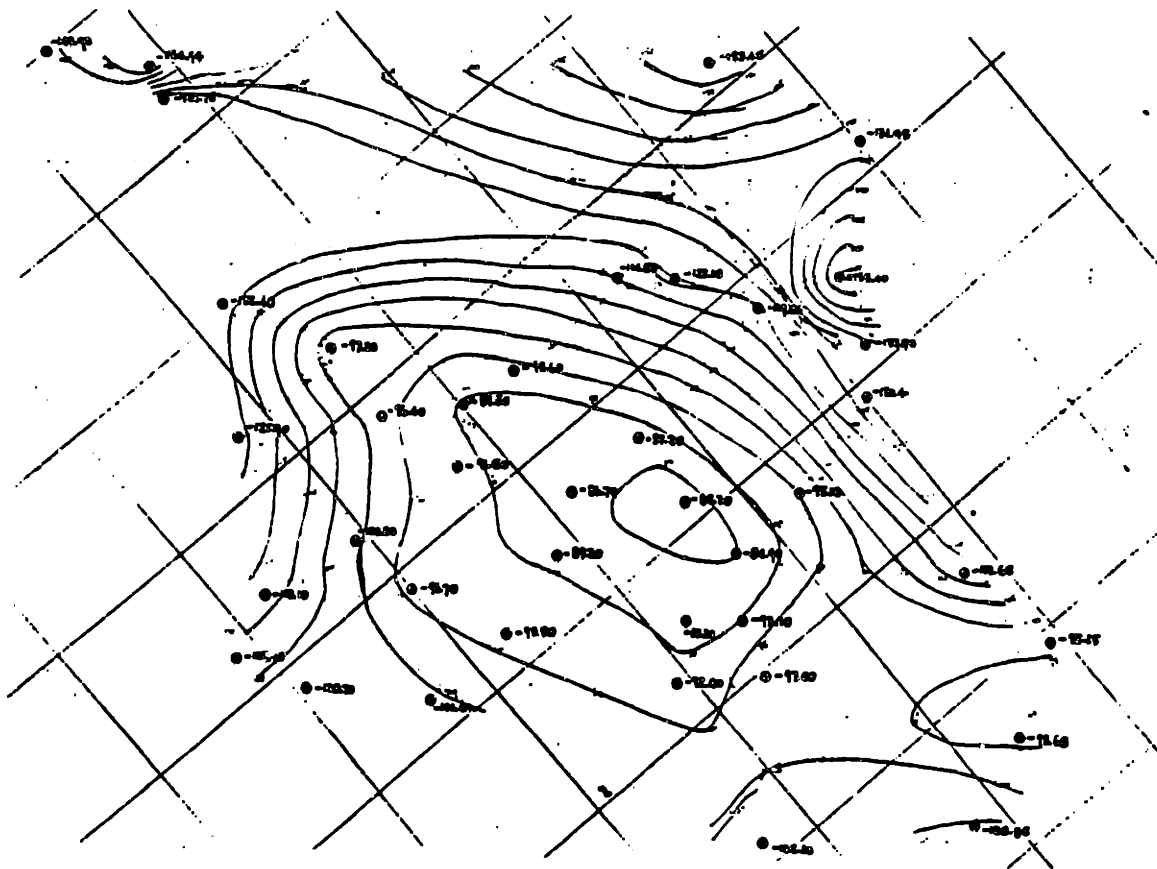
Figure A.4 - Continued. (f) Individual #6,

284
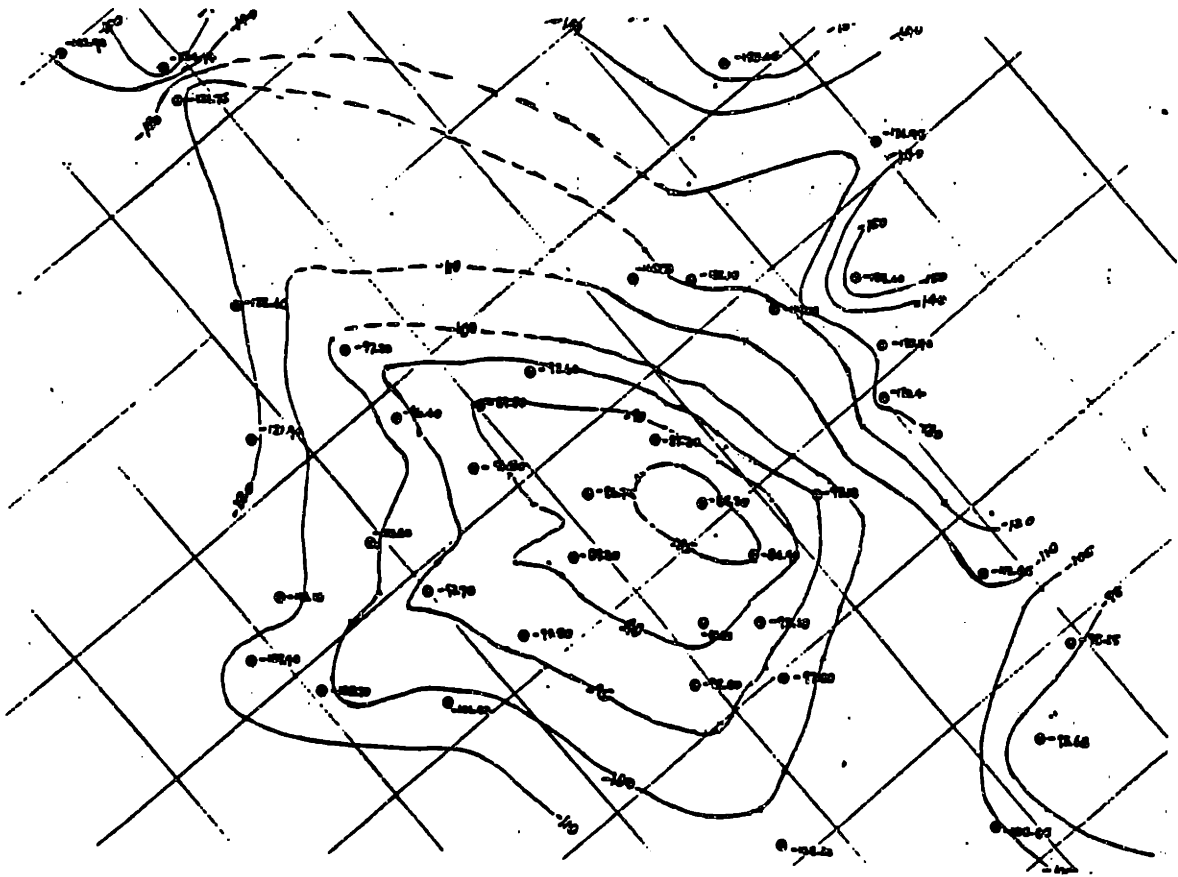
Figure A.4 - Continued. (g) Individual #7,

Figure A.4 - Continued. (h) Individual #8,
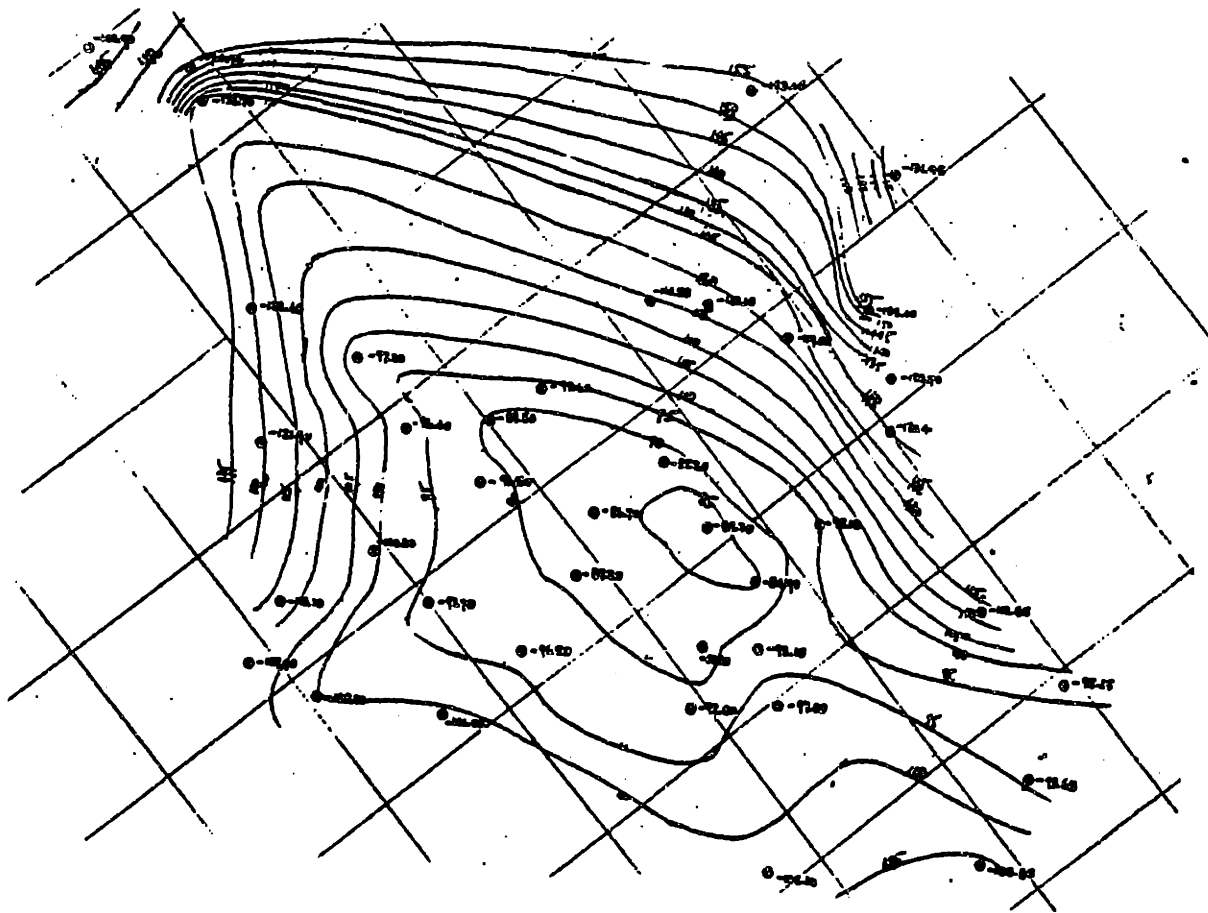
Figure A.4 - Continued. (i) Individual #9.

APPENDIX B

CAMBRIDGE CENTER CASE HISTORY

B.1 Introduction

The Cambridge Center site is a 14 acre site located in the Kendall Square area of Cambridge, Massachusetts (see Figure B.1). The case history area is indicated in Figure B.1. Available subsurface data has been summarized and is presented in summary form in the following sections.

The elevations indicated are referenced to the Cambridge City Base Datum, wherein El. 0 is 10.84 feet below the National Geodetic Vertical Datum (NGVD).

B.2 Subsurface Conditions

The subsurface conditions as indicated by the field explorations consist of seven discernible strata described as follows (starting from the existing bedrock):

Bedrock: The bedrock underlying the site is locally known as Cambridge Argillite. This is the same rock that underlies the Back Bay area. The upper surface of the rock is extremely weathered in some locations. The top of rock was observed at elevations ranging from El. -45 to El. -86.

Glacial Deposits: Strata of glacial till and glacial outwash overlie the bedrock. These strata are not continuous and in some locations are interbedded. The observed strata range in thickness from 3 to 56 feet. Although highly variable in composition, the deposits are typically gray medium to fine sand, silty fine sand, or cobbles and boulders.

Marine Deposits: A stratum of marine clay overlies the glacial deposits. The marine deposits can be sub-divided into three sub-strata. The major sub-strata is the gray silty clay deposit known as the Boston Blue Clay (BBC). In some locations the BBC is overlain by stiff to very stiff, yellow silty clay, which is actually BBC which has dried out to an extent and oxidized during periods of lower groundwater levels. A sub-stratum

288

of sandy clay or clayey sand may be encountered below the BBC and above the glacial deposits. The observed total thickness of the marine deposits ranged from 24 to 50 feet.

Sand: A continuous layer of sand deposits is found over the marine deposits. In very localized areas the continuity of the sand has been disrupted by erosion in the estuarial environment of the harbor or possibly by excavation to construct the canals which were built in this area.

Organic Silt: A discontinuous stratum of organic silt was encountered in many of the test borings. The maximum observed thickness was 8.5 feet. In several of the test borings it appeared that there had been some intermixing of the organic silt and the underlying sand.

Fill: The historical development of the Boston harbor area has included the placement of considerable fill. A continuous blanket of fill covers the Cambridge Center site. The fill material is highly variable in composition.

The major soil strata were further sub-divided for analysis. A brief description of the sub-strata is as follows:

Stratum I: Miscellaneous Fill, variable with location and depth; typically silty medium to fine sand, little gravel, trace brick, concrete, cinders; ranges from fibrous peat, little fine sand to coarse to fine sand, trace silt.

Stratum II: Organic Silt and Peat, variable sand and fiber content; typically, gray organic silt, trace peat; ranges from brown fibrous peat, little fine sand to dark gray, clayey organic silt, trace coarse to medium sand.

Stratum III: Sand, variable with location and depth; tends to become more coarse grained with depth; typically, gray or brown, medium to fine sand, trace silt, coarse sand, fine gravel; ranges from brown fine sand to gray, gravelly coarse to fine sand, trace silt.

<u>Stratum IVA</u>: Stiff Yellow Clay; typically, stiff to very stiff, yellow-brown, silty clay, trace fine sand.

<u>Stratum IVB</u>: Silty Clay (BBC); typically, gray, silty clay, occasionally with trace fine sand to coarse to fine sand, usually in lenses and partings, cobbles and boulders were occasionally encountered.

<u>Stratum IVC</u>: Sandy Clay; typically, gray, medium to fine sandy clay, little gravel, trace coarse sand; sand and gravel content varies with location.

<u>Stratum VA</u>: Glacial Outwash; typically, gray, medium to fine sand, trace silt, coarse sand, fine gravel to silty fine sand, trace coarse to medium sand.

<u>Stratum VB</u>: Glacial Till; Variable with depth and location; typically, gray, silty, medium to fine sand, little gravel, trace coarse sand; ranges from cobbles and boulders to gray, medium to fine sandy clay, trace coarse sand, fine gravel.

<u>Stratum VI</u>: Bedrock; variable with depth and location; upper region ranges from gray silt (completely decomposed Cambridge Argillite) to moderately hard, slightly weathered, moderately fractured, fine-grained, gray, Cambridge Argillite.

For ease of reference, the strata in the Cambridge Center case history are referred to by their Roman numeral designations only throughout the thesis.

B.3 Field Investigations

Over 130 test borings have been drilled in the process of performing the subsurface investigations for proposed structures within Cambridge Center. For the purposes of this case history, the available test boring logs were reviewed and eventually 110 test borings were selected for use. The test borings were selected based on the completeness of the test boring logs, and the detail in the visual descriptions.

The locations of the test borings selected for inclusion in the Cambridge Center case history are shown in Figure B.2.

B.4 Summary Statistics

The soil strata information for the Cambridge Center site was analyzed to determine summary statistics. Summary statistics were calculated for the top of the soil stratigraphy and the observed thickness of the soil deposits. The results are given in Tables B.1 and B.2.

B.5 Transition Matrix

An embedded Markov chain transition matrix was calculated for the Cambridge Center case history. The transition matrix is shown in Table B.3. The transition matrix for the Cambridge Center data is considerably more complex than the matrix for the Back Bay data. There are four strata that are consistent in transition (0.96 to 1.00). These are II to III, IVA to IVB, VA to VB, and VB to VI. The rest of the transition matrix elements, ranging 0.01 to 0.77, indicate that there is considerable intermixing of some of the strata.

B.6 Trend Surface Analysis

Trend surface analysis was performed on the observed strata top and thickness data for the Cambridge Center case history. The goodness-of-fit coefficients for the analysis of the strata tops and thickness, ranging from 0.008 to 0.926, are summarized in Tables B.4 and B.5.

B.7 Delaunay Triangulation Analysis

Delaunay triangulation analysis was performed on the case history data for the observed top and thickness of the soil strata. It should be noted that the Delaunay triangulation estimates can not be made for the exterior points which form the convex hull around the data locations. The results of the jackknifed Delaunay estimates are summarized in Tables B.6 and B.7.

B.8 Kriging Analysis

Kriging analysis was performed on both the observed top of soil strata and observed soil strata thickness data. The analysis was performed using KRM, a modified version of AKRIP. The results are summarized in Tables B.8 and B.9.

Similar to the Back Bay case history, most of the structural models for the Cambridge Center case history are based on zero order intrinsic functions. Only the VA and VI stratum top models were first order intrinsic functions.

B.9 Other Analysis

Probabilistic relaxation analyses were performed on portions of the Cambridge Center case history data. The results of these analyses are discussed in Chapter 6.

Table B.1 - Summary Statistics for Strata Tops, Cambridge Center.

Stratum	No. of Pts., n	Mean (El)	Stand. Dev. (ft)	Median (El)	Range (ft)
II	60	12.20	2.20	12.2	12.0
III	116	9.86	2.33	9.95	12.1
IVA	28	3.03	2.35	2.15	8.2
IVB	116	-1.16	3.32	-0.2	17.2
IVC	27	-29.29	8.99	-31.1	34.3
VA	20	-35.64	5.92	-35.4	24.0
VB	92	-36.04	10.38	-35.95	69.1
VI	42	-63.56	12.64	-62.55	54.0

Table B.2 - Summary Statistics for Strata Thickness, Cambridge Center.
([ ] indicates values for non-zero data, if no brackets are shown then all data were non-zero)

Stratum	No. of Pts., n	Mean (ft)	Stand. Dev. (ft)	Median (ft)	Range (ft)
I	118	8.53	2.23	9.0	12.5
II	118 [59]	1.62 [3.23]	2.17 [2.04]	0.25 [2.5]	8.5 [8.0]
III	118	9.72	3.84	9.0	21.0
IVA	96 [28]	1.34 [4.59]	3.01 [4.04]	0.0 [3.25]	15.0 [14.5]
IVB	93 [92]	33.43 [33.79]	8.24 [7.50]	34.0 [34.0]	53.0 [40.5]
IVC	63 [26]	3.62 [8.77]	6.66 [7.93]	0.0 [6.0]	37.0 [36.0]
VA	50 [17]	3.58 [10.53]	6.22 [6.40]	0.0 [1.15]	23.0 [20.5]
VB	42	25.19	13.18	23.05	56.5

Table B.3 - Strata Change Transition Matrix, Cambridge Center.

To \ From	I	II	III	IVA	IVB	IVC	VA	VB	VI
I	0	0.51		0.01	0	0	0	0	0
II	0	0	0.98	0	0.02	0	0	0	0
III	0	0	0	0.22	0.77	0	0	0.01	0
IVA	0	0	0	0	0.96	0	0	0.04	0
IVB	0	0	0	0	0	0.29	0.15	0.56	0
IVC	0	0	0	0	0	0	0.22	0.70	0.08
VA	0	0	0	0	0	0	0	1.00	0
VB	0	0	0	0	0	0	0.01	0	0.99
VI	0	0	0	0	0	0	0	0	0

Table B.4 - Trend Surface Goodness-of-Fit Values, Strata Tops, Cambridge Center.

Stratum	Order of Polynomial			
	1	2	3	4
II	0.008	0.123	0.265	0.424
III	0.071	0.221	0.271	0.346
IVA	0.527	0.586	0.716	0.858
IVB	0.129	0.351	0.390	0.657
IVC	0.190	0.511	0.598	0.755
VA	0.561	0.809	0.926	0.986
VB	0.255	0.397	0.450	0.553
VI	0.696	0.734	0.761	0.818

Table B.5 - Trend Surface Goodness-of-Fit Values, Strata Thickness, Cambridge Center.

Stratum	Order of Polynomial			
	1	2	3	4
I	0.025	0.104	0.114	0.150
II	0.073	0.190	0.234	0.263
III	0.426	0.491	0.555	0.623
IVA	0.259	0.465	0.596	0.708
IVB	0.289	0.415	0.495	0.583
IVC	0.104	0.159	0.238	0.381
VA	0.040	0.195	0.255	0.328
VB	0.347	0.473	0.510	0.588

Table B.6 - Summary Statistics for Jackknifed Residuals for Delaunay Triangulation Analysis, Strata Tops, Cambridge Center.

Stratum	No. of Pts., n	Mean, (ft)	Stand. Dev. (ft)	Median, (ft)	Range, (ft)
II	53	-0.03	2.45	0.14	13.65
III	107	0.13	2.15	0.07	18.21
IVA	21	0.26	1.75	1.98	5.46
IVB	107	0.01	2.37	0.44	13.25
IVC	19	-0.25	7.62	2.48	32.37
VA	13	-0.07	2.44	2.84	7.84
VB	77	-0.59	10.04	0.11	53.98
VI	33	-0.93	10.04	1.27	51.17

Table B.7 - Summary Statistics for Jackknifed Residuals for Delaunay Triangulation Analysis, Strata Thickness, Cambridge Center.

Stratum	No. of Pts., n	Mean, (ft)	Stand. Dev. (ft)	Median, (ft)	Range, (ft)
I	109	0.22	2.63	0.02	14.67
II	109	-0.32	2.18	-0.22	11.47
III	109	0.08	3.08	-0.01	22.82
IVA	81	-0.09	2.05	0.00	15.72
IVB	77	0.71	6.71	0.38	36.62
IVC	54	0.87	8.01	0.00	54.11
VA	40	-0.01	7.24	0.00	34.83
VB	32	1.47	13.45	4.48	65.97

Table B.8 - Summary of Kriging Coefficients, Strata Tops, Cambridge Center.

Stratum	K	b_0	b_1	b_2	b_3
II	0	0	-.0438	-	-
III	0	0	-.0735	-	-
IVA	0	2.0568	-.0043	-	-
IVB	0	0	-.1390	-	-
IVC	0	0	-.6000	-	-
VA	1	0	0	-2.8E-6	-
VB	0	0	-1.0575	-	-
VI	1	0	-.9908	0	-

Table B.9 - Summary of Kriging Coefficients, Strata Thickness, Cambridge Center.

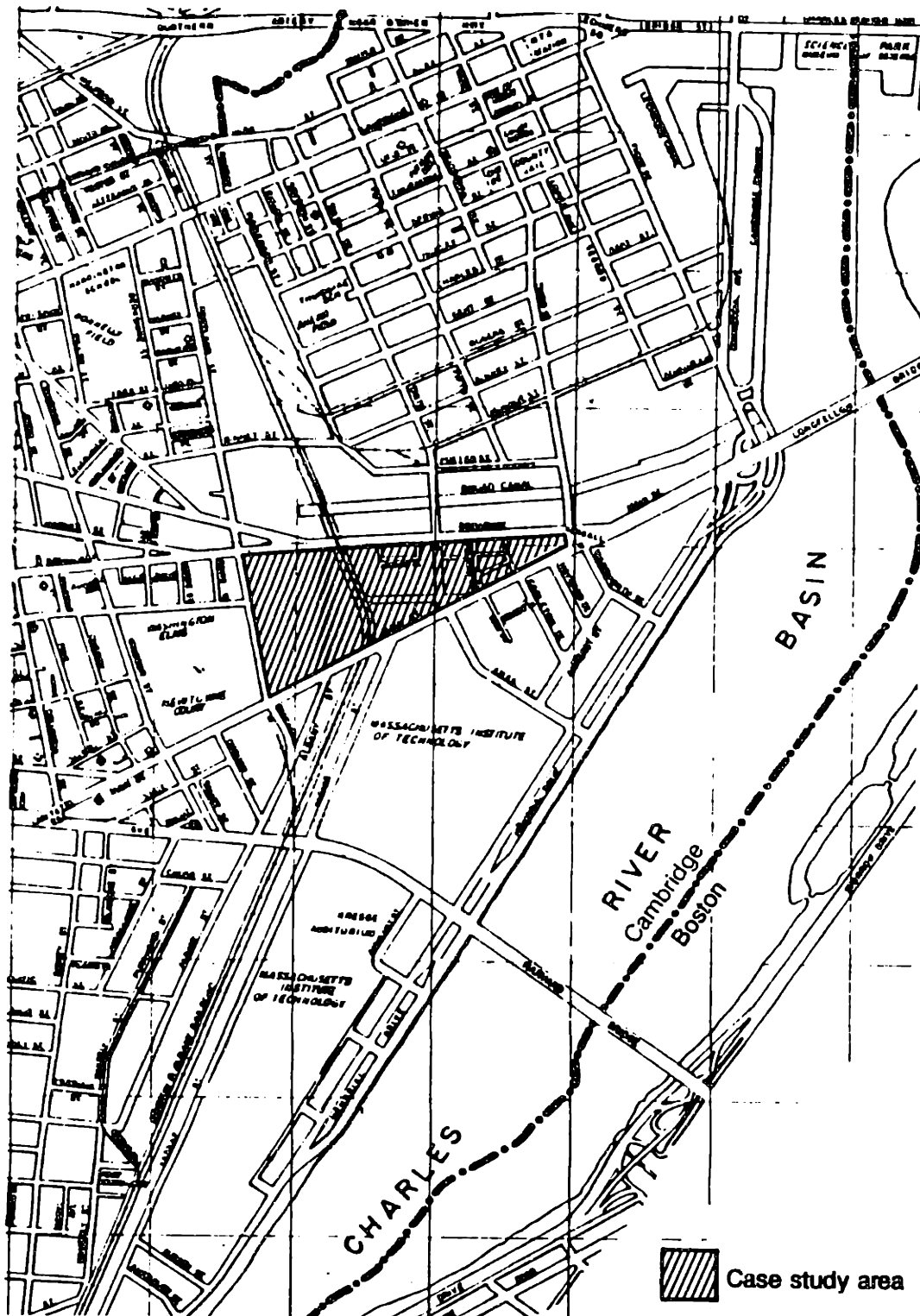| Stratum	K	b_0	b_1	b_2	b_3
I	0	0	-.1087	-	-
II	0	2.3774	-.0221	-	-
III	0	3.2687	-.0689	-	-
IVA	0	0	-.06188	-	-
IVB	0	0	-.8837	-	-
IVC	0	0	-.7349	-	-
VA	0	0	-.5461	-	-
VB	0	0	-2.0046	-	-

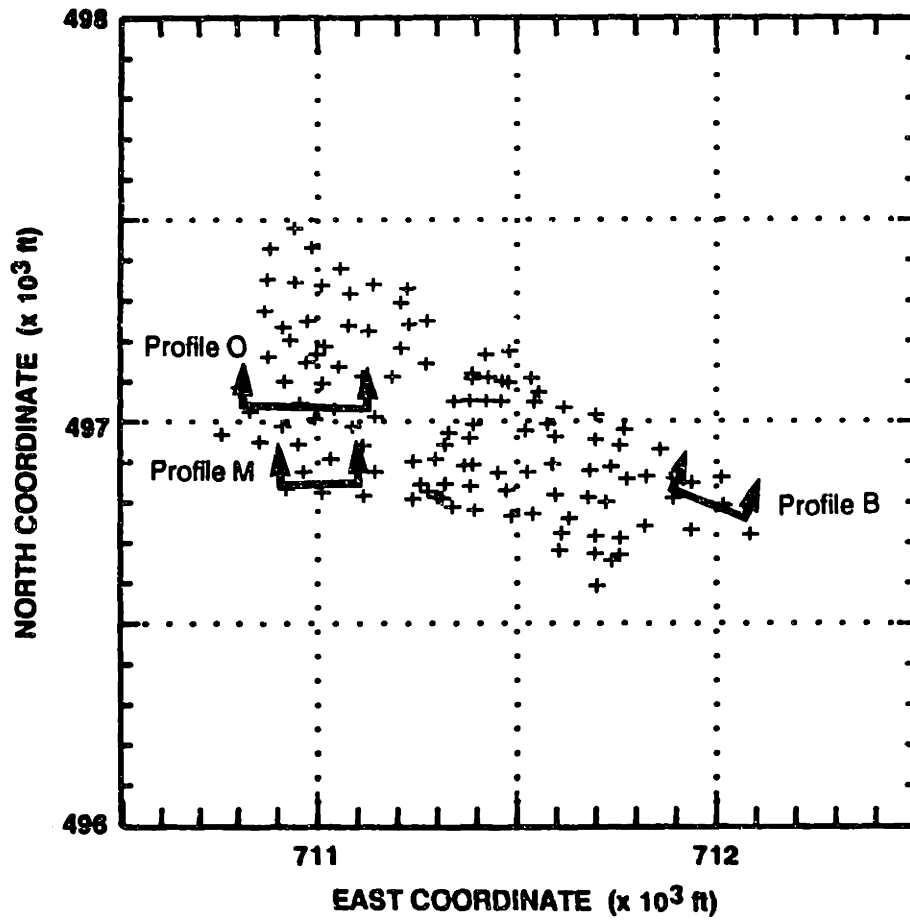Figure B.1 - The Cambridge Center Area, Cambridge, Massachusetts.

Figure B.2 - Test Boring Locations (110), Cambridge Center.